Czech Technical University in Prague
Faculty of Electrical Engineering

Doctoral Thesis

August 2018   Eva Žáčeková

Czech Technical University in Prague
Faculty of Electrical Engineering
Department of Control Engineering

Identification for Model Predictive Control under Closed-loop Conditions

Doctoral Thesis

Eva Žáčeková

Prague, August 2018

Programme: Electrical Engineering and Information Technology (P 2612)
Branch of study: Control Engineering and Robotics (2612V042)

Supervisor: Prof. Ing. Michael Šebek, DrSc.

Thesis Supervisor:

      Prof. Ing. Michael Šebek, DrSc.

      Department of Control Engineering

      Faculty of Electrical Engineering

      Czech Technical University in Prague

      Karlovo náměstí 13

      121 35 Prague 2

      Czech Republic

Abstract

In recent years, modern control algorithms have gained popularity in many fields of industry. One of the methods that has become widely recognized is Model Predictive Controller (MPC). Such controller brings innumerable advantages such as possibility to define control requirements compactly as an objective function, ability to incorporate potential constraints directly into the optimization task and many others—at the same time, it brings some disadvantages as well. Above all, its main drawback is the fact that it crucially needs a mathematical model for its proper functioning. Its internal model not only has to describe the reality (the responses of the real controlled system) accurately but it should also be as simple as possible due to the computational complexity of the resulting task. However, a mathematical model that is not a sufficiently reliable replica of the controlled system can significantly degrade the performance of the controller relying on it. Therefore, extensive attention needs to be paid to the search for an appropriate system behavior predictor.

The first part of this work deals with the problem of identification of a model for a predictive controller under real-world conditions. Methods of minimization of multistep prediction error are introduced—the reason to choose them is the fact that the models they provide are able to predict the behavior of the system even for longer period ahead and therefore, they are suitable for use with MPC. The designed algorithms are thoroughly tested and a significant part of their verification is performed using real-life data gathered from several buildings. Further proof of validity of the provided identification techniques is given by the fact that these models are used by real operational MPCs serving as indoor climate controllers in these buildings.

In the second part of this thesis, a task of ensuring sufficiently excited data for the subsequent re-identification of a model used within the model predictive control framework is discussed. Two novel algorithms tackling this problem are introduced and gradually adapted to suit both the standard MPC formulation with reference tracking requirement and also a class of zone MPCs. Various model structures are considered ranging from linear systems trough linear systems with (partially) predictable disturbances up to a chosen class of nonlinear systems containing bilinear systems and systems with polynomial nonlinearities.

Keywords:

Model predictive control, system identification, model predictive control relevant identification, persistent excitation, closed-loop experiment design, dual control, building climate control.

Abstrakt

V posledných rokoch došlo k rozmachu moderných algoritmov pre riadenie v rôznych odvetviach priemyslu. Jednou z metód, ktorá sa stala veľmi populárnou, je aj prediktívny regulátor založený na modeli. Takýto regulátor prináša nespočetné množstvo výhod, ako napríklad možnosť kompaktne definovať požiadavky na riadenie vo forme účelovej funkcie, schopnosť zahrnúť obmedzenia priamo do optimalizačnej úlohy a mnoho ďalších. Zároveň však tento typ regulátora prináša aj niekoľko nevýhod. Jeho hlavným problémom je predovšetkým fakt, že pre svoje správne fungovanie potrebuje mať k dispozícii matematický model systému. Tento vnútorný model nielenže musí dostatočne presne popisovať realitu (odozvy skutočného riadeného systému), ale mal by byť aj čo najjednoduchší kvôli výpočtovej zložitosti výslednej úlohy. Matematický model, ktorý nie je dostatočne vernou replikou riadeného systému, môže významne degradovať správanie regulátora, ktorý sa na tento model spolieha. Z tohto dôvodu je nevyhnutné venovať hľadaniu vhodného prediktora správania systému náležitú pozornosť.

Prvá časť tejto práce sa zaoberá problémom identifikácie matematického modelu pre prediktívny regulátor v podmienkach reálneho sveta. Sú predstavené algoritmy pre minimalizáciu viackrokovej predikčnej chyby. Tieto metódy sú vybrané kvôli tomu, že modely, ktoré poskytujú, dokážu predikovať budúce správanie systému aj na dlhší čas vopred a sú preto vhodné pre použitie s MPC. Navrhnuté algoritmy sú dôkladne otestované a významná časť ich overenia je vykonaná s využitím skutočných dát získaných z niekoľkých budov. Ďalším dôkazom správnosti poskytnutých identifikačných techník je to, že tieto modely sú používané reálne nasadnými MPC regulátormi, ktoré slúžia na riadenie vnútornej mikroklímy v týchto budovách.

V druhej časti tejto práce je diskutovaná úloha zabezpečenia dostatočne vybudených dát pre následnú reidentifikáciu modelu, ktorý je použitý v rámci prediktívneho regulátora založeného na modeli. Sú navrhnuté dva algoritmy pre riešenie tohto problému, ktoré sú následne upravené tak, aby sa vedeli vysporiadať ako so štandardnou MPC formuláciou s požiadavkou na sledovanie referencie, tak aj s triedou takzvaných zónových prediktívnych regulátorov. Sú uvažované viaceré štruktúry modelu od lineárnych systémov cez lineárne systémy s (čiastočne) predpovedateľnými poruchovými vstupmi až po vybranú triedu nelineárnych systémov obsahujúcu bilineárne systémy a systémy s polynomiálnymi nelinearitami.

Kľúčové slová:

Prediktívný regulátor založený na modeli, identifikácia systémov, identifikácia vhodná pre prediktívny regulátor založený na modeli, vytrvalé vybudenie, návrh experimentu v uzavretej slučke, duálne riadenie, riadenie vnútornej klímy v budovách.

Acknowledgements

First of the all, I would like to express my very great appreciation to Michael Šebek, my supervisor, for his fair approach and patience. Thanks to him, I could participate in many conferences, which enabled me to discover new horizons, fostered my imagination and helped me to gain useful experience.

My gratitude belongs to the members of the groups of Lieve Helsen (Department of Mechanical Engineering) and Dirk Saelens (Department of Civil Engineering) at KU Leuven. I worked with them during my half-year stay in Belgium and I especially appreciate their friendliness and exceptional co-operation. They helped me to gain deeper knowledge and a lot of beautiful memories. My thanks belong namely to Stefan Antonov, Jan Hoogmartens, Wout Parys, Maarten Sourbron and Clara Verhelst. It was my pleasure to work with you.

I would like to thank the people belonging to the group of prof. Francesco Borrelli at UC Berkeley where I spent several months during my studies for their willingness, great attitude and for quantum of fruitful chats which provided me with fresh inspiration and many new ideas. I must not omit homey atmosphere they created in the lab. I spent unforgettable times with you.

My further thanks go to the staff of the Department of Control Engineering for the pleasant and flexible environment for my research. Most of all, I would like to mention Mrs. Petra Stehlíková who always willingly helped me to process every formality, especially during the last three years of my studies.

I want to thank also my family and friends, most notably Ondřej Bruna for many infinite debates about the joys and sorrows of the PhD student life.

Finally and most importantly, I am deeply grateful to Matej Pčolka for his support, patience and innumerable fruitful academic discussions.

Declaration

I hereby declare that this dissertation thesis is my own personal effort and I have carefully cited all the literature sources I had used.

Prague, 20. 8. 2018

Prehlasujem, že som svoju dizertačnú prácu vypracovala samostatne a v predloženej práci dôsledne citovala použitú literatúru.

V Praze, 20. 8. 2018

Contents

Chapter 1

Introduction and Motivation

During the last years, modern control methods relying on use of a model of the controlled system have witnessed significant boom. Being popular not only among the academicians [Mayne, 2014], [Corriou, 2018], these approaches of which the most noticeable one is the Model Predictive Control (MPC) have started to be more and more appreciated also by the community of process control engineers [Darby and Nikolaou, 2012], [Forbes et al., 2015].

The MPC brings a wide variety of new possibilities, opportunities and advantages, the most significant of which are the ability to handle constraints and control multivariable plants and the capability of formulating control requirements in a comprehensive and compact form of an optimization cost function and satisfying them in an optimal way. Going hand in hand with plenty of indisputable benefits, several problems arise with use of this type of controller.

The most crucial bottleneck of this framework is the fact that for its proper functioning, the MPC needs a mathematical model of the controlled system capable of predicting the behavior of the system as accurately as possible since based on these predictions, the MPC optimizes the input actions applied to the system.

While model creation is mentioned only marginally in majority of the academic works dealing with the MPC and these usually assume that the model of the system is either perfectly known or found in literature, the task is much more complicated and time-consuming in case of real applications—sometimes, it can be even more complex and involved than the controller design itself [Zhu, 2001], [Forbes et al., 2015].

As already mentioned, the predictive controller makes use of the model of the controlled system to predict its future behavior over the prediction horizon. Therefore, the chosen model must be able to accurately predict the response of the system for suffi-

ciently long time ahead. However, majority of the commonly used identification methods provide models that are optimized only in the sense of one-step prediction error [Ljung, 1999], [Ljung, 2001]. Predictions of such models might be sufficiently precise for a few steps ahead, however, their multistep predictions are usually not accurate enough, which results in the performance of the MPC being suboptimal. A solution to this issue might be to employ identification methods directly minimizing the multistep prediction error—such methods are able to provide models with reliable multistep predictions appropriate for use with MPC. These approaches are collectively called Model Predictive Control Relevant Identification (MRI) methods [Shook et al., 1992], [Gopaluni et al., 2004], [Zhao et al., 2014].

The next issue making the whole process of obtaining a mathematical model more complicated is the fact that majority of real systems are controlled continually by certain feedback controller. It is often impossible to execute any identification experiment because of either operating or economical reasons and therefore, it is necessary to identify only from the data that are available—closed-loop data. These data use to suffer from several undesired phenomena such as insufficient excitation, correlation between certain input signals or input-disturbance correlation causing that even well-designed identification methods fail.

There exists a broad spectrum of special identification methods capable of handling also closed-loop identification data [Gustavsson et al., 1977], [Van den Hof, 1998], however, most of these methods work well only for simple linear controllers. On the other hand, the MPC framework results in a much more involved controller structure and therefore, it is desirable to search for alternative ways of tackling this task.

A very promising perspective is to focus on methods where the controller itself can bring some additional information which then improves the model of the process—in such case, the controller can be viewed as performing certain kind of closed-loop identification experiment. Relating this to the MPC framework, the controller is designed not just to meet the standard MPC requirements but also to ensure that the gathered data are sufficiently excited [Marafioti et al., 2010], [Rathousky and Havlena, 2013], [Tanaskovic et al., 2014], [Larsson, 2014], [Bustos et al., 2016].

One of the most emerging application areas where the MPC has been steadily gaining popularity is undoubtedly building climate control. According to the available literature, overall expenses spent on heating/cooling of building complexes reach as high as half of the total energy consumption in the building sector, the area to which about 40% of the global energy consumption is attributed. It has turned out that use of advanced control methods

such as MPC opens door to about 30% energy consumption reduction [Oldewurtel et al., 2010], [Ma et al., 2011], [Razmara et al., 2015], [Smarra et al., 2018].

Speaking about data excitation, the building climate control differs significantly from other application areas of control engineering. For example, using an engine test stand, an automotive control engineer can implement basically arbitrarily rich identification experiment thus simplifying the subsequent search for the mathematical model—a situation that is hardly possible when dealing with building climate controller design. However, building climate control area—together with process control and others—is just one of many branches where any identification experiment might be very cumbersome. This might have various reasons of mostly economical nature, nevertheless, focusing on the building climate control in particular, operating reasons join as well since the buildings are usually permanently inhabited. Finally, the difficulties when executing identification experiments in a building are emphasized by the fact that the time constants of a typical building are often in the range of dozens of hours or even several days. It is all these issues accompanying the deployment of MPC in the building climate control area that stood for the motivation for the majority of the research presented in this thesis.

Linking up the thesis with this overview, the thesis focuses mainly on the identification problems that occur in real applications such as the above mentioned inability of performing an extensive open-loop identification experiment and the consequent insufficient excitation and data correlation problems. Even though one of the strongest motivations originated in the building climate control applications, this thesis attempts to provide a general and comprehensive framework enabling efficient identification of models for MPC under the real-life conditions for a broad spectrum of control engineering applications.

1.1   Structure of the Thesis

This doctoral thesis takes the format of a *thesis by publication*, thereby it presents publications of the author relevant to the topic of the thesis. This thesis format is approved by the Dean of Faculty of Electrical Engineering by the *Directive for dissertation theses defense, Article 1*.

The rest of this thesis is organized as follows: Chapter 2 describes the current state of the art in both main topics of the thesis—model predictive control relevant identification and persistently exciting model predictive control. The main contributions of this thesis are introduced in Chapter 3. Two subsequent chapters go into detail and elaborate more

on each subtopic with a special emphasize put on author's principal publications related to the particular subtopic. Chapter 4 focuses on contributions in the area of model predictive control relevant identification while Chapter 5 presents the results achieved for the model predictive control with guaranteed persistent excitation. Last of all, Chapter 6 reviews the results of the work, discusses potential directions for further research and concludes the thesis.

Chapter 2

State of the Art

This chapter covers the state-of-the-art knowledge of the topics elaborated in this thesis. As already mentioned, the thesis focuses on two main problems that are related to process of obtaining a mathematical model for MPC in case of real operation and therefore, also this chapter is divided into two main parts.

The first part of this chapter discusses a specific class of the identification methods that are collectively referred to as model predictive control relevant identification methods. The acronym MRI has become a synonym for those identification approaches that—unlike the traditional identification procedures—minimize multistep prediction errors of the obtained model, which enables them to find models that are capable of providing accurate predictions even for several steps ahead and are thus especially suitable for use with MPC.

The second part of this chapter addresses a process of obtaining suitable closed-loop identification data within the model predictive control framework. The available approaches are explained and the means of providing data that are sufficiently rich on information avoiding costly experiments and not degrading the MPC optimal performance inadmissibly are debated.

2.1 Model Predictive Control Relevant Identification

It belongs to common control engineering knowledge that for proper behavior of a predictive controller, the availability of both sufficiently simple and satisfactorily accurate model of the controlled system is of crucial importance. In order to achieve that the internal MPC model is suitable and accurate enough, the fact that it is intended to be used as

a predictor for a predictive controller needs to be considered far before the design of the identification procedure. Here, the most appropriate approach providing models tailored to use with MPC is to minimize multistep prediction error. It should be mentioned that the commonly used identification methods coming out of the prediction error method [Ljung, 1999], however, minimize only one-step prediction error and thus, predictions of their models are sufficiently precise only for couple of steps ahead while the quality of their multistep predictions is mediocre which results in the suboptimal behavior of the MPC.

The available literature offers several different approaches to handle the problem of multistep prediction error minimization properly. The first sprouts are dated back to early '90s—at that time, the authors of [Shook et al., 1991] and [Shook et al., 1992] proved the equivalence of the multistep prediction error minimization and the pre-filtration of the input-output data using a noise-model-dependent filter with subsequent use of one-step prediction error minimization. While in these first pioneering works, the authors considered only simple single-input/single-output (SISO) model structure, this method was later extended also for more general ones, e.g. Box-Jenkins [Huang and Wang, 1999]. Due to the crucial importance of the knowledge of the process noise model, these methods have never been applicable for the practical use.

These works were followed by [Gopaluni et al., 2003], [Gopaluni et al., 2004] and [Potts et al., 2014]. In these papers, the authors introduced a two-stage algorithm; during the first stage, the deterministic part of the model was estimated while in the second one, coefficients of the noise model were obtained using the deterministic part of the model from the previous step. Employing the second stage, perfect knowledge of the system noise model became unnecessary, nevertheless, at least a correct *structure* of the noise model— an information that is neither available in real applications—had to be at disposal and strongly conditioned the performance of this method. Another drawback discriminating this approach from spreading wider is the fact that the estimation of the noise model coefficients is a highly challenging task especially when dealing with multi-input/multi-output (MIMO) systems since it includes involved polynomial matrix operations.

The next way to tackle the problem of multistep prediction error minimization was given in [Rossiter and Kouvaritakis, 2001] where multiple models were used to generate the predictions. Thus, a separate model specifically optimized for each of the k-step predictions was estimated. Although providing very accurate predictions for the entire inspected horizon, the number of parameters involved can rise very steeply—especially for MIMO processes—already for moderate prediction horizons. Since the variance of the parameter

estimation error is proportional to the ratio between the number of the estimated parameters and the dataset length, this approach usually requires large identification data volumes.

Published several years later, [Laurı et al., 2010] formulated the multistep prediction error minimization as an optimization problem. For models with MIMO ARX (autoregressive with external input) structure considered also in this thesis, this results in a nonlinear programming task. Later, the authors of the mentioned paper provided an extension of their own original work [Laurí et al., 2010] where the so-called partial least squares algorithm was used for the model parameters estimation. Let us note that the proposed algorithm can help in avoiding issues with ill-conditioned data which are typical for the industrial processes. Besides that, these two publications discussed not only theoretical aspects but practically oriented matters and phenomena as well. Still, the models resulting from the aforementioned optimization procedure have input-output structure and these models (such as ARX) might not be particularly suitable for the MPC, since usually, the control requirements are formulated such that they involve also the internal states of the controlled system.

The common problem of the available works is the fact that they consider only black-box models with unconstrained parameters. This might be inappropriate since the real operation data often suffer from lack of information—a bottleneck that can be eliminated or at least remedied as simply as by taking advantage of some additional knowledge about the system model. A methodology for identification of state-space grey-box models was provided in [Rehor and Havlena, 2010] where the authors based their approach on minimization of a weighted combination of the prediction error and the output error.

It should be mentioned that during the last years, a significant boom in the area of nonlinear model predictive control has been witnessed fostering novel contributions in the field of identification for MPC with some noteworthy algorithms for identification of special classes of nonlinear systems provided in [Quachio and Garcia, 2014] or [Quachio and Garcia, 2017].

Last of all, let us remind that the original contributions of this thesis related to this topic are presented in Chapter 4.

2.2 MPC with Guaranteed Persistent Excitation

A very common situation that occurs in industrial practice is that the system is already controlled by certain advanced controller whose control performance starts to deteriorate. This is usually caused by the mathematical model which might loose its ability to describe the system dynamics in a reliable manner and in such case, perhaps the most appropriate step is to re-identify the model.

It has already been noted that in many industrial applications, performing an identification experiment is not admissible due to various reasons. Then, the only available data come from closed-loop operation and these are known to be not persistently excited and suffer from noise-input cross-correlation, in which case the classic open-loop identification methods are not capable of providing models with reasonable quality [Ljung, 1999], [Ljung, 2001]. It can be shown that the accuracy of a model obtained under closed-loop conditions can be improved by a proper choice of the "identification cost function" and also considering constraints on the model parameters. Nevertheless, it is still important to pay much attention to a very delicate nature of the closed-loop data, e.g. input-noise correlation and insufficient excitation.

Following the categorization presented in [Forssell and Ljung, 1998], the traditional closed-loop identification approaches can be divided into three groups as follows:

1. *direct methods*: the feedback presence is ignored and the estimation is performed using unaltered input/output signals;

2. *indirect methods*: the closed-loop system is identified using measurements of the reference r and the output y and the plant model is retrieved making use of an information about the controller structure (use of this method is, however, restricted to situations when the controller is known and linear);

3. *joint input-output methods*: the original inputs and outputs are used as outputs and the reference signal is considered to be an input from the identification point of view. Consequently, an open-loop model is found based on the knowledge of the augmented system with the mentioned inputs and outputs. In case of a linear controller, a two-stage method can be applied, otherwise a more complex projection method [Van Den Hof and Schrama, 1993], [Forssell and Ljung, 2000] is needed. Here, it should be remarked that when using the joint input-output method, the inaccuracy of the estimates increases with the nonlinear character of the controller as well.

Since the MPC brings a piecewise affine feedback into the system [Alessio and Bemporad, 2009] whose parameters depend on the measurements of the current states of the system and also on the future references and/or disturbances acting on the system, even the use of the second two (joint input-output method and indirect method) of the closed-loop identification approaches might not bring the desired results [De Klerk and Craig, 2002].

In the author's paper [A.11], several examples of special de-correlation procedures having the potential to improve the identifiability of the model significantly (even in case of the feedback introduced by the MPC) were presented. However, these and similar procedures that are designed ad hoc for particular process are not versatile, they can not be automated and, moreover, they require considerable amount of time and engineering effort which might complicate the real-life deployment of the whole concept.

A proper way in case of closed-loop identification of an MPC-controlled system might be to use the direct identification method ignoring the presence of the input-noise correlation and rather focus on the second problem causing that the identification methods fail with closed-loop data—(in)sufficient excitation of the data. Here, one should realize that both bottlenecks (insufficient data excitation and input-noise correlation) are strongly related and therefore, correlation between noise and inputs can be significantly reduced making the input signal "sufficiently rich" (the data are much more excited) and in this way, the inaccuracy of the closed-loop estimates can be remedied [Forssell and Ljung, 1998].

A noteworthy and promising concept is the one that makes use of the controller itself to execute a kind of closed-loop identification experiment during the course of operation of the system in order to gather more information about the process and help the subsequent identification. A straightforward way to improve MPC closed-loop data informativeness is to add a constraint that guarantees persistence of excitation of the input calculated by the controller. To be more specific, this means that the MPC cost function is extended with such additional term that the persistent excitation condition [Bitmead, 1984] is satisfied.

A simple and intuitive way of incorporating the persistent excitation condition into the standard MPC formulation[1] is to add it directly as an additional constraint, an idea that was explained in [Shouche, 1996], [Genceli and Nikolaou, 1996] and [Shouche et al., 2002]. The authors of these works used an approximation of the information matrix with the outputs being omitted from the regressor. This approximation, unfortunately, does not ensure persistance of excitation in every direction and leads to biased estimates of those

---

[1]By standard MPC formulation, minimization of squares of the input effort and reference tracking error over the prediction horizon is meant.

parameters that correspond to the omitted outputs. Even with the mentioned approximation, the resulting optimization problem is still non-convex (thanks to the quadratic constraints), which is usually relaxed and solved as a semi-definite programming task.

An alternative solution was provided in [Aggelogiannaki and Sarimveis, 2006] where the approximation with just inputs being considered to affect the information matrix was adopted as well. Here, the authors used a two-stage procedure: in the first step, an optimal value for the data excitation level was obtained and in the second step, the MPC optimization problem with persistent excitation condition serving as an additional constraint was solved. This solution helped to ensure the optimization problem feasibility, the overall optimization problem was still non-convex similarly to the previous works, though.

Likewise, the authors of [Larsson et al., 2016] and [Larsson et al., 2013] added persistent excitation condition as a constraint to the original MPC optimization problem. Unlike the previous works, a full information matrix including also the system outputs was considered. To solve the underlying non-convex optimization task efficiently, several relaxations were utilized.

Yet another approach reported in [Marafioti et al., 2010] made use of the MPC with receding horizon. Following this paradigm, at each time step, only the first sample of the computed input sequence is applied and therefore, for certain class of the systems (e.g. finite input response models), it is possible to solve two quadratic programming problems instead of one semi-definite programming task. This approach, however, suffers from a few disadvantages caused by a cumbersome formulation of the problem since it does not consider the fact that the applied input influences the information brought by the future system outputs. Omitting the rest of the input sequence, the excitation is aggressive in several short "burst" segments and is effective in one direction only, which degrades the results of the original MPC formulation.

The work published in [Rathousky and Havlena, 2011] is also worth mentioning. The authors' approach consisted of a two-step procedure where in the first step, the classical MPC problem was solved. In the second one, the task of the maximization of the information matrix increase was solved such that the control performance did not deviate from the original MPC by more than a predefined threshold. Compared with the previous approaches, this one has one huge advantage: the tuning parameter corresponds to the allowed perturbation and its choice is thus much simpler than just choosing "the required" excitation level. The next indisputable advantage is the fact that with this formulation, the real information matrix increase is handled instead of its approximation, which enables

to optimize the excitation in the output directions as well. The optimization task solved in the second step is non-convex, though. Moreover, in their another publication [Rathousky and Havlena, 2013], the authors provided a so-called ellipsoid algorithm which offered an elegant way to solve this non-convex optimization task for low-order systems.

A considerable number of dual-MPC formulations have occured in the last several years. For example, [González et al., 2014], [Anderson et al., 2018] and others construct a target invariant set where the excitation is possible and thanks to this, both the stability of the closed-loop system and persistently exciting property of the input are ensured. [Heirung et al., 2013] incorporates also minimization of the future parameter error covariance into the original MPC cost function and [Bustos et al., 2016] provides a robust approach guaranteeing recursive feasibility of the MPC task on the one hand and uncorrelated inputs and outputs on the other hand. A self-reflective MPC formulation was proposed in [Feng and Houska, 2018] where the authors aimed at improving the accuracy of the state and parameter estimates by expanding the MPC formulation with a term quantifying how the impreciseness of their estimates influences the MPC performance.

Another way to ensure persistently excited data in an efficient manner without the need to execute costly experiments was described in [Larsson et al., 2011] and [Ebadat, 2017]. The main idea of the approaches described therein was to design input signal maximizing data informativeness while satisfying the MPC requirements. This can be realized either in an open-loop or in a closed-loop fashion. Usually, the solved optimization task consists in maximizing a chosen parameter related to the richness of the input signal subject to requirements of the original MPC, i.e. cost function and constraints. This optimization task is similar to the cases mentioned above: it is non-convex and various relaxations and approximations need to be employed, e.g. a graph-theory-based approach was used in [Ebadat et al., 2017]. While the previously mentioned publications considered mostly classic linear MPC and the identification of relatively simple linear models, several works [Lucia and Paulen, 2014], [Telen et al., 2016] take also presence of certain type of nonlinearity into account.

The author's contributions related to the MPC providing guarantees of persistence of excitation are scrutinizingly discussed in Chapter 5.

Chapter 3

Contributions

The main motivation of this thesis was the fact that although substantial progress in the area of model predictive control has been witnessed recently, still there is at least one aspect significantly complicating its serial deployment in the industry. This showstopper is the process of finding a proper mathematical model, an essential component of the framework, which still remains the most time-consuming and at the same time also the most challenging part of the predictive controller design.

The main goal of this thesis is to provide a methodology for obtaining the mathematical models in real life conditions in such a way that *i)* the identified models are appropriate for use with MPC (i.e. they have bounded complexity and attractive prediction behavior); and *ii)* considering economical, operational and time aspects, the whole identification process is as modest as possible.

The thesis contributions can be divided into the following two fields that can help to improve the procedure of the model identification for MPC and are closely related:

1. **Model predictive control relevant identification.** Extensions of the existing method for the minimization of the multistep prediction error were developed. These enhancements consist in adapting the method such that it can handle different linear state-space structures and even a broad class of nonlinear systems. The developed identification methods were tested also with data obtained from high-fidelity building models and data from real building operation. Some of the models were successfully used as predictors for MPCs operating as governors in several real buildings. A more detailed discussion of the contributions related to the model predictive control relevant identification is provided in Chapter 4.

2. **MPC with guaranteed persistent excitation.** Being another part of the research conducted within this thesis, a two-stage procedure for persistently exciting MPC problem was provided. In the first step of this procedure, an input sequence that is optimal in the sense of the original MPC cost function is computed. During the second stage, the data excitation quantified by the smallest eigenvalue of the information matrix increase is maximized such that the newly obtained control performance does not deviate from the original one (corresponding to the inputs calculated in the previous step) by more than a chosen threshold. Two methods solving the second-stage optimization task were presented in several publications: either *i)* a specific relaxation was used, or *ii)* a gradient-based optimization method was employed to handle the full non-convex optimization task. These methods were first developed for the standard MPC formulation (minimization of a weighted sum of squared input efforts and reference tracking errors over the whole prediction horizon) and were later extended for more complex MPC problems and model structures. A detailed description of this contribution can be found in Chapter 5.

Chapter 4

Model Predictive Control Relevant Identification

This chapter discusses the first contribution of the thesis (see Chapter 3). The main goal of this part of the research was to design a methodology for identification of models that would be optimal with respect to minimization of multistep prediction errors. The outcome of the underlying research can be divided into two parts: the first one presented in Chapter 4.1 pertains to MRI for linear systems and in the second part covered in Chapter 4.2, novel results related to identification of nonlinear systems are presented.

4.1 MRI for Linear Systems

Design of MRI identification methods based on direct minimization of the multistep prediction error represents one of the contributions of this work. The approach proposed in this thesis originated as an extension of [Lauri et al., 2010] and the adaptations standing for the partial contributions of this thesis can be summarized as follows:

- An algorithm for grey-box identification of mutli-input/multi-output state-space models performing minimization of the multistep prediction error was provided. Having added physical constraints on the model parameters, considerable *a apriori* information was brought to the identification procedure. The developed method was used for the identification of a simplified representation of a high-fidelity building model created in *Trnsys* software [Klein, 1988] and the obtained models were used as predictors for a linear and also for a switched-linear MPC for building climate control in [A.6] and [A.7].

- The same method was verified when a mathematical model of the building of Michigan Technological University was acquired. The available data came from real operation and on a series of simulations, the estimated model was tested as a predictor for an MPC manipulating the air-handling unit. Subsequently, the data gathered from the simulations employing the designed MPC were used to "teach" a feedback controller. More details including simulation results are available in [A.8].

- A method combining minimization of the multistep prediction error and partial least squares was utilized for identification of the building of the Czech Technical University in Prague (CTU). For the identification purposes, closed-loop data collected during real operation were exploited. A more detailed evaluation and discussion of the obtained results can be found in [A.9] and in Section 4.3 of [A.2].

- Models identified using the developed MRI identification algorithm were used in the role of internal system dynamics predictors for the MPC controlling the indoor temperature inside the CTU building. With the MPC controller involved, the energy consumption was decreased by more than 20 %. This part of the author's research is described in [A.10] and [A.11], respectively.

As the principal contribution related to the linear MRI identification, the process of identifying a set of mathematical models of a 4-floor office building in Hasselt (Belgium) can be designated. First of all, a linear model structure based on the RC-network modeling approach was proposed and subsequently, the parameters of the structure were estimated by a two-stage approach. At first, several one-step prediction error optimizing grey-box models were identified and then, the parameters from the first stage were used as initial estimates for the second stage during which multistep prediction errors were minimized. This procedure helped in remedying the otherwise significant computational complexity of the optimization of the multistep prediction error by making use of the qualified estimates from the first stage. Despite the questionable data quality, a complex model of the whole building with 8 outputs and 11 inputs could be identified in a very reasonable time with sufficient accuracy.

One of the obtained models was utilized together with MPC for the building climate control of the mentioned office building *in situ* in Haaselt. After the deployment of this model-based controller, about 20 % decrease of the energy consumption was reported [A.22]. The paper [A.3] published in *Applied Energy* goes into much more detail about the overall process of identification starting from data processing procedure and proceed-
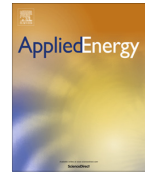
ing with model parameters estimation up to model selection and validation. Starting on the next page, the mentioned paper is presented in the original formatting.

Towards the real-life implementation of MPC for an office building: Identification issues

Eva Žáčeková [a,*], Zdeněk Váňa [a], Jiří Cigler [b]

[a] Department of Control Engineering, Faculty of Electrical Engineering, Czech Technical University in Prague, Czech Republic
[b] University Centre for Energy Efficient Buildings, Czech Technical University in Prague, Czech Republic

HIGHLIGHTS

- The paper describes the process of creation of an office building model for MPC.
- The complete process: the data collection and model acquisition is discussed.
- For parameters estimation, a special approach MPC relevant identification is used.

ARTICLE INFO

ABSTRACT

Modern control methods such as Model Predictive Control (MPC) are getting popular in recent years in many fields of industry. One of the branches that have witnessed great increase of interest in use of the MPC over the last few years is the building climate control area. According to the studies, the energy used in the building sector counts for 20–40% of the overall energy consumption. Almost half of this amount consists of heating, ventilation and air-conditioning (HVAC) costs which implies that energy consumption decrease in this area is one of the most interesting challenges today.

Besides enormous potential in reduction of energy consumed by heating, ventilation and air conditioning (HVAC) systems brought by such controller, it suffers from a bottleneck being the necessity of having a reliable mathematical model of the building at disposal. By finding a mathematical model appropriate for the MPC, it is meant to obtain such a model that is able to predict the behavior of the building sufficiently accurately for several hours ahead, which is an especially delicate task. This task is getting even more complicated in case of a real-life application.

In this paper, we are looking for a reliable model of a huge three-storey office building in Hasselt, Belgium. For parameter estimation, an advanced identification approach is used – its advantage is that it attacks the problem of minimization of multi-step prediction error and in this way, it corresponds to MPC requirements for a good multi-step predictor. Moreover, we discuss not only the identification approach itself but we also focus on accompanying problems with real-operation data acquisition, processing and special treatment which is an indispensable step for achieving satisfactory identification results. The chosen model is now used in real operation with MPC at Hollandsch Huys.

© 2014 Elsevier Ltd. All rights reserved.

1. Introduction

In the last years, significant emphasis on the energy savings can be observed – this effort is strongly supported by the strategy of the European Union called "20-20-20" [1]. This long-term strategy proposed for the whole Europe and lasting until year 2020 encourages the reduction of the greenhouse gases emission of 20%, the renewable energy sources should provide 20% of the consumed energy and also 20% reduction of the primary energy is expected. Out of the overall primary energy consumption, up to 40% is consumed in the building sector [2] and more than half of this energy is spent on heating/cooling of the building complexes. All these numbers are self-speaking and the necessity of search for the saving opportunities especially in the area of building climate control is more than evident. One of the very promising ways to achieve the savings is the use of advanced control techniques such as Model Predictive Control (MPC).

* Corresponding author. Address: Department of Control Engineering, Faculty of Electrical Engineering, Czech Technical University in Prague, Technická 2, 166 27 Praha 6, Czech Republic. Tel.: +420 2 243 57689.
E-mail addresses: eva.zacekova@fel.cvut.cz (E. Žáčeková), zdenek.vana@fel.cvut.cz (Z. Váňa), jiri.cigler@uceeb.cvut.cz (J. Cigler).

Although there is an intensive interest of academicians demonstrated by a huge number of publications on building climate control using MPC (see e.g. [3–10]), the number of applications of the predictive controller for control of real buildings is still very limited [11–14].

One of the possible reasons can be the fact that together with number of benefits and vast potential, the MPC brings also several drawbacks. The most crucial of them is the fact that for its proper functioning, MPC needs a mathematical model of the controlled system which should be able to predict the behavior of the system as accurately as possible as based on these predictions, MPC optimizes the input applied to the system.

While model creation is mentioned only marginally in majority of the academical works dealing with the MPC and these usually assume that the model of the system is either perfectly known or found in literature, the task is much more complicated and time consuming in case of real application – sometimes, it can be even more complex and involved than the controller design itself [15,16].

It has been already mentioned that the predictive controller makes use of the model of the controlled system to predict its future behavior over the prediction horizon. Therefore, the chosen model must be able to accurately predict the behavior of the system for sufficiently long time ahead. However, majority of the commonly used identification methods provide model optimized only in the sense of one-step ahead prediction error [17,18]. Predictions of such models are sufficiently accurate only for couple of steps ahead. Their multi-step predictions are usually not accurate enough which results in the suboptimal behavior of the MPC. The solution can be obtained by the use of the identification methods directly minimizing the multi-step prediction error being able to offer models with good multi-step predictions appropriate for the use within MPC. These approaches are collectively called Model Predictive Control Relevant Identification (MRI) methods [19–21].

The available literature offers several different approaches to handle the problem of multi-step prediction error minimization properly. The first sprouts are dated back to early 1990s – at that time, the authors of [20,19] proved the relevance of the multi-step prediction error minimization and pre-filtration of the input–output data using a noise-model-dependent filter with a subsequent use of one-step prediction error minimization. Due to the importance of the knowledge of process-noise-model, these methods have never been suitable for practical use. These works were later followed by [21–23]; the ideas were improved significantly but the results were still far from practical usability. A few years ago, the task of multi-step prediction error minimization was formulated as an optimization task in [24,25] and attractive properties of the results were shown in an example from chemical industry. The authors extended this method in [26,27] and they successfully used it for identification of the building model from real data.

Current paper describes a real-life application – therefore, we discuss not only the identification approach but we also focus on the accompanying problems as well. The typical situation when dealing with the real-operation data is that even though many variables might be measured, only a very limited number of them can be really exploited for identification purposes. This can be due to either inconvenient sensor placement or bad sensor conditions. These and similar issues appear in industrial applications very often and their solution demands as much attention as the problem of model identification – therefore, one of the objectives of this paper is to show how to improve the practical applicability of the theoretical concepts under real-life conditions and help them to overcome these difficulties.

The paper is organized as follows. Section 2 provides a description of Hollandsch Huys – the building of interest of this paper. In Section 3, the quality of the available data is discussed together with frequent sensor drop-outs as well as pre-filtration and other phenomena which are crucial for real-data identification. Section 4 deals with system identification itself, it describes the choice of model structure and the used identification algorithms. Section 5 summarizes the results of the proposed methods and discusses selection and validation of the resulting models. Finally, Section 6 concludes the paper.

2. Hollandsch Huys building – technical introduction

Hollandsch Huys (Fig. 1) is a large office building in Hasselt (Belgium) which is monitored and studied in the framework of the Geotabs project. This building consists of 5 floors: underground garages, 3 floors with occupied offices and an under-roof apartment. The area of each office floor is approximately 1500 m^2. The building itself is a light-façade (two main façades are oriented south-west and north-east). This building is equipped with triple glazing windows which are not directly on the surface of the façade but are retreated by 40 cm. Each of them is equipped with an external slat shading device that is retracted when there is no incident direct solar radiation and of which the slats angle is adjusted automatically to the solar position. The total window-to-wall ratio is 0.36.

Both the floors and the ceilings are equipped with so-called double layer thermally activated building systems (TABS) where water piping circuits are integrated into the concrete core itself, one circuit at the upper part of the concrete, the other deeper in the concrete. Each layer consists of four separate thermal circuits (Fig. 2 left) which can be controlled independently by two-way valves. The ground floor and the apartment are exceptions – both of them consist of floor-heating. Actual space distribution of the thermally activated building components can be seen in (Fig. 2 right).

A speciality of this building consists in a seasonal ground thermal energy storage – a storage effect is achieved using a series of closed-loop vertical heat exchangers. The bore field consists of 2 linear arrangements of 14 and 8 single *U*-tube ground heat exchangers at both sides of the building with a 75 m depth and approximately 5 m spacing in between. The heat and cold water for the TABS, the main air handling unit (AHU) and the floor heating on the ground floor are generated by a ground coupled heat pump (GCHP). It can operate in heating and active cooling mode, in which the GCHP is active. So-called "free cooling" or passive cooling is a third possible mode in which heat is injected into the ground through direct heat exchange between a brine and a cold storage tank. In addition to the heat pump system, two modulating gas-fired boilers are present in the building. One boiler with a rated thermal output of 35 kW provides heat to the heating coil of the apartment AHU and the apartment floor heating. The other boiler with a rated thermal output of 60 kW is a back-up heat production mainly for the AHU. All three office floors are equipped with VAV-boxes to control the ventilation air flow rate, except in the sanitary zones. The VAV-boxes are on/off controlled based on time schedules.

3. Data acquisition and processing

3.1. Process data acquisition

Design and application of advanced control techniques always require an interface between numerical tools and the building management system. There is a wide variety of such systems providing the users with a Matlab data acquisition tool usually realized by Matlab OPC Toolbox,[1] Matlab Database Toolbox or

---

[1] OPC Toolbox provides a connection to OPC DA and OPC HDA servers, giving you access to live and historical OPC data directly from MATLAB.
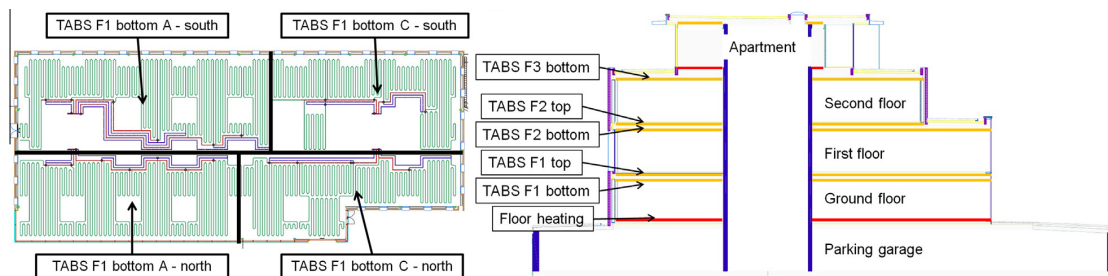
Fig. 1. Hollandsch Huys building.

Fig. 2. Hollandsch Huys building – heating circuits and scheme of TABS components. *A*, *C* labels in description of pipes stand for marking the shaft with main water piping (it was taken from the project, marking as east and west could serve as well). Red and blue colors mark supply and return pipes, respectively, the green pipes are heating coils. (For interpretation of the references to color in this figure legend, the reader is referred to the web version of this article.)

possibly by a different software tool/driver. In this paper, we consider the RcWare building control and management system [28] for process data acquisition in any desired form necessary for analysis and subsequent system identification and validation.

3.2. Measured variables and disturbances

As mentioned in Section 1, TABS is the main exchanger of thermal energy between the thermal medium and the zone. Each TABS contains four heating circuits (Fig. 2), each equipped with a pump ensuring constant nominal mass flow rates through the particular heating circuit. The mass flow rate within each heating circuit can then be controlled independently through the position of the particular valve. One can therefore obtain particular mass flow rates by measuring the positions of valves only. Further measured variables on the Hollandsch Huys follows, Table 1 offers an overview of all measurements. As long as Hollandsh-Huys being a multi-storey administrative building contains more than 80 sensors, it is practically impossible to provide the readers with figures showing exact position of each of them.

- Supply water temperatures (°C) – There are 2 main distribution circuits. One supplies all TABS and the second one delivers the water into the floor heating on the ground floor only. The main reason is that the ground floor is used as a clinic, so its thermal requirements have to be met (to a certain extent) independently of the rest of the building.
- Return water temperatures (°C) – These temperatures are measured at the end of each circuit in the shaft where all pipes from the corresponding heating circuit are collected.
- Concrete core temperatures (°C) – There are as many sensors as heating circuits, one sensor per each circuit. The sensors are placed several centimeters deep in the concrete core.
- Zone air temperatures (°C) – As the heating circuits geometrically split the building into 12 possible zones, each zone was supposed to have at least one temperature sensor. Due to the original control strategy, there are more sensors in the building whilst the above mentioned requirement is satisfied. Graphical depiction of the location of the zone temperature sensors can be found online at https://provoz.rcware.eu:9998/geotabs_hollandsch_huys (username "geotabs", password "hasselt").

Table 1
Table of measured variables.

Measured variables (units)	Number of measurements			Sensitivity
	Total # of sensors	Usable in Spring 2012	Usable in Winter 2012	
Concrete core (°C)	20	12	16	0.1 °C
Zone air (°C)	25	17	15	0.1 °C
Return water (°C)	21	8	8	0.1 °C
Valve position (%)	20	20	20	–
Supply water (°C)	2	2	2	0.1 °C

Except of the measured variables, it was necessary to obtain predictions of disturbances. In the case of Hollandsch Huys building, long-term predictions of the following disturbance variables were at disposal and therefore could be used as additional (uncontrolled) inputs:

- Outside air temperature (°C) – Here, weather forecast provided by NOAA agency[2] for the corresponding area was employed.
- Global solar radiation (W m^{-2}) – Forecast of global solar radiation on horizontal surface provided by NOAA agency was used.
- Occupancy and internal gain profile (W m^{-2}) – This merged disturbance variable covers heating power emitted by occupants, computers and lights. Hollandsch Huys is an office building where different floors are occupied by different companies and therefore, the "occupancy schedule" varies a lot over the day from zone to zone. The typical profiles were created based on the information provided by the building owner and personal investigation.

The last two disturbances were normalized by the area of the particular zone for the identification purposes. It should be noticed that all significant disturbances were measured/predicted and incorporated into the identification procedure as the (uncontrollable) inputs acting on the building.

Despite the fact that quite a wide range of the available measurements were at disposal, many of them turned out to be unusable. Some sensors were showing unreasonable (constant, physically impossible or saturated) values over a long period and, moreover, several concrete core temperature sensors were short-circuited. Several measurements of the return water temperatures were quite problematic as well mainly due to the improper sensors placement. Namely, these return water temperatures were measured in a shaft where both supply and return water pipes are placed one next to the other. This caused that the measured temperatures were strongly affected by each other. Table 1 also shows the number of measurements that were at disposal during Spring 2012 and after a general revision and replacement/maintenance of several wrong sensors during Winter 2012.

3.3. Data pre-processing

The main challenge after the data acquisition is the fact that some of available measurements were of such low quality that they were not suitable for the identification procedure at all.

Measured values are quantified with certain sensitivity which can consequently cause some difficulties with the direct utilization within the system identification. Let us illustrate the problem on an example from a real office building. The zone temperature is measured by Pt1000 sensor with sensitivity of 0.1 °C, so the temperatures between 23.05 °C and 23.15 °C are quantified as 23.1 °C. If the real temperature varies closely around 23.05 °C, undesirable oscillations of the measured value between 23.0 °C and 23.1 °C occurs. Additionally, the hysteresis of the sensor can make it more significant. Such phenomena significantly increase the high frequency portion of the signal which can in turn decrease the quality of the model.

Fig. 3 demonstrate the problem. The light blue range determined mostly by the sensitivity[3] of the sensor is drawn around the dark blue measured value. The real temperature can thus lie anywhere within that range. This enables the user to approximate the measurement and therefore offers possibility to suppress the

undesired fast oscillations. The simplest approximation that eliminates the oscillations is a piece-wise affine approximation which changes only when necessary (red line in Fig. 3 left). However, the temperature (as a physical quantity) is expected to change smoothly. Therefore, except of the oscillations suppression, one should enforce the smoothness of the signal with respect to the real measurements and expected dynamics of the measured quantity as well. Such example is depicted in Fig. 3 right. Smooth approximation need not to lie fully within the light blue range, however (if performed appropriately), the error is insignificant and can be attributed to the measurement noise. For example in Fig. 3 right, the quantification of this error ends up in more than 98% of the data points with the absolute error lower than 0.01 °C (10% of sensitivity of the sensor) and the maximum approximation error of 0.06 °C.

4. Building modeling and identification

4.1. Model structure

Since the main objective of the MPC in the Hollandsch Huys building is to control the zone temperature, the model suitable for control has to have zone temperatures as outputs. In [29], making a black box model of building for control purposes was reasoned as not so good approach since it usually spoils the real system structure. Therefore, Grey box (GB) approach exploiting the model structure was decided to be used. Based on the thermodynamic laws, one can come up with the following general equation [30] describing time derivative of the temperature of interest:

$$C_k \dot{T}_k = \sum_i \frac{(T_i - T_k)}{R_{i,k}} + \sum_j \dot{Q}_j, \tag{1}$$

where i stands for the ith source of temperature T_i, j stands for the jth source of heat flux $\dot{Q}_j$, T_k and C_k are measured temperature and heat capacity of the entity of interest, respectively, and $R_{i,k}$ is the thermal resistance of the mass between measurement points of T_i and T_k. $\dot{Q}_j$ are usually those heat fluxes which cannot be expressed as linearly weighted difference of two temperatures. Moreover, they can include some type of nonlinearity, e.g. heat flux caused by radiation. Constants $R_{i,k}$ can have different physical meanings depending on the considered ways of heat transfer. A detailed thermodynamic RC network model of a zone is depicted in Fig. 4.

Very important task related to the model structure in our case is how to compute the energy delivered to the zone by the supply water. Section 3.2 mentioned that the return water temperature measurements were mostly unreliable, therefore we decided to approximate the heat delivered into the jth zone as $\dot{Q}_{f/c,j} \approx \dot{m}_{j,spec} p_j c_w (T_{SW} - T_{f/c,j})$, where $\dot{m}_{j,spec}$, $T_{f/c,j}$ and p_j are meant to be the specific mass flow rate, floor/ceiling core temperature and the valve position, all corresponding to the jth zone. T_{SW} represents supply water temperature and c_w stands for the specific heat of water flowing in pipes.

To put the way of estimation (return water temperature vs. concrete core temperature) straight, it should be mentioned that this estimation was based on the analysis performed on the available data – for several zones, both the return water temperature and concrete core temperature measurements were at disposal (for more information, see Table 1) and the differences between them were negligible. Moreover, the concrete temperature sensors were placed deeply in the concrete core only several centimeters from the water piping (they were always placed near the place where the piping exits particular zone) and therefore, it can be expected that the dynamic behaviors of these two (return water and concrete core) temperatures are almost the same.

A general zoning was considered so far and the particular zoning of the Hollandsch Huys building follows. At first, the model had
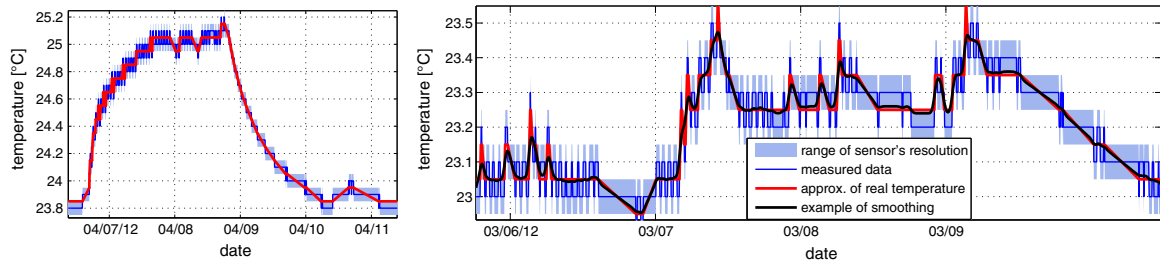
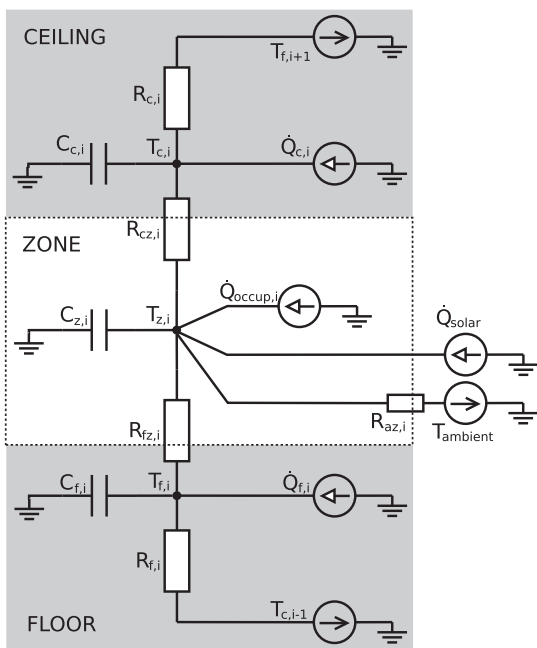**Fig. 3.** Realistic approximation of the measured data.

Fig. 4. RC network of 1 zone. Subscripts f, z, c stand for floor, zone, ceiling, respectively, and subscript i stand for number of floor. T stands for temperature (analogous to voltage) and $\dot{Q}$ stands for heat flux (analogous to electric current). The sources represent constant temperature and constant heat flux sources.

been intended to contain one zone per each heating circuit, i.e. 12 zones in total. Nevertheless, due to an inadequate complexity of such model (in this configuration, the model would have had 25 outputs and approximately 30 inputs) and mainly due to missing or unreliable measurements, the intended zoning had to be changed. Current model represents each floor as a single zone and takes into account 8 outputs (3 zone air temperatures and 5 temperatures of TABS), 6 manipulated variables (temperature of supply water delivered into the ground floor and heat fluxes delivered to the TABS) and 5 disturbance variables (1 ambient temperature, 1 solar radiation and 3 internal loads).

For the sake of completeness, let us note that the zoning with one zone representing the entire floor was chosen mainly because of the lack of quality and accurate measurements (see Table 1). However, besides the considerable simplification, it brings also some problems with dissimilarity of temperatures in the particular building zone. The main problem which could be caused by such zoning is the fact that in this configuration, an undesired situation can occur when certain part of the floor is underheated while some

other can be overheated. This was treated by the design of the low level controller which was implemented in such a way that the temperature distribution over the particular floor was balanced.

4.2. Identification approaches

The aim of the following text is to describe the estimation of the parameters of the model structure which is described in Section 4.1. As was told at the beginning of this paper, the proper methods to obtain a model suitable for MPC are the MRI identification methods.

In the literature, these methods were tested on a wide variety of theoretical examples and the ability to outperform the traditional methods minimizing the one-step prediction error was shown (see e.g. [25,21,20]). One of the approaches is to formulate the minimization of the multi-step prediction error as an optimization task [24,25]. These methods were used by the authors of this paper for identification of a building model for MPC in [31,26] where it was also demonstrated that the minimization of multi-step prediction error can significantly improve the quality of the model not only in case of theoretical systems but in case of real application as well.

However, this optimization task is non-convex and therefore it is necessary to find a good initial guess. To accomplish this, we formulated a two stage identification procedure which consisted of the search for the initial guess being the first step and the estimation of the parameters of the final model being the second step.

Note that based on the model structure, to obtain model parameters using the first principle method seems to be an apparent approach. Nevertheless, such an estimation of unknown parameters is not easy from several reasons. The zone thermal capacity covers not only the inner air but the zone equipment together with eventual interior walls as well. Next, the orientation of the TABS with respect to the position of the sensor (see Fig. 4) is not known, thus all thermal resistances as well as the TABS heat capacities are cumbersome to obtain. Additionally, the knowledge of the construction composition is necessary which is not always available. All above mentioned reasons together with comfort of parameters identification from the measured data resulted in definite choice for system identification. On the other hand, we admit that experienced user can estimate the model parameters reliably and sufficiently accurately, however, we believe that data driven modeling always reaches higher model precision and, furthermore, the user can involve aging and evolution of the model into the whole identification process.

4.2.1. First step – GB as an initial model estimate

Consider that the true system is a linear, time invariant system, that all outputs are also the state variables and that all of them are measured. The discrete formulation of such a system is

$$x_{k+1} = Ax_k + Bu_k + e_k, \tag{2}$$

where k is the discrete time, $x \in \mathbb{R}^n, u \in \mathbb{R}^m, e \in \mathbb{R}^n$ are system state (or output), input and measurement noise vectors, respectively. A and B are system matrices of appropriate dimensions. For the time line, it can be written as

$$
\begin{aligned}
X_1^N &= AX_0^{N-1} + BU_0^{N-1} + E_0^{N-1}, \\
X_1^N &= [A \quad B]\begin{bmatrix} X_0^{N-1} \\ U_0^{N-1} \end{bmatrix} + E_0^{N-1},
\end{aligned} \tag{3}
$$

with $N + 1$ being the number of samples and $X_k^{k+N-1}, U_k^{k+N-1}, E_k^{k+N-1}$ being the matrices of state, input and noise values defined as follows

$$
\begin{aligned}
X_k^{k+N-1} &= [x_k \quad x_{k+1} \quad \ldots \quad x_{k+N-1}] \\
U_k^{k+N-1} &= [u_k \quad u_{k+1} \quad \ldots \quad u_{k+N-1}] \\
E_k^{k+N-1} &= [e_k \quad e_{k+1} \quad \ldots \quad e_{k+N-1}].
\end{aligned} \tag{4}
$$

Eq. (3) can be rewritten as

$$
vecX_1^N = \left(\begin{bmatrix} X_0^{N-1} \\ U_0^{N-1} \end{bmatrix} \otimes I_n \right)^T vec[A \quad B] + vecE_0^{N-1} \tag{5}
$$

with I_n being $n \times n$ identity matrix, n represents system order, $(vec\bullet)$ is vectorization of a matrix and $(\bullet \otimes \bullet)$ is the Kronecker product. The deterministic model of considered system is $x_{k+1} = \widehat{A}x_k + \widehat{B}u_k$ and its structure is determined by linear differential equations in Eq. (1) written for each considered zone and discretized using Euler's discretization [32], which preserves the structure of the matrices A, B. When writing the model structure, one can see that only some of elements of matrices $\widehat{A}, \widehat{B}$ are to be found while the others are zero, which is the point where the strength of the vectorization comes up. Moreover, other none-zero elements can be constrained as well, usually in order to satisfy physical presumptions or demand on the stability. Let $\mathcal{S}$ stand for the model structure including both the structure and constraints and let $\mathcal{A}(\mathcal{S}), \mathcal{B}(\mathcal{S})$ be sets of all matrices $\widehat{A}, \widehat{B}$ with the structure $\mathcal{S}$. Then one-step ahead prediction error is written as follows [18].

$$
vecX_1^N - vec\widehat{X}_1^N = vecX_1^N - \left(\begin{bmatrix} X_0^{N-1} \\ U_0^{N-1} \end{bmatrix} \otimes I_n \right)^T vec\begin{bmatrix} \widehat{A} & \widehat{B} \end{bmatrix}
$$

and the unknown structured model matrices $\widehat{A}, \widehat{B}$ can be estimated via quadratic programming as

$$
\widehat{A}, \widehat{B} = \arg\min_{\widehat{A}, \widehat{B}} \left\| vecX_1^N - \left(\begin{bmatrix} X_0^{N-1} \\ U_0^{N-1} \end{bmatrix} \otimes I_n \right)^T vec\begin{bmatrix} \widehat{A} & \widehat{B} \end{bmatrix} \right\|_2^2
$$

subject to : $\widehat{A} \in \mathcal{A}(\mathcal{S}),$
$\widehat{B} \in \mathcal{B}(\mathcal{S}).$

4.2.2. Second step – model predictive control relevant identification

In the second step, the estimates from the first step are used as the initial conditions. Let us consider a cost function corresponding to minimization of the multi-step prediction error over the whole prediction horizon [24]

$$
J_{MRI} = \sum_{k=0}^{N-P} \sum_{i=1}^{P} [y(k+i) - \hat{y}(k+i|k)]^2, \tag{6}
$$

$\hat{y}(k+i|k)$ is the i-step output prediction created from data up to time k, N corresponds to the number of samples and P $(P < N)$ stands for prediction horizon considered in identification. The multi-step output prediction can be expressed as

$$
\hat{y}(k+i|k) = Z(k+i)\hat{\theta}, \quad i \in 1, 2, \ldots, P, \tag{7}
$$

where regressor $Z(l) = [u(l-n_d), \ldots, u(l-n_b), y(l-1), \ldots, y(l-n_a)]$ and $\hat{\theta} = [\hat{b}_{n_d}, \ldots, \hat{b}_{n_b}, \hat{a}_1, \ldots, \hat{a}_{n_a}]^T$. n_a denotes the number of past outputs in the regressor, n_b is the number of inputs in the regressor and n_d represents their delay compared to the outputs. Note that having all the states at disposal and $n_a = n_b = 1$ (which holds for the above-mentioned GB identification), there exists a direct transformation between θ and matrices $A, B : \theta = [B \quad A]^T$.

It is important to note that not every output contained in regressor $Z(k+i)$ is available at time k, thus the multi-step predictions $y(k+i|i)$ must be obtained recursively by applying i-times the expression $\hat{y}(k+1|k) = Z(k+1)\hat{\theta}$ with initial conditions y_k. Now, the estimate of matrix of parameters $\hat{\theta}$ can be obtained as a solution of the following optimization task:

$$
\hat{\theta}^* = \arg\min_{\theta} \sum_{i=1}^{P} \sum_{k=0}^{N-i} [y(k+i) - Z(k+i,\theta)\theta]^2 \tag{8}
$$

subject to : $\theta_0 = \begin{bmatrix} \widehat{B} & \widehat{A} \end{bmatrix}^T,$
$\theta \in \theta(\mathcal{S}),$

where $\theta(\mathcal{S})$ is set of all matrices $[B \quad A]^T$ with $A \in \mathcal{A}(\mathcal{S}), B \in \mathcal{B}(\mathcal{S})$. Matrices $\widehat{A}$ and $\widehat{B}$ were obtained by Grey box identification in Section 4.2.1.

As the regressor Z from Eq. (8) depends on the optimized parameters θ, the optimization task is nonlinear in parameters and must be solved by a proper algorithm of nonlinear optimization. In our case, the optimization based on Levenberg–Marquardt algorithm was used [33]. It is very important to choose a suitable initial condition for the parameter vector θ_0, which, in our case, was obtained from the first step of the algorithm.

5. Model selection and verification

In this section, we evaluate the results achieved applying the procedures described in the previous sections on the available data.

The ultimate objective of the Geotabs[4] project was the H.H. building to be controlled by MPC by the beginning of the heating season 2012/2013. First attempts on modeling and identification were made as soon as possible at the beginning of 2012 despite the disastrous sensors conditions. As can be found in Table 1, only about half of all needed measurements were at disposal for identification purposes. Besides this, we needed to deal with poorly excited data – H.H. is an administrative building where the temperature is kept by the original controller at a certain pre-set reference, and therefore, the available data were not very rich in information. Moreover, they were correlated (AHU was turned on at the occupants arrival) and so the first identification attempts failed. A long-term identification experiment could not come into consideration due to both high energy consumption increase and the fact that the building is used permanently over the whole year, which means that thermal comfort has to be guaranteed continuously. Therefore, 3 days during the Easter period (when the building was not occupied) were used for a simple and energy non-demanding experiment. At the beginning of the Easter holidays, all valves were closed and the AHU was turned on (temperature and mass flow rate of supply air were chosen as in normal operation). During the second part, the AHU was shut down and the valves and supply water were set to normal regime.

Having performed this short experiment, identification attempts were made. The available data were divided into 4 identification sequences ($I-IV$, a more detailed description is available in Table 2), prepared as described in Section 3 and re-sampled with

---

[4] http://www.geotabs.eu/.

Table 2
Datasets for identification.

Dataset	First identification				Second identification			
	From	To	# Days	# Samples	From	To	# Days	# Samples
I	02/25/2012	03/11/2012	15	720	11/15/2012	12/02/2012	18	864
II	03/12/2012	03/25/2012	14	672	12/05/2012	12/20/2012	16	768
III	03/26/2012	09/04/2012	15	720	01/03/2013	01/15/2013	15	720
IV	05/04/2012	19/04/2012	13	624	–	–	–	–

the sampling period $T_s = 30$ min. Having prepared the data for the identification, GB models were identified first and they were used for subsequent MRI identification, where several models were identified assuming various identification prediction horizons P. Let us note that the analysis of the building performance for various identification prediction horizons is highly important and as shown in [21], the prediction horizon for the identification chosen to be equal to the prediction horizon of the MPC itself might not be the best choice (this phenomena will be discussed later in detail). GB model identified using data set *III* was used because it was the only GB model showing reliable predictions for the 1st and the 2nd floor.

From this set of the identified models, the most suitable model for the control was needed to be chosen. As the model was intended to be used within the MPC strategy, one of the criteria was the accuracy of the predictions over the prediction horizon of the MPC – this was quantified as the root mean square error *RMSE* applied to the multi-step predictions:

$$RMSE = \sqrt{\frac{1}{(N-P)P} \sum_{k=0}^{N-P} \sum_{i=1}^{P} [y(k+i) - \hat{y}(k+i|k)]^2} \qquad (9)$$

where N is the number of samples of verification data. We chose prediction horizon of the MPC as $P = 96$ samples which with the sampling period $T_s = 30$ min corresponds to two days. In the role of the verification data, all the available data were used except of the sequence which was used for the identification of the model.

However, for a properly designed identification method, the main goal should not be to only have the smallest possible prediction error – it is much more important to have a physically reliable model at disposal. Even a model that is able to fit the measured profiles very satisfactorily can be physically unreliable. In case of use of such model in real operation, the controller performance can be unsatisfactory (e.g. with a negative coefficient corresponding to the input variable influence, the controller could try to heat up the building by using water of lower temperature than the temperature of the concrete/air). Such situation (*overfitting*) is more likely to occur in case that the model contains larger number of parameters (which basically means that the identification algorithm can "exploit" large number of degrees of freedom). This can be also the case of a real building identification and therefore, the risk of overfitting should not be underrated.

As long as the very important property which should be satisfied by the model for the MPC is to correspond to the physical nature of the controlled system, therefore the step responses were evaluated for each of the identified models. Here, it should be noted that only the first 2 days of the responses were of interest as the MPC does not take longer predictions into account. Furthermore, the relative influences of particular inputs were compared, e.g. a model predicting that the concrete core would be heated up faster by occupants than by hot water flowing through the pipes is inappropriate for the MPC. Similarly, models with oscillatory modes were considered undesirable.

The *RMSE* comparison of particular models can be found in Table 3(a) (in this table symbol ∞ means unstable model) which shows the prediction errors for all occupied floors – the ground floor, the 1st floor and the 2nd floor. The models which were

excluded due to unreasonable step responses are marked by red color. The models that were not identified are marked by ×.

It is obvious that the initial model identified using GB identification was unable to provide sufficiently accurate multi-step predictions, especially in the case of the ground floor temperature. Its predictions diversed from the real measurements and the model contained unstable mode describing the heat transfer from the floor heating to the ground floor zone temperature. On the other hand, the models obtained by MRI approach resulted in much more accurate prediction properties especially for the longer prediction horizons. In fact, all models obtained by MRI identification were not only able to predict the evolution of the ground floor zone temperature quite accurately (here, the GB model failed) but a significant improvement can be noticed in case of the 1st and the 2nd floor as well. While the mean prediction error (Eq. (9)) of the GB model was 0.5 °C for the 1st floor and 0.42 °C for the 2nd floor, using MRI this error was reduced to 0.17 °C and 0.31 °C, respectively. Let us note that these and all other RMSEs were calculated using validation data gathered from the real operation where the outputs stayed within 21−24 °C range. This can be seen in Figs. 6 and 7 showing part of the validation sets. Improved prediction ability of the models identified by MRI methods is demonstrated also by Fig. 5 showing two-days prediction errors[5] of various models depending on the data set used for the identification and the choice of the identification prediction horizon P.

Most of the MRI models successfully passed the step response test and their step responses appeared to be much closer to the behavior of the real building – no oscillatory or unstable modes were observed and the time constants corresponded to the character of the building. It can be also noticed that the models corresponding to the data sets *III* and *IV* clearly provided more accurate predictions than the others since both of these sets contained data from the Easter experiment. The fact that the predictions of the models identified from the mentioned data sets were more accurate can be observed also looking at Fig. 5. In case of identification data sets *III* and *IV*, darker color representing lower *RMSE* can be seen. This demonstrates that even a simple, economically and operationally non-demanding heating up and cooling down test (which was performed during the Easter holidays) can help to improve the identification significantly and leads to obtaining a better model.

Finally, the model providing the most accurate predictions and showing physically reasonable step responses was chosen to be used within the MPC. The comparison of the predictions of this model with the real data[6] is shown at Fig. 6. It can be argued that the models for longer horizons (up to the MPC prediction horizon) should have been identified (due to the expected improvement in the model accuracy). However, from certain value of the prediction

---

[5] The darker the color, the lower the *RMSE*. The errors in °C are visualized by the colorbar on the right side. The white fields express that the model could not be identified.

[6] Two-days predictions in this case mean that in time 0, $\hat{y}(\text{twodays}|0)$ and $y(\text{twodays})$ are depicted while in time 1, $\hat{y}(\text{twodays}+1|1)$ and $y(\text{twodays}+1)$ are shown, etc. As long as the MPC works with prediction horizon corresponding to two days, this comparison shows the worst-case accuracy of the predictions used by the MPC.

Table 3
Mean multi-step prediction error *RMSE* (°C). MRI$_m$ means that MRI with $P = m$ was used.

Data set floor	I			II			III			IV		
	0	1	2	0	1	2	0	1	2	0	1	2
(a) Results from the first (Spring) identification												
GB	∞	∞	∞	∞	∞	∞	∞	0.50	0.42	∞	∞	∞
MRI$_{10}$	0.63	0.43	1.15	0.29	0.18	0.32	×	×	×	×	×	×
MRI$_{20}$	0.34	0.26	0.43	0.28	0.19	0.29	0.27	0.20	0.31	0.27	0.20	0.31
MRI$_{40}$	0.45	0.32	0.74	0.29	0.19	0.29	0.31	0.22	0.40	0.34	0.18	0.26
MRI$_{60}$	×	×	×	×	×	×	0.27	0.18	0.31	0.27	0.18	0.37

Data set floor	I			II			III		
	0	1	2	0	1	2	0	1	2
(b) Results from the second (Winter) identification									
GB	0.25	0.16	0.26	0.23	0.17	0.26	0.24	0.21	0.27
MRI$_{10}$	0.23	0.16	0.27	0.18	0.15	0.25	0.19	0.18	0.27
MRI$_{20}$	0.25	0.17	0.27	0.19	0.14	0.25	0.19	0.18	0.27
MRI$_{40}$	0.24	0.18	0.26	0.19	0.14	0.27	0.19	0.13	0.26
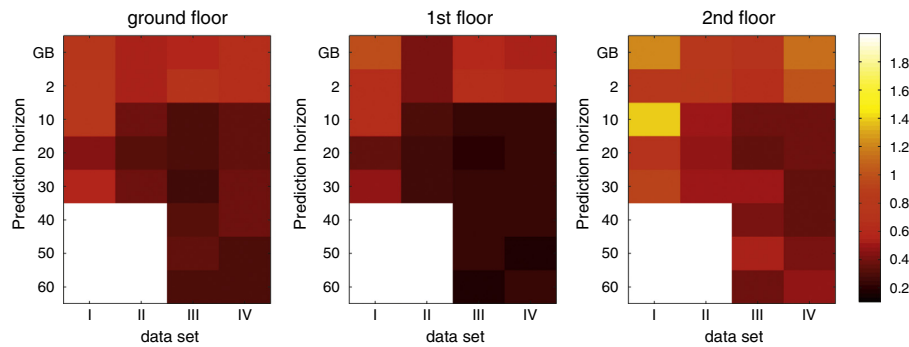
Fig. 5. Comparison of *RMSE*.
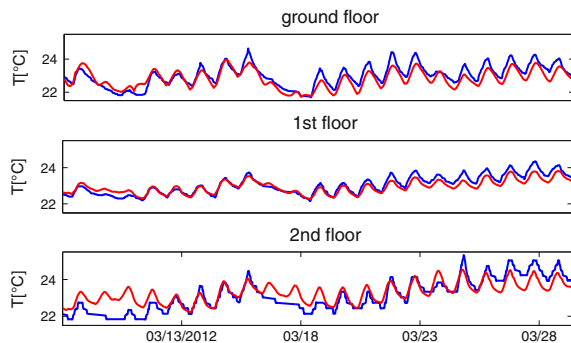
Fig. 6. Comparison of 2 days room temperatures predictions (blue line – real data, red line – model predictions) – the first (spring) identification. (For interpretation of the references to color in this figure legend, the reader is referred to the web version of this article.)

horizon *P*, the quality of the model improves only a little (which is supported by the Table 3(a) while the computational complexity increases, therefore the MRI algorithm had not to be executed for higher prediction horizons. More detailed analysis of this problem can be found in [21].

As was already mentioned, during Winter 2012, maintenance of several sensors was performed and since then, more measurements were available which resulted in the effort to re-identify the current model. For this purpose, new extensive identification Christmas holiday experiment was designed. Unfortunately, due to a database failure on the side of the company maintaining the

H.H. building, the data from this experiment were not stored into database and they could not be used for identification. The available 6-weeks data sequence was divided into three subsequences and several models were identified using these data sets. Similarly to the first Spring identification, *RMSE* properties and step responses computed from the whole data sequence were compared and chosen results are summarized in Table 3(b). One GB model was identified from each of the available identification data set *I–III* and model identified using data set *II* which appeared to be t he best was chosen as the initial model for MRI procedure. The decision to use this model as the initial one for the second stage was influenced not only by the fact that it showed slightly better prediction features (see Table 3(b)) but also the step responses of the model matched the expected behavior of the building.

As in the case of the first identification, it can be observed that the quality of the models depended significantly on the data set that had been used for the identification – the best model was identified from the data set *II* (not only these models had lower values of *RMSE* but also all the identified responses possessed reliable physical properties, none of the corresponding rows in the table is marked with red color).

This phenomena can be explained such that the data set *II* contained the days when the ambient temperature rose and dropped abruptly which resulted in the MPC heating up wildly and performing something like cool down experiment. This situation again confirms that also such a pseudo-experiment can help and improve the quality of the model significantly and therefore it yields better performance of the MPC. It is quite obvious that the new models performed much better (smaller prediction errors and more models corresponding to the physical nature of the H.H. building).
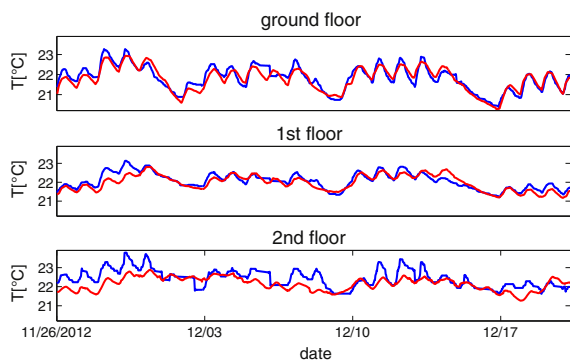
Fig. 7. Comparison of 2 days room temperatures predictions (blue line – real data, red line – model predictions) – the second (winter) identification. (For interpretation of the references to color in this figure legend, the reader is referred to the web version of this article.)

Moreover, it can be noticed that the least accurate predictions were provided for the 2nd floor where only 1 out of 5 installed sensors seemed to measure reliable values.

The next fact that can be found to be very interesting is that after the second identification, GB-identified models also performed quite satisfactorily and they predicted relatively accurately (for none of the models the mean prediction error exceeded $0.3\,°C$) and they successfully passed the step response test. MRI identification did not improve the prediction properties of these models significantly. This can be explained such that in case of the first identification attempts, only a very limited number of the concrete core temperature measurements (only 12 out of 20) were at disposal and it was hardly possible to quantify the delivered heat which resulted into considerable uncertainty into the identification process. Among the identified models, the model MRI_{40} identified from data set *II* was chosen and the comparison of its 2 day prediction are shown in Fig. 7.

This is related to what was shown in [20,19] in 90s that the minimization of the multi-step prediction error is equivalent to the pre-filtration of the input/output data by a noise model and subsequent "common" identification minimizing only one-step prediction error. MRI identification (unlike the GB identification) optimizes the model in the sense of the multi-step prediction error, it "can see" all the uncertainties and disturbances more clearly and deals with them in a better way which enables it to provide models of a higher quality even in case of poorly excited data.

6. Conclusions

In this paper, a very detailed description of the identification process of an office building intended to be controlled by the MPC is provided. Huge attention is paid not only to the estimation procedure itself but the data collection/pre-processing (and number of problems associated with that) and the choice of a model structure (which was quite restricted due to the faulty sensors) are discussed in details as well. These problems are often omitted in literature despite the fact that their solution demands at least as much effort as the identification itself. In this paper, MRI identification approach is used and it is shown that this kind of identification procedure is appropriate for real-life applications in case that the models for MPC are sought. The models obtained by MRI methods are (despite of poor quality of data) able to provide models that predict the zone temperature for 2 days ahead with a mean error approximately $0.3\,°C$ or less even in a situation that the GB minimizing one-step prediction error fails and provides unstable

models. This supports the claim that a properly chosen identification method can improve the overall behavior of the MPC and help to spare more energy.

The finally chosen model is now used in real operation with MPC at Hollandsch Huys and according to the comparison, this controller leads to 17% energy consumption reduction in average compared to the original control strategy [34,35].

References

[1] E.C.E. DG., Report on the implementation of the European charter for small enterprises: communication from the commission to the council and the European parliament, vol. 30, Office for Official Publications of the European Communities; 2005.

[2] Perez-Lombard L, Ortiz J, Pout C. A review on buildings energy consumption information. Energy Build 2008;40(3):394–8.

[3] Oldewurtel F, Gyalistras D, Gwerder M, Jones C, Parisio A, Stauch V, et al. Increasing energy efficiency in building climate control using weather forecasts and model predictive control. In: 10th REHVA world congress Clima, 9–12; 2010.

[4] Freire RZ, Oliveira GH, Mendes N. Predictive controllers for thermal comfort optimization and energy savings. Energy Buildings 2008;40(7):1353–65.

[5] Sourbron M, Verhelst C, Helsen L. Building models for model predictive control of office buildings with concrete core activation. J Build Perform Simul 2013;6(3):175–98.

[6] Cho S. Predictive control of intermittently operated radiant floor heating systems. Energy Convers Manage 2003;44(8):1333–42. http://dx.doi.org/10.1016/S0196-8904(02)00116-4. ISSN 01968904.

[7] Chen T. Application of adaptive predictive control to a floor heating system with a large thermal lag. Energy Build 2002;34(1):45–51. http://dx.doi.org/10.1016/S0378-7788(01)00076-7. ISSN 03787788.

[8] Oldewurtel F, Sturzenegger D, Morari M. Importance of occupancy information for building climate control. Appl Energy 2013;101:521–32.

[9] Wang N, Zhang J, Xia X. Desiccant wheel thermal performance modeling for indoor humidity optimal control. Appl Energy 2013;112:999–1005.

[10] Petersen S, Bundgaard KW. The effect of weather forecast uncertainty on a predictive control concept for building systems operation. Appl Energy 2014;116:311–21.

[11] Široký J, Oldewurtel F, Cigler J, Prívara S. Experimental analysis of model predictive control for an energy efficient building heating system. Appl Energy 2011;88(9):3079–87. http://dx.doi.org/10.1016/j.apenergy.2011.03.009. ISSN 0306-2619.

[12] Ma Y, Kelman A, Daly A, Borrelli F. Predictive control for energy efficient buildings with thermal storage: modeling, stimulation, and experiments. Control Syst, IEEE 2012;32(1):44–64.

[13] Ma Y, Borrelli F, Hencey B, Coffey B, Bengea S, Haves P. Model predictive control for the operation of building cooling systems. In: American Control Conference(ACC). IEEE; 2010. p. 5106–11.

[14] Castilla M, Álvarez J, Berenguel M, Rodríguez F, Guzmán J, Pérez M. A comparison of thermal comfort predictive control strategies. Energy Build 2011;43(10):2737–46. http://dx.doi.org/10.1016/j.enbuild.2011.06.030. ISSN 0378-7788.

[15] Zhu Y. Multivariable process identification for MPC: the asymptotic method and its applications. J Process Control 1998;8(2):101–15.

[16] Zhu Y. Multivariable system identification for process control. Elsevier; 2001.

[17] Ljung L. Prediction error estimation methods. Circuits, Syst Signal Process 2002;21(1):11–21.

[18] Ljung L. System identification. Wiley Online Library; 1999.

[19] Shook D, Mohtadi C, Shah S. Identification for long-range predictive control. In: Control theory and applications, IEE proceedings D, vol. 138, IET; 1991. p. 75–84.

[20] Shook DS, Mohtadi C, Shah SL. A control-relevant identification strategy for GPC. IEEE Trans Automat Control 1992;37(7):975–80.
[21] Gopaluni R, Patwardhan R, Shah S. MPC relevant identification—-tuning the noise model. J Process Control 2004;14(6):699–714.
[22] Rossiter J, Kouvaritakis B. Modelling and implicit modelling for predictive control. Int J Control 2001;74(11):1085–95.
[23] Huang B, Malhotra A, Tamayo EC. Model predictive control relevant identification and validation. Chem Eng Sci 2003;58(11):2389–401.
[24] Laurí D, Martínez M, Salcedo J, Sanchis J. PLS-based model predictive control relevant identification: PLS-PH algorithm. Chemometr Intell Lab Syst 2010;100(2):118–26. http://dx.doi.org/10.1016/j.chemolab.2009.11.008. ISSN 0169-7439.
[25] Laurí D, Salcedo J, Garcia-Nieto S, Martínez M. Model predictive control relevant identification: multiple input multiple output against multiple input single output. Control Theory Appl, IET 2010;4(9):1756–66.
[26] Prívara S, Cigler J, Váňa Z, Oldewurtel F, Žáčeková E. Use of partial least squares within the control relevant identification for buildings. Control Eng Pract 2013.
[27] Záceková E, Prívara S. Control relevant identification and predictive control of a building. In: Control and decision conference (CCDC), 2012 24th Chinese. IEEE; 2012. p. 246–51.
[28] Cigler J, Široký J, Kulvejt M, Chlupáč M, Gyalistras D. Web services based data acquisition from a process database. In: Proceedings of technical computing; 2011.
[29] Prívara S, Váňa Z, Žáčeková E, Cigler J. Building modeling: Selection of the most appropriate model for predictive control. Energy Build 2012.
[30] Barták M, Úvod do přenosových jevu pro inteligentní budovy, CTU Prague, Prague, Czech Republic; 2010.
[31] E. Z ác eková S. Prívara Z. Ván a Model predictive control relevant identification using partial least squares for building modeling. In: Australian control conference (AUCC). IEEE; 2011. p. 422–27.
[32] Franklin GF, Powell JD, Emami-Naeini A, Powell JD. Feedback control of dynamic systems, vol. 3. Reading, MA: Addison-Wesley; 1994.
[33] Bertsekas DP. Nonlinear programming.
[34] Cigler J. Problematika prediktivního řízení budov. <www.stpcr.cz/?download=_/sborinhob2013/13_cigler.pdf?>; 2013.
[35] Bockelmann F, Plesser S, Soldaty H. Advanced system design and operation of GEOTABS buildings. REHVA 2013. ISBN 978-2-930521-12-1.

26

4.2 MRI for Nonlinear Systems

While at the beginning of the millennium, mostly linear MPCs were discussed in the literature, during the last years, also *nonlinear* MPCs have gained popularity among the researchers. Implementing a nonlinear MPC, one can leverage the full potential of the predictive control concept since it uses a nonlinear internal model that is usually capable of predicting the future system responses more precisely and, moreover, it can optimize with respect to a nonlinear cost function enabling to cover a much broader and more general class of optimization tasks. Counting up all these aspects, a significant improvement in control performance can be expected. However, the available literature contains only few entries devoted to identification of nonlinear models using MRI approach and, moreover, these works focus just on certain classes of models.

In [A.4], two methods for MRI identification of nonlinear system models were provided. The first of them computes and optimizes multistep prediction errors of the whole nonlinear system while the second one adopts the following simplification. The parameters corresponding to the nonlinear part of the system model are optimized focusing only on one-step prediction error and just the linear part is identified such that the multistep prediction error is minimized. This simplification reduces the complexity of the underlying problem from general nonlinear optimization task to only polynomially nonlinear one thus alleviating the computational burden of the identification routine.

The publication [A.4] describing the aforementioned contributions is presented in the original formatting on the next page et seq. Here, it should be mentioned that the identification procedure is discussed mainly in Section 3 of this paper.

Contents lists available at ScienceDirect

Control Engineering Practice
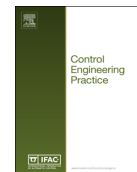
Bridging the gap between the linear and nonlinear predictive control: Adaptations for efficient building climate control

CrossMark

Matej Pčolka [a,*], Eva Žáčeková [a,*], Rush Robinett [b], Sergej Čelikovský [c], Michael Šebek [a]

[a] Department of Control Engineering, Faculty of Electrical Engineering, Czech Technical University in Prague, Technická 2, 166 27 Praha 6, Czech Republic
[b] Mechanical Engineering-Engineering Mechanics, Michigan Technological University, United States
[c] Institute of Information Theory and Automation, Czech Academy of Sciences, Czech Republic

A B S T R A C T

The linear model predictive control which is frequently used for building climate control benefits from the fact that the resulting optimization task is convex (thus easily and quickly solvable). On the other hand, the nonlinear model predictive control enables the use of a more detailed nonlinear model and it takes advantage of the fact that it addresses the optimization task more directly, however, it requires a more computationally complex algorithm for solving the non-convex optimization problem. In this paper, the gap between the linear and the nonlinear one is bridged by introducing a predictive controller with linear time-dependent model. Making use of linear time-dependent model of the building, the newly proposed controller obtains predictions which are closer to reality than those of linear time invariant model, however, the computational complexity is still kept low since the optimization task remains convex. The concept of linear time-dependent predictive controller is verified on a set of numerical experiments performed using a high fidelity model created in a building simulation environment and compared to the previously mentioned alternatives. Furthermore, the model for the nonlinear variant is identified using an adaptation of the existing model predictive control relevant identification method and the optimization algorithm for the nonlinear predictive controller is adapted such that it can handle also restrictions on discrete-valued nature of the manipulated variables. The presented comparisons show that the current adaptations lead to more efficient building climate control.

© 2016 Elsevier Ltd. All rights reserved.

1. Introduction

Presently, energy savings and reduction of energy consumption in buildings are some of the most challenging issues facing the engineering community. The reason is straightforward and the numbers speak for themselves – up to 40% of the total energy consumption can be owed to the building sector (Perez-Lombard, Ortiz, & Pout, 2008). More than half of this 40% is consumed by various building heating/cooling systems. Therefore, the recent significant emphasis on the energy savings in this area is right on target and can be observed in recent years. For example, the strategy of the European Union called "20–20–20" (European Economic & Social Committee, 2005) should be mentioned. Intended to be followed by all of Europe through the year 2020, this strategy aims at 20% reduction of the use of primary energy sources and production of the greenhouse gas emissions, and the

renewable energy sources are expected to provide 20% of the consumed energy. With the clearly evident need for savings in the area of the building climate control, improvements can be found when considering the latest control techniques.

Model Predictive Control (MPC) is one of the most promising candidates for an energetically efficient control strategy (Pčolka, Žáčeková, Robinett, Čelikovský, & Šebek, 2014a, 2014b). This was also demonstrated within the framework of the Opticontrol project. One research team at ETH Zurich (Switzerland) showed via numerous simulations that using MPC instead of the classical control strategies achieves more than 16% savings (Gyalistras & Gwerder, 2010; Oldewurtel et al., 2010) depending on the building type. If one considers real operational conditions, these savings can be even higher when the MPC is modified appropriately for the conditions. This was shown by teams from Prague (Prívara, Široký, Ferkl, & Cigler, 2011; Žáčeková & Prívara, 2012 and UC Berkeley (Ma, Kelman, Daly, & Borrelli, 2012) where the actual cost savings were even better than the theoretical expectations (27% and 25% reduction of the energy consumption, respectively).

However, MPC suffers from several drawbacks including the complexity of the optimization routine and the need for a reliable mathematical model of the building. In order to be feasible and

* Corresponding authors.
E-mail addresses: matej.pcolka@fel.cvut.cz (M. Pčolka),
eva.zacekova@fel.cvut.cz (E. Žáčeková), rdrobine@mtu.edu (R. Robinett),
celikovs@utia.cas.cz (S. Čelikovský), sebekm1@fel.cvut.cz (M. Šebek).

computable, simplified formulations are often considered. Moreover, linear models are usually assumed and exploited by the optimizer. Therefore, in the majority of the MPC applications, the overall task is formulated as a linear/convex optimization problem easily solvable by the commonly available solvers for quadratic or semidefinite programming (Verhelst, Degrauwe, Logist, Van Impe, & Helsen, 2012; Prívara et al., 2011). Although being computationally favorable and able to find the global minimum in case of the convex formulation of the optimization task, their disadvantage is that they do not enable minimization of the nonlinear/nonconvex cost criteria and therefore, only certain approximation of the real cost paid for the control is optimized. Moreover, they resort to the optimization of either the setpoints or the energy delivered to the heating/cooling system while leaving all its distribution to the suboptimal low-level controllers which can lead to a significant loss of the optimality gained by the MPC.

In several recent works, the effort to take the nonlinearities (caused either by the dynamical behavior of the building or by the control requirements formulation) into account within the optimization task can be found (Ma et al., 2012, 2011). In this paper, we discuss both possibilities for the zone temperature control (the linear and the nonlinear MPC) and moreover, we bridge the two banks of the gap between the nonlinear and the linear variant of the MPC by introducing linear model that changes in time. Such model can describe the building dynamics in a more reliable and flexible way than the original linear model while it still keeps the low complexity of the optimization task (since with the linear model, the optimization task to be solved remains convex). The way of obtaining a time-varying model is described and the results of the linear predictive controller with linear model that changes in time are compared with the results of the original (linear and nonlinear) MPCs.

It should be mentioned that a good predictive controller relies on a good system dynamics predictor and therefore, we focus on the identification of such reliable multi-step predictors as well. The MPC employs optimization over certain given prediction horizon and this fact should be taken into consideration also in the design of the identification procedure. Unlike the commonly used identification methods (PEM, Ljung, 1999) which provide models that are able to predict well only over short horizons, the methods based on minimization of multi-step prediction errors (MRI – model predictive control relevant identification, Laurí, Salcedo, Garcia-Nieto, & Martínez, 2010) offer models with more attractive prediction properties. Therefore, we exploit the MRI for identification of both linear and nonlinear models. While several published works deal with application of MRI for estimation of parameters of linear models (Chi, Fei, Zhao, Zhao, & Liang, 2014; Shook, Mohtadi, & Shah, 1991; Zhao, Zhu, & Patwardhan, 2014), no extension, to the best knowledge of the authors of this paper, has been provided for estimation of parameters of *nonlinear* models. Moreover, even the linear version of MRI in the literature is usually validated only on simple artificial examples. On the other hand, this paper presents application of both the linear and the newly proposed nonlinear MRI versions on much more complex and realistic example of building model identification.

Furthermore, a very important practical aspect of the building temperature control is addressed in this work as well. In real-life building applications, water pumps are a crucial part of the actuators used to manipulate the optimized input variables. These water pumps possess nonlinear output dynamics where the amount of mass flow rate which can be provided by the pump is often quantized. Therefore, the achievable water mass flow rates belong to a countable set of discrete values rather than to a continuous interval. The appropriately designed control algorithm should take this information properly into account. This can be performed in several ways: (1) mixed-integer programming

techniques can be employed, (2) additional postprocessing after the calculation of the optimal inputs can be applied, or (3) the (originally continuous-valued) optimization procedure itself can be adapted such that discrete-valued input profiles are obtained.

First of all, the mixed-integer programming approach is the most suitable one in case that one of the manipulated variables should belong to countable set of discrete values. However, the mixed-integer programming problems are known to be NP-hard (Bussieck & Vigerske, 2010; Lenstra, 1983; Pancanti, Leonardi, Pallottino, & Bicchi, 2002) and their solution using mixed-integer programming solvers requires massive computational power. Furthermore, the majority of reliable currently available mixed-integer solvers able to handle nonlinear system description/nonlinear optimization criterion are not free for industrial use. Since the computational burden caused by solving the mixed-integer programming task is huge and it is in direct opposite to the extensive effort to simplify the control schemes and systems used in buildings, this direction is not suitable. Instead of formulating the building temperature control problem as a mixed-integer programming task, the other two mentioned options (additional postprocessing and adaptation of the continuous-valued optimization procedure) are elaborated in the current paper.

The paper is organized as follows: Section 2 illustrates the problem of the building climate control on a simple example. Both the building and the heat delivery system description are provided. Furthermore, control performance criterion, comfort requirements and restrictions are introduced. In Section 3, the models supplying predictions to the model-based controllers are described. The nonlinear model is derived in Section 3.1 based on the thermodynamics while for the linear model, the assumed simplifications are presented in Section 3.2. The linear time-varying model is presented in Section 3.3. A new approach to estimating parameters of the nonlinear model with respect to the multi-step prediction error minimization criterion proposed in Section 3.4. Two alternative versions of this approach are presented which are some of the main contributions of this paper. All models are verified on the data set obtained from TRNSYS environment and their results are discussed. Section 4 describes the controllers including the low level re-calculation (for the linear MPC) and the nonlinear optimization routine (for the nonlinear MPC). In order to address the discrete-valued nature of part of the considered actuators, the nonlinear MPC optimization routine is changed in two ways: either a naive additional post-processing is employed or the *mid-processing* iteration (which is another main contribution of this paper) is incorporated into the routine. In Section 5, building behaviors of all proposed controllers are investigated and their results are presented and examined. Section 6 draws conclusion of the paper.

2. Problem formulation

In this section, the description of the building, constraints and the evaluative performance criterion are formulated.

2.1. Building of interest

The building under our investigation is a simple medium weight one-zone building modeled in the TRNSYS16 (University of Wisconsin-Madison, 1979) environment, which is a high fidelity simulation software package widely accepted by the civil engineering community as a reliable tool for simulating the building behavior.

The building considered in this paper is a medium sized one with a size of $5 \times 5 \times 3$ m and a single-glazed window (3.75 m^2) placed in the south-oriented wall. The Heating, Ventilation and Air
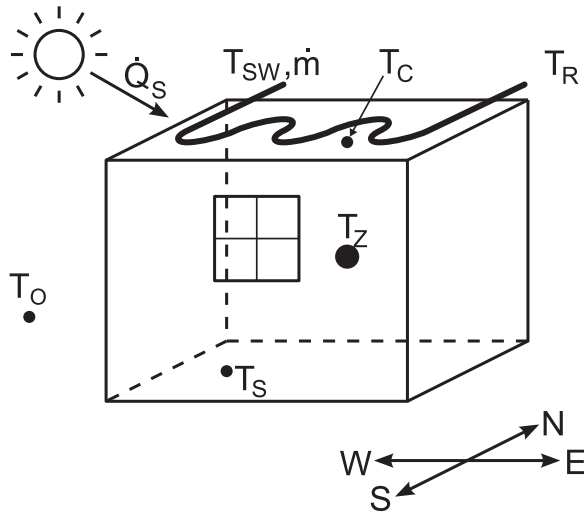
Fig. 1. A scheme of the modeled building.

Fig. 2. A scheme of heat distribution system.

Conditioning (HVAC) system used in the building is of the so-called active layer type. Technically, the HVAC system consists of TABS (thermally activated building system) – a set of metal pipes encapsulated into the ceiling distributing the supply water which then enables thermal exchange with the concrete core of the modeled building consequently heating the air in the room. This configuration corresponds to the commonly used building heating system in the Czech Republic. Ambient environmental conditions (ambient temperature, ambient air relative humidity, solar radiation intensity and others) are simulated using TRNSYS Type15 with the yearly weather profile corresponding to Prague, Czech Republic.

Fig. 1 shows a sketch of the building HVAC system configuration, the "building" variables and the environment variables. Regarding the building inner variables, four of them are considered to be available – zone temperature T_Z, ceiling temperature T_C, temperature of the return water T_R and temperature of the south-oriented wall T_S. From the environmental influences, solar radiation $\dot{Q}_S$ and outside-air temperature T_O are taken into account as disturbances while the supply water temperature T_{SW} and the mass flow rate of the supply water $\dot{m}$ are the controlled input variables. The TRNSYS model in this configuration offers a good numerical test-bed to compare the control approaches, and the results obtained with this model can be generalized without any loss of objectivity.

The next step is to describe the heat distribution system. In the application presented in this paper, the configuration of the heating system as shown in Fig. 2 is considered. Clearly, the storage tank plays a key role as the sole heat supplier in this system. In fact, having obtained the requirements for the supply water temperature T_{SW} and the supply water mass flow rate $\dot{m}$, these two values are "mixed" using the return water with the temperature T_R flowing into the building inlet pipe through the side-pipe at the mass flow rate $\dot{m}_s$ and the water from the storage tank which is kept at certain constant value T_{St} (in this paper, $T_{St} = 60\,^\circ\text{C}$ is considered) and can be withdrawn from the tank at mass flow rate $\dot{m}_{St}$. Based on this, the following set of equations can be written for the upper three-way valve:

$$\dot{m}T_{SW} = \dot{m}_{St}T_{St} + \dot{m}_S T_R$$
$$\dot{m} = \dot{m}_{St} + \dot{m}_S. \tag{1}$$

which can be further rewritten into an expression for the
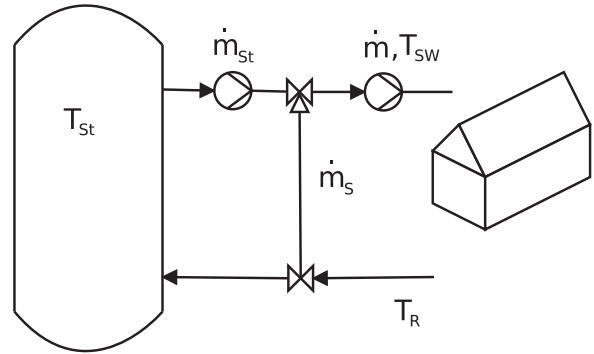
calculation of the storage water mass flow rate,

$$\dot{m}_{St} = \dot{m}\frac{(T_{SW} - T_R)}{(T_{St} - T_R)}. \tag{2}$$

Having the return water temperature values at disposal and extracting the storage water with the temperature of T_{St} at the mass flow rate $\dot{m}_{St}$, both the supply water temperature and supply water mass flow rate related to the heating requirements can be achieved.

2.2. Control performance requirements

Considering the building climate control, one of the most important tasks is to ensure the required thermal comfort which is specified by a pre-defined admissible range of temperatures related to the way of use of the building (office building, factory, residential building, etc.). Under the weather conditions of middle Europe with quite low average temperatures where heating is required for more than half of year, the thermal comfort satisfaction requirement can be further simplified such that the zone temperature is bounded only from below. Since an office building with regular time schedule is considered, the lowest admissible zone temperature $T_Z^{min}(t)$ whose violation will be penalized is defined as a function of working hours as

$$T_Z^{min}(t) = \begin{cases} 22\,^\circ\text{C} & \text{from 8 a. m. to 6 p. m.,} \\ 20\,^\circ\text{C} & \text{otherwise.} \end{cases} \tag{3}$$

Then, the thermal comfort violation is expressed as

$$CV(t) = \max(0, T_Z^{min}(t) - T_Z(t)). \tag{4}$$

Besides the comfort violation $CV(t)$, the price paid for the operation of the building is penalized in the cost criterion as well. Coming out of the considered structure of the building and its energy supply system, the monetary cost includes the price for the consumed hot water and the electricity needed to operate the two water pumps. While the hot water price P_W is considered constant (see Table 1), the electricity price $P_E(t)$ which applies to the operation of the supply and storage water pumps is piece-wise constant and similar to the lowest admissible zone temperature

Table 1
List of the specific parameters.

T_Z^{min} (°C)	22/20	P_W (−)	2.6199
HT (€/kWh)	0.1168	α_0 (−)	9
LT (€/kWh)	0.0502	α_1 (−)	9.25×10^{-3}
T_{St} (°C)	60	α_2 (−)	1.875×10^{-6}
$[\underline{\dot{m}}, \overline{\dot{m}}]$	[15,60]	ΔT (°C)	5

profile, it depends on the working hours as follows:

$$P_E(t) = \begin{cases} HT & \text{from 8 a. m. to 6 p. m.,} \\ LT & \text{otherwise.} \end{cases} \qquad (5)$$

In order to bring the presented case study closer to reality, the values of high and low tariff (*HT* and *LT*) have been chosen in accordance with the real prices approved by the Regulatory Office for Network Industries of Slovak Republic (R.O. for Network Industries, 2011). The exact values of *HT* and *LT* in €/kWh are listed in Table 1.

Thus, the overall performance criterion over a time interval $\langle t_1, t_2 \rangle$ is formulated as

$$J = \int_{t_1}^{t_2} \omega CV(t)\, \mathrm{d}t + \int_{t_1}^{t_2} \left(P_E(t)(P_C(\dot{m}) + P_C(\dot{m}_{St})) + P_W \dot{m}_{St} \right) \mathrm{d}t. \qquad (6)$$

Here, ω is the virtual price for the comfort violation $CV(t)$ which is defined by Eq. (4) and $P_W \dot{m}_{St}$ represents the cost paid for the consumed hot water. Time-varying electricity price is expressed as a function of time by Eq. (5) and the power consumptions of the water pumps corresponding to $\dot{m}$ and $\dot{m}_{St}$ can be calculated as a quadratic function of the particular mass flow rate,

$$P_C(\dot{m}) = \alpha_0 + \alpha_1 \dot{m} + \alpha_2 \dot{m}^2,$$
$$P_C(\dot{m}_{St}) = \alpha_0 + \alpha_1 \dot{m}_{St} + \alpha_2 \dot{m}_{St}^2. \qquad (7)$$

The parameters $\alpha_{0,1,2}$ are listed in Table 1.

Let us note that since the criterion (6) specifies the control requirements for the control of a building in a very compact form, all considered controllers will be evaluated and compared according to this criterion.

2.3. Constraints

In order to ensure proper functionality of the heat distribution system depicted in Fig. 2, the following technical constraints imposed on the manipulated variables need to be taken into account.

First of all, the constraints on mass flow rates which can be achieved by both the supply water pump and storage water tank pump need to be respected. The upper bound of the mass flow rates is given by the maximal power of the considered pumps. Technically, the lower bound on the supply water mass flow rate $\underline{\dot{m}}$ and storage tank mass flow rate $\underline{\dot{m}}_{St}$ is zero, however, the supply water pump is required to always maintain some nonzero supply water mass flow rate. To prevent the supply water pump from damage resulting from water overpressure potentially caused by the storage tank pump, the storage tank mass flow rate must never exceed the supply water mass flow rate. Due to this, the mass flow rate of the supply water and the storage tank mass flow rate are bound together by the relation $\dot{m}_{St} \le \dot{m}$. The last mass flow rate constraint results from a common feature of the water pumps that are very often multi-valued and cannot set the mass flow rate with arbitrarily small sensitivity. Therefore, the mass flow rate values must belong to a countable admissible set of discrete values.

The second group of constraints is imposed on the supply water temperature. Since the storage tank is the only source of hot water and no additional heater that could increase the water temperature to values higher than T_{St} is considered, it is obvious that the highest required supply water temperature must be lower than or equal to storage water temperature. However, the heat losses caused by the transportation of the storage water should be also reflected and therefore, it is more realistic to consider the upper constraint for the supply water temperature to be several degrees lower than the storage water temperature. Last of all, let us note that a situation which requires a value of T_{SW} to be lower than the return water temperature T_R would mean negative storage water mass flow rate $\dot{m}_{St}$, which can not be practically

realized. On the other hand, it is also obvious that such T_{SW} requirement really cannot be satisfied as only the hot water storage is considered in this configuration. With no cold water storage neither water chiller provided, the temperature of the supply water cannot be decreased below the return water temperature and the active cooling mode is not allowed.

Since the storage water mass flow rate is not an independent variable and is uniquely given by the supply water mass flow rate $\dot{m}$ and supply water temperature T_{SW}, the constraints for storage water mass flow rate can be omitted. To sum up, the above mentioned technical constraints are mathematically formulated as follows:

$$\underline{\dot{m}} \le \dot{m} \le \overline{\dot{m}}$$
$$\dot{m} \in \dot{M}_{\mathrm{adm}} = \{ \dot{m}_a | \dot{m}_a = a \times q_{st},\ a \in \mathbb{Z} \},$$
$$\max\{T_R,\ \underline{T}_{SW}\} \le T_{SW} \le T_{St} - \Delta T. \qquad (8)$$

Parameters $\underline{\dot{m}}$, $\overline{\dot{m}}$ and ΔT are provided in Table 1. Several different values of quantization steps q_{st} were considered in this work and their exact values are specified later.

3. Modeling and identification

In this section, the derivation of models for the particular variants of the MPC (being one of the crucial part of the whole control approach) is described and explained. A special emphasis is put on explanation and description of Model Predictive Control Relevant Identification (MRI) approach, the identification procedure providing mathematical models with good prediction behavior on wider range of prediction horizons.

3.1. Nonlinear model (NM)

In the current paper, the methodology that is widely used for modeling of heat transfer effects in buildings (ASHRAE, 2009; Barták, 2010; Lienhard, 2013) is followed. As explained in the dedicated literature, several physical phenomena need to be considered to obtain an appropriate structure reliably describing the building behavior. The most crucial aspects influencing the thermodynamics within the inspected zone are:

1. *Convection from walls*: This phenomenon occurs when fluid (in this case the zone air) moves along the body (wall) with different surface temperature. It affects both the heated wall T_C and the unheated wall T_S and the zone temperature T_Z. Derived from the well known Newton's cooling law, the heat flux $q_{W,\mathrm{conv}}$ caused by convection can be expressed as

$$q_{W,\mathrm{conv}} = h_{W,\mathrm{conv}}(T_W - T_Z).$$

In this expression, $h_{W,\mathrm{conv}}$ denotes the convection heat transfer coefficient and T_W refers to temperature of one of the considered walls, i.e. T_C or T_S.

In case that the fluid is externally forced to move, the convection heat transfer coefficient $h_{W,\mathrm{conv}}$ is independent of the temperature difference $T_W - T_Z$. However, in case that the fluid motion is caused solely by buoyant forces arisen from different temperatures of the fluid and the body (and thus temperature-dependent density of the fluid) and the gravitational effects, the convection heat transfer coefficient $h_{W,\mathrm{conv}}$ is expressed as a function of this temperature difference (ASHRAE, 2009; Lienhard, 2013). A common and empirically proven choice is to express the convection heat transfer coefficient $h_{W,\mathrm{conv}}$ as a weak function of the temperature difference $\Delta T = T_W - T_Z$, typically $h_{W,\mathrm{conv}} \propto |\Delta T^{1/4}|$ or $h_{W,\mathrm{conv}} \propto |\Delta T^{1/3}|$ (Lienhard, 2013; Zmrhal & Drkal, 2006). Based on the technical specification of

the building examined in this paper (absence of the ventilation fan), the forced convection is neglected and the convection heat transfer coefficient is in accordance with ASHRAE (2009), Barták (2010), and Lienhard (2013) modeled as

$$h_{W,\text{conv}} = \bar{h}_{W,\text{conv}} \left| T_W - T_Z \right|^{\frac{1}{3}},$$

where $\bar{h}_{W,\text{conv}}$ accounts also for influence of the surface area of the convecting wall $A_{W,\text{conv}}$. Then, the convection heat flux $q_{W,\text{conv}}$ from particular wall can be summarized as

$$q_{W,\text{conv}} = \bar{h}_W \left| T_W - T_Z \right|^{\frac{1}{3}} (T_W - T_Z). \tag{9}$$

2. *Mutual interactions of the walls*: Out of the three possible heat transfer phenomena – conduction, radiation and convection –, the first two might apply when inspecting the mutual interactions between the considered walls (ASHRAE, 2009; Lienhard, 2013). Conduction heat flux q_{cond} occurs due to the presence of common edges and vertices of the walls and being the simpler one, it is expressed by a formula resembling Newton's cooling law (Balmer, 2010; Lienhard, 2013),

$$q_{W,\text{cond}} = h_{\text{cond}}(T_S - T_C).$$

Here, the conduction heat transfer coefficient $h_{W,\text{cond}}$ is proportional to the surface area of the walls and inversely proportional to the distance between the points at which the temperatures T_C and T_S are provided.

Regarding the radiation, the well known Stefan–Boltzmann law applies:

$$q_{\text{rad}} = h_{\text{rad}}(T_S^4 - T_C^4),$$

with h_{rad} embracing (besides the effect of the Stefan–Boltzmann constant) various influences such as *view factor* between the two irradiating objects, emissivity/absorptivity and the surface area (Balmer, 2010). In case that the temperature difference between the two objects is relatively small (which holds true also for the heated and unheated wall temperatures), radiation heat flux q_{rad} can be with sufficient accuracy approximated by a linear function of the temperature difference,

$$q_{\text{rad}} \approx \bar{q}_{\text{rad}} = \bar{h}_{\text{rad}}(T_S - T_C)$$

and the joint conduction/radiation heat flux can be then expressed as

$$q_{\text{cd,rd}} = q_{W,\text{cond}} + \bar{q}_{\text{rad}} = h_{\text{cd,rd}}(T_S - T_C). \tag{10}$$

3. *Effects of ambient environment*: Here, influences of solar radiation and ambient temperature are considered. The values of the first of them (solar radiation) are provided in terms of the corresponding heat flux and therefore, no further derivations are necessary, $q_{\text{sol}} = \dot{Q}_S$. The latter one is assumed to be "measured" on the outer surface of the unheated wall and is assumed to vary only negligibly across the wall surface. Then, the heat flux resulting from the different inner and outer surface temperatures of the wall is described in terms of conduction through the wall as

$$q_O = h_{O,\text{cond}}(T_O - T_S). \tag{11}$$

Since the heated wall contains metal piping filled with hot supply water, the effect of the ambient temperature T_O on the temperature T_C of its inner surface is neglected.

Due to the presence of the window and possible associated gaps and interstices, the ambient temperature is assumed to directly influence the zone temperature according to the following expression:

$$q_{O,Z} = h_{O,Z}(T_O - T_Z), \tag{12}$$

where the heat transfer coefficient $h_{O,Z}$ reflects all the above mentioned window-related leakage effects.

4. *Thermal energy supplied by the manipulated variables*: In the currently presented case, this energy is provided by the hot supply water of the temperature T_{SW} circulating at mass flow rate $\dot{m}$ in the metal piping encapsulated in the concrete core of the building. The thermal energy that is transferred from the supply water into the concrete core can be quantified as follows:

$$q_{\text{in}} = c_w \dot{m}(T_{SW} - T_R). \tag{13}$$

Furthermore, based on the low thermal resistivity of the metals, it is assumed that the metal piping in which the water circulates has temperature T_P only negligibly different from the return water, $T_P \approx T_R$. Therefore, the return water temperature can be used for expression of the conductive heat transfer from the concrete core to the heated wall surface,

$$q_{R,\text{cond}} = h_{R,\text{cond}}(T_R - T_C), \tag{14}$$

with the heat transfer coefficient $h_{R,\text{cond}}$ covering the effects of the different piping and wall materials and the distance from the water piping to the heated wall surface.

Based on this, thermodynamics of each of the considered inner variables of the building can be summarized:

- dynamics of the zone temperature T_Z is positively influenced by the convection from both considered walls and the heat flux coming from the ambient environment. Furthermore, the zone temperature is also increased due to the presence of solar radiation entering the room directly through the window,

$$\frac{dT_Z}{dt} \propto q_{C,\text{conv}}, \quad \frac{dT_Z}{dt} \propto q_{S,\text{conv}}, \quad \frac{dT_Z}{dt} \propto q_{O,Z}, \quad \frac{dT_Z}{dt} \propto q_{\text{sol}}. \tag{15}$$

- heated wall surface temperature T_C is decreased by the amount of heat that is transferred into the zone air via convection while it is increased by the heat resulting from mutual interaction with the unheated wall and also by the heat transferred from heated supply water piping,

$$\frac{dT_C}{dt} \propto -q_{C,\text{conv}}, \quad \frac{dT_C}{dt} \propto q_{\text{cd,rd}}, \quad \frac{dT_C}{dt} \propto q_{R,\text{cond}}. \tag{16}$$

- similar to the heated wall, the unheated wall is cooled down by the convection into the zone air. Moreover, the unheated wall surface temperature T_S decreases due to the thermal exchange with the heated wall while it is increased due to the effects of the ambient environment (ambient temperature T_O and solar radiation q_{sol}),

$$\frac{dT_S}{dt} \propto -q_{S,\text{conv}}, \quad \frac{dT_S}{dt} \propto -q_{\text{cd,rd}}, \quad \frac{dT_S}{dt} \propto q_O, \quad \frac{dT_S}{dt} \propto q_{\text{sol}}. \tag{17}$$

- finally, the return water temperature T_R is affected by the supplied thermal energy and further heat transfer with the surface of the heated wall,

$$\frac{dT_R}{dt} \propto -q_{R,\text{cond}}, \quad \frac{dT_R}{dt} \propto q_{\text{in}} \tag{18}$$

For further use in a mathematical model, all the building inner variables are considered as the state variables of the mathematical model of the building thermodynamics, $x = [T_Z, T_C, T_S, T_R]$. Moreover, inputs $u = [T_{SW}, \dot{m}]$ stand for the manipulated variables being supply water temperature and the mass flow rate of the supply water and $d = [T_O, q_{\text{sol}}]$ correspond to the predictable

disturbances, namely the temperature of the ambient environment and the solar radiation. Then, the above mentioned phenomena described by Eqs. (15)–(18) are captured by the following set of differential equations:

$$\dot{x}_1 = \overline{p}_1 \left| x_2 - x_1 \right|^{\frac{1}{3}} (x_2 - x_1) + \overline{p}_2 \left| x_3 - x_1 \right|^{\frac{1}{3}} (x_3 - x_1) + \overline{p}_3 (d_1 - x_1) + \overline{p}_4 d_2$$

$$\dot{x}_2 = -\overline{p}_5 \left| x_2 - x_1 \right|^{\frac{1}{3}} (x_2 - x_1) + \overline{p}_6 (x_3 - x_2) + \overline{p}_7 (x_4 - x_2)$$

$$\dot{x}_3 = -\overline{p}_8 \left| x_3 - x_1 \right|^{\frac{1}{3}} (x_3 - x_1) - \overline{p}_9 (x_3 - x_2) + \overline{p}_{10} (d_1 - x_3) + \overline{p}_{11} d_2$$

$$\dot{x}_4 = -\overline{p}_{12} (x_4 - x_2) + \overline{p}_{13} u_2 (u_1 - x_4). \tag{19}$$

To ensure admissible computational complexity of the predictive controller exploiting the nonlinear model, the structure (19) was discretized using Euler discretization method considering fixed a priori known sampling time t_s (Stetter, 1973). In this paper, $t_s = 15$ min is considered. The discretization procedure results in a series of difference equations expressing the one-step predictions of the system behavior,

$$x_{1,k+1} = x_{1,k} + p_1 \left| x_{2,k} - x_{1,k} \right|^{\frac{1}{3}} (x_{2,k} - x_{1,k}) + p_2 \left| x_{3,k} - x_{1,k} \right|^{\frac{1}{3}} (x_{3,k} - x_{1,k})$$
$$\qquad + p_3 (d_{1,k} - x_{1,k}) + p_4 d_{2,k}$$
$$x_{2,k+1} = x_{2,k} - p_5 \left| x_{2,k} - x_{1,k} \right|^{\frac{1}{3}} (x_{2,k} - x_{1,k}) + p_6 (x_{3,k} - x_{2,k}) + p_7 (x_{4,k} - x_{2,k})$$
$$x_{3,k+1} = x_{3,k} - p_8 \left| x_{3,k} - x_{1,k} \right|^{\frac{1}{3}} (x_{3,k} - x_{1,k}) - p_9 (x_{3,k} - x_{2,k})$$
$$\qquad + p_{10} (d_{1,k} - x_{3,k}) + p_{11} d_{2,k}$$
$$x_{4,k+1} = x_{4,k} - p_{12} (x_{4,k} - x_{2,k}) + p_{13} u_{2,k} (u_{1,k} - x_{4,k}), \tag{20}$$

which are more suitable for implementation of the predictive controller than the continuous-time model (19). To obtain estimates of the parameters p of the discretized structure (20), MRI approach (whose explanation is provided later in this Section) belonging to advanced identification techniques was employed.[1]

3.2. Linear model (LM)

In order to simplify the model (19), let us adopt the assumption that the cubic roots of the temperature differences related to the heat convection are constant over the whole range of the operating points of the building. This simplifies the nonlinear terms as follows:

$$p|x_i - x_j|(x_i - x_j)^{\frac{1}{3}} \approx a(x_i - x_j). \tag{21}$$

Furthermore, $q_{in} = c_w \dot{m} (T_{SW} - T_R)$ is assumed to be the control input instead of the pair $\dot{m}$ and T_{SW}. Based on these assumptions, the linear version of the model Eq. (20) can be summarized as a discrete-time state space model as follows:

$$x_{k+1} = Ax_k + Bu_k + B_d d_k \tag{22}$$

with the state matrices having the following structure:

$$A = \begin{bmatrix} a_1 & a_2 & a_3 & 0 \\ a_5 & a_6 & a_8 & a_7 \\ a_9 & a_{10} & a_{11} & 0 \\ 0 & a_{12} & 0 & a_{13} \end{bmatrix}, \quad B = \begin{bmatrix} 0 \\ 0 \\ 0 \\ b \end{bmatrix}, \quad B_d = \begin{bmatrix} b_{d1} & b_{d2} \\ 0 & 0 \\ b_{d3} & b_{d4} \\ 0 & 0 \end{bmatrix}. \tag{23}$$

In this model, state and disturbance variables correspond to the

previously mentioned ones and $u = q_{in}$ refers to the optimized input. The sampling period of the system has been chosen as $t_s = 15$ min. The model parameters a, b, b_d have been estimated by a multistep prediction error minimization procedure (MRI). For further details on this method, the readers are referred to Žáčeková & Prívara (2012).

3.3. Switched linearly approximated model (SLM)

The main idea of this approach is that for a combination of inputs u, disturbances d and state variables x, a linear time-varying approximation of model (20) can be found by replacing particular nonlinearities with time-varying terms. In case of a building, this approach is even more natural and expected as the nonlinear mathematical description of the building contains terms depending on the differences between two state variables, namely $p \left| x_i - x_j \right|^{\frac{1}{3}} (x_i - x_j)$ which are likely to vary much less than the temperatures themselves. As an opposite to the linear models described earlier where the nonlinear terms are linearized "before the identification" and having the gathered data at disposal, parameters of linear time invariant model are estimated considering the purely linear character of the model, in this case, the nonlinear model is identified off-line and using its parameters, the nonlinearities are continuously approximated on-line depending on the actual values of the chosen auxiliary variables which leads to a time-varying linear model.

In order to get rid of the nonlinear terms coupling the states, let us propose an approximation procedure based on the auxiliary variables as follows.

Let us introduce two auxiliary variables, $\delta_{x_{1,2},k}$ and $\delta_{x_{1,3},k}$ defined such that

$$\delta_{x_{1,2},k} = \sqrt[3]{|x_{2,k_m} - x_{1,k_m}|}$$
$$\delta_{x_{1,3},k} = \sqrt[3]{|x_{3,k_m} - x_{1,k_m}|}, \tag{24}$$

where $k \geq k_m$ refers to discrete time and k_m indicates the time instant when the last available values of the state variables arrived. The derived model shall predict the behavior of the building over certain prediction horizon during which no current values of the state variables are available. Therefore, at each "measurement" time instant, the values of $\delta_{x_{1,2},k}$ and $\delta_{x_{1,3},k}$ are calculated and they are used by the optimizer over the whole prediction horizon. The necessity of realizing the difference between the *real-life time* (in which the model is time-varying) and the *internal time of the optimizer* (in which the model stays constant over the prediction horizon) is obvious.

Then, the nonlinear terms appearing in the model Eq. (20) can be approximated as

$$\sqrt[3]{|x_2 - x_1|}(x_2 - x_1) \approx \delta_{x_{1,2},k}(x_{k_m})(x_2 - x_1),$$
$$\sqrt[3]{|x_3 - x_1|}(x_3 - x_1) \approx \delta_{x_{1,3},k}(x_{k_m})(x_3 - x_1) \tag{25}$$

for all $k \geq k_m$. Here, the expressions $\delta_{x_{1,2},k}(x_{k_m})$, $\delta_{x_{1,3},k}(x_{k_m})$ are used to emphasize the fact that the values of auxiliary variables depend only on the last available state values.

The bilinear term in the last differential equation is (similar to the previous approaches) considered as the new controlled input q_{in} while the vector of disturbances d remains unchanged. The linearized difference equations can be now summarized as:

$$x_{k+1} = A_{app}(x_{k_m})x_k + B_{app}u_k + B_d d_k, \tag{26}$$

where

---

[1] Let us note that the parameters p_i of the discrete time model (20), $i \in \{1, 2, ..., 13\}$, differ from the parameters $\overline{p}_i$ of the continuous time model (19) since they incorporate also the effect of the chosen sampling period t_s.

$A_{app}(x_{k_m})$

$$= \begin{bmatrix} 1 - (\tilde{p}_1 + \tilde{p}_2 + \tilde{p}_3) & \tilde{p}_1 & \tilde{p}_2 & 0 \\ \tilde{p}_5 & 1 - (\tilde{p}_5 + p_6 + p_7) & p_6 & p_7 \\ \tilde{p}_8 & p_9 & 1 - (\tilde{p}_8 + p_9 + p_{10}) & 0 \\ 0 & p_{12} & 0 & 1 - p_{12} \end{bmatrix},$$

$\qquad\qquad\qquad\qquad\qquad\qquad\qquad\qquad\qquad\qquad\qquad\qquad$ (27)

with

$$\tilde{p}_1 = p_1 \delta_{x_{1,2},k}, \quad \tilde{p}_2 = p_2 \delta_{x_{1,3},k},$$

$$\tilde{p}_5 = p_5 \delta_{x_{1,2},k}, \quad \tilde{p}_8 = p_8 \delta_{x_{1,3},k} \qquad\qquad\qquad (28)$$

and

$$B_{app} = \begin{bmatrix} 0 \\ 0 \\ 0 \\ p_{13} \end{bmatrix}, \quad B_d = \begin{bmatrix} p_3 & p_4 \\ 0 & 0 \\ p_{10} & p_{11} \\ 0 & 0 \end{bmatrix}. \qquad\qquad (29)$$

At this point, the whole algorithm of obtaining the linear approximated model of the building can be summarized.

At each discrete sample $k = k_m$, the values of the state variables x are provided and the auxiliary variables $\delta_{x_{1,2},k}$, $\delta_{x_{1,3},k}$, are evaluated according to Eq. (24). Making use of the calculated auxiliary variables, a linear discrete-time model (26) of the building is created with the corresponding matrices. This approximated model is used until the new state values arrive, which means that at each discrete time sample, a new model is approximated and used by the optimizer over the following prediction horizon $k \in \{1, 2, ..., P\}$ of the *internal time of the optimizer*.

The readers interested in theoretical properties of the linear MPC exploiting model belonging to widely used family of linear time-/parameter-varying models (which SLM also belongs to) are warmly referred to Falcone, Borrelli, Tseng, Asgari, & Hrovat (2008) where the stability and feasibility of such formulation are discussed in detail. It should be noticed that one of the crucial assumption is that on constancy of the model over the prediction horizon, which is satisfied also by the SLM model and therefore, the results obtained in Falcone et al. (2008) hold also for the case of LMPC with SLM model.

3.4. MRI identification for nonlinear models

Having the model structures at disposal, it is necessary to estimate the parameters of these structures from the available input/output data. Since the obtained models are expected to be used by the predictive controllers as system dynamics predictors, this fact needs to be taken into account as early as at the point of choosing of the identification procedure. Instead of classical identification methods performing minimization of one-step prediction error (the so-called prediction error methods or PEMs Ljung, 2007), advanced approach focusing directly on minimization of multi-step prediction error is exploited since it provides models with better long-term prediction performance which is highly requested when considering use of the model with MPC. The objective is to find such parameters of the given model structure which minimize the multi-step prediction error (Laurí et al., 2010) over the whole prediction horizon,

$$J_{MRI} = \sum_{k=0}^{N-P} \sum_{i=1}^{P} \left[y_{k+i} - \hat{y}_{k+i|k} \right]^2, \qquad\qquad (30)$$

where $\hat{y}_{k+i|k}$ is the i-step output prediction constructed from data up to time k, N corresponds to the number of samples and P stands for prediction horizon considered for identification. In case of linear model structures which is also the case of structure (22), several reliable approaches can be found. Therefore, one particular

algorithm that has already been successfully used for building model parameters identification (interested readers are referred to Žáčeková & Prívara, 2012) will be used also in this paper to estimate the parameters of the linear structure (22).

When talking about identification of models with nonlinear structure performing minimization of (30), no methods of solving of the arisen problem can be found in the available literature according to authors' best knowledge. The proposed extension of the MRI identification methods (Žáčeková & Prívara, 2012) for nonlinear systems is described in the following text.

Without any loss of generality, let us assume nonlinear systems where the multi-step predictor $\hat{y}_{k+i|k}$ can be formulated in the following way:

$$\hat{y}_{k+i|k} = Z_{L,k+i} \hat{\theta}_L + Z_{NL,k+i} \hat{\theta}_{NL}, \quad i \in 1, 2, ..., P, \qquad (31)$$

where $z_{L,k+i} = [u_{k+i-n_d} ... u_{k+i-n_b} y_{k+i-1} y_{k+i-n_a}]$ and $\hat{\theta}_L = [\hat{b}_{n_d} ... \hat{b}_{n_b} \hat{a}_1 ... \hat{a}_{n_a}]$ are regression matrix and the vector of unknown parameters describing the linear part of the model dynamics, respectively. n_a denotes the number of past outputs in the regressor, n_b is the number of inputs in the regressor and n_d represents their delay compared to the outputs. The nonlinear part of the system dynamics is described by $\hat{\theta}_{NL} = [\hat{\theta}_1 \ \hat{\theta}_2 \ ... \ \hat{\theta}_n]^T$ with n being the number of identified parameters and $Z_{NL,k+i} = [f_1(\cdot) f_2(\cdot) ... f_n(\cdot)]$. In general, $f_i(\cdot)$ are functions of $u_{k+i-1}, ..., u_{k+i-n_{b,NL}}$ and $y_{k+i-1}, ..., y_{k+i-n_{a,NL}}$ with parameters $n_{a,NL}$ specifying the number of past outputs in the nonlinear dynamics and $n_{b,NL}$ representing the number of inputs in the nonlinear structure.

It is important to note that not every output contained in regression matrices $Z_{L,k+i}$ and $Z_{NL,k+i}$ is available at time k, thus the multi-step predictions $\hat{y}_{k+i|k}$ must be obtained recursively by applying i-times the expression $\hat{y}_{k+1|k} = Z_{L,k+1} \hat{\theta}_L + Z_{NL,k+1} \hat{\theta}_{NL}$ with initial conditions y_k. Now, the estimate of matrix of parameters $\hat{\theta}$ can be obtained as a solution of the following optimization task:

$$[\hat{\theta}_L, \hat{\theta}_{NL}]^* = \arg \min_{[\theta_L, \theta_{NL}]} \sum_{i=1}^{P} \sum_{k=0}^{N-i} [y_{k+i} - Z_{L,k+i} \theta_L - Z_{NL,k+i} \theta_{NL}]^2$$

subject to :

$$\theta_L \in \theta_L(S_L), \quad \theta_{NL} \in \theta_{NL}(S_{NL}) \qquad\qquad (32)$$

where S_L and S_{NL} correspond to the sets of all admissible estimated parameters. These constraints enable the user to incorporate certain a priori information into the identification procedure, for example to ensure that certain parameters are nonnegative or lie in a constrained interval, etc. In the currently presented case, two different methods of obtaining of $\hat{y}_{k+i|k}$ were exploited:

- *variant A* – for computing of $\hat{y}_{k+i|k}$, the output predictions are used only for recursive calculation of Z_L and for calculation of Z_{NL}, the available output data are exploited. In such case, the optimization task (32) is *polynomial* in parameters and can be solved employing standard solver for nonlinear programming. This is certain kind of approximation where the nonlinear part of the system dynamics is basically identified just in sense of minimization of one-step prediction error while the linear part is still identified with respect to the multi-step prediction error minimization criterion.
- *variant B* – for computing of $\hat{y}_{k+i|k}$, the output predictions are used for recursive calculation of Z_L as well as Z_{NL}. In this case, the parameters of both the linear and nonlinear part of the system dynamics are searched such that the multi-step prediction errors are minimized. It should be noted that in this case, the optimization task (32) is again a nonlinear programming problem, however, it might not be only polynomial in the estimated parameters any more.

3.5. Identification results

Making use of the above mentioned identification procedures, the parameters of all model structures presented in the current Section were identified from the available identification data set.

At first, the comparison of the nonlinear models obtained using variant A and variant B of the nonlinear MRI identification (denoted as nMRIa and nMRIb, respectively) is presented in Fig. 3. For identification purposes, prediction horizon $P=20$ samples was considered which with sampling period $t_s=15$ min corresponds to duration of 5 h. It can be argued that the prediction horizon is shorter than the real prediction horizon of the predictive controllers (in the current application, the predictive controllers perform optimization calculations over 12 h corresponding to 48 samples), however, in Žáčeková, Váňa, & Cigler (2014) and Gopaluni, Patwardhan, & Shah (2004) it was shown that from certain prediction horizon threshold, the increase of the identification prediction horizon can lead to degradation of the performance of the obtained model.

It is obvious that both obtained nonlinear models fit the verification data very well also on longer verification interval with slight superiority of the model identified making use of nMRIb. nMRIa variant provides model with performance which is only slightly worse than that of the model obtained by (seemingly) more computationally demanding variant nMRIb. It is true that within the nMRIb, a more general nonlinear programming task needs to be solved (which is undoubtedly more computationally demanding than just solving of polynomially nonlinear programming performed within nMRIa), however, the overall optimization which is solved within nMRIb takes less computational time than optimization performed within nMRIa. Although one iteration of nMRIb is slower (due to solving of the more general optimization problem), on the other hand less iterations are needed to converge to the solution of the optimization problem. This can be explained such that the task formulated within nMRIb brings the chosen nonlinear structure closer to reality and thus also to the verification data – this of course holds well only in case that a reasonable model structure was chosen. Therefore, it might be more advantageous to choose identification of nonlinear model in variant nMRIb which can be ultimately faster and provides a more accurate and reliable model. Based on this, the model obtained by nMRIb was chosen to be used with the nonlinear predictive controller in the role of the system dynamics predictor.

Now, the graphical and numerical comparison of all above described models follow. Since the models are intended to be used with the MPC, one of their most important features is the ability to provide reasonable predictions over the whole prediction horizon. In this paper, the prediction horizon $T_P=12$ h is considered which with 15-min sampling corresponds to $P=48$ samples. Let us remind that in the role of the nonlinear model, nMRIb was chosen.
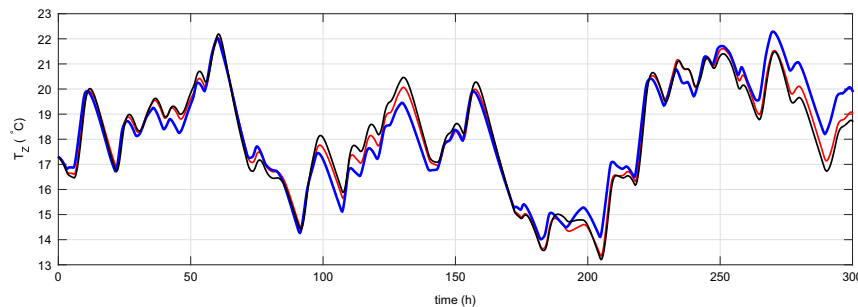
Fig. 4 shows several weeks of comparison of the models which are used for the building behavior predictions with the linear time invariant (LM model), linear time-varying (SLM model) and non-linear MPC (NM model). At each discrete time sample ($t_s=15$ min), 12-h predictions are calculated based on the provided state values. All the predictions of the models are plotted together with the verification data.

Looking at Fig. 4, it is clear that while the NM behavior constraints the quality of the prediction behavior from above with the smallest deviations from the verification data and the LM behavior exhibits the highest prediction errors, the performance of the performance of the time-varying model is somewhere in the middle between these two "limit" cases. The most obvious are the differences in the behavior when looking at the 200-th and the 300-th hour of the comparison. While the absolute value of prediction errors for the off-line identified linear model reaches up to 2 °C, the error obviously decreases through the switched linearly approximated time-varying model down to the nonlinear model which provides the predictions with the least prediction error out of the three compared models, which in turn justifies the use of the predictive controller with the more complex nonlinear model.

In order to compare the models in a more complete way, the statistical comparison of the models is provided in Table 2. The length of the evaluated period was nearly 3 months. In the table, LM specifies the linear model, SLM stands for the switched linearly approximated model and NM represents the nonlinear model. For each model, ε_{av} being the average prediction error over the whole 12-h prediction horizon and the maximum prediction error ε_{max} over the prediction horizon are inspected.

The table clearly demonstrates that the most reliable predictions are provided by the NM model. However, this is not a surprise as this model takes the whole dynamics of the building into account including the nonlinearities. On the other hand, it can be seen that considering the linear time-dependent model, the quality of the predictions fairly improves compared to the linear time invariant model. With SLM model, the reduction of ε_{av} is almost 40% and the reduction of ε_{max} is nearly 37%.

4. Model predictive control

In this section, the considered MPC variants are briefly explained and the optimization routines used to solve the corresponding optimization problems are presented. At the end of this Section, the quantized nonlinear predictive control algorithm is proposed.

4.1. Linear MPC

The control requirements which have been chosen for the linear MPC to be satisfied (minimization of both the thermal comfort
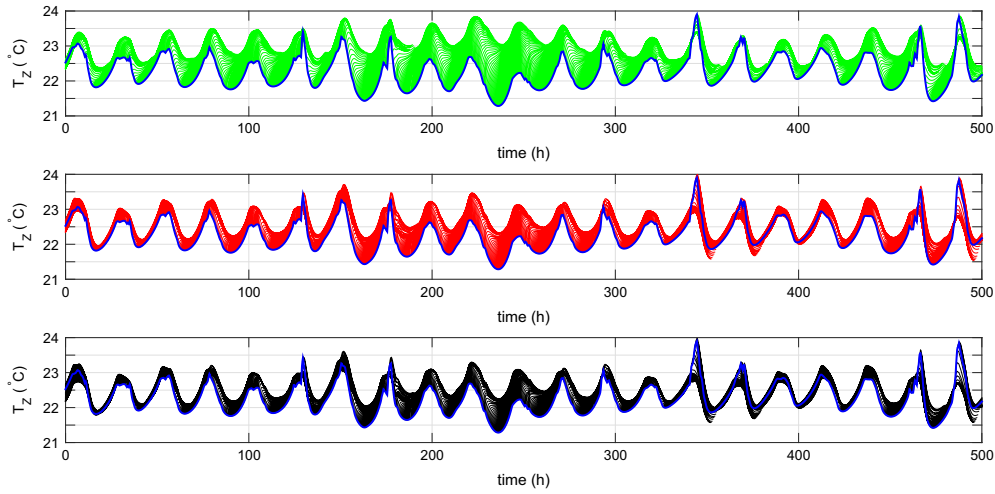

Fig. 3. Comparison of nMRIa (——) and nMRIb (——) models with the verification data (——).

Fig. 4. Comparison of T_Z predictions of the LM (——), SLM (——) and NM (——) models with the verification data (——).

Table 2
Statistical comparison of the models.

	LM	SLM	NM
ε_{av} (°C)	0.57	0.34	0.30
ε_{max} (°C)	1.89	1.20	1.08

violation and the energy consumption) can be mathematically summarized as follows:

$$J_{MPC,k} = \sum_{i=1}^{P} W_{1,\mathbf{p}}(k+i) \| q_{\text{in},k+i} \|_{\mathbf{p}} + \sum_{i=1}^{P} W_{2,\mathbf{p}} \| CV_{k+i} \|_{\mathbf{p}} \tag{33}$$

s. t. : linear dynamics (22)

$0 \le q_{\text{in},k+i} \le \bar{q}_{\text{in},k+i}, \quad i = 1, ..., P$

$\hat{T}_{Z,k+i|k} \ge T_{Z,k+i}^{min} - CV_{k+i}.$

This formulation considers a combination of linear and quadratic penalization indicated by the index $\mathbf{p} \in \{1, 2\}$ which enables us to shape the penalization criterion conveniently. Time-varying weighting matrices W reflecting the time dependence of the electricity tariffs and prediction horizon P stand for the tuning parameters of the controller. Comfort violation is calculated based on the difference between the zone temperature prediction $\hat{T}_Z$ and its lowest acceptable bound T_Z^{min} and the hard constraints are relaxed employing an auxiliary variable CV. Exact values of the optimization problem settings can be found in Table 3.

As the linear version of MPC optimizes supplied heat q_{in}, a post-processing procedure is needed to obtain the particular values of T_{SW} and $\dot{m}$ which correspond to the true control inputs of the thermally activated building system (TABS). This straightforward postprocessing

Table 3
Table of controller parameters.

$W_{1,1}$ (high tariff)	0.01	$W_{1,2}$ (high tariff)	1.6
$W_{1,1}$ (low tariff)	0.005	$W_{1,2}$ (low tariff)	0.8
$W_{2,1}$	2×10^6	$\bar{q}_{\text{in}}$	90×10^4
$W_{2,2}$	10^4	$q_{\text{in},tr}$	700
$\underline{T}_{SW}$	20	$\overline{T}_{SW}$	50
P	48	$\dot{m}_{pp}$	20

holds the mass flow rate fixed $\dot{m} = \dot{m}_{pp}$ and it calculates the supply water command as $T_{SW} = q_{\text{in}}/\dot{m}c_w + T_R$. Should the calculated supply water command be higher than $\overline{T}_{SW}$, $T_{SW} = \overline{T}_{SW}$ is set and the mass flow rate command is calculated as $\dot{m} = q_{\text{in}}/c(T_{SW} - T_R)$. If the heating effort is lower than a threshold value $q_{\text{in},tr}$, the TABS manipulated variables are set to $T_{SW} = T_R$ and $\dot{m} = \underline{\dot{m}}$. The settings of the post-processing procedure are listed in Table 3.

4.2. Nonlinear MPC

Thanks to the use of nonlinear programming optimization method, the nonlinear MPC can exploit the more reliable nonlinear discrete-time state-space description of the building behavior and address directly the minimization of the evaluative criterion (6). To obtain computationally tractable solution, also the criterion (6) needs to be discretized in time. This results in the following nonlinear MPC cost criterion:

$$J_{NMPC,k} = \frac{1}{t_s} \sum_{i=1}^{P} \omega CV_{k+i} + \frac{1}{t_s} \sum_{i=1}^{P} \left(P_{E,k+i}(P_C(u_{2,k+i}) + P_C(\bar{u}_{3,k+i})) \right)$$
$$+ \frac{1}{t_s} \sum_{i=1}^{P} P_W \bar{u}_{3,k+i}, \tag{34}$$

where t_s represents the chosen constant sampling period, P stands for the prediction horizon, $P_C(\cdot)$ corresponds to Eq. (7) and $\bar{u}_3$ represents a virtual input which corresponds to the storage water mass flow rate $\dot{m}_{St}$,

$$\bar{u}_3 = u_2 \frac{u_1 - x_4}{T_{St} - x_4}.$$

The obtained optimal profiles u_1, u_2 are required to satisfy the technical limitations which are formulated as box constraints,

$$\max\{\underline{T}_{SW}, x_4\} \le u_{1,k} \le \overline{T}_{SW},$$
$$\underline{\dot{m}} \le u_{2,k} \le \overline{\dot{m}}. \tag{35}$$

Last but not least, the dynamics of the building must not be violated which is represented by the satisfaction of the model dynamics (20).

In the role of the optimization routine, gradient optimization algorithm (Zhou, Doyle, & Glover, 1996; Bryson, & Ho, 1975) with variable step length is employed. This approach is able to address optimization problems in the following form:

$$\text{minimize } J = \sum_{i=1}^{P} L(x_i, u_i) + \phi(x_P, u_P)$$

such that $u_i \in \langle \underline{u}, \overline{u} \rangle$. \hfill (36)

To find the solution of (36), the following idea is employed: starting from an initial estimate of the optimal input profile u^0, the opposite direction of the gradient of the minimization cost criterion is iteratively followed until convergence to the optimal input vector,

$$u^l = u^{l-1} - \alpha^l \frac{\partial J}{\partial u}. \hfill (37)$$

Here, l represents the iteration of the gradient algorithm and α^l is the step length at l-th iteration.

To obtain computationally tractable solution of this optimization task, the Hamiltonian

$$\mathcal{H} = L_k + \lambda_{k+1}^{\mathrm{T}} f(x_k, u_k) \hfill (38)$$

is created. Here, L_k is the integral or in discrete-time case the *summation* part of the criterion J, $f(x_k, u_k)$ is the vector field representing the dynamics of the controlled system and λ is the so-called co-state vector with the backwards dynamics

$$\lambda_k = \frac{\partial H}{\partial x}(x_k, u_k, \lambda_{k+1}) \hfill (39)$$

and the terminal condition

$$\lambda_P = \frac{\partial J}{\partial x}\bigg|_P. \hfill (40)$$

It can be shown that the gradients of both the cost criterion J and the Hamiltonian H with respect to the input vector u are equal, $\partial J/\partial u = \partial H/\partial u$, and therefore, the iterative search (37) turns into

$$u^l = u^{l-1} - \alpha^l \frac{\partial H}{\partial u}. \hfill (41)$$

To satisfy the input constraints, the input profile u^l is at each iteration projected on the admissible input interval $\langle \underline{u}, \overline{u} \rangle$. The iterative search (41) is used until convergence which is usually defined as

$$|J(u^l) - J(u^{l-1})| \le \epsilon \hfill (42)$$

with some reasonably chosen nonnegative tolerance $\epsilon > 0$.

As can be expected, the search step length α significantly influences the convergence properties of the algorithm. In order to provide smooth and uniform convergence to the optimum, α should be small in case that the cost criterion J decreases rapidly and it should increase in case that the change of the cost criterion $|J(u^l) - J(u^{l-1})|$ is small. To satisfy these requirements, the following formula for the search step length is proposed:

$$\alpha^l = -\beta \log(\gamma \Delta J^l). \hfill (43)$$

Here, $\Delta J^l = |J(u^l) - J(u^{l-1})|$ is the change of the cost function value and $\beta > 0$, $\gamma > 0$ are some suitably chosen constants. Last of all, the step length α^l is constrained at each gradient algorithm iteration,

$$\underline{\alpha} \le \alpha^l \le \overline{\alpha}. \hfill (44)$$

Parameters $\underline{\alpha} > 0$ and $\overline{\alpha} > 0$ are together with β and γ considered to be the tuning parameters of the presented optimization algorithm.

4.3. Quantized MPC

As was mentioned earlier, the mass flow rate should belong to the

admissible set of discrete values $\dot{M}_{\mathrm{adm}}$. In case of the linear MPCs which calculate optimal amount of energy that should be delivered into the zone and subsequently perform the postprocessing to obtain the values of mass flow rate and supply water temperature, the discrete-valued nature of the mass flow rate can be very straightforwardly taken into account. However, the situation is more complicated in case of nonlinear MPC. As already mentioned in the Introductory Section, two ways how to obtain discrete-valued mass flow rate sequence are considered in this work.

The first of them consists in use of additional postprocessing which is performed after the continuous-valued optimization is finished. The most straightforward postprocessing routine is pure rounding of the obtained continuous-valued mass flow rate sequence u_2 away from zero to the nearest multiple of the quantization step,

$$u_{2,q} = q_{st} \cdot \text{round}\left(\frac{u_2}{q_{st}}\right), \hfill (45)$$

with $\text{round}(\cdot) = \text{sgn}(\cdot) \lceil |\cdot| \rceil$. Major advantage of this approach is its simplicity – the a posteriori quantization can be performed by a hardware component and therefore, no increase of the computational complexity occurs. However, it can be expected that such naive approach significantly degrades the control performance of the original controller since the fact that the manipulated variable will be quantized a posteriori is not taken into account in the used optimization routine.

This drawback is solved by the adaptation of the original Hamiltonian-based method representing the second way of achieving that discrete-valued mass flow rate profile is obtained. Here, a regular *mid-processing* iteration is performed each **I**-th iteration of the gradient search. Thanks to this, the information about the discrete-valued nature of one of the manipulated variables is incorporated into the optimization procedure and the optimality of the original continuous-valued optimization technique is preserved.

The *mid-processing* is performed at particular iterations $l = m \times \mathbf{I}$, $m \in \mathbb{N}^+$ after the gradient step is made and it can be described as follows: first of all, the quantized mass flow rate sequence $u_{2,\bigcirc}^l$ is obtained by projecting the continuous-valued mass flow rate vector $\hat{u}_2^l$ on the admissible set $\dot{M}_{\mathrm{adm}}$ given by (8) with respect to the chosen quantization step q_{st},

$$u_{2,\bigcirc}^l = q_{st} \cdot \text{round}\left(\frac{\hat{u}_2^l}{q_{st}}\right). \hfill (46)$$

These P predicted quantized mass flow rate samples are connected with n_f past mass flow rate samples $\overleftarrow{u}_2 = [u_{2,k-n_f}, u_{2,k-n_f-1}, \ldots, u_{2,k-1}]$ with k representing the current time step, and vector $\overleftrightarrow{U}_2 = [\overleftarrow{u}_2, u_{2,\bigcirc}^l]$ is received. The vector $\overleftrightarrow{U}_2$ represents all mass flow rate samples that will have been applied into the system until time $k + P$ and have influence on the frequency properties of the manipulated variable u_2.

Then, $\overleftrightarrow{U}_2$ is filtered with a suitably defined low-pass filter with order n_f which helps us to suppress the undesired high frequencies and decrease oscillations in the last P-sample subvector representing the currently optimized input sequence. This P-sample subvector is extracted and after quantization and projection on its admissible range is used for the next iteration of the gradient search.

The overall control algorithm is then summarized as follows:

Algorithm agqNPC
1. obtain current values of the state variables $x_{curr,k}$
2. consider input profiles from the previous iteration

$\{u_1^{l-1}, u_2^{l-1}\}$ and obtain state trajectories $X = [x_0, x_1, ..., x_P]$ according to the model (20) with $x_0 = x_{curr,k}$;

3. according to the co-state dynamics (39), obtain the co-state trajectory $\Lambda = [\lambda_0, \lambda_1, ..., \lambda_P]$ with terminal condition (40);

4. calculate gradients $\partial H/\partial u_1$, $\partial H/\partial u_2$, and perform gradient step (41), obtain u_1^l and $\hat{u}_2^l$;

5. **if** $\text{mod}(l, \mathbf{I}) = 0$
   then perform the *mid-processing*:

   (i) quantize mass flow rate $\hat{u}_2^l$ according to (46) with chosen q_{st}, obtain $u_{2,\bigcirc}$,

   (ii) create sequence $\overleftrightarrow{U}_2^l = [\overleftrightarrow{u}_2^l, u_{2,\bigcirc}^l]$,

   (iii) filter $\overleftrightarrow{U}_2^l$ using a low-pass filter of order n_f with the chosen characteristics, obtain $\overleftrightarrow{U}_{2,\text{filt}}^l$,

   (iv) quantize $\overleftrightarrow{U}_{2,\text{filt}}^l$ with chosen q_{st}, obtain $\overleftrightarrow{U}_{2,\text{filt},\bigcirc}^l$,

   (v) extract u_2^l as the last P samples of $\overleftrightarrow{U}_{2,\text{filt},\bigcirc}^l$;

   else $u_2^l = \hat{u}_2^l$;

6. project the sequences u_1^l and u_2^l on the admissible intervals $\langle \max\{\underline{T}_{SW}, x_4\}, \overline{T}_{SW} \rangle$ and $\langle \underline{\dot{m}}, \overline{\dot{m}} \rangle$;

7. **if** $|J(\{u_1^l, u_2^l\}) - J(\{u_1^{l-1}, u_1^{l-1}\})| \le \epsilon$
   then terminate,
   else $l = l + 1$, repeat from (2);

8. apply the first sample of the calculated input profiles into the system, in the next time instance repeat from (1).

The performance of both the naive a posteriori quantization and the algorithm employing the *mid-processing* iteration is verified in the following section. In order to provide a better comparison, the results of the original continuous-valued nonlinear MPC are provided together with the results of the linear versions of predictive controller.

5. Results

First of all, visual comparison of the thermal comfort performance is presented in Fig. 5.

Fig. 5 shows the zone temperature profiles over a 6-day period for the linear predictive controllers with LM and SLM and the nonlinear continuous-valued predictive controller. From this figure, it can be seen that al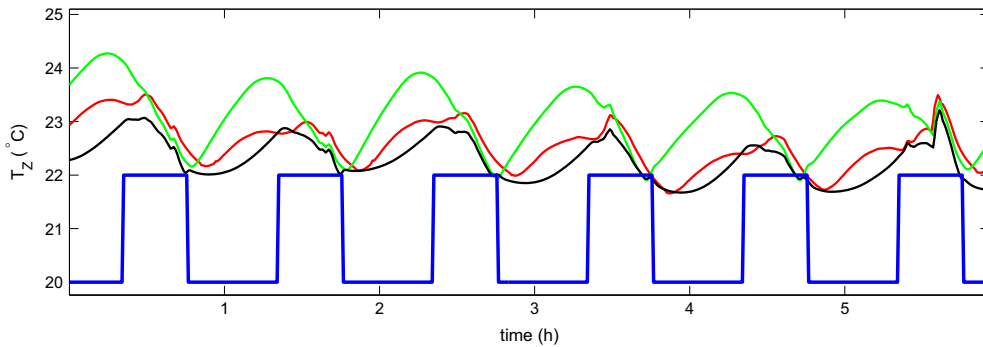l controllers are carefully tuned to achieve satisfactory thermal comfort performance since all of them are able to satisfy the room temperature requirements and maintain the zone temperature within the admissible zone above the zone temperature threshold. This feature is very crucial since a controller that does not fulfill the thermal comfort requirements and violates the zone temperature threshold significantly is literally useless for building temperature control. Out of all considered controllers, the nonlinear MPC (NMPC) exhibits the most superior performance – it satisfies the required thermal comfort keeping the zone temperature within the admissible range and on the other hand, it obviously does not waste too much energy keeping the zone temperature just as high above the threshold as needed. This result could have been expected as the NMPC combines the model with the best prediction performance out of the considered set and it also directly addresses the minimization of the optimization criterion corresponding to the ultimate evaluative performance criterion (6).

Fig. 6 provides the second part of the visual comparison – it depicts the monetary cost that is being paid for the control at each time instance.

All profiles exhibit sinusoidal-like trends – this is caused by the consideration of time-varying price of the electricity. The higher parts of the profiles correspond to low-tariff hours while the lower parts match the non-working hours with cheap electricity. Also from this figure, the monetarily more economical nature of the NMPC can be observed. The NMPC spares significant amount of expenses compared to its linear counterparts. This superiority comes from the use of more precise nonlinear model and it is of course caused also by the nonlinear cost function of the NMPC which directly corresponds to the amount of money that is paid for the control. It can be also seen that the SLM model which is closer to the nonlinear one enables also the controller with approximated cost function to achieve better economical performance than the original linear model. For further illustration, the cumulative sum of the monetary cost of the control is depicted in Fig. 7. The provided profiles are normalized with respect to the total price TP_{LM} that is paid by the linear MPC with the ordinary time-invariant linear model.

The statistical comparison of the energy consumption can be found in Table 4. *TP* expresses the overall price paid for zone temperature control. Moreover, the particular energy consumptions normalized with respect to the consumption of the linear MPC using the ordinary off-line identified linear model are expressed. Furthermore, also the comparison of the average computational time T_{av} and the maximum computational time T_{max} per discrete time instance is provided.

The superiority of the NMPC is demonstrated once again. It can be seen that although the comparison of the identified models was very optimistic in the case of linear time-dependent model versus the linear time-invariant one, the resulting effect of the good
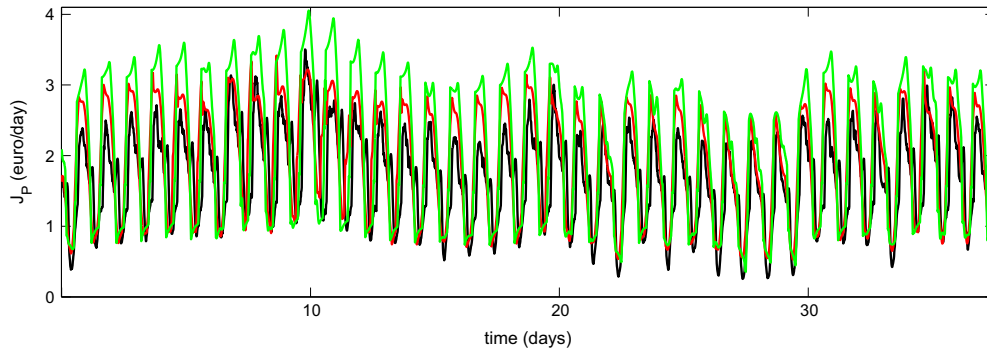

Fig. 5. Zone temperature control (━━ – linear MPC with LM, ━━ – linear MPC with SLM, ━━ – nonlinear continuous-valued MPC with NM, ━━ – T_z^{min}).

Fig. 6. Overal price of the control effort (■■■ – linear MPC with LM, ■■■ – linear MPC with SLM, ■■■ – nonlinear continuous-valued MPC with NM).

model on the overall monetary cost of the control is not so attractive. This can be simply explained by the fact that although the good predictor is crucial for the proper functioning of the MPC (either linear or nonlinear), so is the properly chosen optimization criterion. Based on this observation, in the building climate control, the need for the use of nonlinear MPCs which are able to address the task of the real-life price minimization in a direct way instead of using certain approximation is obvious. However, one more aspect needs to be taken into account when choosing the controller type – its computational complexity. Table 4 shows two factors related to the computational demands of the particular control strategy: T_{av} being the average computational time needed for the calculation of the optimal input and T_{max} corresponding to the maximum calculation time. Let us mention that this calculation time includes also the time needed to obtain the model which (as will be shown) might contribute considerably to the overall calculation time. The comparison is evaluated depending on the type of the model which is used by the optimizer. The simplest controller being the LMPC with LM needs the shortest time to calculate the optimal input. As this variant does not consume any time to obtain the model and the same optimizer is used also by second member of the family of the linear MPCs (the controller with SLM model), one can get a very good insight into how long does it take to obtain the SLM model for the predictions. As the SLM variant performs the approximation of the nonlinear model at each sampling instant, the increase of the average computational time is understandable. Although in case of the LMPC with SLM, the average calculation time is longer than in case of the LMPC with LM, this is compensated by the better control performance.

Let us summarize the performance of the particular variants. Regarding the control performance and the energy consumption, the NMPC is the best candidate for the real-life application. On the

Table 4
Comparison of the energy consumption and computational complexity.

	LM	SLM	NM
TP	83.7	77.0	66.8
TP/TP_{LM} (%)	100	92	80
T_{av}(s)	0.81	0.93	4.41
T_{max}(s)	1.20	1.49	6.21

other hand, the LMPC with the simplest off-line identified model is able to provide the fastest calculation of the optimal input sequence. Looking for a trade-off between the optimality and the time complexity, the presented time-varying approach exploiting SLM model is able to bridge the gap between these two and therefore, it stands for a promising candidate for the real-life application especially in case of large buildings complexes where it can be expected that the nonlinear optimization task can take too long to be solved.

Since one of the main objectives of this paper was to adapt the nonlinear MPC such that it provided discrete-valued mass flow rate profile, let us present a comparison of the performance of the following alternatives – the naive a posteriori quantization that is referred to as nqNPC and the adaptation of the gradient algorithm named agqNPC are compared with the continuous-valued NMPC from the previous comparison. At first, the situation with 7 admissible values for mass flow rate was considered. All three compared controllers (continuous-valued NMPC, nqNPC and agqNPC) were tuned to achieve approximately the same thermal comfort and therefore, only the economical part of the criterion might be focused on. At first, the calculated mass flow rate profiles are presented in Fig. 8.

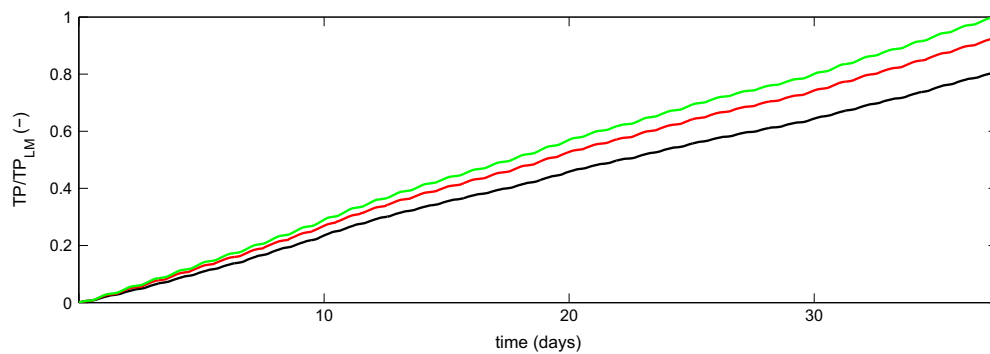Based on the visual comparison, it can be expected that the

Fig. 7. Normalized cumulative price of the control effort (■■■ – controller with LM , ■■■ – controller with SLM, ■■■ – controller with NM).
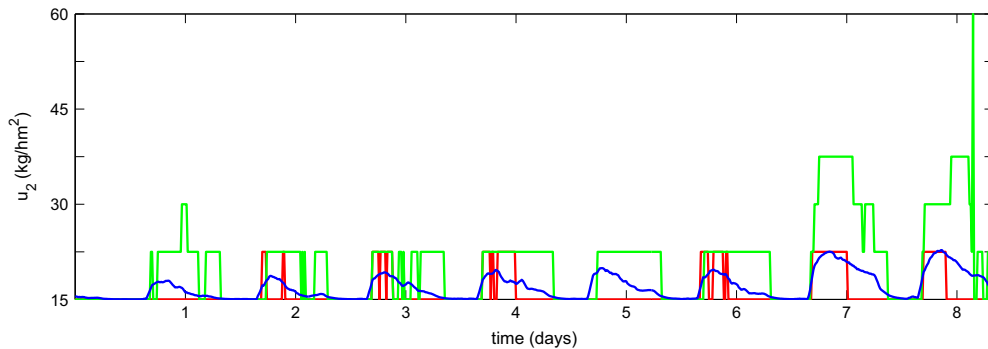
39

Fig. 8. Mass flow rates, $N_{qst} = 7$ (▬▬ – continuous-valued NMPC, ▬▬ – nqNPC, ▬▬ – agqNPC).

nqNPC pays the most for the operation of the building. On the other hand, the agqNPC with advanced handling of the quantization phenomena behaves more similar to the original continuous-valued NMPC. This demonstrates the fact that while within the agqNPC, the mid-processing iteration enables us to adapt the calculation of the mass flow rate *inside* the optimization procedure and take the quantization into account, the naive quantization does not provide such possibility and therefore, significant part of the optimality is lost. Moreover, a posteriori quantization obviously leads to more oscillatory profiles which stands for another drawback of such approach. Since the mass flow rate is not the only manipulated variable, it might be interesting to inspect how much affected is u_1 by the quantization of u_2. Such comparison is provided in Fig. 9 where the profiles of supply water temperature applied by the inspected controllers are shown.

Comparing Figs. 8 and 9, a waterbed effect of the quantization can be observed since the quantization of one manipulated variable causes oscillatory performance that "leaks" into the other manipulated variable profile. The situation might seem a little bit paradoxically – although the mass flow rate is the manipulated variable that is quantized, the other manipulated variable also strongly oscillates when comparing the quantized version with the original continuous-valued version of the controller. This is more significant in case of the nqNPC where the oscillations of the supply water temperature are much more aggressive than the oscillations of the mass flow rate. This can be explained by the fact that while the quantization of the mass flow rate projects the values belonging to particular interval to the same quantized value, no such "damping" applies to the supply water temperature and therefore, its oscillations fully develop.

The last part of the comparison is the numerical evaluation of the economical aspects of the control under the quantization conditions

provided in Table 5. Besides the total control cost (denoted as NMPC, nqNPC and agqNPC according to the evaluated control algorithm) shown in euros, also percentage increases of energy consumption normalized with respect to the consumption achieved by continuous-valued NMPC are provided (in Table 5, the increases are referred to as EI_{nqNPC} and EI_{agqNPC}, respectively). To obtain a more reliable comparison, situations with 3 up to 8 quantization steps N_{qst} were compared. The range of quantization levels $N_{qst} \in \{3, ..., 8\}$ was chosen based on the actual market research – it turned out that none of the currently available water pumps offers use of more than 8 pre-programmed different speeds/mass flow rates and therefore, values of N_{qst} higher than 8 were not considered. On the other hand, the theory of optimal bang-bang (2-valued) control is nearly as mature and elaborated as the optimal control theory itself (Anderson & Moore, 1971; Kaya & Noakes, 1996; Ledzewicz & Schättler, 2002; Wonham & Johnson, 1964) – therefore the optimization problem with 2-valued valve was omitted and the lowest number of quantization levels was chosen as $\underline{N}_{qst} = 3$.

Inspecting Table 5, it is obvious that the increase of the quantization steps N_{qst} leads to decrease of the cost paid for the control – this holds for both the naive and advanced quantization handling. However, a considerable difference can be observed in the actual value of the control cost increase. While for the naive quantization algorithm nqNPC the control cost can be increased by as high portion as 28%, the control cost increase never exceeds 17% with the use of advanced agqNPC algorithm. The difference can be nicely illustrated on an example of $N_{qst} = 4$ steps. The advanced quantization algorithm agqNPC consumes only about 10% more energy than the continuous-valued NMPC while the naive quantization algorithm nqNPC cost increase is nearly twice as high – moreover, even with $N_{qst} = 6$ quantization steps, the nqNPC algorithm achieves worse control cost. The difference between the two algorithms turns
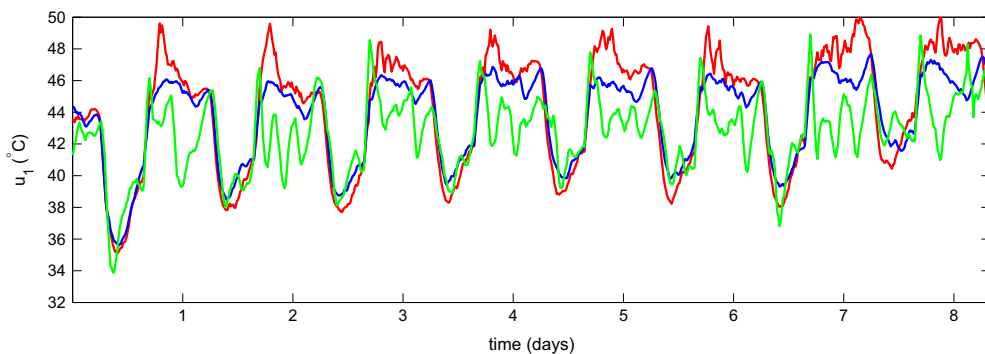

Fig. 9. Supply water temperatures, $N_{qst} = 7$ (▬▬ – continuous-valued NMPC, ▬▬ – nqNPC, ▬▬ – agqNPC).

Table 5
Comparison of the energy cost.

N_{qst}	NMPC	nqNPC	EI_{nqNPC}	agqNPC	EI_{agqNPC}
3	66.8	85.6	28.1	78.1	17.0
4	66.8	80.2	20.1	73.6	10.2
5	66.8	76.1	13.9	72.5	8.5
6	66.8	75.2	12.6	69.0	3.3
7	66.8	72.4	8.3	67.6	1.2
8	66.8	67.5	1.0	67.1	0.4

insignificant only for the highest number of quantization steps $N_{qst} = 8$. However, although the control cost increase might not be significant, the difference in handling the oscillatory effects should not be forgotten as documented in Fig. 10 which clearly shows that the high-frequency portion of both the mass flow rate and the supply water temperature signals is decreased by the agqNPC and brought closer to the continuous-valued NMPC.

Last but not least, the computational complexity should be mentioned. Since the naive quantization algorithm nqNPC involves only a post-processing procedure to handle the quantization, virtually no computational time increase compared with the continuous-valued NMPC is observed. In case of the advanced quantization algorithm agqNPC, the *mid-processing* iteration causes a constant average increase of the computational complexity $\Delta_{ct} = 0.28$ s representing about 6% of the average computational time of the continuous-valued NMPC. Here, it should be highlighted that the computational complexity increase introduced by the use of the agqNPC is *independent* of the number of quantization levels N_{qst} which strongly distinguishes it from the commonly used mixed-integer programming methods where the computational time rises very steeply even when using massive computational power (Causa et al., 2008; Geyer, Larsson, & Morari, 2003; Lenstra, 1983; Pancanti et al., 2002).

Given the combination of less oscillatory and more economical performance (compared with the naive quantization) and constant trifling time complexity increase, it can be concluded that the agqNPC is the better and more attractive choice for the industrial application of control with discrete-valued input variables.

6. Conclusion

The task of advanced building climate control was formulated, several ways how to solve it using model based predictive control paradigm (namely linear MPC with ordinary linear model, nonlinear MPC and linear MPC with time-varying linear model) were presented and chosen practically oriented aspects were discussed in this paper.

Since the modeling and the estimation of the unknown parameters of the model structures is crucial for proper functionality of the predictive controller, the first part of the paper was devoted to the related problems. MRI method that is known to be the appropriate choice for the identification for predictive controllers with linear model was used for identification of the linear model structure and furthermore, it was adapted for use in case of nonlinear model structures. With both presented variants of the nonlinear MRI algorithm, models with good prediction properties were obtained. Furthermore, a bridge between the nonlinear and linear model structure was introduced by a switched linear approximated model (SLM). All identified models (linear model, nonlinear model and SLM model) were tested on a series of verification data and the achieved results certified them for use within the MPC scheme.

The next part of the paper covers the design of the predictive controller. The algorithm for both linear and the nonlinear MPC were provided. According to the specifications of the control systems presented in the Introductory Section, one of the manipulated variables might not be set with infinite resolution. Therefore, certain adaptations of the predictive controllers were necessary. For the linear MPCs, the adaptation consisted only in change of admissible post-processing values for mass flow rate and therefore, it was not discussed in the paper. However, the adaptation of nonlinear MPC was more delicate. Out of the three possible options (use of mixed-integer programming, naive a posteriori quantization and inclusion of mid-processing iteration into the optimization routine), the first one was abandoned due to its high computational requirements. While the naive a posteriori quantization represents only another post-processing procedure, the last option with the mid-processing iteration of the optimization algorithm adapts the original continuous-valued optimization and incorporates the information about the quantization directly into the optimization routine.

All the presented controllers were compared with respect to the pre-defined evaluative criterion based on the real-life requirements and costs. The results demonstrate that although the nonlinear continuous-valued predictive controller addresses the minimization of the given evaluative criterion in the best way, it was also quite time consuming. Therefore, the linear MPC exploiting the SLM model can be regarded as a reasonable trade-off between the optimality of the solution and the time complexity of the underlying optimization, especially in case of huge centrally-controlled building complexes where the complexity of the optimization task can be very high.
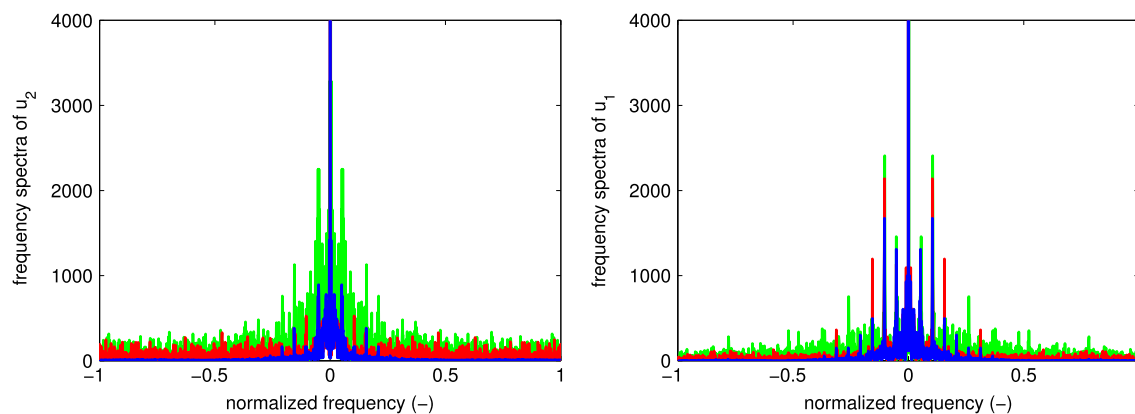
Fig. 10. Frequency spectra of the optimized variables, $N_{qst} = 8$ (━━ – continuous-valued NMPC, ━━ – nqNPC, ━━ – agqNPC).

41

The other part of the comparison was focused on evaluation of the performance of the nonlinear controllers under the restrictions on the discrete-valued nature of the mass flow rate. The provided comparison shows that the advanced of the inspected methods agqNPC is not only able to keep the economical aspects of the control closer to standard of the original continuous-valued controllers but also helps us to reduce the oscillations of the manipulated variables for the cost of a negligible *constant* time complexity increase. Therefore, it can be suggested that the advanced agqNPC algorithm be used in practice instead of naive but commonly frequently used a posteriori quantization.

Regarding the future work, it would be interesting to examine the effect of incorporation of the persistent excitation condition into the predictive controller procedure. Based on the available literature, if the persistent excitation condition is included, more informative data are obtained which then turns into a better ability to estimate the model parameters accurately. The suggested procedure should be compared with the advanced Kalman filtering algorithms such as Extended or Unscented Kalman filtering. Moreover, a procedure for the model parameter update should be designed for the nonlinear model. Last but not least, based on the performed numerical experiments the authors suggest the strategies be tested on a building in real operation.

Acknowledgment

References

Anderson, B. D. & Moore, J. B. (1971). *Linear optimal control* (Vol. 197). Englewood Cliffs: Prentice-Hall.

ASHRAE. (2009). *ASHRAE-handbook fundamentals*. NE Atlanta, GA: American society of heating, refrigerating and air-conditioning engineers, Inc.

Balmer, R. T. (2010). *Modern engineering thermodynamics-textbook with tables booklet.* Academic Press, Oxford, UK.

Barták, M. (2010). *Úvod do přenosových jevu pro inteligentní budovy*. Prague, Czech Republic: CTU Prague.

Bryson, A. E., & Ho, Y. C. (1975). *Applied optimal control: optimization, estimation, and control.* Taylor and Francis, Oxford, UK.

Bussieck, M. R. & Vigerske, S. (2010). MINLP solver software. In *Wiley encyclopedia of operations research and management science*.

Causa, J., Karer, G., Núñez, A., Sáez, D., Škrjanc, I., & Zupančič, B. (2008). Hybrid fuzzy predictive control based on genetic algorithms for the temperature control of a batch reactor. *Computers & Chemical Engineering, 32*(12), 3254–3263.

Chi, Q., Fei, Z., Zhao, Z., Zhao, L., & Liang, J. (2014). A model predictive control approach with relevant identification in dynamic PLS framework. *Control Engineering Practice, 22*, 181–193.

European Economic and Social Committee. (2005). S.M. act: Communication from the commission to the council, The European parliament, The European economic and social committee and the committee of the regions.

Falcone, P., Borrelli, F., Tseng, H. E., Asgari, J., & Hrovat, D. (2008). Linear time-varying model predictive control and its application to active steering systems: *Stability analysis and experimental validation. International Journal of Robust and Nonlinear Control, 18*(8).

Geyer, T., Larsson, M., & Morari, M. (2003). Hybrid emergency voltage control in power systems. In *Proceedings of the European control conference*, 2003.

Gopaluni, R., Patwardhan, R., & Shah, S. (2004). MPC relevant identification—Tuning the noise model. *Journal of Process Control, 14*(6), 699–714.

Gyalistras, D., & Gwerder, M. (2010). Use of weather and occupancy forecasts for optimal building climate control (OptiControl): Two years progress report. Terrestrial Systems Ecology ETH Zurich, Switzerland and Building Technologies Division, Siemens Switzerland Ltd., Zug, Switzerland.

Kaya, C. Y., & Noakes, J. L. (1996). Computations and time-optimal controls. *Optimal Control Applications and Methods, 17*(3), 171–185.

Laurí, D., Salcedo, J., Garcia-Nieto, S., & Martínez, M. (2010). Model predictive control relevant identification: *Multiple input multiple output against multiple input single output. Control Theory & Applications, IET, 4*(9).

Ledzewicz, U., & Schättler, H. (2002). Optimal bang–bang controls for a two-compartment model in cancer chemotherapy. *Journal of Optimization Theory and Applications, 114*(3), 609–637.

Lenstra, H. W., Jr. (1983). Integer programming with a fixed number of variables. *Mathematics of Operations Research, 8*(4), 538–548.

Lienhard, J. H. (2013). *A heat transfer textbook*. Courier Corporation, Cambridge, Massachusetts, USA.

Ljung, L. (1999). *System identification*. Wiley Online Library.

Ljung, L. (2007). System identification toolbox for use with {MATLAB}.

Ma, J., Qin, S. J., Li, B., & Salsbury, T. (2011). Economic model predictive control for building energy systems. In *2011 IEEE PES innovative smart grid technologies (ISGT)* (pp. 1–6). IEEE, Piscataway, NJ, USA.

Ma, Y., Kelman, A., Daly, A., & Borrelli, F. (2012). Predictive control for energy efficient buildings with thermal storage: *Modeling, stimulation, and experiments. IEEE Control Systems, Magazine, 32*(1), 44–64.

Oldewurtel, F., Gyalistras, D., Gwerder, M., Jones, C., Parisio, A., Stauch, V., et al. (2010). Increasing energy efficiency in building climate control using weather forecasts and model predictive control. In *10th REHVA world congress clima* (pp. 9–12).

Pancanti, S., Leonardi, L., Pallottino, L., & Bicchi, A. (2002). Optimal control of quantized input systems. In *Hybrid systems: computation and control* (pp. 351–363). Springer, Berlin Heidelberg, Germany.

Perez-Lombard, L., Ortiz, J., & Pout, C. (2008). A review on buildings energy consumption information. *Energy and Buildings, 40*(3), 394–398.

Prívara, S., Široký, J., Ferkl, L., & Cigler, J. (2011). Model predictive control of a building heating system: *The first experience. Energy and Buildings, 43*(2), 564–572.

Pčolka, M., Žáčeková, E., Robinett, R., Čelikovský, S., & Šebek, M. (2014). Economical nonlinear model predictive control for building climate control. In *American control conference (ACC), 2014* (pp. 418–423). IEEE, Piscataway, NJ, USA.

Pčolka, M., Žáčeková, E., Robinett, R., Čelikovský, S., & Šebek, M. (2014). From linear to nonlinear model predictive control of a building. In *IFAC world congress 2014* (Vol. 19, pp. 587–592).

R.O. for Network Industries. (2011). Approved electricity tariffs for the household consumers for 2011 (online). ⟨http://www.urso.gov.sk/doc/dokumenty/Por ovnanieMaxCienEEpreDomacnisti2011.pdf⟩, accessed: 03/11/2013.

Shook, D. S., Mohtadi, C., & Shah, S. L. (1991). Identification for long-range predictive control. In *IEEE proceedings D (Control theory and applications)* (Vol. 138, pp. 75–84). IET, Piscataway, NJ, USA.

Stetter, H. J. (1973). *Analysis of discretization methods for ordinary differential equations* (Vol. 23). Springer, Berlin Heidelberg, Germany.

University of Wisconsin-Madison, Solar Energy Laboratory, & Klein, S. A. (1979). *TRNSYS, a transient system simulation program*. Solar Energy Laboratory, University of Wisconsin–Madison.

Verhelst, C., Degrauwe, D., Logist, F., Van-Impe, J., & Helsen, L. (2012). Multi-objective optimal control of an air-to-water heat pump for residential heating. *Building Simulation, 5*, 281–291.

Wonham, W. M., & Johnson, C. (1964). Optimal bang–bang control with quadratic performance index. *Journal of Fluids Engineering, 86*(1), 107–115.

Žáčeková, E., & Prívara, S. (2012). Control relevant identification and predictive control of a building. In *2012 24th Chinese control and decision conference (CCDC)* (pp. 246–251). IEEE, Piscataway, NJ, USA.

Žáčeková, E., Váňa, Z., & Cigler, J. (2014). Towards the real-life implementation of MPC for an office building: *Identification issues. Applied Energy, 135*, 53–62.

Zhao, J., Zhu, Y., & Patwardhan, R. (2014). Some notes on MPC relevant identification. In *American control conference (ACC), 2014* (pp. 3680–3685). IEEE, Piscataway, NJ, USA.

Zhou, K., Doyle, J. C., Glover, K., (1996). *Robust and optimal control* (Vol. 40). New Jersey: Prentice Hall, Upper Saddle River, New Jersey, USA.

Zmrhal, V., & Drkal, F. (2006). The influence of heat convection on room air temperature. In *Proceedings of 17th air-conditioning and ventilation conference*.

Chapter 5

MPC with Guaranteed Persistent Excitation

In this chapter, the second contribution of the thesis (see Chapter 3) related to the persistently exciting MPC is addressed. It starts with an explanation of fundamental results for the standard MPC formulation given in Chapter 5.1. Than, an enhancement of the algorithm tailored for zone MPC is discussed in Chapter 5.2 and finally, an adaptation for predictive control for a class of nonlinear systems—namely bilinear systems— is presented in Chapter 5.3.

5.1   Standard MPC

In the previous chapter, it has been shown that applying a proper identification procedure, one can obtain a model suitable for the MPC even in case that the identification is performed using imperfect identification data suffering from quantization, correlation or strong noisiness. However, if more information can be "encoded" into data already when gathering them (ideally by means of an inexpensive identification experiment), the model identification process could be even further simplified and the resulting MPC performance could be considerably improved. In this thesis, one of a variety of possible procedures trying to accomplish this goal is provided. Apart from satisfying the classic MPC requirements, the presented MPC design ensures that the collected data are persistently excited, which is particularly beneficial for the subsequent re-identification.

The author's research devoted to this area started with the basic MPC formulation for which two novel algorithms leading to a persistently exciting MPC were developed. Both

of the designed methods are based on the following two-stage procedure:

1. In the first stage, the original MPC problem is solved which in case of the standard MPC formulation consists in minimization of squared input effort and squared reference tracking error subject to input inequality (box) constraints. This can be solved by any standard quadratic programming solver [Boyd and Vandenberghe, 2004].

2. The second stage aims at maximizing the future data informativeness quantified by the smallest eigenvalue of the information matrix increase. This optimization is performed in such a way that the original MPC performance corresponding to the input sequence obtained in the previous step is not violated by more than certain predefined value.

In total, three different variants of solving the optimization task formulated in the second stage of the aforementioned procedure were provided:

- **One-sample algorithm.** This candidate for the second-stage optimization takes advantage of the fact that the industrial MPC utilizes the receding horizon principle[1]. Based on this, the smallest eigenvalue of the information matrix increase calculated over an "excitation" horizon of M future steps is maximized, but only the first input sample is considered free and available for optimization with the rest of the input sequence being fixed and equal the original MPC input profile obtained in the previous step. Thanks to looking into the M-step future, the ability to excite also output directions is preserved and while the resulting optimization problem still remains non-convex, its dimension reduces to a single one and its globally optimal solution can be found executing a line search with reasonable time complexity. More details were given in [A.13].

- **Gradient algorithm.** To find the whole input sub-sequence of length M maximizing the smallest eigenvalue of the future increment of the information matrix, an algorithm based on the gradient search was designed. This approach benefits from more degrees of freedom available for informativeness maximization and even though finding the global optimum of the posed optimization task cannot be ensured, higher values of the informativeness quantifier can be reached than with the one-sample

---

[1]At each time instant, an input sequence for the entire prediction horizon is computed, but actually only the first input sample is applied to the system.

approach. The price to be paid, however, is the corresponding increase in computational complexity and longer calculation times. This approach was presented in [A.1] and [A.17].

- **Semi-receding horizon principle algorithm.** The last of the variants relies on a relaxation of the feedback the MPC introduces by obeying the receding horizon paradigm. The bottom line is as follows: having computed the input sequence optimizing the MPC cost function (stage 1), optimize M input samples with respect to the provided excitation criterion and then apply *the whole M-sample sequence.* Thanks to this relaxation, it is ensured that the inputs that are applied to the system are indeed those chosen as optimal with respect to bringing enough information. It can be argued that this might slightly degrade the closed-loop performance due to loosening the feedback, but for stable systems with $M \ll P$ (i.e. the excitation horizon is much shorter than the prediction horizon, which holds in most cases), the control performance is not harmed noticeably. This algorithm was introduced in [A.17].

A more detailed description of the first two mentioned algorithms (one-sample algorithm and gradient algorithm) including two comprehensive case studies and a comparison of their results was published in [A.1] while the algorithm applying the semi-receding horizon principle was presented in [A.17]. Both these papers are provided in the the original formatting and follow starting on the next page.

CrossMark

Persistent excitation condition within the dual control framework

Eva Žáčeková*, Samuel Prívara, Matej Pčolka

Department of Control Engineering, Faculty of Electrical Engineering, Czech Technical University in Prague, Czech Republic

ARTICLE INFO

ABSTRACT

Model Predictive Control framework is currently used in many different fields of expertise. The inherent part and very often also the main bottleneck is the model of a process used for the computation of predictions.

Due to many reasons e.g. ageing, from time to time there exists a need to adjust/re-identify (if there was already some kind of a model-based controller) or to construct a brand new model (in other cases). Frequently, the process generating the data is under some kind of control, imposing thus problems when classical open loop identification methods are considered. The need for models identified from the data gathered in a closed-loop fashion and a request for possible re-identification of the model parameters lead to the emerge of dual control where the problems of control and system identification are addressed simultaneously.

In this paper, we present a new algorithm based on the persistent excitation condition when the minimal eigenvalue of the information matrix is maximized in order to have sufficiently exciting optimal control signal satisfying the control requirements.

© 2013 Elsevier Ltd. All rights reserved.

1. Introduction

1.1. Motivation

Advanced control algorithms based on a system model such as Model Predictive Controller (MPC) have been a standard solution in many different fields and industries such as process [1], chemical [2], automotive [3,4], electronics [5] or even in so conservative field as building climate control [6–10].

The MPC possesses a number of advantages, e.g. it is able to handle constraints, has a capability of controlling the multivariable plants, incorporate model uncertainties, and moreover, it is easy to tune [11,12]. The main bottleneck of this framework is the necessity of a good mathematical model of the controlled process.

1.2. Closed-loop identification

It is a very frequent case that the data gathered for identification come from the operation under feedback conditions. The other usual case is a need for adaptive changes or the reconfiguration of model parameters. Standard open loop identification techniques usually fail in providing the model with a reasonable quality which could be subsequently used for predictive control. This is mostly caused by the input-noise correlation or the input being insufficiently excited [13,14].

Closed-loop identification was first introduced rather as a theoretical concept [15] but the motivation eventually changed [16] with possible use of the model for optimization in some advanced control technique [17]. There is a large amount of papers dealing with the problem of closed-loop identification, see e.g. [18–20] and especially nice overview of the whole range of possible approaches by [21], where the closed-loop identification approaches are based on (i) direct method in which the feedback is completely ignored and just the standard estimation is employed; or (ii) indirect method when a closed-loop system is identified using measurements of the reference input r_k and the output y_k. The plant model is retrieved using the known structure of the controller. This approach, however, requires a linear feedback and is therefore improper to use when MPC is considered; and finally, (iii) joint input–output method which uses y_k and u_k as outputs and r_k as an input for identification. Such an augmented system makes it possible to find an open loop model. A two-stage method [22] can be readily used in case that the controller is linear, otherwise the projection method [23] is available.

Later, the simultaneous control and identification formulations became the objective of the research. The pioneering work [24,25] showed that certain way of control of a process enriches the informative content of control input, improving thus subsequent adjustments/re-identification of the model of that process. The so

called dual control (DC) concept when control and identification problems are solved in parallel was introduced by [26]. However, the problem is analytically unsolvable [27] and numerical algorithms are usually computationally extensive [28–30]. One possible approximation modifies the MPC formulation such that the persistent excitation (PE) condition becomes one of the MPC constraints [31,32]. Unfortunately, this formulation results in a non-convex optimization task as well. Another approach presented in [33] utilizes the MPC with the receding horizon (RH) and the non-convex optimization is reformulated resulting in two quadratic programming (QP) tasks. The full regressor in this approach is replaced by inputs only leading to a poorer excitation in directions corresponding to the outputs. A partial solution was proposed by [34] where the maximization of the information matrix increment is considered such that the performance does not deviate from the original MPC by more than certain predefined bound, however, this approach leads again to a non-convex optimization. Moreover, the formulation is effective only for those single input single output (SISO) systems which are of the first order with autoregressive external input (ARX) model structures.

1.3. Contribution of the paper

In this paper, we introduce an algorithm which modifies the standard MPC formulation with RH to enable the effective incorporation of the PE condition. Compared to the current solutions, the presented algorithm is faster and enables identification of more complex systems.

It comprises two stages. In the first stage, a constrained optimization problem is solved providing thus the explicit solution to the second stage. The PE condition is included into the MPC criterion in the form of the maximization of the minimal eigenvalue of the information matrix increase. The optimal input u maximizes the information matrix increase and guarantees that the value of control criterion stays within the pre-defined range. An efficient implementation solving the DC problem is provided as well.

1.4. Organization of the paper

The paper is structured as follows. The formulation of a typical MPC problem is introduced in Section 2. Section 3 reviews the problem of the PE condition and its specifics within the DC framework. The key part of the paper is presented in Section 4 where the formulation of the maximization of the information matrix (MIM4DC) algorithm is provided. Moreover, a numerical algorithm GNA4DC being an alternative to the algorithms presented in the literature is proposed in this section. The case study in Section 5 demonstrates the properties of the MIM4DC algorithm and compares it to the numerical algorithm GNA4DC while the last section concludes the paper.

2. Problem formulation

In the following, we will formulate models used for the subsequent control problem, namely the standard ARX and the state space models.

2.1. Models used within the MPC framework

In the rest of the paper, we will use ARX(n_a, n_b, n_d) for the ARX model

$$y_k = -\sum_{i=1}^{n_a} a_i y_{k-i} + \sum_{i=1}^{n_b} b_i u_{k-n_d-i+1} + \varepsilon_k \tag{1}$$

with n_a, n_b and n_d denoting numbers of lagged inputs and outputs and the relative delay of the outputs w.r.t. the inputs, respectively and y_k, u_k and ε_k referring to the system output, input and white zero-mean Gaussian noise sequences. The predictor for parameters estimation in Eq. (1) can be written as:

$$y_{k|k-1} = Z_k^T \hat{\theta}, \tag{2}$$

with the parameters $\theta = [\hat{b}_{n_d}, \ldots, \hat{b}_{n_b}, -\hat{a}_1, \ldots, -\hat{a}_{n_a}]^T$ and regressor $Z_k = [u_{k-n_d}, \ldots, u_{k-n_b}, y_{k-1}, \ldots, y_{k-n_a}]^T$ and $y_{k|k-1}$ denoting one step-ahead predictions in time k based on information up to time $k-1$. Representation (1) is equivalent to the well-known state-space description [35]

$$\begin{aligned} x_{k+1} &= Ax_k + Bu_k + Ww_k, \\ y_k &= Cx_k + Du_k + w_k, \end{aligned} \tag{3}$$

where k is the discrete time, $x \in \mathbb{R}^n$, $u \in \mathbb{R}^m$, $w \in \mathbb{R}^v$, $y \in \mathbb{R}^p$ and A, B, C, D, W are the matrices of appropriate dimensions.

2.2. Formulation of the control problem

The typical formulation of the MPC can be readily expressed as follows

$$J_{MPC,k} = \sum_{i=1}^{P} \left\| Q(y_{k+i} - y_{k+i}^{ref}) \right\|_2^2 + \left\| Ru_{k+i} \right\|_2^2$$

$$\begin{aligned} s.t. : & \text{ linear } dynamics \, (3), \\ & x_k = x_{init}, \\ & u_{k+i}^{min} \le u_{k+i} \le u_{k+i}^{max}, \\ & \Delta u_{k+i}^{min} \le \Delta u_{k+i} \le \Delta u_{k+i}^{max}. \end{aligned} \tag{4}$$

with y_k^{ref} specifying the reference trajectory, Q and R are the control algorithm tuning matrices of the appropriate size and P is the prediction horizon. Formulation (4) can be readily solved by commonly available solvers.

The classical MPC is usually used with the receding horizon (RH) where at each time step k, the optimization task (4) is solved, that is, the optimal input sequence on the horizon P is computed, however, only the first sample u_k is applied and the procedure is repeated. This formulation ensures constraints satisfaction and attractive performance compared to the alternative methods. The bottleneck of the approach is its dependence on the model quality (here, the model refers to a mathematical description of the system used by MPC to obtain the future predictions), i.e. its ability to predict the future behavior of the controlled process. In many cases, it is necessary to re-identify model parameters. As the data are gathered from the real operation—from the process which is under control—the commonly used identification methods fail, mostly due to the input-noise correlation and/or insufficient excitation.

The insufficient excitation is problematic and especially urgent when the reference changes slowly (causing a very low information content of the data). One possible approach to tackle this problem in the MPC framework is to include the PE condition into the cost function (4). If the PE is guaranteed, the input-noise correlation problem is partly solved. The input-noise correlation has an influence on the accuracy of the identified parameters as well, i.e. the accuracy of the estimation depends on the signal-to-noise ratio (SNR). In the following, we will discuss the problem of incorporating the PE condition into the MPC cost function.

3. Persistent excitation condition within the dual control problem

In the current paper, we consider the model-based control approaches when a model-plant mismatch has direct consequences on the quality of predictions causing thus control performance degradations. The use of the closed-loop (CL) system identification, i.e. identification with the running controller, can lead to a better model [34]. On the other hand, to apply this approach, a sufficiently informative input (PE condition) is required, which unfortunately can not be attained by a standard formulation (e.g. Eq. (4)) of the control problem. DC is an approach that formulates identification and control problems in a unified manner. Unfortunately, the DC problem can not be (in general) solved analytically [27].

There is a number of approximative solutions and some of them are based on the PE condition. As the new algorithm presented in this paper is based on the PE condition, a short introduction is provided here. Considering the model given by Eq. (2), the increment of information matrix from the time k to the time $k+M$ can be written as:

$$\Delta I_k^{k+M} = \sum_{t=k+1}^{k+M} Z_t Z_t^T. \tag{5}$$

Then, the PE condition can be formulated in the following form:

$$\Delta I_k^{k+M} \geq \gamma I > 0 \tag{6}$$

where γ is a scalar specifying the level of the required excitation, I is a unit matrix of corresponding dimensions. The most straightforward solution is to include the condition (6) as one of the MPC constraints (4). This approach, however, suffers from several drawbacks, e.g. Eq. (6) comprises the output predictions (besides the inputs) which are problematic to formulate within Eq. (4). One way how to solve this problem which can be found in the available literature [36,37] is to use the following approximation of the information matrix increase:

$$\Delta \tilde{I}_k^{k+M} = \sum_{t=k+1}^{k+m} \psi_t \psi_t^T \tag{7}$$

with $\psi_t = [u_{t-n_d} \cdots u_{t-n_b}]^T$. This approximation, unfortunately, does not ensure PE in every direction and leads to a biased estimate of parameters $a_1, \ldots, a_{n_a}$ in θ. Note that Eq. (7) introduces a quadratic matrix inequality which can be transformed into a linear matrix inequality [32] and then, a semi-definite programming task can be solved.

Yet another approach by [33] utilizes the MPC with RH. The non-convex optimization problem is thus significantly simplified. At each time step, only the first sample of the computed input sequence is applied and therefore, it is possible to replace a semi-definite program with a doubly solved QP problem. This approach, however, suffers from a few disadvantages caused by the very obscure formulation of the problem as it does not consider the fact that the applied u influences the information brought by the future system outputs. Omitting the rest of the input sequence, the excitation is aggressive in a few short segments and it is effective in one direction only which perturbs the results of the original MPC formulation. An alternative solution was proposed by [34]. This approach consists of a two-step procedure where in the first step, the classical MPC problem Eq. (4) is solved. In the second step, the task of the maximization of the information matrix increase is solved such that the performance does not deviate from the original MPC by more than certain predefined bound as follows:

$$\begin{aligned}
&\mathcal{U}^* = \underset{\mathcal{U}}{arg\max} \gamma \\
&\text{s.t.} : \Delta I_k^{k+M} \geq \gamma I, \\
&J_{MPC,k}(\mathcal{U}^*) \leq J_{MPC,k}^* + \Delta J, \\
&u_k^{min} \leq u_k \leq u_k^{max}, \\
&\Delta u_k^{min} \leq \Delta u_k \leq \Delta u_k^{max},
\end{aligned} \tag{8}$$

where ΔJ specifies the maximum allowed increment of the original MPC cost function (4). Compared to the previous approaches, this one has one huge advantage: here the tuning parameter is directly the allowed perturbation—its choice is simpler than the choice of the required excitation level γ. This increase can be (depending on Q and R) simply transformed into control costs increase and/or the reference deviation which is advantageous especially in practical applications. The next indisputable advantage is the fact that in this formulation, the real information matrix increase ΔI is handled directly instead of its approximation $\Delta \tilde{I}$ which enables to optimize the excitation in the output directions as well. However, the main drawback of this approach is the fact that the optimization task solved in the second step is non-convex and search for the global optimum is very time consuming. The authors of [38] used so called ellipsoid algorithm to solve the optimization task (8). This algorithm is based on the idea of constraining the smallest eigenvalue of the inverse of the information matrix from above by a specific quadratic form. As the authors note, the disadvantage of this approach is the fact it can be effectively used only for systems of lower orders.

4. Algorithms for maximization of information matrix

The new algorithm for solving the DC problem is proposed here. This approach comes out of the one provided by [34], however, it makes the original algorithm more effective, less time consuming and also able to cope with higher order systems.

First, let us remark that the industrial MPCs usually work with RH repeating the optimization procedure from the beginning at each step of the iterations using the current measurements which brings the desired feedback into the concept. Trying to solve the optimization task (8), the authors of [38,34] optimize $k+M$ elements of the input sequence to maximize the information matrix increase. However, as only the first element of the calculated sequence is to be applied, the actual information matrix increase might not correspond to the one calculated by their algorithm.

In the current paper, we extend the mentioned algorithm such that we only look for the u_k element and next elements of $\mathcal{U}$ are the same as calculated by the MPC. This adaptation enables us to reduce the complex non-convex problem into a one-dimensional optimization which can be effectively solved via exhaustive search. Assuming that the remaining elements of the $\mathcal{U}$ sequence are close to those calculated by the MPC, this formulation leads to a better algorithm performance.

In the following, the proposed algorithm is described in more detail in Section 4.1. Then, a numerical solution to the problem (8) is presented in order to compare the presented algorithm with the original formulation from [34].

4.1. MIM4DC algorithm

Now, the MPC-based procedure solving the DC problem can be formulated. After choosing proper values of ΔJ and M, the two-stage MIM4DC algorithm is able to solve the problem of the sufficient excitation in all directions at the cost of minimal

48

perturbation of the original MPC cost function (4). This solution outperforms the existing algorithms. Detailed description of both stages of MIM4DC follows.

4.1.1. Stage I

In the first stage, the optimization task (4) is solved resulting into the optimal control sequence $\mathcal{U}_{MPC}^* = [u_{MPC,k} \; u_{MPC,k+1} \cdots u_{MPC,k+P}]^T$. Then, the cost function $J_{MPC,k}^* = J_{MPC,k}(\mathcal{U}_{MPC}^*)$ is evaluated and its value becomes the threshold for the second stage. Afterwards, the maximal allowed ΔJ perturbation is chosen. In order to solve the maximization of the information matrix increment easily, it is possible to rewrite the constraint $J_{MPC,k}(\mathcal{U}) \leq J_{MPC,k}^* + \Delta J$ into a form $\mathcal{U}^{min} \leq \mathcal{U} \leq \mathcal{U}^{max}$. Recall that only the first element u_k of $\mathcal{U}$ is applied. Only u_k^* instead of $\mathcal{U}^*$ is needed and the rest is fixed as:

$$u_{k+i}^* = u_{MPC,k+i} \quad \text{for } i \in \{1, \cdots, M-2\}. \tag{9}$$

Now, the constraints $J_{MPC,k}(\mathcal{U}) \leq J_{MPC,k}^* + \Delta J$ can be transformed into $\overline{u}_k^{min} \leq u_k \leq \overline{u}_k^{max}$, where $\overline{u}_k^{max}$ and $\overline{u}_k^{min}$ are the values for which the cost function $J_{MPC,k}$ reaches values $J_{MPC,k}^* + \Delta J$ assuming that Eq. (9) holds. It could appear that the following matrix quadratic equation needs to be solved:

$$\frac{1}{2}\mathcal{U}^T H \mathcal{U} + j\mathcal{U} - (J + \Delta J) = 0, \tag{10}$$

in order to obtain $\overline{u}_k^{min}$ and $\overline{u}_k^{max}$. In Eq. (10), H is a symmetric positive definite $P \times P$ matrix and j is a row vector of length P, obtained by rewriting the MPC formulation (4) into the quadratic programming problem [39].

However, realize that due to Eq. (9), all the elements of $\mathcal{U}$ except for u_k are known, the following simple scalar quadratic equation can be solved instead of Eq. (10):

$$au_k^2 + bu_k + c = 0, \tag{11}$$

where

$$a = \frac{1}{2}h_{k,k},$$
$$b = \frac{1}{2}\sum_{i=1}^{P-1} u_{MPC,k+i}h_{1,k+i} + j_k, \tag{12}$$
$$c = \sum_{i=1}^{P-1} u_{MPC,k+i}j_{k+i} + \frac{1}{2}\sum_{j=k}^{P}\sum_{i=1}^{P-1} u_{MPC,k+i}h_{k+i,j} - (J + \Delta J).$$

Symbol $h_{m,n}$ refers to the element of H in the m-th row and in the n-th column. $\overline{u}_k^{min}$ and $\overline{u}_k^{max}$ are then found as the roots of Eq. (11). In order to satisfy constraints given by Eq. (4), the found constraints $\overline{u}_k^{min}$ and $\overline{u}_k^{max}$ should be compared with the original constraints u_k^{min} and u_k^{max}. Finally, the constraints to use in the second stage are computed as follows:

$$\tilde{u}_k^{max} = \min\{\overline{u}_k^{max}, u_k^{max}\}, \tag{13}$$

$$\tilde{u}_k^{min} = \max\{\overline{u}_k^{min}, u_k^{min}\}. \tag{14}$$

The process of looking for $\tilde{u}_k^{max}$, $\tilde{u}_k^{min}$ is depicted in Fig. 1.

4.1.2. Stage II

The goal of the second stage is to find u_k^* that ensures the best excitation in all directions by the maximization of the information matrix increment (8). $\tilde{u}_k^{max}$, $\tilde{u}_k^{max}$ obtained in the first step are used to restrict the perturbation of the original MPC cost function (4). It is possible to formulate the maximization of the information matrix increment as the minimal eigenvalue maximization. The general problem (8) can be then formulated as the following simple task:

$$\begin{aligned}
u_k^* &= \arg \max_{u_k} \left(\lambda_{\min}\left(\Delta \hat{I}_k^{k+M}\right)\right) \\
&\text{s.t.: } \tilde{u}_k^{min} \leq u_k \leq \tilde{u}_k^{max}, \\
&u_{k+i} = u_{MPC,k+i}, \quad \text{for } i \in \{1, \cdots, M-2\}.
\end{aligned} \tag{15}$$

Note that $M < P + 1$. To make Eq. (15) unambiguous, $\hat{Z}_t$ is defined as follows:

$$\hat{Z}_t = \begin{bmatrix} u_{t-n_d} & \cdots & u_{t-n_b} & y_{t-1}^{\alpha} & \cdots & y_{t-n_a}^{\alpha} \end{bmatrix}^T, \tag{16}$$

where

$$y_t^{\alpha} = \begin{cases} \hat{y}_{t|k-1} & \text{if } t > k-1, \\ y_t & \text{if } t \leq k-1. \end{cases} \tag{17}$$

It follows that $\hat{y}_{t|k-1}$ is in the form of Eq. (2) with Eq. (16).

The remaining issue is to solve this non-convex optimization problem for which it is generally difficult to obtain a global optimum. However, given the optimization task reformulated as a one-dimensional optimization on a bounded interval and a constrained solution from above and below $\mathcal{U}_{add} = \{u_k^* : \tilde{u}_k^{min} \leq u_k^* \leq \tilde{u}_k^{max}\}$, the most straightforward approach is to search through the whole interval $\mathcal{U}_{add}$. This is usually not that demanding from the computational time point of view as the tightness of the boundaries
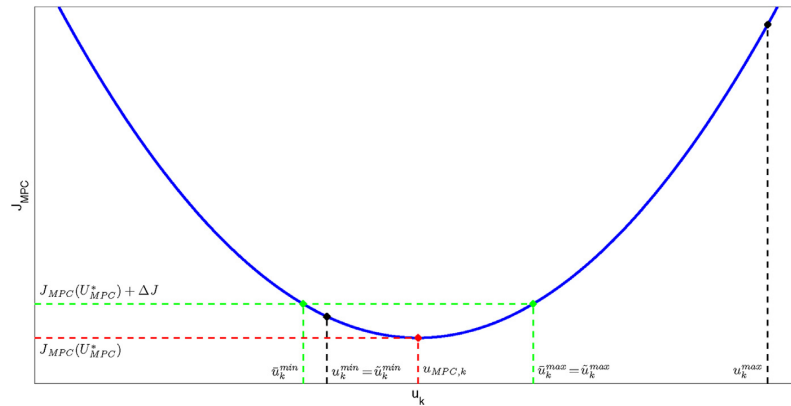

Fig. 1. Search for $\tilde{u}_k^{min}$ and $\tilde{u}_k^{max}$.

49

of u_k^* rise (the computational demand decreases) with the decrease of the maximal allowed perturbation ΔJ. Additional computational relaxation can be achieved by choosing a proper sampling of the admissible input set $\mathcal{U}_{add}$, which can be easily accomplished considering the resolution of the sensors measuring u in practical applications.

In case of higher significance of the PE compared to the performance quality given by Eq. (4), the maximal allowed perturbation ΔJ is larger and the computational cost of the search grows. In that situation, the following hint for the search of u_k^* is suggested. Consider $\mathcal{U}_{add}$: in such case, it undoubtedly holds that the smallest eigenvalue of the matrix rises towards the boundaries of the interval $(\mathcal{U}_{add}, \pm\infty)$. Thus, if the chosen ΔJ is sufficiently large and the interval $\mathcal{U}_{add}$ is sufficiently broad (which does not necessarily mean it is infinite), the boundary values of the interval ensure maximization of the minimal eigenvalue of the information matrix increment.

This property can be explained intuitively (for sufficiently large $\mathcal{U}_{add}$) as well. As the MPC drives the system into a certain stationary point where the information increase is minimal, the input maximizing the information increase corresponds to the boundary value that is farthest from the optimal value computed by the MPC.

4.2. Gradient Numerical Algorithm for Dual Control (GNA4DC)

In this subsection, the numerical solution to the problem Eq. (8) is described. The algorithm GNA4DC is based on the classical gradient approach which is well known in the area of numerical optimization [40].

The initialization of this algorithm is quite similar to the initialization of the previously mentioned MIM4DC algorithm. First of all, the optimization task Eq. (4) is solved and the optimal input sequence $\mathcal{U}_{MPC}^* = [u_{MPC,k}\, u_{MPC,k+1} \cdots u_{MPC,k+P}]^{\mathrm{T}}$ and the corresponding MPC cost function value $J_{MPC,k}^* = J_{MPC,k}(\mathcal{U}_{MPC}^*)$ are obtained. The first M samples of the input sequence $\mathcal{U}_{MPC}^*$ are further used as the initial guess $\mathcal{U}_0$ for the gradient search while the corresponding MPC cost function value $J_{MPC,k}^*$ serves as the constraint in the further procedure.

Basically, the main idea of this numerical algorithm can be formulated as follows: at each sampling instant k, we are looking for such input sequence that the amount of provided information contained in the corresponding input/output data is maximal while the behavior of the original MPC should not be degraded of more than ΔJ. To examine this amount, the smallest eigenvalue of the information matrix increase is inspected. Then, assuming a performance criterion $\mathcal{J} = \lambda_{min}$ being the smallest eigenvalue of the information matrix increase, the optimal input sequence $\mathcal{U}^*$ maximizing this criterion,

$$\mathcal{U}^* = \arg\max_{\mathcal{U}} \left(\lambda_{\min} \left(\Delta \hat{I}_k^{k+M} \right) \right) \tag{18}$$

can be found iteratively starting from an initial guess $\mathcal{U}_0$. The iterative procedure can be explained as a search in the direction of the gradient of the performance criterion λ_{min} and mathematically, it is formulated as:

$$\mathcal{U}_{i+1} = \mathcal{U}_i + \alpha \nabla \lambda_{min}. \tag{19}$$

Here, α is the gradient search step and $\nabla \lambda_{min}$ stands for gradient of the λ_{min} with respect to the optimized sequence $\mathcal{U}$. The algorithm is terminated if the improvement of the optimized criterion λ_{min} is less than a chosen tolerance. Last but not least, let us note that as the initial guess $\mathcal{U}_0$, the corresponding subsequence of the optimal input calculated by the original MPC is used.

Regarding the convergence and performance quality, both the choice of the search step α and calculation of the gradient $\nabla \lambda_{min}$ are of crucial importance. Firstly, the gradient of the optimization

criterion might be sometimes very difficult to calculate analytically which requires alternative ways of its computation. Secondly, even the already calculated gradient is valid only in a small region in the multidimensional space of the samples of the optimized sequence $\mathcal{U}$ around the "operating point" at which it was calculated. In the current paper, both these aspects are taken into consideration and a simple yet very effective solution is proposed.

First of all, let us recapitulate the optimization task which is to be solved: we are looking for such input sequence $\mathcal{U}$ which maximizes the smallest eigenvalue λ_{min} of the information matrix (being the quality criterion for this optimization task) while the MPC cost function perturbation is smaller than a pre-defined value and the original input constraints are satisfied. Mathematically, this task can be formulated as follows:

$$\mathcal{U}^* = \arg\max_{\mathcal{U}} \left(\lambda_{\min} \left(\Delta \hat{I}_k^{k+M} \right) \right)$$
$$\text{s.t.} : \mathcal{U}^{min} \leq \mathcal{U} \leq \mathcal{U}^{max}, \tag{20}$$
$$J_{MPC}(\mathcal{U}^*) \leq J_{MPC,k}^* + \Delta J,$$

M is the number of input samples that can be optimized.

It has been already mentioned that the analytical calculation of the gradient $\nabla \lambda_{min}$ of the quality criterion might be very cumbersome and this is exactly the case of the maximization of the smallest eigenvalue. Instead of analytical calculation, a numerical alternative is proposed as follows:

Let us assume that at each iteration i of this algorithm, the starting (unperturbed) input sequence u_{unp} represents the input sequence found at the end of the previous iteration and its application to the system results in the information matrix with the smallest eigenvalue $\lambda_{min,unp}$. Here, we recall that the smallest eigenvalue is directly the optimized performance criterion in this optimization task. At every iteration, each of the input samples (one by one) u_l can be perturbed with some set of additive perturbations $\boldsymbol{\Delta}_{\mathcal{AP}}$ being a set of multiples of a chosen least perturbation step LPS. Then, a set $\mathbf{S}^l$ of the input vectors can be created representing a group of such input vectors $[u_1, u_2, \ldots, u_{l,q}^{\Delta}, \ldots, u_M]$[1] where the l-th sample $u_{l,q}^{\Delta} = u_l + \Delta_{ap,q}$ is perturbed with certain perturbation $\Delta_{ap,q}$ from the chosen set. In this application, the set of perturbations $\boldsymbol{\Delta}_{\mathcal{AP}} = \{\Delta_{ap,q}\}$ is considered as follows:

$$\boldsymbol{\Delta_{AP}} = \{[-20, -4, -2, -1, 0, 1, 2, 4, 20] \times LPS\}.$$

Let us note that the rest of the input samples remains unchanged (equal to their values in the starting input sequence u_{unp}). Then, assuming particular $\mathbf{S}^l$, the set of smallest eigenvalues $\boldsymbol{\Lambda}^l$ resulting from application of each vector from the group $\mathbf{S}^l$ to the system can be calculated. Here, the superscript l refers to the position of the perturbed input sample. In our case, the set $\boldsymbol{\Lambda}^l$ has 9 members, each of them corresponding to particular perturbation element from the set $\boldsymbol{\Delta_{AP}}$ while the middle member (corresponding to $\Delta_{ap,5} = 0$) is in fact equal to the "unperturbed" smallest eigenvalue $\lambda_{min,unp}$ and therefore, it is not necessary to evaluate it once again at that iteration.

Having done this, it can be seen that considering particular l the changes of the smallest eigenvalue are caused only by the perturbation of the l-th input sample u_l and therefore, the obtained values of $\boldsymbol{\Lambda}^l$ can be used to approximate $\boldsymbol{\Lambda}^l$ as a piecewise polynomial function of the input perturbation $\boldsymbol{\Delta}$ using spline interpolation technique,

$$\boldsymbol{\Lambda}^l = s^l(\boldsymbol{\Delta}).$$

---

[1] Here, M is the number of the input samples that can be optimized.

As the explanation of the principles and the practical realization of the spline interpolation is beyond the scope of this paper, interested readers are referred to [41]. The piecewise polynomial nature of the spline interpolation can be used with advantage to find such value of perturbation Δ_{ap}^* for which the improvement of the smallest eigenvalue is maximal. Note that this extreme point might not belong to the original set $\boldsymbol{\Delta}_{\mathcal{AP}}$, however, it should be searched for only within the interval $\langle \min(\boldsymbol{\Delta}_{\mathcal{AP}}), \max(\boldsymbol{\Delta}_{\mathcal{AP}})\rangle$. The mentioned spline interpolation and subsequent choice of the extreme point can be performed for each position l of the perturbed input sample and the obtained perturbation values $\Delta_{ap}^{*,l}$ can then be stored in a vector $\mathcal{G} = [\Delta_{ap}^{*,1}, \Delta_{ap}^{*,2}, \ldots, \Delta_{ap}^{*,M}]$. The vector $\mathcal{G}$ has a very interesting property – as it was chosen as a set of extreme points for various position l of the perturbed input sample, it can be directly substituted for the expression $\alpha \nabla \lambda_{min}$ in the iterative procedure Eq. (19) which is then changed as follows:

$$\mathcal{U}_{i+1} = \mathcal{U}_i + \mathcal{G}_i. \tag{21}$$

Here, the subscript i in $\mathcal{G}_i$ refers to particular iteration of the iterative procedure.

In order to satisfy the input constraints, a simple projection of the input profile on the admissible interval is performed,

$$\mathcal{U}_{i+1} = \max(\mathcal{U}_{min}, \min(\mathcal{U}_{max}, \mathcal{U}_i + \mathcal{G}_i)) \tag{22}$$

ensuring that at each iteration i, the values of the samples of input profile lie within the acceptable interval $\langle \mathcal{U}_{min}, \mathcal{U}_{max}\rangle$.

The constraint for the original MPC cost function violation are handled evaluating also the MPC cost function $J_{MPC}(\mathcal{U}_i)$ at every iteration i of this iterative gradient search algorithm and comparing it to the maximal allowed perturbation ΔJ. If at certain iteration i such situation occurs that the current MPC cost function $J_{MPC}(\mathcal{U}_i)$ is higher than $J_{MPC,k}^* + \Delta J$, the iterative gradient search algorithm is terminated. By choosing sufficiently small least perturbation step $LPS \to \mathrm{d}u$ and by assuming continuous and smooth dependence of the original MPC cost function violation on the change of the input samples, the MPC cost function violation constraint is effectively and satisfactorily handled using this approach.

Last of all, let us mention that unlike the algorithm proposed in [38], GNA4DC algorithm is able to solve the task of information matrix maximization for arbitrarily large systems and is therefore more general and applicable than the mentioned one.

5. Case study

First we provide the comparison of MIM4DC, GNA4DC and classical MPC algorithms and discuss the choice of settings on a simple example. Second, we introduce an example representing the system with varying parameters to demonstrate the ability of the MIM4DC algorithm to perform well in the role of an adaptive controller which can handle the change of the system parameters while satisfying the required control performance.

5.1. Scholar example

To show the basic properties and to demonstrate the performance of the MIM4DC, a simple SISO system with ARX structure was chosen

$$y_k = Z_k^{\mathrm{T}}\theta + \epsilon_k$$

$$y_k = 0.01u_{k-1} + 0.0008u_{k-2} + 0.00087u_{k-3} + 0.996y_{k-1} \tag{23}$$
$$+ 0.36y_{k-2} - 0.376y_{k-3} + \epsilon_k$$

with y, u, ϵ being output, input and white noise sequences. In fact, this example was not chosen arbitrarily as it mimics a simplified heat transfer model between the heating medium and zone air in

a one-zone building with the constant ambient temperature and sampling period $T_s = 15$ min.

This model is used for the design of the controller implemented within the MPC framework with the objective of minimizing supplied energy (temperature of the heating medium u) and satisfying thermal comfort (to keep the output y as close to reference value as possible). Following Eq. (4), the MPC cost function is formulated as

$$J_k = \sum_{i=1}^{P} \left\| Q(\hat{y}_{k+i} - y_{k+i}^{ref}) \right\|_2^2 + \left\| Ru_{k+i} \right\|_2^2 \tag{24}$$

subject to

$$\begin{aligned} &\text{linear } dynamics\,(3) \\ &20\,^\circ\mathrm{C} \le u_{k+i} \le 55\,^\circ\mathrm{C}, \\ &-1\,^\circ\mathrm{C} \le \Delta u_{k+i} \le 1\,^\circ\mathrm{C}, \end{aligned} \tag{25}$$

where the required outputs y^{ref} are generated in accordance with the seven-day schedule with night and weekend setbacks:

$$\begin{aligned} y^{ref} &= 22\,^\circ\mathrm{C}, \text{ work days } 8:00\,am - 6:00\,pm \\ y^{ref} &= 20\,^\circ\mathrm{C}, \text{ weekend, holidays } 6:00\,pm - 8:00\,am. \end{aligned} \tag{26}$$

The chosen prediction horizon $P = 60$ steps corresponds to 15 h ($T_s = 15$ min). Weighting matrices are $Q = 1000$ and $R = 1$. Initially, the closed loop data with length $N = 10000$ was generated controlling the system Eq. (23) with noise variance $\sigma_e = 0.015$ using the MPC described earlier. Note that in order to get closer to the real situation and to simulate the model inaccuracy, the model of the system used by MPC did not fully correspond to the real model Eq. (23) but it was slightly changed $\hat{a}_1 = -0.99$, $\hat{a}_2 = -0.359$, $\hat{a}_3 = 0.372$, $\hat{b}_1 = 0.01$, $\hat{b}_2 = 0.00079$, $\hat{b}_3 = 0.0009$. The same set-up is used also for MIM4DC for several tuning parameter settings $M = 6$, …, 12 and $\Delta J = 60, 80, 100$ and for parameter settings $M = 6, \ldots, 12$ a $\Delta J = 80, 100, 120$. These choices of ΔJ were picked up intentionally to obtain controllers with the closest settings as in both algorithms, the choice of ΔJ is of different meaning - while in case of MIM4DC, the whole maximal perturbation ΔJ is caused only by u_k, in case of GNA4DC is this perturbation divided amongst all M input samples. Let us remark that we intentionally chose M such that $M \ge n_a + n_b$ as if $M < n_a + n_b$ then $n_a + n_b - M$ eigenvalues of the information matrix increase Δl_k^{k+M} are equal to zero as we sum M multiplications vv^{T} where v is a vector $(n_a + n_b) \times 1$.

All three algorithms MPC, MIM4DC and GNA4DC were then compared from two points of view. The first factor we were interested in was how well the particular algorithm satisfied the control performance defined by the cost function J_{MPC}. Here, we inspected both the average reference tracking error $e_y = \frac{1}{N}\sum_{k=1}^{N}|y_k - y_k^{ref}|$ and the energy consumption of both MIM4DC and GNA4DC compared to the classical MPC. The energy consumption comparison is expressed as

$$I_E = \frac{\sum_{k=1}^{N} u_{M,k}^2}{\sum_{k=1}^{N} u_{MPC,k}^2}(\%), \tag{27}$$

where $u_{M,k}$ stands for the input generated by one of the proposed algorithms for dual control with tuning parameter M. Finally, we evaluated also the overall increase of the cost function for the cases of the proposed algorithms compared to the original *MPC* which we expressed using the following relations.

Let us consider the overall value of the cost function over the whole experiment:

$$J_{res} = \frac{1}{N}\sum_{k=1}^{N} \left\| Q(y_k - y_k^{ref}) \right\|_2^2 + \left\| Ru_k \right\|_2^2. \tag{28}$$

Table 1
Results for MIM4DC with different parameter settings.

	$\Delta J = 60$					$\Delta J = 80$					$\Delta J = 100$				
	e_y	$I_e(\%)$	$\overline{\Delta J}$	$\lambda_{min}(\Delta I_1^N)$	q_e	e_y	$I_e(\%)$	$\overline{\Delta J}$	$\lambda_{min}(\Delta I_1^N)$	q_e	e_y	$I_e(\%)$	$\overline{\Delta J}$	$\lambda_{min}(\Delta I_1^N)$	q_e
$M=6$	0.089	0.93	21.4	1.26	669.1E−9	0.098	1.21	28.1	1.61	172.2E−9	0.097	1.57	34.9	1.92	804.3E−10
$M=7$	0.078	1.07	20.3	1.30	146.5E−10	0.082	1.42	27.1	1.62	220.3E−8	0.088	1.83	34.0	1.94	256.7E−10
$M=8$	0.074	1.21	21.6	1.47	120.1E−8	0.076	1.64	28.5	1.86	725.8E−9	0.081	2.06	35.3	2.27	855.9E−9
$M=9$	0.077	1.19	21.6	1.23	279.9E−8	0.081	1.57	28.8	1.48	815.3E−9	0.086	1.92	35.8	1.65	260.1E−9
$M=10$	0.079	1.14	22.4	0.90	947.7E−10	0.084	1.57	29.2	1.08	874.7E−10	0.088	1.92	35.9	1.28	535.2E−9
$M=11$	0.080	1.14	22.7	0.94	990.5E−11	0.085	1.57	30.1	1.10	147.3E−8	0.090	2.00	37.3	1.30	140.6E−9
$M=12$	0.076	1.21	22.8	1.03	648.5E−9	0.081	1.64	30.2	1.21	669.2E−9	0.086	2.06	37.5	1.44	645.8E−9
MPC	0.068	0.00	0.0	0.28	240.0E−5	0.068	0.00	0.0	0.28	240.0E−5	0.068	0.00	0.0	0.28	240.0E−5

Then,

$$\overline{\Delta J} = J_{res,MPC} - J_{res,M} \qquad (29)$$

where the subscript *MPC* specifies the value of the cost function of the original MPC while the subscript *M* denotes the particular setting of the dual control algorithm (MIM4DC or GNA4DC).

Besides the evaluation of the control performance satisfaction, we are also interested in how much information contains the data and if it is possible to identify the parameters well. To evaluate the information content of the data generated by the respective algorithms, the smallest eigenvalue of the information matrix increase is taken and evaluated at each k (denoted as $\lambda_{min}(\Delta I_1^N)$). In fact, by this parameters we measure how well are we able to identify the parameters with the worst identifiability. In order to measure how the amount of gathered information improves the identifiability of the particular parameters, we introduce q_E expressing the quality of parameter estimation as follows:

$$q_E = (E(\hat{\Theta}) - \theta_0^{\mathrm{T}}) S (E(\hat{\Theta}) - \theta_0^{\mathrm{T}})^{\mathrm{T}}, \qquad (30)$$

where

$$S = \frac{1}{n-1}(\hat{\Theta} - E(\hat{\Theta}))^{\mathrm{T}}(\hat{\Theta} - E(\hat{\Theta})) \qquad (31)$$

is a sample covariance matrix. Here, $\hat{\Theta} = [\hat{\theta}_1 \ldots \hat{\theta}_n]^{\mathrm{T}}$. Parameters θ_i specify identified parameters from i-th set of data and n is the number of identified models.

Before summing-up the results, recall that the main objective is to acquire (provided by the controller) data with a rich information content while not to deteriorate control by more than the predefined value.

Tables (1) and (2) compare the behavior of the classical MPC, MIM4DC and GNA4DC for various settings. Looking at the energy consumption, it can be observed that both dual control algorithms consume slightly more energy than the classical MPC, however, the energy consumption increase I_e stays within 0.5–2% depending on the current setting. For the reference tracking, one can observe the same result being a negligible aggravation in case of each of the dual control algorithms. However, the most important factor in this comparison is the satisfaction of the sufficient excitation requirement. The outcome is that both proposed dual control algorithms provide data which are much more excited than those provided by the classical MPC for all the settings. While for the classical MPC, $\lambda_{min}((\Delta I_1^N))$ is approximately 0.28, it is 4–8 times higher with the dual control algorithms. The superior ability of MIM4DC and GNA4DC to identify parameters θ accurately is demonstrated by q_E which measures inaccuracy of the estimation – this value is significantly lower for an arbitrary setting of these algorithms.

The next phenomenon that can be observed is that increasing ΔJ, both dual control algorithms consume more and more energy (measured by I_e) and this is accompanied by the increase of delivered information. This was of course expected as increase of ΔJ basically offers more freedom for excitation which is reflected by the data of higher quality. The next interesting thing is the comparison of the dual control algorithms—the novel MIM4DC algorithm utilizing RH nature on one hand and the numerical algorithm as an alternative solution to the algorithm presented in [38]) on the other. From Tables (1) and (2), it can be seen that MIM4DC usually consumes slightly more energy, has a little bit higher tracking error and thus, it perturbs the MPC cost function with higher ΔJ. However, this slightly worse control performance is almost negligible. On the other hand, comparing the data excitation and the subsequent ability to identify the system parameters, MIM4DC algorithm clearly proves its superiority as the values of q_e expressing the inaccuracy of the estimates are usually of one order lower than in the case of the GNA4DC.

We are ready to show both the comparison of the estimated parameters of the models identified from the data using the dual control algorithms and the classical MPC with the real system parameters from Eq. (23). We also add the comparisons of the step responses of all these models. We chose such settings of dual control algorithms for which both perturb the original MPC cost function equivalently. For GNA4DC we chose $\Delta J = 120$ and $M = 8$ and for MIM4DC $\Delta J = 60$ and $M = 10$. Both dual control algorithms result in estimated models that are much closer to the real ones than those identified from the data provided by the classical MPC (see Fig. 2 and 3).

Table 2
Results for GNA4DC with different parameter settings.

	$\Delta J = 100$					$\Delta J = 120$					$\Delta J = 140$				
	e_y	$I_e(\%)$	$\overline{\Delta J}$	$\lambda_{min}(\Delta I_1^N)$	q_e	e_y	$I_e(\%)$	$\overline{\Delta J}$	$\lambda_{min}(\Delta I_1^N)$	q_e	e_y	$I_e(\%)$	$\overline{\Delta J}$	$\lambda_{min}(\Delta I_1^N)$	q_e
$M=6$	0.074	0.45	8.9	0.91	441.5E−8	0.076	0.53	10.6	1.03	501.6E−8	0.076	0.61	11.4	1.11	405.2E−8
$M=7$	0.071	0.92	15.6	1.18	423.6E−9	0.071	1.09	18.6	1.34	116.2E−8	0.071	1.26	20.4	1.50	788.6E−8
$M=8$	0.065	1.20	18.6	1.70	367.6E−8	0.066	1.46	22.6	2.04	148.9E−9	0.067	1.66	25.5	2.27	249.1E−8
$M=9$	0.068	1.00	16.6	1.39	305.0E−9	0.068	1.17	18.6	1.55	154.6E−8	0.069	1.38	21.8	1.77	184.1E−8
$M=10$	0.068	0.77	12.6	0.95	107.4E−8	0.068	0.92	15.6	1.07	736.3E−8	0.068	1.04	16.8	1.15	280.5E−8
$M=11$	0.073	0.76	13.6	0.82	725.9E−8	0.074	0.93	16.6	0.96	800.2E−8	0.075	1.07	18.7	1.05	251.9E−8
$M=12$	0.070	0.78	12.9	1.25	711.8E−8	0.071	0.93	15.6	1.44	168.9E−8	0.070	1.09	17.4	1.62	991.7E−9
MPC	0.068	0.00	0.0	0.28	240.0E−5	0.068	0.00	0.0	0.28	240.0E−5	0.068	0.00	0.0	0.28	240.0E−5
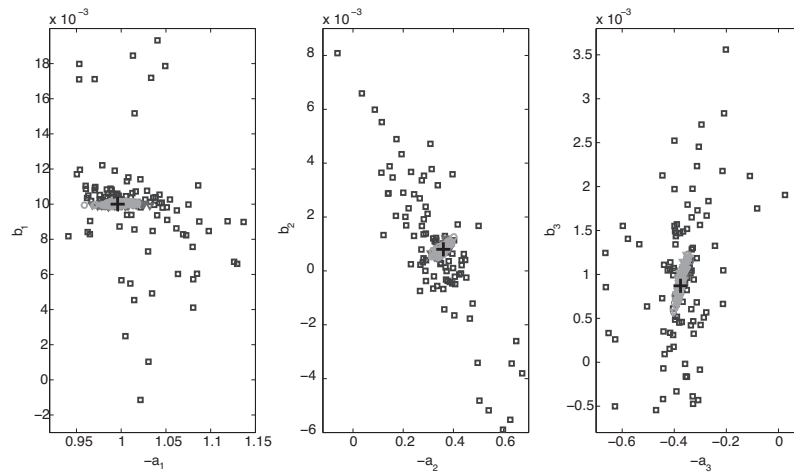
Fig. 2. Comparison of the identified parameters. Black cross – true values, blue squares – clasical MPC, red triangles – GNA4DC $M = 8$ $\Delta J = 120$, green rings – MIM4DC $M = 10$ $\Delta J = 60$. (For interpretation of the references to color in this figure legend, the reader is referred to the web version of the article.)
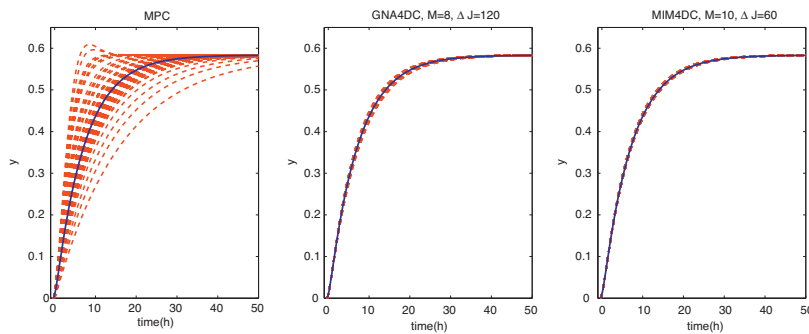
Fig. 3. Step plots of identified models, blue – true system, red – estimated models. (For interpretation of the references to color in this figure legend, the reader is referred to the web version of the article.)

Table 3
Time consumptions of algorithms [s] ($M = 9$).

ΔJ	60	80	100
MIM4DC	0.054	0.058	0.060
ΔJ	100	120	140
GNA4DC	2.24	2.59	3.72
MPC		0.039	

Following the discussion above, it should not be a surprise that given the same perturbation of the original cost function, MIM4DC is able to provide data which enable even more accurate estimates than GNA4DC (see Figs. 3 and 2). Realize that besides the fact that MIM4DC slightly outperforms the GNA4DC (as an alternative to the algorithm presented in [38]), it brings also other advantages as it performs exhaustive search over a small set of values which in this case is easy to implement and is computationally time-friendly while ensuring that the global optimum is always found.

In the Table 3, we present the average duration of one run[2] of the particular algorithm for $M = 9$ (this setting was chosen because it is in the middle of the considered scale) and for various ΔJ. It shows that while one iteration takes approximately 60 ms in the

case of MIM4DC (which is the same value as the duration of one iteration of the classical MPC), the duration is approximately 3 s in the case of GNA4DC. From the Table 3, it can be seen that the computational complexity of the algorithms rises with increasing ΔJ which is quite natural as the space to be explored gets wider as well.

The next advantage of MIM4DC is that except for M and ΔJ, no other additional parameters need to be specified. This is not the case of GNA4DC algorithm, where (except for M and ΔJ) besides the LPS parameter (which can be chosen the same for all the excited/optimized input samples), also the whole perturbation vector (namely the multiples of LPS) needs to be chosen. On one hand, by increasing the density and extent of the perturbation vector, a better spline approximation can be found, on the other hand, the duration of the optimization per one sampling period gets increased as well. The question that could come into one's mind is what is the "best" choice of the tuning parameters of the algorithm M a ΔJ. Unfortunately, in neither case it can be said explicitly what are the rules for the "best" choice. It has been already mentioned that $M < n_a + n_b$ is not suitable at all. Of course, the algorithm can be used also with this setting, however, some of the eigenvalues stay zero and thus, the corresponding directions remain unexcited. On the other hand, M should not be chosen to be very high as it is not exactly known what inputs will be actually applied to the system from the time $k + 1$ ahead (the calculated values are only estimates)

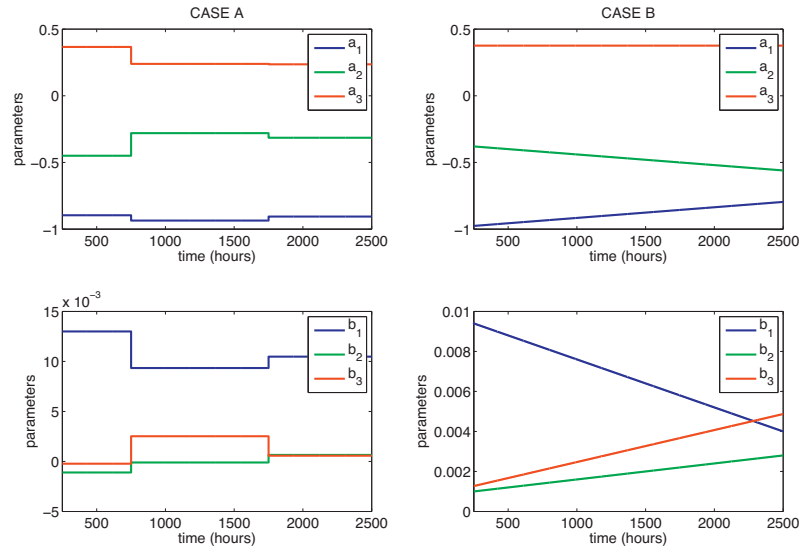[2] The simulations were performed on a computer with 2.4 GHz CPU.
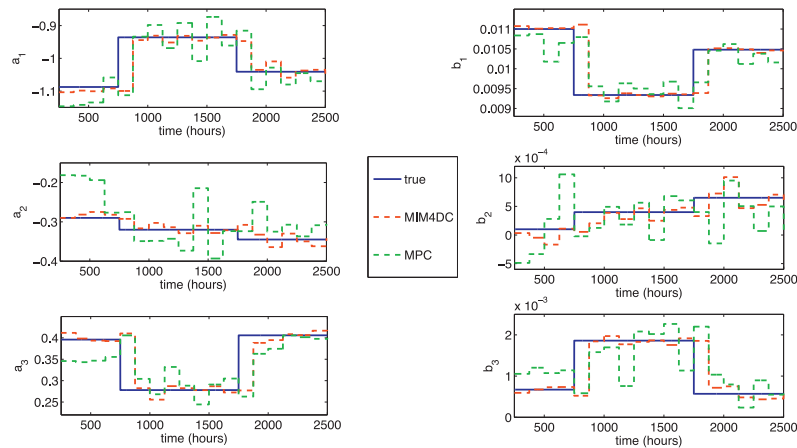
Fig. 4. Changes of the parameters.

Fig. 5. Parameter estimations – Case A.

and with increasing M, the number of these inputs rises as well and so does the uncertainty. The next reason against too high M is the eventual inaccuracy of the multistep predictions.

In Tables (1) and (2) no significant performance improvement or degradation can be observed with changing M. As the best choice for both algorithm, medium-height M should be chosen which in this case corresponds to $M = 8$ or $M = 9$. As already mentioned, the exact formula for the choice of M does not exist, nevertheless, it is a reasonable choice to pick up M slightly higher than $n_a + n_b$ but not too high as it can be observed from Tables (1) and (2) that for higher M, the resulting behavior is not adequately improved. Regarding the choice of ΔJ, it is mainly up to the user preferences and it also depends on how big degradation of the original controller performance can be accepted. As the tuning parameter here is directly related to the increase of the cost function (and not to the excitation level as in the case of [32,33]), based on the knowledge of the weighting matrices Q and R and model of the process, the impact of this perturbation on the change of the inputs and outputs can be estimated.

5.2. MIM4DC as an adaptive controller

Now we are ready to focus on MIM4DC in the role of an adaptive controller. As in the previous subsection, we adapt the system (23) with parameters varying during the experiment. In the first case, the change is slow (see Fig. 4, Case B) while in the second case, the change is abrupt (see Fig. 4, Case A). The goal is to design a predictive controller which is able to satisfy the requirements defined by the cost function (24) and constraints (25) even when the parameters of the system alter. To be able to respond to the change of parameters, the controller needs a model with parameters being re-identified periodically. To satisfy this request, the controller optimizes cost function (24) given

$$
\begin{aligned}
&\text{linear } dynamics\,(3) \\
&20\,^\circ\text{C} \le u \le 55\,^\circ\text{C}, \\
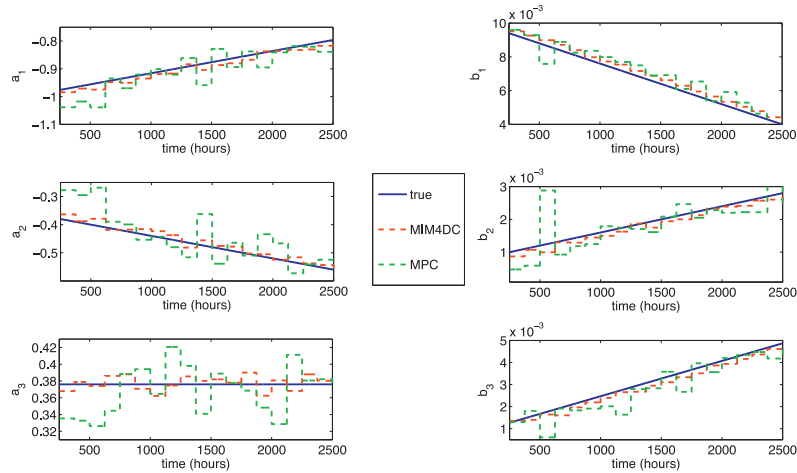&-1\,^\circ\text{C} \le \Delta u \le 1\,^\circ\text{C},
\end{aligned}
\tag{32}
$$

Fig. 6. Parameters estimations – Case B.

where

$$
\hat{\theta}(k) = \begin{cases} \left(\displaystyle\sum_{i=1}^{N_i} \lambda^i Z_{k-i} Z_{k-i}^{\mathrm{T}} \right)^{-1} \displaystyle\sum_{i=1}^{N_i} Z_{k-i}^{\mathrm{T}} y_{k-1} & \text{if} \quad \mathrm{mod}(k, 500) = 0, \\ \hat{\theta}_{k-1} & \text{elsewhere,} \end{cases}
$$

(33)

with λ being the forgetting factor, $\lambda \in (0, 1)$.

With this MPC settings, an experiment similar to the one described in the previous sections with $\lambda = 0.99$ and $N_i = 700$ was performed. This time, MIM4DC was tested with $\Delta J = 80$ and $M = 7$. As can be seen in Figs. (5) and (6) (in both cases the reference is changing), MIM4DC is able to react to the changes of parameters and tracks both abruptly and slowly varying parameters during the whole experiment. The classical MPC has slight problems with adaptation to parameter changes, especially, the estimates of a_1, a_2, a_3 are considerably biased.

6. Conclusions

In this paper, we have introduced a new algorithm MIM4DC for solving the problem of dual control. Moreover, we have presented an alternative solution to the dual control problem by introducing a numerical gradient-based algorithm. Both of these algorithms ensure a rich information content of the generated optimal input enabling thus accurate estimation of the time invariant system parameters. The newly presented algorithms outperforms the classical MPC in the sense of information content of the data (thus accuracy of parameter estimation) at a price of a small (and predefined) deterioration of the reference tracking and energy consumption.

Our new formulation utilizes receding horizon principle when MIM4DC is not only able to find the global optimum during approximately 60 ms but also slightly outperforms more complex and time consuming GNA4DC. MIM4DC was also tested as an adaptive controller with a system with time varying parameters with encouraging results. Moreover, unlike to the solution proposed in the literature, both of the presented algorithms have the ability to solve the posed problem for arbitrarily large systems.

References

[1] Y. Zhu, Multivariable process identification for MPC: the asymptotic method and its applications, Journal of Process Control 8 (2) (1998) 101–115.
[2] D. Bonvin, B. Srinivasan, D. Ruppen, Dynamic optimization in the batch chemical industry, in: AIchE Symposium Series, American Institute of Chemical Engineers, 2002, pp. 255–273.
[3] S. Di Cairano, A. Bemporad, I. Kolmanovsky, D. Hrovat, Model predictive control of magnetically actuated mass spring dampers for automotive applications, International Journal of Control 80 (11) (2007) 1701–1716.
[4] S. Di Cairano, D. Yanakiev, A. Bemporad, I. Kolmanovsky, D. Hrovat, An MPC design flow for automotive control and applications to idle speed regulation, in: 47th IEEE Conference on Decision and Control, 2008, pp. 5686–5691.
[5] P. Cortés, M. Kazmierkowski, R.M. Kennel, D.E. Quevedo, J. Rodríguez, Predictive control in power electronics and drives, IEEE Transactions on Industrial Electronics 55 (12) (2008) 4312–4324.
[6] J. Široký, F. Oldewurtel, J. Cigler, S. Prívara, Experimental analysis of model predictive control for an energy efficient building heating system, Applied Energy 88 (9) (2011) 3079–3087.
[7] Y. Ma, F. Borrelli, B. Hencey, B. Coffey, S. Bengea, P. Haves, Model predictive control for the operation of building cooling systems, IEEE Transactions on Control Systems Technology 20 (3) (2012) 796–803.
[8] P. May-Ostendorp, G.P. Henze, C.D. Corbin, B. Rajagopalan, C. Felsmann, Model-predictive control of mixed-mode buildings with rule extraction, Building and Environment 46 (2) (2011) 428–437.
[9] S. Prívara, Z. Váňa, E. Žáčeková, J. Cigler, Building modeling: selection of the most appropriate model for predictive control, Energy and Buildings (2010).
[10] S. Prívara, J. Cigler, Z. Váňa, F. Oldewurtel, C. Sagerschnig, E. Žáčeková, Building modeling as a crucial part for building predictive control, Energy and Buildings 56 (2012) 8–22.
[11] M. Bacic, M. Cannon, Y.I. Lee, B. Kouvaritakis, General interpolation in MPC and its advantages, IEEE Transactions on Automatic Control 48 (6) (2003) 1092–1096.
[12] P. Orukpe, I. Jaimoukha, H. El-Zobaidi, Model Predictive Control based on Mixed H2/H Control Approach, in: American Control Conference, IEEE, 2007, pp. 6147–6150.
[13] L. Ljung, Prediction error estimation methods, in: Circuits, Systems, and Signal Processing, Birkhauser, Boston, 2001, pp. 11–21.
[14] L. Ljung, System Identification, Wiley Online Library, 1999.
[15] I. Gustavsson, L. Ljung, T. Soderstrom, Identification of processes in closed loop-identifiability and accuracy aspects, Automatica 13 (1) (1977) 59–75.
[16] P. Van Den Hof, R. Schrama, Identification and control – closed-loop issues, Automatica 31 (12) (1995) 1751–1770.
[17] P. Van den Hof, Closed-loop issues in system identification, Annual Reviews in Control 22 (1998) 173–186.
[18] O. Sotomayor, D. Odloak, L. Moro, Closed-loop model re-identification of processes under MPC with zone control, Control Engineering Practice 17 (5) (2009) 551–563.

[19] Y. Shardt, B. Huang, Closed-loop identification condition for ARMAX models using routine operating data, Automatica 47 (7) (2011) 1534–1537.

[20] R. Hildebrand, G. Solari, Closed-loop optimal input design: the partial correlation approach, in: IFAC Symposium on System Identification, 2009, pp. 928–933.

[21] U. Forssell, L. Ljung, Closed-loop identification revisited, Automatica 35 (7) (1999) 1215–1241.

[22] P. Van Den Hof, R. Schrama, An indirect method for transfer function estimation from closed loop data, Automatica 29 (6) (1993) 1523–1527.

[23] U. Forssell, L. Ljung, A projection method for closed-loop identification, IEEE Transactions on Automatic Control 45 (11) (2000) 2101–2106.

[24] H. Hjalmarsson, H. Jansson, Closed-loop experiment design for linear time invariant dynamical systems via LMIs, Automatica 44 (3) (2008) 623–636.

[25] H. Hjalmarsson, From experiment design to closed-loop control, Automatica 41 (3) (2005) 393–438.

[26] A. Feldbaum, Dual control theory I, Automation and Remote Control 21 (9) (1960) 874–1039.

[27] J. Sternby, A simple dual control problem with an analytical solution, IEEE Transactions on Automatic Control 21 (6) (1976) 840–844.

[28] B. Wittenmark, Adaptive dual control methods: an overview, in: 5th IFAC Symposium on Adaptive Systems in Control and Signal Processing, Citeseer, 1995.

[29] J. Lee, J. Lee, An approximate dynamic programming based approach to dual adaptive control, Journal of process control 19 (5) (2009) 859–864.

[30] N. Filatov, H. Unbehauen, Survey of adaptive dual control methods, in: IEE Proceedings-Control Theory and Applications, vol. 147, IET, 2000, pp. 118–128.

[31] H. Genceli, M. Nikolaou, New approach to constrained predictive control with simultaneous model identification, AIChE Journal 42 (1996) 2857–2868.

[32] M. Shouche, H. Genceli, V. Premkiran, M. Nikolaou, Simultaneous constrained model predictive control and identification of DARX processes, Automatica 34 (12) (1998) 1521–1530.

[33] G. Marafioti, R. Bitmead, M. Hovd, Persistently exciting model predictive control using FIR models, in: International Conference Cybernetics and Informatics, 2010.

[34] J. Rathousky, V. Havlena, Multiple-Step Active Control with Dual Properties, in: IFAC World Congress, vol. 18, 2011, pp. 1522–1527.

[35] P. Antsaklis, A. Michel, A Linear Systems Primer, Birkhauser, 2007.

[36] M. Shouche, Closed-loop Identification and Predictive Control of Chemical Processes, Ph.D. Thesis, Texas A&M University, 1996.

[37] E. Aggelogiannaki, H. Sarimveis, Multiobjective constrained MPC with simultaneous closed-loop identification, International Journal of Adaptive Control and Signal Processing 20 (4) (2006) 145–173.

[38] J. Rathouský, V. Havlena, MPC-based approximate dual controller by information matrix maximization, International Journal of Adaptive Control and Signal Processing (2013) (in press).

[39] S. Boyd, L. Vandenberghe, Convex Optimization, Cambridge Univ Press, 2004.

[40] J. Nocedal, S.J. Wright, Numerical Optimization, Springer Science, Business Media, 2006.

[41] C.D. Boor, A practical guide to splines, Springer Verlag, 1978.

Semi-receding Horizon Algorithm for "Sufficiently Exciting" MPC with Adaptive Search Step

Eva Žáčeková, Matej Pčolka, Sergej Čelikovský, Michael Šebek

Abstract— In this paper, the task of finding an algorithm providing sufficiently excited data within the MPC framework is tackled. Such algorithm is expected to take action only when the re-identification is needed and it shall be used as the "least costly" closed loop identification experiment for MPC. The already existing approach based on maximization of the smallest eigenvalue of the information matrix increase is revised and an adaptation by introducing a *semi-receding horizon* principle is performed. Further, the optimization algorithm used for the maximization of the provided information is adapted such that the constraints on the maximal allowed control performance deterioration are handled more carefully and are incorporated directly into the process instead of using them just as a termination condition. The effect of the performed adaptations is inspected using a numerical example. The example shows that the employment of the semi-receding horizon brings major improvement of the identification properties of the obtained data and the proposed adaptive-search step algorithm used for the "informativeness" optimization brings further significant increase of the contained information while the aggravation of the economical and tracking aspects of the control are kept at acceptable level.

I. Introduction

Over the few decades since its introduction, model predictive control (MPC)—being perhaps the most perspective member of the broad family of the advanced control approaches—has been cured of most of the "childhood" diseases, its theoretical properties have been well-proven and therefore, it has gained much popularity within both the theoretically- and practically-oriented branches of the control community. Thanks to numerous advantages, the areas in which MPC is employed have accrued rapidly and nowadays, its practical use is no more restricted to chemical engineering where it started [1]. The evolution in the field of numerical optimization [2] enabling implementation of MPC algorithms on low-demand industrial computers and PLCs and their use for control of the fast systems opens the door for more and more challenging industrial applications of MPC.

However, not all drawbacks related to the deployment of MPC have been eliminated satisfactorily. The crucial role played by the mathematical model of the controlled system still restricts its usage. Furthermore, it is usually the process of obtaining of the suitable model candidate which is the most time-consuming part of the whole procedure of bringing MPC to life and requires much more time than the design, implementation and tuning of the controller itself. Actually, some references indicate that the identification phase may take up to $90\,\%$ of the overall time [3]. Taking this enormous percentage into account, it is desirable to pay sufficiently much attention to the identification of the model for MPC.

The identification aspects of MPC use are very often omitted in the literature. Usually, it is assumed that certain identification experiment has been performed to obtain a suitable model. This, however, does not correspond to the real life situation – in industrial practice, it is generally impossible to execute such experiment due to numerous economical and operational reasons. In such case the only data which are available for identification purposes are those from ordinary closed-loop operation of the controlled process. Such data suffer from lack of contained information and from negative aspects related to input-to-noise correlation.

So far, several methods for closed-loop identification have been introduced [4], [5]. The main disadvantage of these approaches is that while they work well for simple controllers with properties which are favorable from the identification point of view (causality, linearity), they do not work properly in case of advanced optimization based controllers [6]. The most effective way how to tackle this task in case of MPC seems to be simultaneous control and excitation of the system. If performed carefully, such approach has the potential to provide well-excited data suitable for identification purposes while also satisfying the given performance criteria.

The first approaches mentioned in the literature come up with adding of an external so-called dithering signal [7] to the control input while the next group of approaches is based on use of sufficiently excited reference signal. Both these branches can lead to a situation that the resulting closed-loop behavior will be far away from the desired control performance. In several other works [8], [9], an alternative method has been presented. The requirement on informativeness of the data has been added to the MPC cost function as an additional constraint. This demands solving of a complicated nonconvex task which is solved by the authors using a suitable relaxation as the semi-definite programming task. This approach suffers from one serious drawback – the excitation in the output directions is usually omitted.

In [10], [11], the authors have utilized the receding horizon principle which has enabled them to split the process of solving of the originally non-convex problem into two steps by solving twice the quadratic programming task. However, the output excitation has been omitted as well.

The approach published recently in [12] offers another alternative. It works in two stages – in the first one, the original MPC task is solved and in the second step, the maximization of the information matrix is performed while the maximal allowed perturbation of the original MPC cost function is employed as the constraint. To simplify the second-stage optimization, elliptic approximation is exploited.

The authors themselves have also contributed to the lastly mentioned two-stage branch. Unlike [12], they performed no approximation and optimized directly the quantization of the

4142

provided information contained in data. In [13], two algorithms have been provided: the first of them considers only the first input sample for the optimization of informativeness while the second based on gradient optimization optimizes certain chosen subsequence of the whole optimal input sequence pre-calculated by MPC. According to comparison provided in [13], the two algorithms are equivalent for the class of the reference-tracking MPCs. In [14], the second (gradient-optimization-based) approach has been tested for the rapidly spreading class of zone MPC. Its versatility with respect to the used optimization criterion and considered constraints has been shown.

In the current paper, the authors provide several improvements of the existing methodology. First of all, in order to fully exploit the pre-calculated input samples ensuring sufficient excitation, *semi-receding horizon approach* is proposed. The authors provide also improvement of the optimization algorithm that is employed at the second stage in the view of constraints handling. Instead of keeping the optimization steps constant, the distance from the constraints on the allowed MPC performance deterioration is taken into account and the optimization steps are adapted accordingly. The semi-receding horizon approach together with the adaptive step provide major increase of the information gathered from the system.

The paper is organized as follows. In Section II, the problem to be solved is introduced including the model description, control requirement formulation and quantification of the amount of the information contained in the obtained data. Section III presents the proposed solution. Firstly, constraints-dependent step adaptation of the two-stage algorithm is provided and secondly, semi-receding horizon approach is introduced. Section IV presents the case study on which the performance of the proposed improvements is demonstrated. After the brief description of the considered system and the comparison quantifiers, the results are summarized and corresponding discussion is provided. The paper is concluded by Section V.

II. PROBLEM FORMULATION

In the following paragraph, the necessary background is provided. The descriptions of the model and the considered controller follow.

A. Model under investigation

In this paper, a simple linear time-invariant (LTI) model is considered. Such model can be described by the well-known ARX structure as

$$y_k = Z_k^T \theta + \varepsilon_k, \qquad (1)$$

where y_k and u_k are the system output and input sequences and ε_k stands for zero-mean white noise. The vector of parameters θ is considered in the following form:

$$\theta = [b_{n_d} \dots b_{n_b} - a_1 \dots - a_{n_a}]^T \qquad (2)$$

while $Z_k = [u_{k-n_d} \dots u_{k-n_b} y_{k-1} \dots y_{k-n_a}]^T$ is the regressor. Parameters of the structure n_a, n_b, n_d specify numbers of lagged inputs and outputs and a relative input-to-output delay ($n_d = 0$ means direct input-output connection).

B. Model predictive control

The objective of MPC is to find the optimal input sequence that minimizes the given performance criterion. The model of the system is used for predictions of the future behavior. Typical MPC formulation penalizes both the energy consumed for the control and the deviation of the outputs from the pre-defined reference trajectory. Such formulation can be mathematically expressed as:

$$J_{MPC,k} = \sum_{i=1}^{P} \left\| Q(y_{k+i} - y_{k+i}^{ref}) \right\|_2^2 + \|Ru_{k+i}\|_2^2$$

$$\text{s.t.: linear dynamics (1),}$$
$$u_{k+i}^{min} \le u_{k+i} \le u_{k+i}^{max}, \qquad (3)$$

with y_k^{ref} specifying the reference trajectory, Q and R being the control algorithm tuning matrices of the appropriate size and P being the prediction horizon. Formulation (3) can be solved by common solvers for quadratic programming.

Although MPC possesses many favorable properties, its potential and utilization crucially depend on the availability of a high accuracy mathematical model with good prediction behavior. In the real-life operation, it oftentimes happens that a model that used to work properly and reliably looses its accuracy and ability to provide good predictions and then, it is inevitable to obtain a new one. This illustrates the need for designing such controllers that are able to generate data which are sufficiently rich and contain enough information that can enable the occasional re-identification. Still, the overall control performance must not be significantly degraded and the resulting behavior should meet the requirements defined by the cost function (3). This might be a welcomed alternative to lengthy, complicated and (often also) cumbersome identification experiments which sometimes might not even be realizable due to either economical or operational reasons. The very first straightforward question before formulating the problem itself is how the "informativeness" of a set of data should be evaluated. One way is to quantify the information content of the data set based on the so-called information matrix [15] and the persistent excitation condition.

C. Persistent excitation condition

Let us consider ARX model structure (1). Then, the matrix ΔI_k^{k+M} defined as

$$\Delta I_k^{k+M} = \sum_{t=k+1}^{k+M} Z_t Z_t^{\mathrm{T}}. \qquad (4)$$

represents the increment of the information matrix from the time k to the time $k + M$ and quantifies the amount of the gathered information. Knowing this matrix, the so-called persistent excitation condition can be formulated as follows

$$\Delta I_k^{k+M} \ge \gamma E > \mathbf{0}, \qquad (5)$$

where γ is a scalar specifying the level of the required excitation and E is a unit matrix of corresponding dimension.

III. PERSISTENT EXCITATION WITHIN MPC

As already mentioned, the goal of this paper is to provide algorithm for the MPC which will be able to not only satisfy the control requirements but also to provide sufficiently excited data making the re-identification easier. Similarly to the recent work [12], we propose a two-stage algorithm

based on the maximization of the information matrix. The procedure is as follows: firstly, the original MPC task (3) is solved and then the maximization of the information matrix is performed in the second step while the maximal allowed perturbation of the original MPC cost function is employed as the constraint:

$$U^* = \arg\max_U \gamma$$
$$\text{s.t.: } \sum_{t=k+1}^{k+M} Z_t Z_t^T \geq \gamma E,$$
$$J_{MPC,k}(U) \leq J_{MPC,k}^* + \Delta J,$$
$$u_{k+i}^{min} \leq u_{k+i} \leq u_{k+i}^{max}, i = 1, \ldots, P \qquad (6)$$

Here, ΔJ specifies the maximum allowed increment of the original MPC cost function $J_{MPC,k}^*$. Note that in [12], the involved non-convex task which is to be solved in the second step is approximated using an elliptic approximation which works reliably only for simple low-order systems. On the other hand, we try to propose an algorithm that is able to solve the second-stage optimization task without any approximations with acceptable computational demands and favorable performance independent of the order of the system. The following subsection brings a more detailed description of the algorithm.

A. Optimization with adaptive constraints-dependent step

In the following text, the two-stage procedure that leads to the solution of the task of persistent excitation within the MPC is described. In the first stage, the original MPC problem is solved while in the second stage, numerical optimization algorithm with adaptive constraint-dependent search steps is employed to attack the optimization task (6).

First stage
The first step of the algorithm can be viewed as a kind of initialization for the second stage. The MPC task formulated by (3) and supplied by the corresponding constraints on the inputs is solved. As the output of the first stage, both the optimal input sequence $U_{MPC}^* = [u_{k+i}], i = 1, 2, \ldots, P$ and the corresponding cost function value $J_{MPC,k}(U_{MPC}^*)$ are obtained. While the optimal input sequence U_{MPC}^* is used for the initialization of the numerical gradient search algorithm as the initial guess of the optimal input sequence $U^0 = U_{MPC}^*$, the optimal cost function value $J_{MPC,k}(U_{MPC}^*)$ is used as a constraint.

Second stage
In the second stage, the optimization task related directly to the maximization of the gathered information is solved. The performance criterion to be optimized is formulated as:

$$\mathcal{J}(U) = \max\left(\min \text{eig}(\Delta I_k^{k+M})\right) \qquad (7)$$

where ΔI_k^{k+M} corresponds to (4). Here, let us mention that several other choices of the maximization criterion (e.g. determinant or the trace of the increment of the information matrix) can come to mind. The reason why the minimal eigenvalue has been chosen is that it corresponds to the direction in the gathered data which contains the least information. In other words, the criterion (7) reflects that the identifiability of the most difficultly identifiable parameter shall be improved.

The direct input constraints $u_{k+i}^{min} \leq u_{k+i} \leq u_{k+i}^{max}$ that are to be satisfied ensure that the calculated control action is practically realizable. Moreover, the optimizer in the second stage is allowed to perturb the original MPC criterion by at most ΔJ which is mathematically expressed as $J_{MPC,k}(U) \leq J_{MPC,k}^* + \Delta J, i = 1, 2, \ldots, P$.

The optimal input sequence from the first stage U_{MPC}^* is then split into two parts –the first M samples are available for the optimization of the informativeness while the rest $P - M$ samples are kept fixed and with the first M samples, they are used to evaluate the original MPC cost function. The reason to optimize more than just 1 sample in the sense of data excitation is very pragmatical. Optimizing just 1 particular input sample, only a single direction corresponding to particular estimated parameter can be excited. The more parameters are to be identified, the more input samples should be taken into account. The numerical optimization of these samples is then performed utilizing a modified gradient search as follows.

The first M samples of the input sequence calculated by the MPC in the previous step are used as the initial guess U^0 of the profile which is optimized iteratively following the direction of the increase of the cost function (7),

$$U^{l+1} = U^l + \beta \star G^l, \qquad (8)$$

where G^l is the search direction for the l-th iteration of the gradient search, β is the vector of lengths of the performed steps and $\star$ denotes element-wise multiplication of vectors. The gradient of the criterion (7) is calculated numerically: one by one, all M samples of U^l are gradually perturbed with chosen Δu. Performing this, a set of M perturbed input vectors is obtained,

$$\mathcal{U} = \{U_i = [u_1, u_2, \ldots, u_i + \Delta u, u_{i+1}, \ldots, u_M,],$$
$$i = 1, 2, \ldots, M\}. \qquad (9)$$

Then, evaluating the change of the performance criterion for the second stage defined by (7) for each of the perturbed input profiles

$$\Delta \mathcal{J}_i = \mathcal{J}(U_i) - \mathcal{J}^c$$

with $\mathcal{J}^c$ denoting the current criterion value, the vector of numerical gradients G can be obtained as follows:

$$G = \left[\frac{\Delta \mathcal{J}_1}{\Delta u}, \frac{\Delta \mathcal{J}_2}{\Delta u}, \ldots, \frac{\Delta \mathcal{J}_i}{\Delta u}, \ldots, \frac{\Delta \mathcal{J}_M}{\Delta u}\right]. \qquad (10)$$

Now, let us return to the search step vector β. While in the previous work, all samples of the vector β had the same magnitude (the movements in all M optimized dimensions was uniform), adaptive constraint-dependent search steps β are employed in the current paper. In the previous work, the maximal deterioration of the MPC performance was used as one of the terminating conditions – at each iteration, the actual deterioration was calculated and if it was higher than ΔJ, the gradient algorithm was terminated and the input subsequence from the previous iteration (which did not violate the MPC performance condition) was used as the output of the algorithm. In the current work, we combine the MPC-performance constraints with the search for the optimally excited inputs and the MPC performance criterion is directly incorporated into the optimization. In case that the perturbation of i-th input sample should cause deterioration

close to the ΔJ, the gradient search step β_i in the corresponding i-th dimension is decreased and the movement in that corresponding direction is slowed down.

To accomplish that, the search steps are adapted using hyperbolic tangent function with the argument being the difference between the actual and maximal allowed degradation of the MPC cost function. In order to prevent the algorithm from "falling back" in case that the expected deterioration should be greater than ΔJ, the steps are restricted to be greater than or equal to 0. The resulting search steps β_i then correspond to

$$\beta_i = \max(0, \tanh(w(\Delta J - \Delta J_i))). \quad (11)$$

where ΔJ specifies the maximal allowed perturbation and ΔJ_i corresponds to the violation of the MPC cost function considering i-th perturbed input sequence U_i. The parameter w is used to shape the expression for the search step appropriately and is considered as the tuning parameter of the algorithm. With lower w, the algorithm is more "careful" and pays more attention to the distance from the maximal allowed perturbation. With $w \to \infty$, the expression (11) approaches $\max(0, \text{sign}(\Delta J - \Delta J_i))$ and only the input perturbations causing unacceptable deteriorations $\Delta J_i \geq \Delta J$ are banned while the others are not handled at all. Let us note that at each iteration l of the gradient search algorithm, a new set of search steps β is obtained.

The box-constraints for the values of the particular input samples are satisfied performing a simple projection on the admissible input interval $\langle u^{min}, u^{max} \rangle$. The iterative search is terminated if the improvement of the criterion (7) is less than a chosen threshold.

B. Semi-receding horizon approach

In the following text, the adaptation of the usually followed methodology is proposed and explained.

Freely spoken, the main idea of the above mentioned approaches based on optimization can be summarized as follows: first, let us calculate the optimal input minimizing the MPC cost function. Then, let us consider that the first M samples of the optimal sequence are available for the optimization of the excitation and can be perturbed in order to maximize the obtained information. Meanwhile, the rest $(P - M)$ of the original input sequence calculated by MPC is considered fixed. The restrictions on the perturbation of these M samples are given by the original hard constraints on the applied inputs and by the maximal deterioration of the optimal value of the cost function calculated by MPC (here, the deterioration is obviously calculated for the whole prediction horizon of MPC). Following the well-known receding horizon control principle, once the second-stage optimization is accomplished, the first perturbed input sample is applied and the whole procedure is repeated.

Unfortunately, it can be expected that as long as the last $M-1$ samples optimized in the second stage are never applied to the system, the achieved excitation might not reach the calculated level. From this perspective, the difference between optimizing the whole subsequence of length M and optimizing just the first applied input might be negligible.

In the current work, we come up with a *semi-receding horizon approach* which decreases the gap between the expected and achieved excitation level and therefore obtains more informative data. The procedure is as follows:

1) calculate the input sequence optimizing the MPC cost function

2) optimize the first M samples of the P-sample sequence with respect to the provided excitation
3) apply the whole M-sample sequence, go to 1).

Obviously, this approach makes use of the receding horizon principle in order to ensure sufficient feedback which is necessary to satisfy the control/safety requirements while it also introduces certain type of relaxation which favors the data excitation effort. Moreover, for stable systems with $M \ll P$ such relaxation of the feedback does not bring observable control performance degradation compared to the receding horizon approach which is also demonstrated in the following Section.

IV. CASE STUDY

A. Description

To show the properties and demonstrate the performance of the proposed algorithm, we consider a SISO system with ARX structure with the parameters $n_a = 3$, $n_b = 3$, $n_d = 1$, and $\theta_0 = [0.01 \quad 0.0008 \quad 0.00087 \quad 0.996 \quad 0.36 \quad 0.376]^{\mathrm{T}}$ and with white noise with variance $\sigma_e = 0.05$.

In fact, this example has not been chosen arbitrarily – it mimics a simplified heat transfer model between the heating medium (heating circuits in concrete ceiling) and zone air in a building with the constant ambient temperature and sampling period $T_s = 15\,\text{min}$. Let us mention that rather than providing a procedure to design a controller for the building control, the objective of this illustrative example is to demonstrate the properties of both the newly proposed methodology and the improved numerical optimization algorithm. Therefore, certain level of simplification of both the model and controller is adopted.

The system is controlled by the MPC corresponding to (3) minimizing the supplied energy (u corresponds to the temperature of the heating medium) and satisfying thermal comfort (to keep the output y as close to reference value as possible) with constraints $u^{max} = 50°C, u^{min} = 20°C$ while y^{ref} is generated according to the following 7 days schedule with night and weekend setbacks:

$$y^{ref} = \begin{cases} 22°\,\text{C} & \text{from } 8\,\text{a.m. to } 6\,\text{p.m.,} \\ 20°\,\text{C} & \text{otherwise.} \end{cases} \quad (12)$$

Weighting matrices are chosen as $Q = 10000$ and $R = 1$, the prediction horizon $P = 40$ steps (with the sampling period $T_s = 15\,\text{min}$, it is equivalent to $10\,\text{h}$) is assumed. In order to bring the example as close to reality as possible, the model which is used by the MPC for the predictions does not perfectly match the real system but its parameters are slightly shifted and are considered as $\hat{\theta} = [0.99 \quad 0.35 \quad 0.37 \quad 0.01 \quad 0.0007 \quad 0.0009]^{\mathrm{T}}$. The comparison is based on a numerical example with length $N = 10000$ samples (for the above mentioned sampling period, this corresponds to 3 months). The tuning parameters have been set as: input perturbation $\Delta u = 0.1$, search step shaping parameter $w = 0.02$, number of samples optimized in the second stage $M = 6$ and maximal allowed MPC function deterioration $\Delta J = 1500$. For a more detailed discussion of the tuning of the parameters, see [13].

B. Results

Let us remind the objective of the current work which is to develop an algorithm that is able to both satisfy the control performance defined by (3) and provide the data containing such amount of information that is sufficient for

the re-identification. The evaluation of the performance can be found in the following table. In Table I, first the overall "informativeness" of data quantified by the normalized value of the smallest eigenvalue of the increment of the information matrix $\lambda_{min,n}$ is listed. The smallest eigenvalues for each particular algorithm are normalized with respect to the eigenvalue achieved by the original gradient algorithm making use of the ordinary receding horizon principle [13]. In the table, this algorithm is referred to as GA and the normalization basically means that the GA approach provides 1 "unit of information". The algorithms belonging into RH class make use of the classical receding horizon principle (contrary to GA, the second-stage optimization performed within the aGA algorithm employs adaptive search step) while algorithms listed in SRH class are those following the newly introduced semi-receding horizon approach (GA$_{SRH}$ algorithm employs constant search step, the aGA$_{SRH}$ employs the adaptive search steps proposed in the current paper). Regarding the last abbreviation, MPC refers to classical MPC control without sufficient excitation condition.

The tracking performance of the algorithms is evaluated using the absolute value of the overall tracking error,

$$e_y = \frac{1}{N} \sum_{k=1}^{N} \|y_k^{ref} - y_k\|,$$

while the consumed energy is evaluated using the quantifier:

$$I_E = \left(\frac{\sum_{k=1}^{N} u_k^2}{\sum_{1}^{N} u_{k,MPC}^2} - 1 \right) (\%).$$

Here, u_{MPC} represents the input applied by the classical MPC without the sufficient excitation condition. Here, the question of why a comparison with the original non-exciting MPC is provided could arise. The reason is that the proposed excitation-optimizing algorithm is supposed to restrict the deviation of the control performance from the ordinary operational conditions. Providing such comparison, it can be checked that our algorithm for the identification experiment does cause only negligible deviation from the ordinary regime, however, it is able to provide more excited data and therefore, it offers better conditions for the re-identification.

TABLE I

RESULTS COMPARISON.

	RH		SRH		MPC
	GA	aGA	GA$_{SRH}$	aGA$_{SRH}$	
$I_E(\%)$	0.9	2.1	1.5	2.2	0
$e_y(°C)$	0.03	0.04	0.05	0.07	0.02
$\lambda_{min,n}$	1	1.9	2.4	4.2	0.2

As shown in Table I, the energy consumption increase for each of the tested algorithms compared to the original MPC never exceeds 2.2%. Here, it should be noted that this aggravation is expected only during the performance of the excitation algorithm until the sufficiently informative data appropriate for the model re-identification are gathered. This together with hardly observable violation of the average reference tracking guarantees very satisfactory control behavior even during the performance of the excitation experiment for which the algorithms have been developed. Even for the semi-receding horizon approaches, the deviation from the

ordinary operational regime is insignificant which supports the claim that for $M \ll P$, the relaxation of the feedback does not cause serious degradation. The control performance is even more promising when realizing that nonzero noise and imperfect MPC model have been considered.

Regarding the "informativeness" of the provided data, it can be witnessed that the proposed improvements clearly fulfill their purposes – while the incorporation of the adaptive search step within the second-stage optimization improves the information quantifiers almost twice, the employment of the semi-receding horizon leads to even higher improvement ratio. As a result, when combined both adaptations, the results of the original GA algorithm have been improved by the aGA$_{SRH}$ algorithm by a factor greater than 4.

In order to visualize how the improvement of the smallest eigenvalue of the information matrix increase affects the identifiability, another comparison is provided. All 5 sets (one for each of the algorithms listed in Table I) of the obtained data containing $N = 10000$ samples have been used for identification. More than 100 models have been identified per each provided data set and their step responses have been confronted with the step response of the original system. The graphical comparison of all of them is shown in Fig. 1.
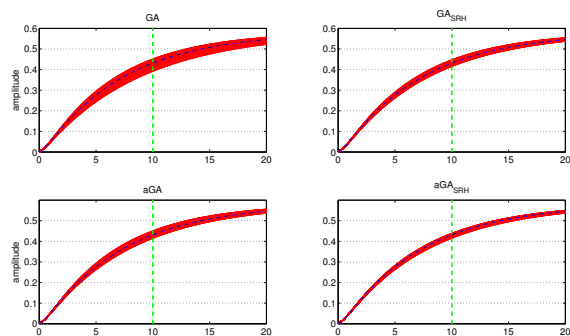
Fig. 1. Comparison of the step responses (red - identified models, blue dashed - real system).

Comparing the two step responses either in one row or one column, it can be observed that they get improved both when employing semi-receding or the adaptive search step proposal. In accordance with Table I, the biggest deviations from the real system step response occur for the GA algorithm while the models identified from the data provided by aGA$_{SRH}$ algorithm match the real step response almost perfectly. Here, the green dashed line marks the prediction horizon of the MPC being 10 h. Freely spoken, the prediction performance of the model on the horizons larger than P are of small interest as the behavior of the system for such horizons is not taken into account within the controller and neither the input is optimized for these horizons.

Fig. 2 compares the ultimate deviations from the real step response for the three most interesting candidates – MPC, GA and aGA$_{SRH}$. While in the previous work, the improvement which was provided by the GA algorithm cut the deviations from the real system response in half in average, very similar improvement has been obtained also in the current work. As can be seen, the deviations for the aGA$_{SRH}$ algorithm are condensed more tightly around zero and also the magnitude of the worst case deviation is at most
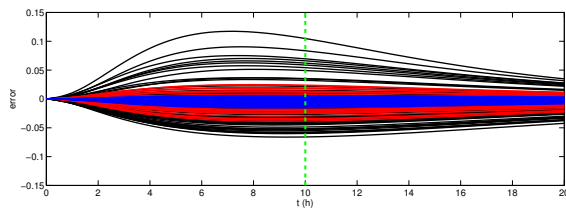
Fig. 2. Deviations from the real step response (black - MPC, red - GA, blue - aGA$_{SRH}$).

one half of the worst case deviation for the GA. Again, green dashed line marks the horizon of $10\,\text{h}$.

As long as considerable part of the presented improvement can be owed to the incorporation of the adaptive search step exploited during the second stage, Fig. 3 illustrates its performance at the chosen sampling instance.

Fig. 3. Adaptive constraints-dependent step algorithm – illustration.

The subfigure in the left upper corner depicts the value of the smallest eigenvalue of the information matrix increase as the function of algorithm iterations. In each subfigure, two significant points (iterations) where its slope changes considerably are marked. Lo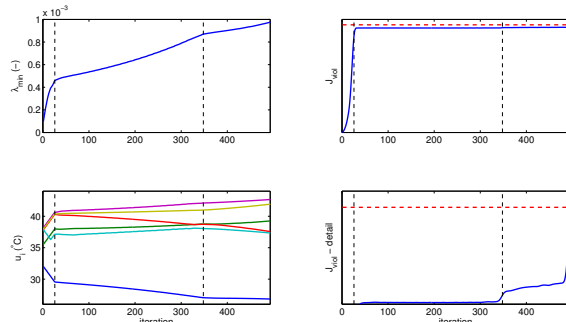oking at the subfigures located in the right upper and right lower corner showing the actual violation of the MPC cost function ΔJ^l at l-th iteration, it is obvious that these two points are strongly related to the distance from the maximal allowed perturbation ΔJ (represented by the red dashed line). For the better clarity, the subfigure located in the right lower corner shows a detail of the subfigure located above it – here, the second point is clearly visible. In case that the algorithm approaches considerably the ΔJ threshold, the adaptive search step should "slow down" the movement in the most critical dimension. This can be witnessed inspecting the subfigure placed in the lower left corner which shows the evolution of the particular perturbed input samples u_i, $i = 1, 2, \ldots, M$. Here, it can be also seen that while at the first marked point, all optimized input samples "slow down", at the second marked point not all input samples are affected (apparently, the one plotted in dark green is not affected at all) which illustrates the performance of the incorporated adaptive step. Here, let us note that with the constant search step, the original algorithm would be terminated soon after the first marked point, the current improved algorithm continues in optimization and is able to improve the value of λ_{min} approximately twice compared to the value at the first marked point.

Last of all, let us note that the computational demands are kept admissibly low – in average, the calculations that need to be performed at particular sampling instance do not take more than $4\,\text{s}$.

V. Conclusion

Two improvements of the approach for sufficiently exciting MPC have been proposed. First of them modifies the utilization of the input samples optimized for the sufficient excitation. Instead of commonly considered receding horizon principle, its relaxed version called semi-receding horizon principle is employed. Second improvement introduces adaptive constraint-dependent search step for algorithm used in the second stage of the whole procedure. The adaptive step reflects the actual distance from the maximal allowed perturbation of the original MPC cost function. As long as both of them are able to provide approximately twofold increase of the information contained in the data, their combination improves the "informativeness" quantifier by a factor of more than 4 compared to the previously used algorithm. The control performance degradation has been also inspected – with the average energy consumption increase of no more than $2.2\,\%$ and negligible average tracking error, the solution presented in the current paper is highly suitable for utilization as a closed loop experiment for MPC.

References

[1] M. Morari and J. H Lee, "Model predictive control: past, present and future," *Computers & Chemical Engineering*, vol. 23, no. 4, pp. 667–682, 1999.

[2] S. Richter, C. N. Jones, and M. Morari, "Computational complexity certification for real-time mpc with input constraints based on the fast gradient method," *Automatic Control, IEEE Transactions on*, vol. 57, no. 6, pp. 1391–1403, 2012.

[3] Y. Zhu, "System identification for process control: Recent experience and outlook," in *System Identification*, vol. 14, no. 1, 2006, pp. 20–32.

[4] U. Forssell and L. Ljung, "Closed-loop identification revisited &Updated Version," *Report no. LiTH-ISY*, 1998.

[5] P. Van den Hof, "Closed-loop issues in system identification," *Annual reviews in control*, vol. 22, pp. 173–186, 1998.

[6] E. de Klerk and I. Craig, "Closed-loop system identification of a mimo plant controlled by a mpc controller," in *Africon Conference in Africa, 2002. IEEE AFRICON. 6th*, vol. 1. IEEE, 2002, pp. 85–90.

[7] M. J. Doma, P. A. Taylor, and P. J. Vermeer, "Closed loop identification of mpc models for mimo processes using genetic algorithms and dithering one variable at a time: application to an industrial distillation tower," *Computers & chemical engineering*, vol. 20, pp. S1035–S1040, 1996.

[8] M. Shouche, H. Genceli, P. Vuthandam, and M. Nikolaou, "Simultaneous constrained model predictive control and identificatoin of darx processes," *Automatica*, vol. 34, pp. 1521–1530, 1998.

[9] H. Genceli and M. Nikolaou, "New approach to constrained predictive control with simultaneous model identification," *AIChE journal*, vol. 42, no. 10, pp. 2857–2868, 1996.

[10] G. Marafioti, F. Stoican, R. Bitmead, and M. Hovd, "Persistently exciting model predictive control for siso systems," in *Nonlinear Model Predictive Control*, vol. 4, 2012, pp. 448–453.

[11] G. Marafioti, "Enhanced model predictive control: Dual control approach and state estimation issues," Ph.D. dissertation, Norwegian University of Science and Technology, 2010.

[12] J. Rathouský and V. Havlena, "Mpc-based approximate dual controller by information matrix maximization," *International Journal of Adaptive Control and Signal Processing*, 2012.

[13] E. Žáčeková, S. Prívara, and M. Pčolka, "Persistent excitation condition within the dual control framework," *Journal of Process Control*, vol. 23, no. 9, pp. 1270–1280, 2013.

[14] E. Žáčeková, M. Pčolka, and M. Šebek, "On satisfaction of the persistent excitation condition for the zone mpc: Numerical approach," in *The 19th World Congress of the International Federation of Automatic Control, IFAC 2014*, 2014.

[15] T. Söderström and P. Stoica, *System identification*. Prentice-Hall, Inc., 1988.

5.2 Zone MPC

As already mentioned, many problems tackled in this thesis were inspired by issues occurring when an MPC is deployed to control a heating/cooling system in a building. Likewise, motivation to focus on the so-called zone MPC arose from the building climate control area.

With the standard MPC formulation, the deviation of the output from a predefined reference trajectory is penalized in the cost criterion. On the other hand, when satisfaction of thermal comfort in a building is expected, a formulation with the indoor temperature preferably kept inside an output *zone* is chosen instead. Such formulation where the reference tracking requirement is replaced with the requirement to keep the system output within some range is referred to as zone MPC and—similarly to the original MPC—can be solved by the quadratic programming solvers.

Enhancement of the persistently exciting MPC algorithm for a class of the zone MPCs represents another contribution of this thesis. To tailor the one-sample algorithm to the zone MPC, a specifically designed algorithm searching for the so-called *breakpoint* was added to its second stage [A.15]. Aiming at the same target, an adaptation of the gradient algorithm was provided as well; further information and debate about the algorithm itself and its results can be found in [A.16].

Next phenomenon observed when deploying the MPC in real operation is the fact that the behavior of the system is also affected by external (partially) predictable disturbances (e.g. solar radiation or ambient temperature when the building climate control area is considered). The presence of the predictable disturbances does not affect the design of the identification procedure itself, but from the excitation point of view, the difference between the predictable disturbances and the manipulated inputs is substantial. While the system input can be influenced to excite the data, the disturbances are determined by external factors and are *uncontrollable*. Since they are often correlated with the manipulated variables, their influence should be taken into account not only when trying to solve the control problem but also when the excitation is optimized.

The variants of both the one-sample algorithm and the gradient algorithm for the zone MPC for linear systems with predictable disturbances were elaborated in a manuscript submitted for review to *Journal of the Franklin Institute* [A.5]. This contribution examines the specifics of the system under the influence of the predictable disturbances from the data excitation point of view. A discussion of the problem solvability and guidelines for choosing a suitable value of the algorithm tuning parameters and cost function are provided including several theoretical findings. The validations are performed using an auxiliary example and

a high-fidelity building model created in *Trnsys* software as well. The mentioned article is presented starting on the next page.

Zone MPC with guaranteed identifiability in presence of predictable disturbances

Eva Žáčeková[a,*], Matej Pčolka[a], Michael Šebek[a]

[a]*Department of Control Engineering, Faculty of Electrical Engineering, Czech Technical University in Prague, Czech Republic*

Abstract

In this paper, a task of ensuring sufficiently excited data for the subsequent re-identification of a model used within the model predictive control framework is tackled. It introduces two algorithms that are developed specifically for the so-called zone MPC for systems with external disturbances, which is a commonly encountered control engineering task. Both of them work in two steps and exploit the original zone MPC solution, which enables that the degradation of their control performance is limited by a user-defined threshold. Moreover, a new optimization criterion quantifying data informativeness is introduced. Both proposed algorithms are described in detail, their theoretical properties are discussed and they are successfully verified on an artificial example and also considering a real-life building climate control task using a high-fidelity testbed model. The results show that they significantly outperform the classic zone MPC while maintaining acceptable zone violation and energy consumption.

1. Introduction

During the last years, modern control methods relying on use of model of the controlled system have witnessed significant boom. Being popular not only among the academicians [1, 2], these approaches of which the most noticeable one is the Model Predictive Control (MPC) have started to be more and more appreciated also by the community of process control engineers [3, 4].

MPC brings wide variety of new possibilities and advantages, the most significant of which are the ability to handle constraints and control multivariable plants and capability of formulating control requirements in a comprehensive and compact form of the optimization cost function. Except of plenty of undisputable benefits, several problems arise with use of this type of controller. The main bottleneck of this framework is the necessity of a good mathematical model of the controlled system by which the favorable controller performance is conditioned. It is actually the search for such appropriate model that is many times more time-demanding than the controller design itself [5].

A very common situation that occurs in industrial practice is that the system is already controlled by some kind of advanced controller whose control performance starts to deteriorate. This is usually caused by the mathematical model which might loose its ability to describe the system dynamics in a suitable manner and the appropriate step is to re-identify the model. Classic open-loop identification experiments might be inadmissible due to operational and/or economical reasons. In such cases, the commonly used identification methods tend to fail and are not able to ensure models of reasonable quality. This is usually caused by failing to satisfy the basic conditions of the open loop identification methods such as no input-noise correlation or persistently exciting input [6, 7].

---

*Corresponding author at Department of Control Engineering, Faculty of Electrical Engineering, Czech Technical University in Prague, Technická 2, 166 27 Praha 6, Czech Republic, tel.: +420 2 243 57689

Email addresses: `eva.zacekova@fel.cvut.cz` (Eva Žáčeková), `matej.pcolka@fel.cvut.cz` (Matej Pčolka), `michael.sebek@fel.cvut.cz` (Michael Šebek)

A broad spectrum of special identification methods able to handle also closed-loop identification data has been developed so far [8, 9, 10], however, most of these methods work well only for simple linear controllers. On the other hand, the MPC framework results in much more complex controller structure and therefore, it is desirable to search for alternative variants of solving this task.

A very promising perspective is to focus on methods where the controller itself can bring some additional information and thus improve the model of the process – in such case, the controller performs certain kind of closed-loop identification experiment. Several works can be found in the available literature that have addressed this problem [11, 12, 13, 14, 15]. So far, mainly their theoretical properties have been discussed [16] and these methods have been validated mostly on simple auxiliary examples [14, 15].

One of the most emerging application areas where the MPC has been steadily gaining popularity is undoubtedly building climate control. According to the available literature, overall expenses spent on heating/cooling of building complexes reach as high as half of the total energy consumption in the building sector which represents about 40 % of the global energy consumption. It has turned out that use of advanced control methods such as MPC opens door to up to 30 % energy consumption reduction [17, 18, 19, 20, 21, 22]. This supplements the motivation of the current paper in which the already presented theoretical methods [23, 24] are extended to enable solving the above-mentioned task of MPC for zone temperature control providing sufficient data excitation. Zone temperature control task is quite specific – unlike the traditional and most frequently used MPC formulation where the given reference is to be tracked, the controller is designed such that the output is kept within a pre-defined zone. This even reduces the effect of natural control-action-induced excitation and provides data of less information quality than the traditional tracking MPC. On the other hand, zone formulation provides certain freedom which–if exploited wisely–can be used for potential system excitation thus improving its identifiability. The next important phenomenon is the fact that besides the manipulated inputs, the output dynamics is influenced also by the predictable disturbance variables (e.g. ambient environment effects). The currently available methods, however, consider only use of classic ARX model structure where the disturbance variables are omitted.

1.1. Contribution of the paper

The algorithm presented in this paper makes use of the receding horizon framework and comprises two stages. In the first stage, a zone control problem is solved providing the explicit solution. This is then passed to the second stage in which the persistent excitation condition is optimized with respect to chosen control performance deterioration allowance. This formulation leads to the optimal input u maximizing the information matrix increase and guaranteeing not to deteriorate the control criterion more than the pre-defined fixed value. As a result, the data used for re-identification are sufficiently excited and the estimate of the system parameters is better than in case of poorly excited data gathered during the operation of the classic zone MPC. Regarding the optimization criterion, a new more robust alternative consisting in maximization of a pre-defined number of smallest eigenvalues of the information matrix increase is presented alongside with the maximization of just the smallest eigenvalue. In addition, the standard MPC formulation using reference tracking control (set-point control) is replaced by "set-range" control (funnel control or zone MPC) since in many practical applications, it is more appropriate to maintain the controlled variable in some predefined range—this is also the case of building climate control chosen as a practical verification testbed. An efficient implementation solving the dual control problem is provided as well.

Compared with the available state-of-the-art methods, the current paper presents several improvements: *i)* external disturbances are considered and their handling in the data excitation task is discussed in detail; *ii)* an alternative optimization criterion especially suitable for the disturbance presence is proposed; *iii)* practically oriented verification of the theoretical concepts is provided using an in-silico example exploiting a high fidelity model of a building.

1.2. Organization of the paper

The paper proceeds as follows. Section 2 introduces the task to be solved, including the used model, MPC formulation and also a description of the PE condition. The main contribution of the paper is presented in Section 3, where two algorithms (one-step algorithm and multi-step algorithm) for the persistently exciting MPC are presented and a suitable choice of the optimization criterion especially focusing on

the disturbance presence is discussed. Section 4 brings a detailed verification of the theoretical concepts: both an artificial and a real-life example are presented and a detailed comparison is provided. Section 5 concludes the paper.

2. Task formulation

This section explains the task this manuscript attempts to solve. At first, the considered model representing the basic system dynamics is described. Then, the formulation of the MPC control problem is provided and finally, the persistent excitation condition is introduced.

2.1. Considered model

Let us consider an extension of the most widely used LTI model for MPC with external disturbances:

$$y_k = \sum_{i=1}^{n_a} a_i y_{k-i} + \sum_{i=1}^{n_b} b_i u_{k-i} + \sum_{i=1}^{n_d} d_i d_{k-i} + e_k \tag{1}$$

where y_k, u_k and d_k are the system output, input and disturbances sequences and e_k zero-mean white noise and n_a, n_b, n_d specify number of lagged inputs, outputs and disturbances. Then, the model structure (1) can be reformulated as

$$y_k = Z_k^{\mathrm{T}} \theta + e_k, \tag{2}$$

with the parameters vector

$$\theta = \begin{bmatrix} a_1 & \dots & a_{n_a} & b_1 & \dots & b_{n_b} & d_1 & \dots & d_{n_d} \end{bmatrix}^{\mathrm{T}}$$

and regressor

$$Z_k = \begin{bmatrix} y_{k-1} & \dots & y_{k-n_a} & u_{k-1} & \dots & u_{k-n_b} & d_{k-1} & \dots & d_{k-n_d} \end{bmatrix}^{\mathrm{T}}.$$

From identification point of view, the disturbances d are equivalent to the manipulated inputs u and the provided structure can be handled as a MISO (Multiple Input - Single Output) one. The representation (1) is then equivalent to the well-known state-space description [25]

$$\begin{aligned} x_{k+1} &= A x_k + B u_k + B_d d_k + W e_k, \\ y_k &= C x_k + D u_k + D_d d_k + e_k, \end{aligned} \tag{3}$$

where k is the discrete time, $x \in \mathbb{R}^n$, $u \in \mathbb{R}$, $d \in \mathbb{R}^p$, $e \in \mathbb{R}^v$, $y \in \mathbb{R}$ are system state, input, noise and output vectors, A, B, B_d, W, C, D and D_d are system matrices of appropriate dimensions and n, v, p specifies number of states, independent sources of noise and disturbances. For the sake of simplicity and with no harm to generality, let us assume that D, D_d are zero matrices thus can be omitted in the subsequent text.

Here, it should be noted that both structures are provided intentionally—while the advantages of structure (1) are exploited the identification, structure (3) is more suitable for implementation with the MPC controller, which is described in more detail in the following section.

2.2. Predictive control

MPC is a modern control technique, that is able to handle constrained optimal control problems. It is usually formulated in a receding horizon (RH) fashion meaning that at each time step, a constrained optimization problem over finite horizon is solved for the current state of the system and the solution—actually, only the first element of the whole optimal input sequence—is then applied to the plant. In the building context, at each time step, a plan for heating, cooling, ventilation, etc. is computed for the whole optimization horizon based on predictions of future weather conditions and other disturbances (e.g. occupancy or internal gains). The usual MPC objectives in the building environment control are minimization

3

of the energy consumption (input effort) and satisfaction of the requirements on technical constraints and user comfort—these are usually required to stay within certain range in contrast to the classic set-point formulation.

In order to satisfy the above-mentioned requirements, the following cost function to be minimized is chosen:

$$J_{MPC,k} = \sum_{i=1}^{P} W_1 \|u_{k+i}\|_p + \sum_{i=1}^{P} W_2 \|\psi_{k+i}\|_p \tag{4}$$

$$\text{s.t. :} \qquad \text{linear dynamics (3)}$$

$$u_{k+i}^{min} \leq u_{k+i} \leq u_{k+i}^{max}, \quad i = 1, \dots, P$$

$$y_{k+i}^{min} \leq \hat{y}_{k+i|k} + \psi_{k+i}$$

where y^{min} is the minimal required output value, u^{min} and u^{max} are input constraints. Weighting matrices are denoted as W_1, W_2 and P specifies the prediction horizon. Symbol ψ represents auxiliary variables used to relax the output constrains and p denotes the norm of the weighting of particular terms in the cost function. If $p = 1$ or $p = 2$ is considered (1- or 2-norm penalization), it is possible to rewrite (4) to a quadratic programming problem [26]:

$$\min \mathcal{U}^{\mathrm{T}} H \mathcal{U} + j^{\mathrm{T}} \mathcal{U} \tag{5}$$

w.r.t.

$$\text{linear dynamics (3)}$$

$$\begin{bmatrix} -I_{P \times P} & \mathbf{0}_{P \times Pn} \\ I_{P \times P} & \mathbf{0}_{P \times Pn} \\ -\mathbb{CB} & -I_{Pn \times Pn} \end{bmatrix} \mathcal{U} \leq \begin{bmatrix} U^{min} \\ U^{max} \\ \mathbb{CA}x_k + \mathbb{CB}_d D - Y^{min} \end{bmatrix} \tag{6}$$

where $\mathcal{U} = \begin{bmatrix} U^{\mathrm{T}} & \Psi^{\mathrm{T}} \end{bmatrix}^{\mathrm{T}}$ is a vector of optimized variables. Throughout the paper,

$$U = \begin{bmatrix} u_k & u_{k+1} & \dots & u_{k+P-1} \end{bmatrix}^{\mathrm{T}}$$

is a vector of inputs over the whole prediction horizon and

$$\Psi = \begin{bmatrix} \psi_{1,k} & \dots & \psi_{n,k} & \psi_{1,k+1} & \dots & \psi_{n,k+1} & \dots & \psi_{1,k+P-1} & \dots & \psi_{n,k+P-1} \end{bmatrix}^{\mathrm{T}}$$

is a vector of zone violations. Similarly, the other vectors D, U^{max}, U^{min} and Y^{min} are created. Matrices $\mathbb{A}, \mathbb{B}, \mathbb{B}_d, \mathbb{C}$ depend on the system dynamics, serve for the computation of the output predictions and the way they are constructed is described in [26]. Matrices H and j are used to shape the penalty function and $I_{P \times P}, I_{Pn \times Pn}$ and $\mathbf{0}_{P \times Pn}$ specify identity and zero matrices of the corresponding dimensions.

The above mentioned approach ensures the attractive properties of the controller such as desirable control performance and constraints satisfaction. However, the resulting performance depends on model quality, particularly on its ability to predict the future behavior. In many cases, the performance of the currently used model is not sufficient (e.g. gradual changes to the plant, aging, etc.) and it is necessary to re-identify the process. In this situation, commonly used identification methods fail, mostly due to two reasons: input-noise correlation and insufficient excitation. The insufficient excitation problem is especially urgent if the controlled variable is required to stay within a certain range during a long period and the data does not contain enough information. Considering the use of MPC, one of the possible and especially efficient approaches is to extend the cost function (4) with a term ensuring sufficiently informative data and in turn also good identifiability of the model. Such term comes out of the sufficient excitation condition, whose formulation is provided in the following text.

4

2.3. Persistent excitation condition

As already mentioned, one of the goals is to develop such an approach that leads to both control requirements satisfaction and sufficiently informative data generation. To be more specific, the obtained input-output data should enable exponential convergence of the parameter estimation error to zero.

Let us consider model structure (2) and let us use linear regression to estimate the parameters of this structure. Then, the *identifiability* of the parameters of this structure from a given set of measured input-output data is defined as follows.

Definition 1 (*Information Matrix Increment*)**.** Having measured data $\{Z_i\}$, $i \in \{1, \ldots, \mathcal{T}\}$, at disposal, *the increment of information matrix* over period $\mathcal{T}$, $\mathcal{T} \in \mathbb{N}^+$, is defined as

$$\sum_{i=1}^{\mathcal{T}} Z_i Z_i^{\mathrm{T}} \tag{7}$$

Definition 2 (*Persistent Excitation Condition*)**.** For a set of measured data $\{Z_i\}$, there exist $\mathcal{T} \in \mathbb{N}^+$, $\sigma_1 \in \mathbb{R}^+$, $\sigma_2 \in \mathbb{R}^+$, $\sigma_1 < \sigma_2$, such that

$$\sigma_1 I \leq \sum_{i=1}^{\mathcal{T}} Z_i Z_i^{\mathrm{T}} \leq \sigma_2 I, \tag{8}$$

where I is an identity matrix of the corresponding dimension.

Definition 3 (*Sufficiently Excited Data*)**.** Measured data $\{Z_i\}$, $i \in \{1, \ldots, \mathcal{T}\}$, satisfying (8) for some $\mathcal{T}$, σ_1 and σ_2 are said to be *sufficiently excited*.

Definition 4 (*Parameters identifiability*)**.** Parameters θ of structure (2) are said to be *identifiable* from measured data $\{Z_i\}$, $i \in \{1, \ldots, \mathcal{T}\}$, satisfying condition (8) for some $\mathcal{T}$, σ_1 and σ_2.

Remark 1. As already noted in [27], the upper bound σ_2 in **PE** condition (8) is not crucial for obtaining of sufficiently excited data and thus, the further text focuses on the satisfaction of the lower bound σ_1.

All three ingredients presented above, namely model of the system, predictive control framework and persistent excitation condition, constitute a sufficiently-exciting MPC whose description and a detailed discussion is provided in the next section.

3. MPC with guaranteed persistent excitation condition

In this paper, the model-based control approach is considered. In such case, a model-plant mismatch has direct consequences on the quality of predictions causing control performance degradation. The use of closed-loop (CL) system identification, i.e. identification with the running controller, can lead to a more precise model [28], however, use of this approach assumes sufficiently excited data, which, unfortunately, cannot be attained by the standard formulation of the control problem, e.g. (4). To make this assumption valid, not only control requirements but also the PE condition (8) should be taken into account. The first straightforward solution presented in the literature [29, 11] consists in adding the PE condition as an additional constraint into the MPC problem formulation. Here, the main bottleneck is that the resulting optimization task us too complex, difficult to solve and to finish the calculations in reasonable time, various approximations need to be employed. Most of the later works devoted to this problem alleviate the computational complexity by solving the task in two stages [30, 16, 31, 12, 32, 33], however, the simplistic basic MPC formulate they consider (penalizing only the reference tracking error) limits their usability. For zone MPC formulation, which is requisite and wide-spread not only in building control but also in chemical industry, only a few works dealing with this task can be found [34, 24, 23, 35].

In this Section, descriptions of our own algorithms are provided. These algorithms lead to zone MPC with guaranteed sufficiently excited data generation for systems with structure (1).

The presented algorithms are adaptations and extensions of the previous ones [24, 23]. It is necessary to remark that in this paper, we consider an improved and a more realistic model structure. In our previous

5

work, a simple SISO ARX structure was assumed while in the current manuscript, a structure with both controlled inputs and predictable disturbance variables is considered. Similarly to the MPC control task, these disturbance inputs can not be optimized, but their predictions are taken into account.

Both algorithms work in two steps as follows: in the first step, the solution to the original zone MPC problem (4) is found and in the second step, the following optimization task is solved:

$$U^* = \arg\max_U \mathcal{J}$$

subject to :

$$u_{k+i}^{min} \leq u_{k+i} \leq u_{k+i}^{max}, \, i = 0, \ldots, P-1$$
$$d_{k+i} = \hat{d}_{k+i}, \, i = 0, \ldots, P-1$$
$$J_{MPC,k}(U) \leq J_{MPC,k}^* + \Delta J,$$

(9)

where $J_{MPC,k}^*$ is the optimal MPC cost function value corresponding to the solution obtained in the first step, ΔJ is a user-defined maximal allowed degradation of the original MPC cost function (4), $\mathcal{J}$ quantifies the data excitation and $\hat{d}$ stands for disturbance prediction.

More detailed descriptions of the algorithms follow.

3.1. Algorithm I. – One-sample approach

This algorithm relies on the fact that MPC controller works according to the receding horizon principle, which can be explained as follows: at each discrete time step k, the optimal control sequence for P steps ahead is calculated but only the first element u_k of the calculated input sequence is exploited and applied to the system. Coming out of the receding horizon principle, the one-sample approach manipulates only the first sample u_k when optimizing data excitation expressed by (9). However, the excitation is calculated over a horizon of M samples where the last $(M-1)$ samples (2-nd up to M-th one) correspond to the samples calculated by the original MPC. Similarly, deterioration of the control performance is limited by evaluating the original MPC cost function over the whole prediction horizon P. The resulting procedure is described as follows.

Algorithm 1 (*One-sample algorithm*).

Stage I

1) minimize (4), obtain the optimal input sequence $U_{MPC}^* = \begin{bmatrix} u_{MPC,k} & u_{MPC,k+1} & \cdots & u_{MPC,k+P-1} \end{bmatrix}^T$ and the optimal value of MPC cost function $J_{MPC,k}^* = J_{MPC,k}(U_{MPC}^*)$;

2) find constraints $\bar{u}_k^{min}$ and $\bar{u}_k^{max}$ for Stage II;
   (a) find values $\underline{u}$ and $\bar{u}$ by Algorithm (2) such that

   $$J_{MPC,k}(\tilde{U}) \leq J_{MPC,k}^* + \Delta J \quad \forall \tilde{U} = \begin{bmatrix} \tilde{u}_k & u_{MPC,k+1} & \cdots & u_{MPC,k+P-1} \end{bmatrix}^T; \, \tilde{u}_k \in \langle \underline{u}, \bar{u} \rangle$$

   (b) perform the following projection

   $$\bar{u}_k^{max} = \min\{\bar{u}, u_k^{max}\},$$
   $$\bar{u}_k^{min} = \max\{\underline{u}, u_k^{min}\}.$$

Stage II

1) compute $\mathcal{J}(\tilde{U})$ with $\tilde{U} = \begin{bmatrix} \tilde{u}_k & u_{MPC,k+1} & \cdots & u_{MPC,k+M-1} \end{bmatrix}^T$ for all $\tilde{u}_k = w \, s_u$ where $s_u \in \mathbb{R}^+$ is a user-defined parameter and $w \in \mathbb{Z}$, $\frac{\bar{u}_k^{min}}{s_u} \leq w \leq \frac{\bar{u}_k^{max}}{s_u}$;

6

70

2) find $\tilde{u}_k^*$ such that $\tilde{U}^* = \arg\max \mathcal{J}(\tilde{U})$, $\tilde{U}^* = \begin{bmatrix} \tilde{u}_k^* & u_{MPC,k+1} & \cdots & u_{MPC,k+M-1} \end{bmatrix}^T$;

3) terminate Stage II; apply $\tilde{u}_k^*$ to the system; wait for new measurements at time $k+1$, repeat from 1) of Stage I.

The crucial part of the algorithm is to find the constraints $\underline{u}$ and $\overline{u}$ for Stage II, which corresponds to search for such values u_k that the MPC cost function (4) equals $J_{MPC,k}^* + \Delta J$. With the classic MPC formulation penalizing the reference tracking error, this collapses to a search for intersections of a parabola with a line parallel to the horizontal axis. In the case discussed in this paper with zone MPC formulation, the cost function remains quadratic, nevertheless, it is necessary to find intersections of two distinct parabolas. This results from the asymmetry introduced by the zone penalization, where only certain range of output values is penalized. Before the zone MPC algorithm looking for $\underline{u}$ and $\overline{u}$ can be described, it is suitable to provide the following definition.

Definition 5 (*Breaking point*). Such input sample $u_{b,k}$ that

$$u_{b,k} = \max\{u_k : \exists i \; : \hat{y}_{k+i|k}(u_k) - y_{k+i}^{min} \leq 0\}, \; i \in \{1, 2, \ldots, P\}, \tag{10}$$

is called *breaking point*.

Freely spoken, $u_{b,k}$ is such value that lower values of the first input sample cause the output zone to be violated at certain point of time during the prediction horizon P. Now, the following theorem can be formulated.

Theorem 1. Consider $u_{b,k}$ given by Definition (5). Next, consider $U_k = \begin{bmatrix} u_k & u_{k+1} & \cdots & u_{k+i} \end{bmatrix}^T$, $i \in \{0, 1, \ldots, P-1\}$, with u_{k+i} fixed for $i \neq 0$. Then, the following holds:

$$J_{MPC,k}(U_k) \cong \widehat{J}_{MPC,k}(u_k) = \begin{cases} p_2^l u_k^2 + p_1^l u_k + p_0^l & u_k \in \langle u_k^{min}, u_{b,k} \rangle, \\ p_2^r u_k^2 + p_1^r u_k + p_0^r & u_k \in (u_{b,k}, u_k^{max} \rangle, \end{cases} \tag{11}$$

with $p_2^l, p_1^l, p_0^l, p_2^r, p_1^r, p_0^r \in \mathbb{R}$.

Proof. First of all, it is obvious that with $U_k = \begin{bmatrix} u_k & u_{k+1} & \cdots & u_{k+i} \end{bmatrix}^T$ where only u_k is allowed to change, the original multivariable function $J_{MPC,k}(U_k)$ collapses into a function of a single variable. Similarly, output predictions $\hat{y}_{k+i}$ depend on u_k and y_k only.

Next, it can be shown that $J_{MPC,k}(U_k)$ can be expressed as a piece-wise quadratic function of u_k with up to P sections. Then, all sections where $\hat{y}_{k+i|k}(u_k) - y_{k+i}^{min} \leq 0$ for some $i \in \{0, 1, \ldots, P\}$ are unified into a single interval $\langle u_k^{min}, u_{b,k} \rangle$ or $(u_{b,k}, u_k^{max} \rangle$ and the MPC cost function is approximated by a single quadratic function over that interval. In the rest of the input range, the MPC cost function is expressed by a quadratic function precisely.

As a result, a piecewise quadratic expression of $\widehat{J}_{MPC,k}(u_k)$ with two intervals can be obtained. This completes the proof. $\square$

To obtain $\underline{u}$ and $\overline{u}$ used in Algorithm 1, the following efficient algorithm is proposed.

Algorithm 2 (*Search for $\underline{u}$ and $\overline{u}$*).

1) Find value $u_{b,k}$ satisfying Definition (5) using Algorithm 3 and compute $J_{MPC,k}(U_{B,k})$, where

$$U_{B,k} = \begin{bmatrix} u_{b,k} & u_{MPC,k+1} & \cdots & u_{MPC,k+P-1} \end{bmatrix}^T.$$

2) Compute values of MPC cost function $J_{MPC,k}(U_{+\Delta})$ and $J_{MPC,k}(U_{+2\Delta})$ where

$$U_{+\Delta} = \begin{bmatrix} u_{b,k} + \Delta_u & u_{MPC,k+1} & \cdots & u_{MPC,k+P-1} \end{bmatrix}^T$$

7

and

$$U_{+2\Delta} = \begin{bmatrix} u_{b,k} + 2\Delta_u & u_{MPC,k+1} & \cdots & u_{MPC,k+P-1} \end{bmatrix}^{\mathrm{T}},$$

$\Delta_u \geq 0$. Use $J_{MPC,k}(U_{u_b})$, $J_{MPC,k}(U_{+\Delta})$, $J_{MPC,k}(U_{+2\Delta})$ to estimate parameters p_2^r, p_1^r, p_0^r.

3) Compute roots r_1^r, r_2^r of equation $p_2^r u_k^2 + p_1^r u_k + p_0^r - (J_{MPC,k} + \Delta J) = 0$.

4) **if** $u_{b,k} = u_k^{min}$
   then
   5a) Set $\underline{u} = \min\{r_1^r, r_2^r\}$ and $\overline{u} = \max\{r_1^r, r_2^r\}$; terminate.
   else
   5b) Compute values of MPC cost function $J_{MPC,k}(U_{-\Delta})$ and $J_{MPC,k}(U_{-2\Delta})$ where

$$U_{-\Delta} = \begin{bmatrix} u_{b,k} - \Delta_u & u_{MPC,k+1} & \cdots & u_{MPC,k+P-1} \end{bmatrix}^{\mathrm{T}}$$

and

$$U_{-2\Delta} = \begin{bmatrix} u_{b,k} - 2\Delta_u & u_{MPC,k+1} & \cdots & u_{MPC,k+P-1} \end{bmatrix}^{\mathrm{T}},$$

$\Delta_u \geq 0$. Use $J_{MPC,k}(U_{u_b})$, $J_{MPC,k}(U_{-\Delta})$, $J_{MPC,k}(U_{-2\Delta})$ to estimate parameters p_2^l, p_1^l, p_0^l.

6b) Compute roots r_1^l, r_2^l of equation $p_2^l u_k^2 + p_1^l u_k + p_0^l - (J_{MPC,k} + \Delta J) = 0$.

7b) Set $\underline{u} = \min\{r_1^l, r_2^l\}$ and $\overline{u} = \max\{r_1^r, r_2^r\}$; terminate.

To complete all necessities for Algorithm 1, $u_{b,k}$ appearing in Algorithm 2 is found following the procedure below. The procedure is illustrated by Fig. 1.

Algorithm 3 (*Search for the breaking point $u_{b,k}$*).

1) Set $u_L = u_k^{min}$, $u_R = u_k^{max}$, $\mathcal{I}_{\mathbf{n}} = u_L$.

2) Divide the considered interval $\langle u_L, u_R \rangle$ into 6 single-sub-intervals $\mathcal{I}_i$ as follows:

$$\mathcal{I}_i = \langle \mathfrak{u}_{i-1}, \mathfrak{u}_i \rangle, \ i \in \{1, 2, \ldots, 6\},$$

$$\mathfrak{u}_j = \left(\frac{u_R - u_L}{6} j + u_L \right), \ j \in \{0, 1, \ldots, 6\}. \tag{12}$$

Next, create double-sub-intervals $\mathcal{I}_h^d$ as follows:

$$\mathcal{I}_h^d = \mathcal{I}_h \cup \mathcal{I}_{h+1} = \langle \mathfrak{u}_{h-1}, \mathfrak{u}_{h+1} \rangle, \ h \in \{1, 2, \ldots, 5\}. \tag{13}$$

3) Compute approximations of the second derivative $\widehat{J}_{uu,h}$ of $J_{MPC,k}$ over $\mathcal{I}_h^d$ as follows:

$$\left. \frac{\partial^2 J_{MPC,k}}{\partial u_k^2} \right|_{\mathcal{I}_h^d} \approx \frac{J_{MPC,k}(\mathfrak{u}_{h+1}) - 2J_{MPC,k}(\mathfrak{u}_h) + J_{MPC,k}(\mathfrak{u}_{h-1})}{\mathfrak{u}_{h+1} - 2\mathfrak{u}_h + \mathfrak{u}_{h-1}} = \widehat{J}_{uu,h}. \tag{14}$$

4) Find the longest sub-sequence s_L consisting of m almost equal elements $\widehat{J}_{uu}$,

$$s_L = \{\widehat{J}_{uu,n} | \forall o \, \|\widehat{J}_{uu,o} - \widehat{J}_{uu,o+1}\| \leq \epsilon; \, n \in \{1, 2, \ldots, m\}, \, o \in \{1, 2, \ldots, m-1\}, \, \epsilon \in \mathbb{R}, \, \epsilon > 0\}. \tag{15}$$

5) **if** the length m of s_L is 5, i.e. $u_{b,k} \notin (u_L, u_R)$
   then set $u_{b,k} = (\bigcup s_L) \cap \{\min(\mathcal{I}_{\mathbf{n}}), \max(\mathcal{I}_{\mathbf{n}})\}$ and terminate
   else continue

8

6) Find the closest admissible neighboring single-sub-interval $\mathcal{I}_\mathbf{n} \in \{\mathcal{I}_i\}$ such that:

$$\mathcal{I}_\mathbf{n} \cap \left(\bigcup s_L\right) = u_{bd}, \ u_{bd} \in \mathrm{bd}(\mathcal{I}_\mathbf{n}), \ u_{bd} \in \mathrm{bd}(s_L), \ \mathcal{I}_\mathbf{n} \backslash u_{bd} \neq \emptyset,$$

where $\mathrm{bd}(A)$ denotes boundary of A.
7) Set $u_L = \min(\mathcal{I}_\mathbf{n})$ and $u_R = \max(\mathcal{I}_\mathbf{n})$
8) **if** $|u_R - u_L| < 2s_u$
   then set $u_{b,k} = \frac{u_R - u_L}{2}$ and terminate
   else go to step 2)
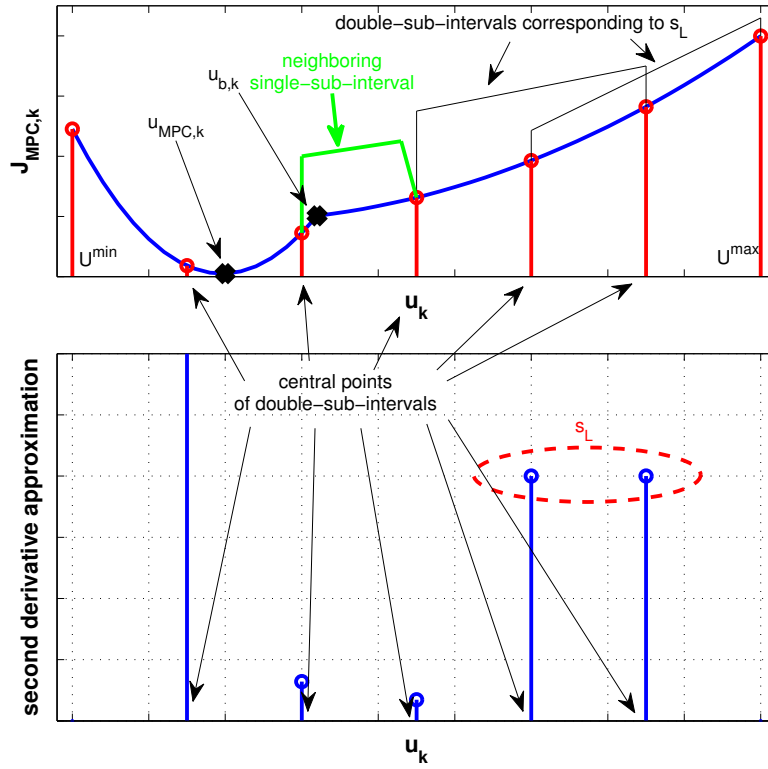
Figure 1: Search for $u_{b,k}$.

Remark 2. Considering one breaking point $u_{b,k}$ and cost function J_{MPC} consisting of two sub-parabolas, it can be shown that 6 is the smallest sufficient number for which the longest sub-sequence s_L (see the step 4) of Algorithm 3) has at least two elements, thus the single-sub-interval containing the breaking point can be uniquely determined. For better illustration, see Fig. 1 where the most crucial elements of Algorithm 3 are graphically presented. Last of all, let us mention that using the proposed procedure, the error in determining the breaking point $u_{b,k}$ is never higher than the user-defined parameter s_u.

9

As an alternative to the above described one-sample approach minimizing only the first one of the M input samples evaluated with respect to data excitation, one can optimize all M input samples. In that case, however, a simple exhaustive search does not even come into consideration due to potential time complexity. To make the data excitation optimization for M samples tractable, a gradient-based algorithm described below is used. In Stage II, an iterative procedure is performed as follows: one by one, all input samples are perturbed and the relative changes of the excitation criterion are gathered to form the numerical gradient that is used to update the first M samples of the input vector. Control performance degradation is guarded by an adaptive search step β whose particular element decreases as the deterioration of the MPC cost function value caused by the corresponding input sample approaches the user-defined threshold ΔJ. The procedure is terminated if the improvement is less than a chosen tolerance ϵ. Let us remark that as in the previous case, data excitation is evaluated over the horizon of M while the MPC cost function is inspected for all P samples. The formulation of the algorithm follows.

Algorithm 4 (*Multi-sample algorithm*).

Stage I
1) minimize (4) and obtain optimal input sequence $U_{MPC}^* = \begin{bmatrix} u_{MPC,k} & u_{MPC,k+1} & \cdots & u_{MPC,k+P-1} \end{bmatrix}^{\mathrm{T}}$;
2) compute optimal value of MPC cost function $J_{MPC,k}^* = J_{MPC,k}(U_{MPC}^*)$;
3) calculate $\mathcal{J}_0 = \mathcal{J}(U_{MPC,M}^*)$ for $U_{MPC,M}^* = \begin{bmatrix} u_{MPC,k} & u_{MPC,k+1} & \cdots & u_{MPC,k+M-1} \end{bmatrix}^{\mathrm{T}}$, initialize the iteration counter $l = 1$;

Stage II
1) obtain a set of M perturbed input vectors

$$\{ \tilde{U}_i = [u_{MPC,k}, \ \ldots, u_{MPC,k+i-1} + \Delta u, \ \ldots, u_{MPC,k+M-1}]^{\mathrm{T}},$$
$$i \in \{1, 2, \ldots, M\}, \ \Delta u \in \mathbb{R}^+ \};$$

2) evaluate excitation criterion $\mathcal{J}(\tilde{U}_i)$ for each perturbed vector;
3) calculate numerical gradient

$$G^l = \left[\frac{\Delta \mathcal{J}_1}{\Delta u}, \frac{\Delta \mathcal{J}_2}{\Delta u}, \ldots, \frac{\Delta \mathcal{J}_i}{\Delta u}, \ldots, \frac{\Delta \mathcal{J}_M}{\Delta u} \right]^{\mathrm{T}},$$

where $\Delta \mathcal{J}_i = \mathcal{J}(\tilde{U}_i) - \mathcal{J}_0$;
4) calculate search step $\beta^l = \begin{bmatrix} \beta_1^l, & \beta_2^l, & \ldots, & \beta_M^l \end{bmatrix}^{\mathrm{T}}$ as follows:

$$\beta_i^l = \max(0, \tanh(\mathfrak{s}(\Delta J - (J_{MPC,k}^* - J_{MPC,k}(\tilde{U}_{i,P}))))),$$

where $\tilde{U}_{i,P} = [u_{MPC,k}, \ \ldots, u_{MPC,k+i-1} + \Delta u, \ \ldots, u_{MPC,k+P-1}]^{\mathrm{T}}, i \in \{1, 2, \ldots, M\}$, and $\mathfrak{s} \in \mathbb{R}^+$ is a user-defined tuning parameter;
5) update the input vector in the direction of the gradient G^l using step β^l

$$\hat{U}^l = U^{l-1} + \beta^l \star G^l;$$

here, $\star$ denotes element-wise multiplication;
6) project the updated input vector on the admissible interval,

$$U^l = \max\{u^{min}, \min\{\hat{U}^l, u^{max}\}\};$$

10

7) **if** $|\mathcal{J}(U^l) - \mathcal{J}(U^{l-1})| \leq \epsilon, \epsilon \in \mathbb{R}^+$
   then terminate Stage II; set $u_k = U_1^l$ and apply it to the system; wait for new measurements in time $k+1$, repeat from step 1) of Stage I,
   else set $\mathcal{J}_0 = \mathcal{J}(U^l), l = l+1$, repeat from step 1) of Stage II.

Despite its more compact formulation, the multi-sample algorithm is more computationally demanding than the one-sample approach. However, it profits from enhanced optimization "freedom" provided by optimizing all M samples, which can be expected to turn into better parameter estimation results. Moreover, both these aspects (time consumption and accuracy of the parameter estimates) can be adjusted using a suitably chosen data excitation criterion, whose choice is discussed in the next subsection.

3.3. Data excitation criteria

One of the key aspects of both algorithms is how the data excitation $\mathcal{J}$ is quantified. The quantifier formulation should reflect that the amount of information contained in the acquired data is to be maximized. Several formulations can be exploited [36] ranging from maximization of trace of the information matrix increase through maximization of its determinant up to maximization of its smallest eigenvalue. In this paper, the following quantifier based on the last mentioned is considered:

$$\mathcal{J} = \lambda_{min}\left(W_p \sum_{i=k-M_P}^{k-1} Z_i Z_i^T + \sum_{i=k}^{k+M} Z_i Z_i^T\right). \tag{16}$$

Here, parameters M_P, M, $W_P \geq 0$ are user-defined tuning parameters. Parameters M and M_P specify how many future/past time steps are taken into account and parameter W_p expresses the relative importance of the information brought by the past obtained data compared with the future ones. With no harm to generality, let us define that $M_P = 0$ is equivalent to $W_P = 0$, i.e. the past samples are ignored.

Considering $\mathcal{J}$ calculated using formula (16) means that the algorithm maximizes the smallest eigenvalue λ_{min} of the information matrix increase. In other words, the algorithm tries to bring as much information as possible in the data direction which has been least informative.

Such choice turns out to be correct in case that the system is of the traditional ARX structure (without any external disturbances). However, if the structure (1) is considered with both the controlled inputs u and *disturbance variables d* coming to play, the above mentioned quantifier definition $\mathcal{J}$ might not be suitable. The samples d_k being part of the regression vector Z_k and thus possibly influencing also the smallest eigenvalue of the information matrix increase cannot be manipulated. Under certain "lucky" conditions, the data might be informative enough even when it comes to estimation of the disturbance parameters.

However, a situation can occur in which the smallest eigenvalue is strongly related to the disturbance variable and cannot be efficiently affected by the manipulated variables. The ultimate scenario is that all n_d samples of d_k are identically zero. Then, also the corresponding elements of Z_k summed in (16) will be zero. Recall that the information matrix increase is calculated as a sum of dyadic products and as such, its rank is equal to the number of the nonzero linearly independent dyads entering (16). In case n_d disturbance samples are zero, the sum appearing in (16) can be re-ordered and transformed such that n_d zero dyads appear. Then, the rank of $\mathcal{J}$ decreases by n_d. Since the rank of a matrix corresponds to number of nonzero eigenvalues and $\mathcal{J}$ is a positive semi-definite matrix having only non-negative eigenvalues, thus n_d smallest eigenvalues will also be zero. The most worrying fact is that this happens no matter the control actions applied to the system and the optimization performed during Stage II would not be effective in such case. An intuitive explanation is that if the disturbance parameters are multiplied by disturbance samples all being identically zero, their values cannot be effectively estimated and, moreover, the data even cannot be excited enough since the disturbances cannot be manipulated.

Therefore, in this paper we propose the following adaptation of the data excitation quantifying criterion:

11

$$\mathcal{J}_{n_d+1} = \sum_{j=1}^{n_d+1} \lambda_j \left(W_p \sum_{i=k-M_p}^{k-1} Z_i Z_i^{\mathsf{T}} + \sum_{i=k}^{k+M} Z_i Z_i^{\mathsf{T}} \right), \tag{17}$$

where λ_j are sorted eigenvalues such that

$$\lambda_1 \leq \lambda_2 \leq \cdots \leq \lambda_m$$

with m being the size of the information matrix increase. Loosely speaking, such formulation of $\mathcal{J}_{n_d+1}$ represents the sum of $n_d + 1$ smallest eigenvalues of the information matrix increase.

In this way, we provide robust efficiency of the Stage II optimization by guaranteeing that the algorithm does not try to optimize the single least eigenvalue since–as mentioned above–it might correspond to the disturbance and might not be effectively affected by the manipulated input. It can be shown that maximizing the sum of $n_d + 1$ smallest eigenvalues instead ensures that at least one element of the sum can be made nonzero and thus the control effort is exploited in a more effective way. Thus, we provide a criterion that is a compromise between maximizing certain function of *all* eigenvalues (e.g. determinant), which is effective but prone to favoring the highest eigenvalues excessively, and maximizing just the *smallest* one, which focuses on the most "problematic" part of the model but might be ineffective in case that disturbances come to play.

Let us discuss another important effect of choosing an "unlucky" optimization criterion which is a degradation of the convergence properties of the optimization routine. This phenomenon, fortunately, does not affect the convergence speed of the one-sample approach since its Stage II optimization consists in an exhaustive search over a predefined interval/set of discrete values and as such, depends only on the size of the explored space. However, the multi-sample approach exploits a numerically computed gradient $\Delta \mathcal{J} / \Delta u$ of the optimization cost function. Gradient-based algorithms work satisfactorily only in case that the change of the optimized variable(s) *can* cause a meaningful change of the optimization criterion, i.e.

$$\exists \, \Delta u \quad \text{s.t.} \quad \left| \frac{\delta \mathcal{J}}{\delta u} \right| \approx \left| \frac{\Delta \mathcal{J}}{\Delta u} \right| \geq \sigma, \quad \sigma \gg 0 \tag{18}$$

otherwise, the convergence to an optimum can be harmed significantly. Recall that also *unaffectable* disturbance variables influence the system whose model is to be identified and as mentioned above, the smallest eigenvalue of the information matrix increase can correspond to estimation of certain disturbance parameter. Then, it is obvious that maximizing only the smallest eigenvalue expressed by criterion (16), such a situation can occur that this eigenvalue cannot be effectively influenced by the optimized input samples, i.e. $|\Delta \mathcal{J} / \Delta u| < \sigma \quad \forall \Delta u$, and the performance of the gradient search can be aggravated. This drawback, however, is overcome by criterion (17) since it focuses on optimizing $n_d + 1$ smallest eigenvalue and even in the ultimate case that all disturbance samples are zero i.e. n_d smallest eigenvalues are zero, it still *ensures* that condition (18) for good gradient algorithm convergence is satisfied. Therefore, it can be expected that the gradient search looking for an optimum of (16) is slower and also might provide worse results than the gradient search optimizing (17). All these expectations are discussed in the following section using a numerical example.

Now, let us formulate several assumptions related to the proposed algorithms, theoretical expectations and their consequences for the ability to solve the persistent excitation task.

Assumption 1. For the meta-parameters of the algorithms, it holds that

$$
\begin{array}{ll}
(\textit{stronger version}) & M_p + M \geq n_a + n_b + n_d, \\
(\textit{weaker version}) & M_p + M \geq n_a + n_b,
\end{array}
$$

where M_p is the number of the past considered samples and M denotes the future considered samples.

12

Assumption 2. The algorithms are initialized such that

$$\text{(stronger version)} \qquad \text{if } M_p + M \geq n_a + n_b + n_d \text{ and } M < n_a + n_b + n_d, \text{ then}$$

$$\text{rank}\left(\sum_{i=k-M_P}^{k-1} Z_i Z_i^{\mathsf{T}}\right) = \min\{M_p, n_a + n_b + n_d\};$$

$$\text{(weaker version)} \qquad \text{if } M_p + M \geq n_a + n_b \text{ and } M < n_a + n_b, \text{ then}$$

$$\text{rank}\left(\sum_{i=k-M_P}^{k-1} Z_i Z_i^{\mathsf{T}}\right) = \min\{M_p, n_a + n_b\}.$$

Assumption 3. The disturbance samples are linearly independent, i.e.

$$\text{rank}\left(\sum Z_{i,d} Z_{i,d}^{\mathsf{T}}\right) = n_d,$$

where $Z_{i,d}$ is a subvector of Z_i consisting of the last n_d samples corresponding to the disturbance samples, $Z_{i,d} = [d_{i-1}, \ldots, d_{i-n_d}]$, $Z_i = [\ldots, Z_{i,d}^{\mathsf{T}}]^{\mathsf{T}}$.

Based on these assumptions, let us formulate the following theorems.

Theorem 2. Satisfaction of Assumptions 1 (stronger version), Assumption 2 (stronger version) and Assumption 3 is a necessary condition for the task of maximization of criterion (16) to be well-posed.

Theorem 3. Satisfaction of Assumption 3 is not a necessary condition for solvability of maximization of criterion (17). Satisfaction of Assumptions 1 (weaker version) and 2 (weaker version) is a necessary condition for the task of maximization of criterion (17) to be well-posed.

Following the discussion of the assumptions presented above, let us provide a combined proof as follows.

Proof (of Theorem 2 and 3). For the task of maximization of criterion (16) to be well-posed, it must be possible to influence the smallest eigenvalue of the information matrix increase. This requires that:

i) At least $n_a + n_b + n_d$ dyadic products are summed (Assumption 1, stronger version).
If less than $n_a + n_b + n_d$ products are summed, there will always be some zero eigenvalues that cannot be increased and thus the optimization task solved by the algorithms is not well-posed.

ii) If less than $n_a + n_b + n_d$ future dyadic products are summed, the sum of the past dyadic products must be of sufficient rank (Assumption 2, stronger version).
In case that $M \geq n_a + n_b + n_d$, the sum of the past dyadic products need not have any specific rank since the summation of M future dyadic products can theoretically ensure that the information matrix increase has full rank and thus, no unaffectable zero eigenvalues appear. Otherwise, the sum of M_p past dyadic products must be added and moreover, it must have such rank that the resulting information matrix increase can be made to have full rank $n_a + n_b + n_d$.

iii) The disturbance acting on the system must be sufficiently excited (Assumption 3).
The disturbance variable cannot be influenced externally and to enable that the information matrix increase has full rank, the disturbance samples must be linearly independent.

Since $(n_d + 1)$ smallest eigenvalues are considered in maximization of criterion (17), the last condition (Assumption 3) is not crucial and has no influence on solvability of the considered optimization task. The necessity of satisfying the weaker versions of Assumption 1 and 2 can be proven following the same reasoning as in case of maximization of criterion (16).
This completes the proof. □

13

4. Case study

In this section, the behavior of the proposed algorithms (multi-sample and one-sample) is investigated. The first part (Section 4.1) demonstrates attractive theoretical properties and inspects the performance of the algorithms with an artificial example. The second part (Section 4.2) focuses on a practical example—a building model created in Trnsys (high-fidelity modeling environment) is used to show that the proposed algorithms represent a promising perspective for the real-life applications.

4.1. Artificial example

In this part of the case study, the behavior of the proposed algorithms is investigated considering a system with the following dynamics

$$y_k = 0.4y_{k-1} + 0.15y_{k-2} + 0.1y_{k-3} + 0.4u_{k-1} + 0.15u_{k-2} + 0.1u_{k-3} \\ + 0.42d_{k-1} + 0.05d_{k-2} + \varepsilon_k$$

(19)

$\varepsilon_k \in \mathcal{N}(0, 0.01^2)$, and controlled by an MPC with the cost function and constraints formulated as follows:

$$J_{MPC,k} = \sum_{i=1}^{P} W_{11}\|u_{k+i}\|_1 + \sum_{i=1}^{P} W_{12}\|u_{k+i}\|_2 + \sum_{i=1}^{P} W_{21}\|\psi_{k+i}\|_1 + \sum_{i=1}^{P} W_{22}\|\psi_{k+i}\|_2$$

(20)

$$\text{w.r.t.} : \qquad \text{linear dynamics (19)},$$
$$0 \le u_{k+i} \le 5, \quad i = 1, \dots, P,$$
$$y_{k+i}^{min} \le \hat{y}_{k+i|k} + \psi_{k+i}.$$

Here, the lower boundary for the system output y_k^{min} was generated according to the following schedule:

$$y_k^{min} = \begin{cases} 4 & 10^3 q + 1 \le k < 10^3(q+1) + 1, \quad q \text{ is even} \\ 6 & 10^3 q + 1 \le k < 10^3(q+1) + 1, \quad q \text{ is odd}. \end{cases}$$

(21)

Regarding the disturbances in this artificial example, perfect knowledge of the disturbance ($\hat{d} = d$) was considered for both the MPC and the identification. The weighting matrices were chosen as $W_{11} = 10^{-2}$, $W_{12} = 9 \times 10^3$, $W_{21} = 10^5$ and $W_{22} = 10^3$ while the prediction horizon $P = 30$ steps was considered. With these settings, a simulation with the length of $N = 15 \times 10^3$ samples was performed.

Similarly, the simulations were run also for both algorithms (one-sample and multi-sample algorithm) developed in this paper with various settings as follows. For $M_p = 0$, the following $M = 9, 10, 11, 12$ were used, while for $M_p = 20$, $M = 4, 6, 8, 10$ were considered. Next, four different maximal allowed perturbations $\Delta J_1 < \Delta J_2 < \Delta J_3 < \Delta J_4$ were considered to inspect the control aspects (energy consumption and zone violation) of the evaluated algorithms. Last of all, both optimization criteria mentioned in the previous section ($\mathcal{J}_{n_d+1}$ and $\mathcal{J}$) were examined.

The obtained data were then split into $\mathcal{N} = 30$ smaller 500-samples subsets and each of them was used to estimate the parameters of the considered structure. The evaluation of the performance of the inspected algorithms is presented in the subsection below.

4.1.1. Results

Let us remind that the objective of the current work was to develop an algorithm able to both satisfy the control performance and provide the data containing amount of information sufficient for the successful re-identification. Therefore, we provide a comparison of the presented algorithms with the original MPC to demonstrate that for the price of only small control performance degradation, the presented algorithms are able to generate data that are much richer on information.

Two viewpoints were considered when evaluating the results of the algorithms presented in the paper, namely *i)* the possibility of system re-identification (parameter adjustment); and *ii)* the control performance quality requirements and restrictions imposed by the MPC problem formulation.

14

To evaluate the satisfaction of the first sub-objective, the following quantifiers were used. Since the main goal of our algorithms was to maximize the smallest or $(n_d + 1)$ smallest eigenvalue(s), the cumulative sum of the smallest eigenvalue $(\sum \mathcal{J})$ and the cumulative sum of the $(n_d + 1)$ smallest eigenvalues $(\sum \mathcal{J}_{n_d+1})$ during the whole experiment were computed. To be more illustrative, the values are normalized with respect to the cumulative sums achieved by the classic MPC.

Recall that the chosen optimization criteria–i.e. certain kind of maximization of the information matrix increase–were chosen to reflect the true objective being the effort to provide the most accurate possible estimates of the parameters of the ARX structure (19). Parameter estimation accuracy was quantified using ε_{AB} and ε_{AB_d} defined as follows:

$$
\varepsilon_{AB} = \frac{1}{\mathcal{N}} \sum_{\mathcal{N}} \left(\sum_{i=1}^{n_a} \frac{\|\hat{a}_i - a_i\|}{a_i} + \sum_{i=1}^{n_b} \frac{\|\hat{b}_i - b_i\|}{b_i} \right),
$$

$$
\varepsilon_{AB_d} = \frac{1}{\mathcal{N}} \sum_{\mathcal{N}} \left(\sum_{i=1}^{n_a} \frac{\|\hat{a}_i - a_i\|}{a_i} + \sum_{i=1}^{n_d} \frac{\|\hat{d}_i - d_i\|}{d_i} \right),
$$

where $\{a_i, b_i, d_i\}$ and $\{\hat{a}_i, \hat{b}_i, \hat{d}_i\}$ stand for the system parameters and their estimates and $\mathcal{N}$ is the number of data subsets used for estimation. According to their definition, ε_{AB} and ε_{AB_d} represent the normalized estimation error for the {output, input} and {output, disturbance} parameters averaged over all $\mathcal{N}$ estimated models.

To inspect the ability to satisfy the original MPC requirements, the following two evaluators were considered. ΔE being the first of them calculates the difference between the total energy consumption E_{PE} of the persistently exciting MPC and the total energy consumption E_{MPC} of the original MPC expressed in per cents of the original MPC consumption, $\Delta E = (E_{PE} - E_{MPC})/E_{MPC}$. The second of the MPC-requirements-satisfaction evaluators is the mean of the normalized zone violation $\overline{ZV}$ over the whole simulation,

$$
\overline{ZV} = \frac{1}{N} \sum_{k=1}^{N} \frac{\max \left(y_k^{min} - y_k, 0 \right)}{y_k^{min}}.
$$

Last of all, average computational time t_{comp} normalized with respect to average computational time of the pure MPC being a measure of computational complexity and the convergence properties of the Stage II optimization routine is provided as well.

The obtained results are summarized in Table 1 - Table 4. In the tables, most cells contain two values of the inspected evaluator. Here, the first value corresponds to the lowest and the second one to the highest achieved value of the evaluator for the whole inspected range of allowed perturbations $\{\Delta J_1, \Delta J_2, \Delta J_3, \Delta J_4\}$.

First of all, the tables confirm the basic expectations: increasing maximal allowed perturbation ΔJ, the control performance gets worse (both the zone violation and the energy consumption increase), on the other hand, the ability to estimate the parameters improves (the parameter estimation error ε_{AB} decreases and the smallest eigenvalue/sum of $(n_d + 1)$ smallest eigenvalues increases).

Inspecting the satisfaction of the MPC control requirements, for both provided algorithms it can be observed that in vast majority of the inspected cases, the energy consumption increase (compared with the classic MPC) is not higher than several per cents while the average zone violation is below 0.4 %. This control performance degradation is compensated by significant decrease of the estimation error. In some cases, the parameter estimation error ε_{AB} for the algorithms presented in the current paper is as low as $10\times$ less than in case of the MPC. Similarly, the cumulative sums of the smallest eigenvalue/$(n_d + 1)$ smallest eigenvalues are several times higher.

Inspecting the presented tables, also a very interesting observation can be made. Even with the most strict ΔJ_1, the average {output, input} estimation error ε_{AB} combining inaccuracy of estimating the a_i and b_i parameters is several times smaller for the algorithms presented in this paper than in case of the classic MPC. However, this does not hold for ε_{AB_d} expressing the combined error in estimating the a_i and d_i

15

Table 1: Comparision of the results - one-sample algorithm, $M_p = 0$

		$\Delta E(\%)$	$\overline{ZV}(\%)$	ε_{AB}	ε_{AB_d}	$\sum \mathcal{J}$	$\sum \mathcal{J}_{n_d+1}$	t_{comp}
$\max \mathcal{J}$	M=9	0.61/1.92	0.00/0.00	1.96/1.34	8.90/ 9.71	5.83/12.95	2.91/5.18	2.01
	M=10	2.00/3.44	0.00/0.00	1.60/1.47	8.47/ 9.60	6.59/14.57	3.12/6.06	2.08
	M=11	3.25/4.47	0.01/0.00	1.68/1.22	9.11/11.70	6.86/15.77	3.21/6.45	2.12
	M=12	4.29/5.42	0.01/0.00	1.87/1.20	8.57/ 8.87	7.14/16.59	3.21/6.64	2.15
$\max \mathcal{J}_{n_d+1}$	M=9	5.08/15.28	0.04/0.04	2.05/1.73	9.01/8.85	3.36/4.15	1.39/1.71	1.98
	M=10	5.05/15.82	0.03/0.04	2.07/1.80	9.35/8.86	3.91/4.48	1.38/1.64	2.02
	M=11	4.85/16.03	0.04/0.04	1.77/1.62	8.90/8.93	4.76/4.94	1.41/1.61	2.10
	M=12	4.59/16.09	0.04/0.04	1.80/1.66	8.97/8.58	4.84/5.66	1.44/1.58	2.18
MPC		0	0.00	7.99	11.17	1	1	1

Table 2: Comparision of the results - one-sample algorithm, $M_p = 20$

		$\Delta E(\%)$	$\overline{ZV}(\%)$	ε_{AB}	ε_{AB_d}	$\sum \mathcal{J}$	$\sum \mathcal{J}_{n_d+1}$	t_{comp}
$\max \mathcal{J}$	M=4	0.80/4.16	0.03/0.04	1.52/1.10	8.75/9.87	5.62/16.69	2.55/6.50	2.11
	M=6	0.54/3.98	0.03/0.03	1.71/1.15	8.83/9.00	6.33/17.07	2.56/6.36	2.24
	M=8	0.55/3.94	0.03/0.03	1.77/1.11	8.83/8.89	5.89/17.30	2.66/6.39	2.33
	M=10	0.66/3.94	0.03/0.03	1.65/1.36	8.89/8.45	5.89/19.44	2.65/6.46	2.40
$\max \mathcal{J}_{n_d+1}$	M=4	0.85/ 9.19	0.06/0.07	2.05/1.26	8.06/9.20	4.90/19.16	1.99/6.83	2.18
	M=6	1.26/10.06	0.06/0.07	1.96/1.26	8.87/9.28	4.50/20.01	1.94/7.17	2.27
	M=8	1.75/13.38	0.06/0.07	1.80/1.30	8.91/9.29	4.36/19.30	1.88/7.22	2.38
	M=10	2.32/16.06	0.06/0.07	1.84/1.19	8.84/9.23	4.44/20.07	1.81/7.20	2.42
MPC		0	0.00	7.99	11.17	1	1	1

Table 3: Comparision of the results - multi-sample algorithm, $M_p = 0$

		$\Delta E(\%)$	$\overline{ZV}(\%)$	ε_{AB}	ε_{AB_d}	$\sum \mathcal{J}$	$\sum \mathcal{J}_{n_d+1}$	t_{comp}
$\max \mathcal{J}$	M=9	2.06/7.91	0.31/0.40	1.30/1.11	12.44/8.71	25.61/47.60	10.54/19.45	20.51
	M=10	1.22/5.27	0.32/0.42	1.22/0.99	12.68/8.48	23.66/35.11	9.80/14.67	22.43
	M=11	0.32/3.31	0.26/0.35	1.22/0.95	12.90/9.27	17.75/28.63	7.46/11.97	23.91
	M=12	0.15/1.09	0.20/0.27	1.07/0.97	12.98/8.95	19.58/24.76	6.62/ 9.39	26.48
$\max \mathcal{J}_{n_d+1}$	M=9	0.87/8.79	0.13/0.19	1.06/0.91	9.47/8.74	31.91/69.81	13.18/37.96	9.38
	M=10	0.44/7.45	0.11/0.17	1.26/0.84	9.51/8.93	30.56/63.81	12.52/33.71	9.62
	M=11	0.10/5.60	0.12/0.18	1.46/0.93	9.41/9.09	31.31/68.61	12.86/36.44	10.82
	M=12	0.01/4.17	0.13/0.18	1.40/0.91	9.54/9.15	26.73/61.16	10.91/31.27	11.51
MPC		0	0.00	7.99	11.17	1	1	1

parameters. For our algorithms, the value of ε_{AB_d} is usually only slightly lower than for the classic MPC and sometimes, it gets even higher. Moreover, this error does not strictly decrease with the increase of

16

Table 4: Comparision of the results - multi-sample algorithm, $M_p = 20$

		$\Delta E(\%)$	$\overline{ZV}(\%)$	ε_{AB}	ε_{AB_d}	$\sum \mathcal{J}$	$\sum \mathcal{J}_{n_d+1}$	t_{comp}
$\max \mathcal{J}$	M=4	3.89/13.70	0.16/0.19	1.15/0.77	9.97/10.16	26.24/44.65	11.04/22.43	18.32
	M=6	1.33/ 7.89	0.23/0.30	1.20/1.02	10.10/10.01	23.05/35.62	9.04/17.04	19.68
	M=8	0.14/ 8.50	0.15/0.22	1.37/1.00	10.01/10.11	18.40/39.12	7.55/18.16	20.81
	M=10	0.01/ 3.33	0.13/0.19	1.63/1.01	10.15/ 9.91	11.79/27.95	5.16/11.67	22.51
$\max \mathcal{J}_{n_d+1}$	M=4	6.46/19.22	0.23/0.30	1.22/1.15	11.14/10.16	21.58/31.91	11.96/17.70	7.32
	M=6	1.01/ 5.78	0.21/0.27	1.41/1.21	11.35/ 9.32	18.81/27.23	9.40/13.23	7.72
	M=8	0.40/ 1.31	0.15/0.19	1.81/1.57	11.14/ 9.78	12.63/17.13	6.49/ 8.64	8.16
	M=10	0.01/ 0.50	0.11/0.14	2.13/1.74	11.59/ 9.52	9.61/13.38	5.14/ 6.95	9.65
MPC		0	0.00	7.99	11.17	1	1	1

$\Delta \mathcal{J}$. This can be explained as follows: Stage II optimization of our algorithms can directly improve the estimation of the input parameters b_i and indirectly affect the estimation accuracy of the output parameters a_i, however, *no* change of the input values can influence the values of the disturbance variables. The best that can be achieved is that a suitable choice of the input values decorrelates the disturbances from both the inputs and the outputs which in turn slightly increases the accuracy of the disturbance parameters d_i.

The ability of both our algorithms to provide more precise parameter estimates is demonstrated also by Fig. 2 and Fig. 3 where the estimation errors for the model parameters considering chosen algorithm settings are depicted. Looking at the pictures, it is obvious that our algorithms yield a_i and b_i estimation errors with significantly smaller variance and also mean value than the MPC with no additional excitation. On the other hand, the improvement in accuracy of the disturbance parameters estimates is only marginal, which confirms the discussion presented above.
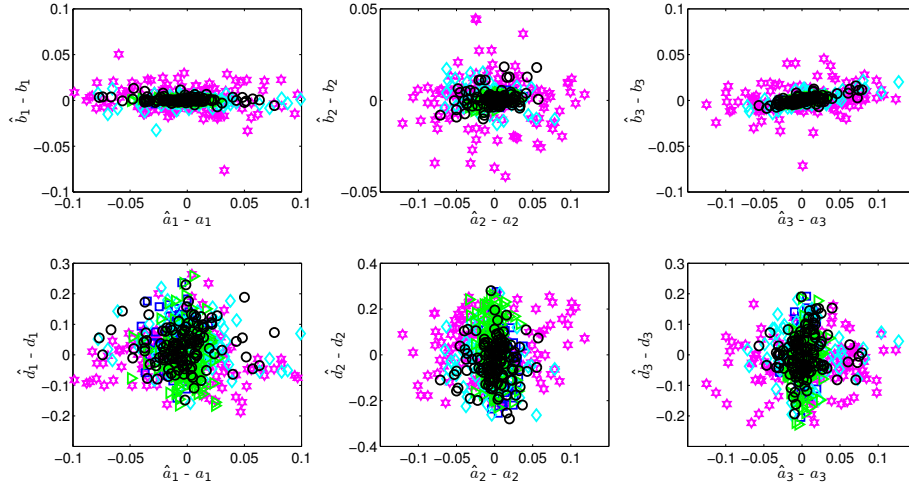

Figure 2: Parameter estimation errors – one-sample algorithm (magenta – MPC, blue – $\{M_p = 0, \mathcal{J}\}$, green – $\{M_p = 20, \mathcal{J}\}$, cyan – $\{M_p = 0, \mathcal{J}_{n_d+1}\}$, black – $\{M_p = 20, \mathcal{J}_{n_d+1}\}$).
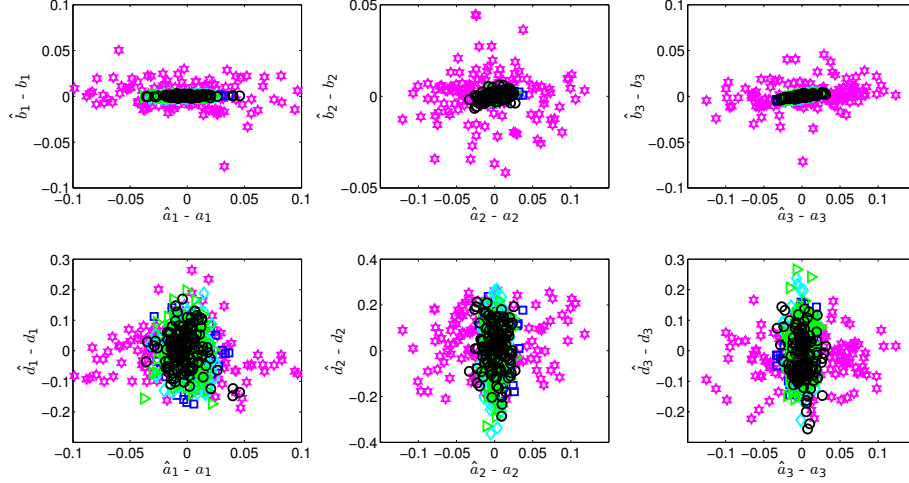
17

Figure 3: Parameter estimation errors – multi-sample algorithm (magenta – MPC, blue – $\{M_p = 0, \mathcal{J}\}$, green – $\{M_p = 20, \mathcal{J}\}$, cyan – $\{M_p = 0, \mathcal{J}_{n_d+1}\}$, black – $\{M_p = 20, \mathcal{J}_{n_d+1}\}$).

Another interesting observation to be made based on the provided pictures is how the accuracy improvement is spread among the estimated parameters. First of all, the most significant improvement of the one-step algorithm estimates corresponds to the b_1 parameter. This following explanation can be provided: during its Stage II optimization, only a single input sample is optimized. Therefore, the algorithm tries to achieve the whole informativeness increase by suitable major changes of the first input sample. This turns into the most evident enhancement of the estimates of the first input parameter b_1 corresponding to this input sample. Of course, the algorithm makes use of the mathematical model and thanks to large M, it improves the excitation also in the directions appertaining to the rest of the parameters. This statement is supported by the depicted estimation errors of the $a_{1,2,3}$ and $b_{2,3}$ parameters – their accuracies have also been ameliorated compared with the MPC case, although not in such significant way. Since just one degree of freedom is available, the gain in the rest of the parameters is not as distinguished as in case of the multi-sample algorithm. The multi-sample algorithm has more degrees of freedom at disposal since it optimizes as much as M input samples. The ability to distribute the excitation effort among multiple input samples considerably improves the identifiability of *all* output/input parameters and as shown in the corresponding pictures, the decrease in the estimation inaccuracy is spread more evenly among all of them as well.

Now, let us compare the table pairs with $M_P = 0$ and $M_P = 20$ for the introduced algorithm i.e. Table 1 with Table 2 and Table 3 with Table 4. Such comparison provides an interesting insight into how the performance of the algorithms changes when they are provided with information about the past system excitation. Recall that $M_P = 0$ means that the algorithm takes only the future excitation into account while with $M_P = 20$, also the information about the past system excitation is exploited. Comparing Table 1 with Table 2, it is obvious that such information improves the performance of the one-sample algorithm and the data excitation is better, which leads to more accurate parameter estimates. On the other hand, no such enhancement of the multi-sample algorithm behavior can be seen inspecting Table 3 and Table 4. This is related to the number of the input samples that can be manipulated by the algorithms. The one-sample algorithm manipulates only with a single input sample and therefore, when provided with additional information about the past measured data, this input sample can be used in a more suitable way. On the other hand, the multi-sample algorithm optimizes a much broader set of the input samples ($9 - 12$ with

18

$M_P = 0$). Thus, even with $M_P = 0$, enough maneuverability freedom is at disposal and the system excitation can be laid out quite appropriately even looking only into the future. This means that the information about the past excitation of the system does not pose such advantage as for the one-sample algorithm and therefore, also the positive effect on the obtained results is lesser.

Last of all, let us inspect the average computational time t_{comp} for various settings of the algorithms. Based on the values listed in the tables, the one-sample algorithm can be generally regarded as faster and apparently also less computationally demanding than the multi-sample algorithm. This results from the fact that the one-sample algorithm optimizes only a single input sample compared with M samples optimized by the multi-sample algorithm. Furthermore, as discussed in the previous section, maximizing $(n_d + 1)$ smallest eigenvalues instead of the single smallest one does not bring any improvement in time complexity of the one-sample algorithm since the explored interval does not change with the change of the optimization criterion. However, the situation is completely different in case of the multi-sample algorithm where maximization of $\mathcal{J}_{n_d+1}$ yields several times shorter computational time compared with maximization of $\mathcal{J}$ and thus, the time requirements of the multi-sample algorithm maximizing criterion (17) become more comparable to those of the one-sample algorithm. Let us also have a look at the calculation time of the variants that do "look back" and those that do not (i.e. $M_P = 0$ vs. $M_P = 20$). Speaking about the one-sample algorithm, no significant difference can be observed between the two variants. This can be attributed to the fact that the time consumption is mainly determined by the length of the inspected input values interval, while the number of input samples considered in calculation of the informativeness increase influences it only marginally. For the multi-sample algorithm, however, the situation is completely different. Since the complexity of the optimization task is directly given by the dimension of the optimization space, the higher M is, the longer the calculation takes. Here, let us remind that the variant with $M_P = 0$ require higher M to preserve the full rank of the information matrix increase. As a result, $M_P = 0$ yields generally longer computational times than $M_P = 20$.

To conclude this case study, the observations can be summarized as follows: the multi-sample algorithm provides the best performance in the sense of data informativeness, however, it is also more computationally demanding. This can be improved exploiting the newly introduced data excitation criteria. The one-sample algorithm, on the other hand, is more suitable for situations with limited computational resources. It still significantly outperforms the original zone MPC, however, at only a gentle increase of computational time.

4.2. Building modeling example

In this part of the case study, the persistently exciting MPC framework was applied to temperature zone control in a one-zone building. This more practical example is provided not to show only good theoretical properties of the persistently exciting MPC framework but also to demonstrate the fact that it is sufficiently robust and capable of performing well even under imperfect real-life conditions. Here, the one-sample algorithm was chosen due to several reasons. In industrial practice, the available hardware resources and computational time are often very limited. For rather small-scale tasks (e.g. one-zone building climate control), the limitations are even more strict. This favors the one-sample algorithm being the less computationally demanding variant. Moreover, as presented in the previous example, even the simple one-sample algorithm provides sufficiently excited data leading to a significant improvement in parameters identifiability compared with the use of non-exciting MPC.

Building model considered in this work was created in Trnsys, an engineering simulation software [37]. Trnsys is a frequently used tool for a wide range of purposes [38], which can be mostly attributed to the fact that particular physical phenomena are modelled in detail ensuring a very high level of fidelity. Therefore, such building model can be exploited as a sufficiently accurate simulator of a real building.

The used model is schematically depicted in Fig. 4. It represents a medium weight building with one zone. Its sizes are $5 \times 5 \times 3$ m and the south oriented wall contains a window of area of $3.75\,\mathrm{m}^2$. The pipes encapsulated into the ceiling referred to as thermally activated building system (TABS) distribute supply water which then performs thermal exchange with the concrete core of the building consequently heating the air in the room. Time-step of the simulation was set to $T_s = 15\,\mathrm{min}$, which guarantees proper convergence of Trnsys internal algorithms.
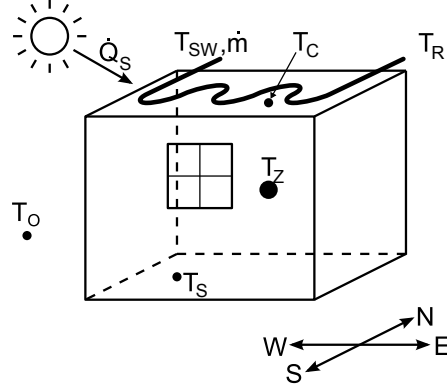
19

Figure 4: A scheme of the modelled building

First, the Trnsys model was utilized as a generator of data used for identification of a linear model exploited by the MPC as a predictor. From the gathered data, the parameters of a model with the following structure were estimated:

$$T_{Z,k} = -\sum_{i=1}^{n_a} a_i T_{Z,k-i} + \sum_{i=1}^{n_b} b_i Q_{k-i} + \sum_{i=1}^{n_d} d_i T_{amb,k-i} + e_k, \tag{22}$$

where T_Z, $\dot{Q}$ and T_{amb} specify the zone temperature (output), the energy supplied by the TABS system (optimized input) and the predictions of the ambient temperature (disturbance variable). Models with this structure are commonly used as a simplified expression of the building dynamics for the control purposes. The chosen set of variables was picked up to represent the real application as reliably as possible – in vast majority of the MPC applications for real buildings, these variables are usually available as measurements and/or predictions. To estimate the parameters of the presented structure, identification method used in [39] for building model identification was employed. Following a procedure given in [39], the meta-parameters of this structure were chosen as $n_a = n_b = n_d = 3$.

Trying to bring this case study even closer to reality, real outdoor temperature profiles for Prague were used as the ambient temperature T_{amb}. It should be noted that the predictions were not perfect and at the beginning of each day, a 2-day forecast of certain accuracy was provided to both the classic MPC and our sufficiently exciting algorithm. At each discrete step, the algorithms extracted a 12-hour subsequence out of this forecast, which they used as the disturbance prediction.

This identified model was then incorporated into the MPC controller optimizing energy supplied to the system while satisfying thermal comfort restrictions in the building zone over the prediction horizon P.

The controllers optimized over a prediction horizon of 12 hours resulting in $P = 48$ samples. T_Z^{min} was generated in accordance with the following 7-days schedule with night and weekend setbacks:

$$T_Z^{min} = \begin{cases} 22°C & \text{work days from 8 a.m. to 6 p.m} \\ 20°C & \text{weekends, holidays, work days from 6 p.m. to 8 a.m..} \end{cases} \tag{23}$$

The following tuning was used: for thermal comfort, the quadratic and the linear weight were set to 1000 and 10000, respectively, while for the consumed energy, the quadratic and the linear weight of 50 and 0.1 were considered.

At first, the classic zone MPC with these settings was used to control the testbed building over a 3-month period (starting at the beginning of January). The same simulation was then performed using the exciting MPC with various settings for maximal allowed perturbation $\Delta J = 1000$ and $\Delta J = 1300$ and

20

various excitation horizon $M = \{2, 4, 6, 8\}$. This enabled to compare the behavior of the non-exciting MPC formulation and the persistently exciting MPC algorithm with different choice of the tuning parameters. Note that both algorithms used the same model (without any adjustments or re-identification) over the whole 3-month simulation. This model was identified from a 2-week period from 1 January to 15 January.

4.2.1. Results

Similarly to the artificial example case, two viewpoints can be considered when evaluating the provided algorithms, namely *i)* the possibility of system re-identification; *ii)* the original MPC requirements and restrictions satisfaction.

Since the primary goal is to re-identify the parameters of the model for the predictive controller using the closed-loop data, the first comparison is focused on the amount of information contained in the data quantified by $\mathcal{J}$. Here, higher amount of information–a result of the data being excited in a more appropriate way–enables identification of better and more accurate models. Estimation of the model parameters was performed with the 3-month data set in a "receding horizon" fashion as follows: for every run of the identification routine, a 500-sample data subset was used and then, the beginning of the identification period was shifted by 100 samples. Using this approach, a sufficiently rich set of models was obtained for both the traditional non-exciting MPC and for each setting of the sufficiently exciting MPC as well.

To inspect the quality of the identified models, a validation data set of 30 days was exploited while both T_{amb} and $\dot{Q}$ were excited by a pseudo-random binary signal with a sufficient bandwidth in order to investigate the accuracy of the model on the frequencies corresponding to those of the implemented control strategy. Considering the prediction horizon of 12 h, frequencies higher than approximately 10^{-5} Hz are of the main interest.

Besides the ability to re-identify the model, it is also important to verify how well do the designed controllers satisfy the control requirements, respect the imposed constraints and how much "do they cost". To investigate the control performance, the following aspects were considered: average control zone violation $\overline{CV}$ (underheating), maximal control zone violation over the whole simulated period MCV and energy consumption EC. Dealing with building climate control applications, both the energy consumption and the control zone violation have their own reasonable physical interpretations: the overall energy consumption can be measured in kWh and the control zone violation represents the violation of the user thermal comfort (underheating in this case) and can be given in Celsius degrees. This is the reason why unlike the artificial example, the energy consumption increase and the control zone violation are presented in absolute numbers instead of being normalized.

The obtained results for both the classic zone MPC formulation and the sufficiently exciting MPC algorithm with different settings are presented in Table 5.

Table 5: Building climate control – results

		MIM4DC				MPC
		M=2	M=4	M=6	M=8	
Δ J=1000	$\overline{CV}$ (°C)	0.01	0.01	0.01	0.01	0.02
	MCV (°C)	0.16	0.17	0.16	0.16	0.12
	EC (kWh)	1567	1574	1568	1574	1482
	$\mathcal{J}$	1.596	1.747	1.745	1.784	1
Δ J=1300	$\overline{CV}$ (°C)	0.005	0.006	0.006	0.006	0.021
	MCV (°C)	0.18	0.19	0.18	0.19	0.12
	EC (kWh)	1625	1637	1639	1726	1482
	$\mathcal{J}$	1.523	1.766	1.798	1.838	1

At first, let us have a look at the consumed energy. From Table 5, it is obvious that the classic MPC con-

21

sumes the smallest amount of energy among all the tested controllers, however, note that the consumption increase due to incorporation of the persistent excitation condition is not dramatic; usually, it is not higher than 10 %. This demonstrates that for a low price (i.e. little energy consumption increase), sufficiently excited data that enable to re-identify the parameters of the system more accurately are obtained.

Inspecting the thermal comfort violation, it can be observed that in some cases, the classic MPC violates the comfort requirements even more than the sufficiently exciting MPC (see Table 5), which can be explained in a simple way. For zone control strategy, the cost function is assymetric and the constraints for the second stage obtained in the first stage of the algorithm are assymetric with respect to the original u^*_{MPC} as well. In other words, $\bar{u}^{max}$ is usually further away from u^*_{MPC} than $\bar{u}^{min}$. Moreover, from the information gain point of view, it is usually also more advantageous to choose the optimal $\bar{u}^*_k$ closer to $\bar{u}^{max}$ which results in gentle zone temperature increase. Nevertheless, the violations are negligible for both MPC variants and in most cases, they lie bellow the sensitivity threshold of majority of the temperature sensors. Therefore, it can be concluded that the persistent excitation condition incorporated into the presented algorithm does not have a significant negative impact on the thermal comfort.

From the comparison given in Table 5, a dependence of $\mathcal{J}$ representing the minimal eigenvalue of the information matrix increase and quantifying the data informativeness on maximal allowed perturbations $\Delta J = 1000$, $\Delta J = 1300$ can be observed. From the obtained values, it can be seen that although the maximal allowed perturbation increase comes hand in hand with increase of gathered information (better conditions for the required re-identification), it causes also higher energy consumption.

As in real life, also in case of a high-fidelity building model the parameters of the structure are not known exactly. Since the Trnsys testbed is a highly complex model with a detailed and complicated non-linear structure, it was not possible to determine how close the estimated parameters to the true system parameters were. Unlike the first part of case study presented in Section 4.1.1, we thus decided to evaluate the model quality by comparing a normalized root mean square error (NRMSE) fitness value defined as

$$fit_{NRMSE} = \left(1 - \sum_{k=1}^{N} \frac{\left\|T_{Z,k} - \hat{T}_{Z,k}\right\|_2}{\left\|T_{Z,k} - E(T_Z)\right\|_2}\right) [100\%]. \tag{24}$$

In this formulation, E stands for the mean value operator. Fig. 5 compares fit_{NRMSE} of the models identified from data provided by sufficiently exciting MPC for $M = 6$ and both allowed values of ΔJ with the fit_{NRMSE} values of the models identified from the data gathered from the classic MPC. The figure demonstrates the ability of our algorithm to excite the data in a more appropriate way thus leading to better re-identification of the model with average fit_{NRMSE} about 90%. The same evaluation applied to the classic MPC results only in 80% fitness value. Looking at the trend of the gathered information (see Table 5), better results–i.e. models with better prediction properties–are achieved by the sufficiently exciting algorithm with higher allowed perturbation.

5. Conclusions

In this paper, two algorithms for MPC with guaranteed identifiability were provided for a class of problems commonly encountered in control engineering practice, namely for zone MPC for linear systems with external predictable disturbances. Both algorithms are based on a two-stage procedure where in the first stage, the original zone MPC problem is solved, while in the second stage, the data excitation is optimized by manipulating either the first one or M first input samples.

Apart from attractive theoretical properties that were demonstrated on an example of artificial system, also validation using a high-fidelity building model was provided. Both of the proposed algorithms *significantly* outperform the classic zone MPC without excitation and the obtained results make them promising candidates for energy efficient closed loop experiment design for predictive control.

The future ambition is to use these algorithms in combination with methods for detection of model deviation as follows: the system would be controlled by the classic MPC and if a significant deviation of the model predictions from the measured data is detected, a short-term switch to either of the provided algorithms ensuring sufficiently excited data for the re-identification would be performed.
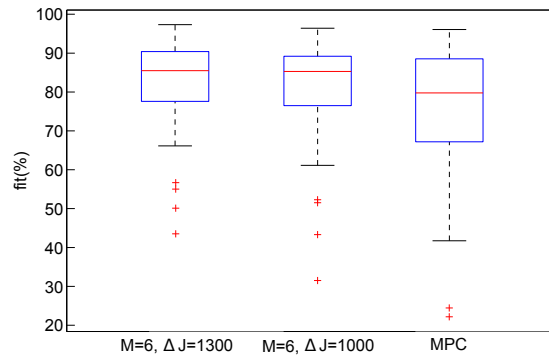
22

Figure 5: Normalized root mean square error fitness – comparison.

References

[1] D. Q. Mayne, Model predictive control: Recent developments and future promise, Automatica 50 (12) (2014) 2967–2986.

[2] J.-P. Corriou, Model Predictive Control, in: Process Control, Springer, 631–677, 2018.

[3] M. G. Forbes, R. S. Patwardhan, H. Hamadah, R. B. Gopaluni, Model predictive control in industry: Challenges and opportunities, IFAC-PapersOnLine 48 (8) (2015) 531–538.

[4] M. L. Darby, M. Nikolaou, MPC: Current practice and challenges, Control Engineering Practice 20 (4) (2012) 328–342.

[5] Y. Zhu, Multivariable system identification for process control, Elsevier, 2001.

[6] L. Ljung, Prediction error estimation methods, in: Circuits, Systems, and Signal Processing, Birkhauser Boston, ISBN 1531-5878, 11–21, 2001.

[7] L. Ljung, System identification, Wiley Online Library, 1999.

[8] I. Gustavsson, L. Ljung, T. Soderstrom, Identification of processes in closed loop–identifiability and accuracy aspects, Automatica 13 (1) (1977) 59–75.

[9] P. Van Den Hof, R. Schrama, Identification and control – closed-loop issues, Automatica 31 (12) (1995) 1751–1770.

[10] P. Van den Hof, Closed-loop issues in system identification, Annual reviews in control 22 (1998) 173–186.

[11] M. Shouche, H. Genceli, P. Vuthandam, M. Nikolaou, Simultaneous Constrained Model Predictive Control and Identificatoin of DARX Processes, Automatica 34 (1998) 1521–1530.

[12] E. Žáčeková, S. Prívara, M. Pčolka, Persistent excitation condition within the dual control framework, Journal of Process Control 23 (9) (2013) 1270–1280.

[13] M. Tanaskovic, L. Fagiano, M. Morari, On the optimal worst-case experiment design for constrained linear systems, Automatica 50 (12) (2014) 3291–3298.

[14] G. Bustos, A. Ferramosca, J. Godoy, A. González, Application of Model Predictive Control suitable for closed-loop re-identification to a polymerization reactor, Journal of Process Control 44 (2016) 1–13.

[15] A. Ebadat, P. E. Valenzuela, C. R. Rojas, B. Wahlberg, Model predictive control oriented experiment design for system identification: a graph theoretical approach, Journal of Process Control 52 (2017) 75–84.

[16] J. Rathouský, V. Havlena, MPC-based approximate dual controller by information matrix maximization, International Journal of Adaptive Control and Signal Processing 27 (11) (2013) 974–999.

[17] Y. Ma, F. Borrelli, B. Hencey, B. Coffey, S. Bengea, P. Haves, Model Predictive Control for the Operation of Building Cooling Systems, Control Systems Technology, IEEE Transactions on PP (99) (2011) 1–8, ISSN 1063-6536, doi:\bibinfo{doi}{10.1109/TCST.2011.2124461}.

[18] B. Coffey, F. Haghighat, E. Morofsky, E. Kutrowski, A software framework for model predictive control with GenOpt, Energy and Buildings 42 (7) (2010) 1084 – 1092, ISSN 0378-7788, doi:\bibinfo{doi}{10.1016/j.enbuild.2010.01.022}.

[19] F. Oldewurtel, A. Parisio, C. N. Jones, M. Morari, D. Gyalistras, M. Gwerder, V. Stauch, B. Lehmann, K. Wirth, Energy efficient building climate control using stochastic model predictive control and weather predictions, in: American control conference (ACC), 2010, IEEE, 5100–5105, 2010.

[20] M. Razmara, M. Maasoumy, M. Shahbakhti, R. Robinett, Optimal exergy control of building HVAC system, Applied Energy 156 (2015) 555–565.

[21] P. H. Shaikh, N. B. M. Nor, P. Nallagownden, I. Elamvazuthi, T. Ibrahim, A review on optimized control systems for building energy and comfort management of smart sustainable buildings, Renewable and Sustainable Energy Reviews 34 (2014) 409–429.

[22] D. Gyalistras, M. Gwerder, (Eds.), Use of weather and occupancy forecasts for optimal building climate control (OptiControl): Two years progress report, Tech. Rep., ETH Zurich, Switzerland and Siemens Building Technologies Division, Siemens Switzerland Ltd., Zug, Switzerland, 2009.

[23] E. Zacekova, S. Privara, Z. Vána, J. Cigler, L. Ferkl, Dual control approach for zone model predictive control, in: Control Conference (ECC), 2013 European, IEEE, 1398–1403, 2013.

23

[24] E. Záceková, M. Pčolka, M. Šebek, On satisfaction of the persistent excitation condition for the zone mpc: Numerical approach, in: The 19th World Congress of the International Federation of Automatic Control, IFAC, vol. 2014, 2014.

[25] P. Antsaklis, A. Michel, A linear systems primer, Birkhauser, 2007.

[26] J. Maciejowski, Predictive control: with constraints, Pearson education, 2002.

[27] G. C. Goodwin, K. S. Sin, Adaptive filtering prediction and control, Courier Corporation, 2014.

[28] J. Rathousky, V. Havlena, Multiple-Step Active Control with Dual Properties, in: IFAC World Congress, vol. 18, 1522–1527, 2011.

[29] H. Genceli, M. Nikolaou, New approach to constrained predictive control with simultaneous model identification, AIChE journal 42 (10) (1996) 2857–2868.

[30] C. A. Larsson, Application-oriented experiment design for industrial model predictive control .

[31] A. Ebadat, P. E. Valenzuela, C. Rojas, H. Hjalmarsson, B. Wahlberg, Applications oriented input design for closed-loop system identification: a graph-theory approach, in: Decision and Control (CDC), 2014 IEEE 53rd Annual Conference on, IEEE, 4125–4130, 2014.

[32] T. A. N. Heirung, B. Foss, B. E. Ydstie, MPC-based dual control with online experiment design, Journal of Process Control 32 (2015) 64–76.

[33] A. Ebadat, P. E. Valenzuela, C. R. Rojas, B. Wahlberg, Model Predictive Control oriented experiment design for system identification: A graph theoretical approach, Journal of Process Control 52 (2017) 75 – 84, ISSN 0959-1524, doi:\bibinfo{doi}{https://doi.org/10.1016/j.jprocont.2017.02.001}, URL `http://www.sciencedirect.com/science/article/pii/S0959152417300185`.

[34] O. Sotomayor, D. Odloak, L. Moro, Closed-loop model re-identification of processes under MPC with zone control, Control Engineering Practice 17 (5) (2009) 551–563.

[35] G. Bustos, A. Ferramosca, J. Godoy, A. GonzÄˇlez, Application of Model Predictive Control suitable for closed-loop re-identification to a polymerization reactor, Journal of Process Control 44 (2016) 1 – 13, ISSN 0959-1524, doi:\bibinfo{doi}{https://doi.org/10.1016/j.jprocont.2016.04.011}, URL `http://www.sciencedirect.com/science/article/pii/S095915241630035X`.

[36] D. Telen, B. Houska, M. Vallerio, F. Logist, J. Van Impe, A study of integrated experiment design for NMPC applied to the Droop model, Chemical Engineering Science 160 (2017) 370–383.

[37] L. Thermal Energy System Specialists, Transient System Simulation Tool, URL `http://www.trnsys.com`, 2012.

[38] M. Trčka, J. Hensen, M. Wetter, Co-simulation of innovative integrated HVAC systems in buildings, Journal of Building Performance Simulation 2 (3) (2009) 209–230.

[39] E. Žáčeková, Z. Váňa, J. Cigler, Towards the real-life implementation of MPC for an office building: Identification issues, Applied Energy 135 (2014) 53–62.

5.3 Bilinear and Polynomial Systems

Thanks to a better availability of high computational power, nonlinear MPCs are getting more attention and have become usable also in real-life tasks and therefore, algorithms for persistent excitation of nonlinear systems are discussed in this thesis as well focusing on a special class of bilinar/polynomial nonlinear systems. Again, the inspiration came from the building sector where the bilinearity is commonly encountered and should be considered in this regard since very often, the manipulated variables "enter" the system being multiplied by its internal variables.

In [A.18], modifications of both the one-sample and the gradient algorithm for persistently exciting MPC for bilinar systems were designed and tested. The first-stage "MPC" optimization was formulated as a quadratic programming problem with quadratic constraints (QPQC). Regarding the second stage, both the one-sample and the gradient algorithm were still applicable for the data excitation optimization. Moreover, the class of the systems to be handled by these two approaches was extended to include also systems with polynomial nonlinearities. Under this assumption, the first-stage optimization still remains a QPQC task (although of a higher dimension depending on the degree of the polynomial), however, the second-stage optimization changes slightly. While the gradient algorithm remains more or less the same, the one-sample approach requires finding roots of a squared polynomial instead of a parabola and the subsequent one-dimensional search gets also slightly more involved.

To conclude the current chapter, the aforementioned paper is presented on the next page et seq.

MPC for a Class of Nonlinear Systems with Guaranteed Identifiability

Eva Žáčeková[1], Matej Pčolka[1], Michael Šebek[1], Sergej Čelikovský[1,2]

Abstract— **This paper addresses the problem of model predictive control for a class of nonlinear systems which satisfies persistent excitation condition. The conditions under which a nonlinear system description can be handled are specified and two algorithms (one optimizing the first input sample and the other considering optimization of an M-sample subsequence of the input profile) solving the persistent excitation condition within a predictive controller for nonlinear systems are developed, both maximizing the smallest eigenvalue of the information matrix increase. The numerical experiments performed on a test-bed system demonstrate that the algorithms are able to successfully improve identifiability of a nonlinear system description while keeping the original controller performance lower than arbitrarily chosen level.**

I. Introduction

During the last years, modern control methods have witnessed significant boom. Being popular not only among the academicians, these approaches of which the most noticeable one is the Model Predictive Control (MPC) have started to be more appreciated also by the control engineers.

MPC brings wide variety of new possibilities and advantages, it can simply handle various input/state/output constraints and simplifies the way the multi-input/multi-output systems are controlled. Except of plenty of undisputable benefits, several problems arise. Their main disadvantage is the crucial necessity of a good mathematical model by which the favorable controller performance is conditioned. It is actually the search for such appropriate model that is many times more time-demanding than the controller design itself [1].

A very common situation that occurs in industrial practice is that the system is already controlled by some kind of advanced controller whose control performance starts to deteriorate. This is usually caused by the mathematical model which might loose its ability to describe the system dynamics in a suitable manner and the appropriate step is to re-identify the model. Classical open-loop identification experiments might be inadmissible due to operational and/or economical reasons. In such case, commonly used identification methods fail and are not able to ensure that the identified models reach reasonable quality [2], [3]. Although relatively wide variety of methods are able to cope with the closed-loop identification data, they work reliably only for simple linear controllers [4]. Since the MPC structure is much more complex, it is inevitable find alternative way of dealing with this problem.

Therefore, it is useful to focus on methods where the controller itself brings additional information and thus improves the model of the process – in such case, the controller performs some kind of closed-loop identification experiment. Several works can be found in the available literature that

[1]Department of Control Engineering, Faculty of Electrical Engineering of Czech Technical University in Prague, Technická 2, 166 27 Praha 6, Czech Republic
[3]Institute of Information Theory and Automation, Czech Academy of Sciences, Pod Vodárenskou věží 4, 182 08 Praha 8, Czech Republic

have addressed this problem [5], [6], [7], [8]. Their common drawback is that they provide solution valid only for linear systems.

Since majority of the industrial processes possess a nonlinear dynamics and thanks to the progress in numerical optimization which makes the nonlinear-programming solvers more affordable and usable in real operation, it is not uncommon to design an MPC making use of nonlinear system model. Therefore, this paper focuses on design of such predictive controller that ensures sufficiently excited data suitable for identification of a class of polynomial nonlinear systems. Of a special interest is a sub-class containing bilinear systems since such system dynamics description appears in many areas of biochemical engineering [9], building control [10], electrical engineering [11] and elsewhere [12].

This paper provides adaptation and extension of the algorithms that have already been successfully validated on examples of linear systems [8], [13]. The adaptations make the algorithms suitable for use also in case that nonlinear system description is assumed. As already indicated, the extensions focus on bilinear systems and possibilities of use of the adapted algorithms for more general polynomial nonlinear systems are discussed.

The paper is organized as follows. Sec. II introduces the considered problem and the necessary background. In Sec. III, the problem of persistently exciting MPC for the class of nonlinear systems specified in Sec. II is discussed and two algorithms solving this task are developed – both the one-sample and the multi-sample algorithm are described in detail. The performance of the proposed algorithms is demonstrated in Sec. IV. Sec. V concludes the paper.

II. Problem Statement

In this Section, the necessary background is provided.

A. Model of the system

In this paper, single-input/single-output (SISO) nonlinear systems with the following description [14] are considered:

$$y_k = \beta_0(u_{k-1}, \ldots, u_{k-n}) + \sum_{i=1}^{n} \beta_i(u_{k-1}, \ldots, u_{k-n})y_{k-i} + \varepsilon_k, \tag{1}$$

where y_k and u_k are the system output and input sequences, ε_k represents zero-mean white noise and β_i are such polynomials of arguments $u_{k-1}, \ldots, u_{k-n}$ that

$$\beta_i(u_{k-1}, \ldots, u_{k-n}) = \theta_i^{\mathrm{T}} Z_{k,i} + \alpha_i, \tag{2}$$

where θ_i are constant real vectors, α_i are constant real scalars (with $\alpha_0 = 0$) and $Z_{k,i}$ are vectors of scalar monomials of $u_{k-1}, \ldots, u_{k-n}$. Parameter n specifies number of lagged inputs in structure (1). Then, the model structure (1) can be reformulated as

$$y_k = \theta^{\mathrm{T}} Z_k + \varepsilon_k, \tag{3}$$

163

where $\theta = \begin{bmatrix} \theta_0^T & \theta_1^T & \alpha_1 & \theta_2^T & \alpha_2 & \dots & \theta_n^T & \alpha_n \end{bmatrix}^T$ and $Z_k = \begin{bmatrix} Z_{k,0}^T & Z_{k,1}^T y_{k-1} & y_{k-1} & \dots & Z_{k,n}^T y_{k-n} & y_{k-n} \end{bmatrix}^T$.

Parameters of structure (3) can be straightforwardly estimated by linear regression $\hat{\theta} = Y \backslash \mathcal{Z}^T$, where $Y = \begin{bmatrix} y_1 & y_2 & \dots & y_N \end{bmatrix}^T$, $\mathcal{Z} = \begin{bmatrix} Z_1 & Z_2 & \dots & Z_N \end{bmatrix}^T$ and N is the length of identification data [2].

Example. Let us consider the following system with the structure corresponding to (1):

$$y_k = ay_{k-1} + by_{k-2} + cu_{k-1}y_{k-1} + du_{k-2}y_{k-1} \tag{4}$$
$$+ eu_{k-1}^2 + fu_{k-1}^2 y_{k-1} + gu_{k-2}y_{k-2}.$$

Let us denote $\theta_0 = \begin{bmatrix} e \end{bmatrix}$, $\theta_1 = \begin{bmatrix} c & d & f \end{bmatrix}^T$, $\theta_2 = \begin{bmatrix} g \end{bmatrix}$, $Z_{k,0} = \begin{bmatrix} u_{k-1}^2 \end{bmatrix}$, $Z_{k,1} = \begin{bmatrix} u_{k-1} & u_{k-2} & u_{k-1}^2 \end{bmatrix}^T$, $Z_{k,2} = \begin{bmatrix} u_{k-2} \end{bmatrix}$, $\alpha_1 = a$, $\alpha_2 = b$. Then, the system (4) can be reformulated into the compact form (3) with

$$Z = [u_{k-1}^2 \ u_{k-1}y_{k-1} \ u_{k-2}y_{k-1}$$
$$u_{k-1}^2 y_{k-1} \ y_{k-1} \ u_{k-2}y_{k-2} \ y_{k-2}]^T$$

and

$$\theta = \begin{bmatrix} e & c & d & f & a & g & b \end{bmatrix}^T.$$

B. Persistent excitation condition

One of the sub-objectives of the successful closed-loop experiment algorithm is to provide the control engineer with sufficiently informative data. By this it is meant to provide input-output data which enable (in ideal case with Gaussian white zero mean noise, etc.) exponential convergence of the parameter estimation error to zero. First of all, it is necessary to formulate requirements related to the data informativeness.

Let us consider the model structure (3). If linear regression is to be used to estimate the parameters of this structure, the convergence of the estimates of the parameters is equivalent to existence of such parameters $M \in \mathbb{N}^+$, $\sigma_1 \in \mathbb{R}^+$ and $\sigma_2 \in \mathbb{R}^+$ for which the data satisfy the following condition [15]:

$$\sigma_1 I \le \sum_{i=k}^{k+M} Z_i Z_i^T \le \sigma_2 I, \tag{5}$$

where I is a unit matrix of the corresponding dimension. The expression (5) is referred to as *persistent excitation* (PE) condition. If the input-output data satisfy this condition, they are *sufficiently excited*, they ensure unique estimates of the parameters of the structure (3) and the parameters of such structure are then *identifiable*.

Let us remark that the upper bound σ_2 in condition (5) is not crucial for obtaining of sufficiently excited data [15] and thus the further text focuses on the satisfaction of the lower bound σ_1.

C. Controller

Besides the sufficiently excited data, one of the requirements is the satisfactory control performance specified by the chosen control performance criterion. The objective of the MPC is then to minimize the given criterion by finding the optimal input sequence. Typically, the MPC criterion includes both the penalization of the tracking error with respect to a reference trajectory y_k^{ref} and the penalization of the energy consumption, which can be summarized as:

$$J_{MPC,k} = \sum_{i=0}^{P-1} \left\| Q(y_{k+i} - y_{k+i}^{ref}) \right\|_2^2 + \left\| Ru_{k+i} \right\|_2^2$$
$$\text{s.t.: dynamics (3), } u_{k+i}^{min} \le u_{k+i} \le u_{k+i}^{max}, \tag{6}$$

with weighting matrices Q and R and prediction horizon P.

In case that the dynamics of the controlled system is linear, the optimization problem formulated in this way is convex and it can be simply and quickly solved by any available quadratic programming solver. For nonlinear model structure (1), the above formulated optimization task represents minimization of a quadratic criterion with respect to nonlinear constraints.

Definition 1. Let us define the *extended degree of the i-th sub-regressor* $\bar{\delta}_i \in \mathbb{N}^+$ as $\bar{\delta}_i = \delta_i + 1$, where δ_i is the highest monomial degree of all entries of sub-regressor $Z_{k,i}$ for $i \in \{1, 2, \dots, n\}$.
Let us define the *degree of the absolute sub-regressor* $\bar{\delta}_0 \in \mathbb{N}^+$ as the highest monomial degree of all entries of the *absolute* sub-regressor $Z_{k,0}$.
Then the *total regressor degree* $D \in \mathbb{N}^+$ is defined as the highest sub-regressor degree, $D = \max\{\bar{\delta}_i | i = 0, 1, \dots, n\}$.

Lemma 1. Let us consider optimization task with quadratic cost criterion and polynomial model structure (3) with total regressor degree D. Such optimization task can be reformulated as a quadratic programming task with quadratic constraints (QPQC) introducing p suitable auxiliary variables.

The number of auxiliary variables p can be calculated as

$$p = d_0 - 1 + \sum_{i=1}^{n2} i \, d_i,$$

where the coefficients $d_i \in \{0, 1\}$ satisfy

$$D = \sum_{i=0}^{n2} d_i 2^i.$$

Then, every optimization problem (6) with system dynamics (1) is re-formulated as:

$$\min \overline{X}^T H \overline{X} + j^T \overline{X} \tag{7}$$

subject to

$$\overline{X}^T Q_i \overline{X} + q_i^T \overline{X} + r_i \le 0 \text{ for } i = 1, 2, \dots, m, \tag{8}$$

where the vector of optimized variables is

$$\overline{X} = [X^T \ \overline{u}_{1,k} \ \dots \ \overline{u}_{1,k+P-1} \ \dots \ \overline{u}_{p,k} \ \dots \ \overline{u}_{p,k+P-1}]^T$$

with $m = P(p+2)$. Here,

$$X = \begin{bmatrix} u_k & \dots & u_{k+P-1} & y_k & \dots & y_{k+P-1} \end{bmatrix}^T$$

is the vector of original optimized variables and $\overline{u}_1, \dots, \overline{u}_p$ are the auxiliary variables.$\square$

Even though the problem (7) with constraints (8) is in general a non-convex one, there exists wide variety of convex relaxations of such problems [16], [17]. Furthermore, there are even several freely-available solvers able to find the global optimum of such problem in reasonable time [18].

Remark 1. It should be remarked that for systems with $D \le 2$, $p = 0$ and thus no auxiliary variables are added

which means that the complexity of the optimization task does not increase. Indeed, it can be straightforwardly shown that systems with $D = 1$ are linear systems while $D = 2$ means either systems where the inputs are multiplied by each other or by other lagged inputs or the output of the system is multiplied by certain (eventually lagged) input. Allowing also quadratic constraints, no additional auxiliary variables are needed to handle such tasks. As was already indicated in the introductory part of the paper, many real-life applications include bilinear system dynamics and therefore, such systems are of great practical interest. Since all bilinear systems belong to the group with $D = 2$, the fact remarked in the above paragraph is especially beneficial from the computational point of view.

III. MPC WITH GUARANTEED PERSISTENT EXCITATION

Even though the currently available literature offers several works discussing either the identifiability of certain classes of nonlinear systems [19], [14] or the optimal experiment design for nonlinear systems [20], [21], there are no algorithms dealing with the design of nonlinear MPC respecting the PE condition. The situation is very different in case of linear systems where significant number of relevant works offers algorithms for PE-MPC [6], [5], [7].

In this Section, descriptions of our own algorithms are provided. The objective of the algorithms is to not only satisfy the control requirements but also to provide sufficiently excited data and in such way enable accurate estimation of the parameters of the controlled nonlinear system with polynomial dynamics. The presented algorithms are adaptations and extensions of the previous ones (which work satisfactorily for linear systems [13], [8]) for the class of nonlinear systems.

Both algorithms work in two steps as follows: in the first step, the solution of the problem (6) is found and in the second step, the following optimization task is solved:

$$U^* = \arg\max_{U} \ \mathcal{J}$$
$$\text{s.t.:} \ \ u_{k+i}^{min} \le u_{k+i} \le u_{k+i}^{max}, \, i = 0, \dots, P-1$$
$$J_{MPC,k}(U) \le J_{MPC,k}^* + \Delta J,$$
$$\tag{9}$$

where ΔJ is the user-defined maximal allowed degradation of the original MPC cost function (6) and $\mathcal{J}$ quantifies the data excitation. In the current paper,

$$\mathcal{J} = \lambda_{min} \left(W_p \sum_{i=k-M_P}^{k-1} Z_i Z_i^{\mathrm{T}} + \sum_{i=k}^{k+M} Z_i Z_i^{\mathrm{T}} \right) \tag{10}$$

is assumed. Here, parameters $M_P, M, W_P \ge 0$ are user-defined tuning parameters. In other words, $\mathcal{J}$ represents the smallest eigenvalue of the information matrix increase which means that by maximizing $\mathcal{J}$, the algorithm tries to bring as much information as possible in the direction which has been least informative. Parameter W_p expresses how important is the information brought by the past obtained data and parameters M and M_P specify how many past/future time steps are take into account.

The two designed algorithms differ mainly in the way they address the optimization task (9). Their descriptions follow.

A. Algorithm I. – One-sample approach

This algorithm relies on the fact that MPC controller usually works according to the receding horizon principle. This principle can be explained as follows: at each discrete time step k, the optimal control sequence for P-step ahead is calculated but only the first element u_k of the calculated input sequence is exploited and applied to the system. Due to the use of the receding horizon principle, the one-sample approach considers only u_k for optimization of the data excitation expressed by (9). The whole procedure is described as follows.

One-sample algorithm
Stage I
1) minimize (6) and obtain optimal input sequence $U_{MPC}^* = \begin{bmatrix} u_{MPC,k} & u_{MPC,k+1} & \cdots & u_{MPC,k+P} \end{bmatrix}^{\mathrm{T}}$;
2) compute optimal value of MPC cost function $J_{MPC,k}^* = J_{MPC,k}(U_{MPC}^*)$;
3) find constraints $\bar{u}_k^{min}$ and $\bar{u}_k^{max}$ for Stage II;
   a) find values $\underline{u}$ and $\overline{u}$ such that $\tilde{u}_k \in \langle \underline{u}, \overline{u} \rangle$ and $J_{MPC,k}(\tilde{U}) \le J_{MPC,k}^* + \Delta J$ are equivalent for

   $$\tilde{U} = \begin{bmatrix} \tilde{u}_k & u_{MPC,k+1} & \cdots & u_{MPC,k+P} \end{bmatrix}^{\mathrm{T}};$$

   b) perform the projection

   $$\bar{u}_k^{max} = \min\{\overline{u}, u_k^{max}\}, \ \ \bar{u}_k^{min} = \max\{\underline{u}, u_k^{min}\}.$$

Stage II
1) compute $\mathcal{J}(\tilde{U}) \,\hat{=}\, \mathcal{J}(\tilde{u}_k)$ with

   $$\tilde{U} = \begin{bmatrix} \tilde{u}_k & u_{MPC,k+1} & \cdots & u_{MPC,k+P} \end{bmatrix}^{\mathrm{T}}$$

   for all

   $$\tilde{u}_k \in \{\bar{u}_k^{min}, \bar{u}_k^{min} + s_u, \bar{u}_k^{min} + 2s_u, \dots, \bar{u}_k^{max}\},$$

   where s_u is a user-defined parameter;
2) find $\tilde{u}_k^* = \arg\max \mathcal{J}(\tilde{u}_k)$;
3) terminate Stage II; set $u_k = \tilde{u}_k^*$ and apply it to the system; wait for new measurements in time $k+1$, repeat from Stage I 1).

The crucial part of the algorithm is to find the constraints $\bar{u}_k^{min}$ and $\bar{u}_k^{max}$ for Stage II. In order to solve this task, let us define the i-step prediction degree and the maximal prediction degree as follows.

Definition 2. Let us consider y_k to be given and fixed and let us express all $(k+1)$- up to $(k+P)$-step predictions $y_{k+1|k}$, $y_{k+2|k}, \cdots y_{k+P|k}$ as polynomials in u_k. The i-step prediction degree $\varrho_i \in \mathbb{N}$ is the degree of u_k in the i-step ahead prediction $y_{k+i|k}$. Then the maximal prediction degree $\bar{\varrho} \in \mathbb{N}$ is the maximal degree of u_k that appears in $(k+1)$- up to $(k+P)$-step predictions, $\bar{\varrho} = \max\{\varrho_i | i = 1, 2, \dots, P\}$.

Lemma 2. Quadratic MPC cost function (6) can be expressed as a polynomial of u_k of degree $2\bar{\varrho}$.

The proof of Lemma 2 is straightforward by substituting all i-step predictions $y_{k+i|k}$ for $i \in \{k+1, \dots, P\}$ into the MPC criterion (6).

Lemma 2 gives us an indication how to find the values $\underline{u}$ and $\overline{u}$ from step 3) of Stage I. Since all but the first sample in $\tilde{U}$ are fixed and equal to the corresponding samples in U_{MPC}^*, J_{MPC} is a polynomial in u_k of order $2\bar{\varrho}$. Considering

165

a bilinear system, $J_{MPC}(u_k)$ is a 2-nd order polynomial. In such case, $\underline{u}$ and $\overline{u}$ are found as roots of the quadratic equation $\alpha_2 u_k^2 + \alpha_1 u_k + (\alpha_0 - \Delta J) = 0$ where the coefficients $\alpha_{\{0,1,2\}}$ are obtained by substituting i-step predictions $y_{k+i|k}$ into (6).

This approach works also for polynomial systems with $\overline{\varrho} > 1$. The only difference from the case with $\overline{\varrho} = 1$ is that instead of finding roots of a quadratic function, roots of a polynomial of order $2\overline{\varrho}$ are searched for. Having obtained $2\overline{\varrho}$ roots $u_{r,1}, u_{r,2}, \ldots, u_{r,2\overline{\varrho}}$, they split the domain of the polynomial $J_{MPC}(\tilde{u}_k)$ into $2\overline{\varrho} + 1$ subintervals $\mathcal{I}_1, \mathcal{I}_2, \ldots, \mathcal{I}_{2\overline{\varrho}}$ out of which the proper subintervals satisfying

$$J_{MPC,k}(\tilde{u}_k) \leq J^*_{MPC,k} + \Delta J, \ \tilde{u}_k \in \mathcal{I}_i$$

for $i \in \{1, 2, \ldots, 2\overline{\varrho} + 1\}$ can be straightforwardly chosen.

Since the optimization performed in Stage II is only a 1-dimensional task, it can be quickly and globally solved by direct optimization approach. This holds even in case that several discontinuous intervals $\mathcal{I}$ are found. Here, s_u is usually equivalent to the resolution with which the input u_k can be set.

B. Algorithm II – Multi-sample approach

Unlike the first alternative presented in the previous Subsection where only the first input sample u_k was available for the Stage II optimization of (10), the second proposed algorithm considers that the whole M-sample sub-sequence of inputs can be used for optimization of (10). The description of Algorithm II. follows.

Multi-sample algorithm
Stage I
  1) minimize (6) and obtain optimal input sequence $U^*_{MPC} = \begin{bmatrix} u_{MPC,k} & u_{MPC,k+1} & \cdots & u_{MPC,k+P} \end{bmatrix}^{\mathrm{T}}$;
  2) compute optimal value of MPC cost function $J^*_{MPC,k} = J_{MPC,k}(U^*_{MPC})$;
Stage II
  1) obtain a set of M perturbed input vectors

$$\{\tilde{U}_i = \begin{bmatrix} u_{MPC,k} \cdots u_{MPC,k+i} + \Delta u \ldots, u^*_{MPC,k+M} \end{bmatrix},$$
$$i = 1, 2, \ldots, M\};$$

  2) evaluate criterion $\mathcal{J}$ for each perturbed vector;
  3) calculate numerical gradient

$$G_l = \begin{bmatrix} \dfrac{\Delta \mathcal{J}_1}{\Delta u}, \dfrac{\Delta \mathcal{J}_2}{\Delta u}, \ldots, \dfrac{\Delta \mathcal{J}_i}{\Delta u}, \ldots, \dfrac{\Delta \mathcal{J}_M}{\Delta u} \end{bmatrix}^{\mathrm{T}};$$

  4) follow the gradient

$$U^l = U^{l-1} + \beta^l \star G^l,$$

where β^l is step length computed in the following way

$$\beta_i^l = \max(0, \tanh(w(\Delta J - (J^*_{MPC,k} - J_{MPC,k}(\tilde{U}_i)))))$$

and $\star$ denotes element-wise multiplication;
  5) **if** $|\mathcal{J}(U^l) - \mathcal{J}(U^{l-1})| \leq \epsilon$
     then terminate Stage II; set $u_k = U_1^l$ and apply it to the system; wait for new measurements in time $k+1$, repeat from Stage I 1),
     else $l = l+1$, repeat from Stage II 1).

The second proposed algorithm performs a gradient-search with iteration-varying search step length. Here, w is a user-defined tuning parameter related to the caution with which the algorithm proceeds in the space of the optimization parameter – the smaller w is, the more carefully the algorithm handles the MPC cost function constraint and the further from the boundary $(J^*_{MPC,k} - J_{MPC,k}(\tilde{U}_i)) = \Delta J$ it starts to slow down.

Here it can be remarked that in case of the multi-sample algorithm, the implementation and the maximization of the informativeness is the same for systems with $\overline{\varrho} = 1$ and $\overline{\varrho} > 1$.

IV. Case study

In this Section, the results of the proposed algorithms are presented.

In order to show the properties and demonstrate the performance of the proposed algorithms, the following SISO system with bilinear dynamics was considered:

$$y_k = 0.4y_{k-1} + 0.15y_{k-2} + 0.1y_{k-3}$$
$$+ 0.42u_{k-1}y_{k-1} + 0.05u_{k-2}y_{k-2} + \varepsilon_k. \tag{11}$$

This model structure can be reformulated into the form (3) with

$$\theta = [0.4 \ 0.15 \ 0.1 \ 0.42 \ 0.05]^{\mathrm{T}}$$

and

$$Z_k = \begin{bmatrix} y_{k-1} & y_{k-2} & y_{k-3} & y_{k-1}u_{k-1} & y_{k-2}u_{k-2} \end{bmatrix}^{\mathrm{T}}.$$

The variance of the noise ε_k was $\sigma_e = 0.01$.

The system was controlled by the MPC (6) minimizing the supplied energy and the reference tracking error with constraints $u^{max} = 1$, $u^{min} = 0$. The reference trajectory y_k^{ref} was generated according to the following schedule:

$$y_k^{ref} = \begin{cases} 1 & 10^3 q + 1 \leq k < 500(q+1), q \text{ is even} \\ 0.5 & 10^3 q + 1 \leq k < 500(q+1), q \text{ is odd} \end{cases} \tag{12}$$

Weighting matrices were chosen as $Q = 1000$ and $R = 1$, the prediction horizon P and the sampling time T_s were $P = 15$ steps and $T_s = 1$ s. In order to bring the example closer to reality, the model which was used by the MPC for the predictions did not perfectly match the real system but its parameters were slightly shifted to

$$\hat{\theta} = \begin{bmatrix} 0.35 & 0.38 & 0.08 & 0.12 & 0.12 \end{bmatrix}^{\mathrm{T}}.$$

With this setting, a simulation with the length of $N = 10 \times 10^3$ samples was performed. Similarly, the simulations were run also for the algorithms developed in this paper with settings provided in Tab. I. The obtained data were then split into several smaller sub-sets with length 500 samples and each data sub-set was used to estimate the parameters of the considered structure.

TABLE I
NOTATION AND SETTINGS.

Notation	Algorithm	ΔJ	M	M_P	W_P
AlgI.	One-sample	20	5	–	0
AlgII.	Multi-sample	25	5	–	0
AlgI.P	One-sample	20	5	15	1/3
AlgII.P	Multi-sample	25	5	15	1/3

Let us remind the objective of the current work which is to develop an algorithm that is able to both satisfy the

control performance and provide the data containing certain amount of information that is sufficient for the successful re-identification. Therefore, we provide the comparison of the presented algorithms with the original MPC to demonstrate that for the price of just relatively small control performance degradation, the presented algorithms are able to generate data which are much more rich on information.

A. Results

Two viewpoints are considered when evaluating the results of the algorithms presented in the paper, namely: *i)* possibility of system re-identification (parameter adjustment); and *i)* the quality requirements and restrictions imposed by the MPC problem formulation. To evaluate the satisfaction of the first sub-objective, the following quantifiers are used.

First of all, the smallest eigenvalue $\lambda_{min}(\Delta I_1^N)$ of the information matrix increase calculated cumulatively over the whole numerical experiment is inspected since this was the quantifier chosen to express the data informativeness. In order to validate the choice of this data informativeness quantifier, determinant of sample covariance matrix of parameters estimation error $\det(S)$ (see [2]) is also investigated. This evaluator is proportional to the size of the ellipsoid which the identified parameters lie in. Investigating both quantifiers, it can be verified whether the maximization of the smallest eigenvalue of the information matrix increase is equivalent to improvement of the parameter identifiability.

Not only the ability to provide data ensuring successful model re-identification but also the satisfaction of the original MPC requirements is interesting. Several evaluators are introduced to provide a comprehensive comparison of the control performance. The first one – relative tracking error e_{ref} – expresses how well the controller tracks the pre-defined reference profile y^{ref},

$$e_{ref} = \frac{1}{N} \sum_{k=1}^{N} \left| \frac{y_k^{ref} - y_k}{y_k^{ref}} \right|.$$

The second important question is "how much does it cost to have sufficiently informative data?". Since even the use of pure non-exciting MPC controller results in some non-zero energy consumption, the question should be reformulated as "how much *more* does it cost to have sufficiently informative data instead of poor data?". To quantify the additional energy which was used to have the possibility to identify the model parameters more precisely, let us introduce a relative energy consumption ΔEC normalized with respect to the MPC-consumption:

$$\Delta EC = \left(\frac{\sqrt{\sum_{k+1}^{N} u_{PE,k}^2}}{\sqrt{\sum_{k+1}^{N} u_{MPC,k}^2}} - 1 \right) \times 100\,(\%),$$

where u_{MPC} and u_{PE} denote the inputs generated by the MPC and PE algorithms, respectively. Last but not least, value J_{res} of the MPC cost function (6) evaluated over the whole duration of the numerical experiment,

$$J_{res} = \sum_{k=1}^{N} \left(\left\| Q(y_k - y_k^{ref}) \right\|_2^2 + \|Ru_k\|_2^2 \right),$$

was calculated and expressed with respect to the nominal MPC,

$$\Delta J_{res} = \left(\frac{J_{res,PE}}{J_{res,MPC}} - 1 \right) \times 100\,(\%).$$

Here, the subscripts MPC and PE indicate the original non-exciting MPC and one of the provided persistently-exciting MPC algorithms, respectively.

The summary of the results is given in Tab. II. From the provided tables it is obvious that the algorithms presented in this paper are able to generate data which are much richer on information. The smallest eigenvalues $\lambda_{min,norm}$ are several times higher than 1 for the presented algorithms while normalized determinants $\det(S_{norm})$ are much lower than in case of the nominal MPC. Here, let us remark that the smallest eigenvalue λ_{min} as well as $\det(S)$ are normalized with respect to the MPC, e.g. $\lambda_{min,norm} = \lambda_{min,PE}/\lambda_{min,MPC}$.

The possibility to estimate model parameters with better accuracy is illustrated also by Fig. 1 and 2, where the estimates of the particular parameters of the structure (11) are depicted. Red asterisks denote parameters identified from data provided by pure non-exciting MPC, green circles show parameters identified from one-sample algorithm data, parameters identified from multi-sample algorithm data are represented by blue crosses and the real values of the parameter are marked by black x-marks. It can be observed that the parameters estimated from the data provided by the MPC are usually quite far from the real parameter value. On the other hand, estimates are more precise in case of one-sample and multi-sample algorithm, respectively.
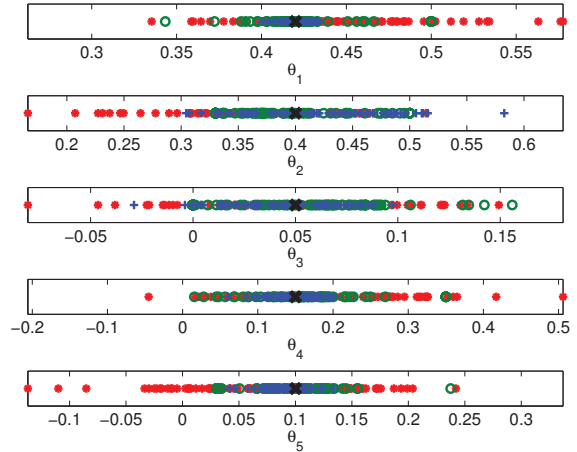

Fig. 1. Parameter estimates ($W_P = 0$).

However, such improvement does not come for free and the price to pay is reflected in the controller performance. Still, from Tab. II it can be seen that the energy consumption increase stays between 1.2 and $2.3\,\%$ depending on the algorithm variant. Also reference tracking error e_{ref} is not critical in case of the presented PE algorithms and stays within $3 - 4\,\%$ range with respect to the reference profile. The cost function values J_{res} are also presented – again, no critical increase can be witnessed in case of the PE algorithms. Furthermore, it should be realized that the degradation of controller performance is only a short-term affair and therefore, this degradation might not be critical even in the industrial practice. The reason is that the closed-loop identification experiment is needed only in case that the controller that makes use of the model
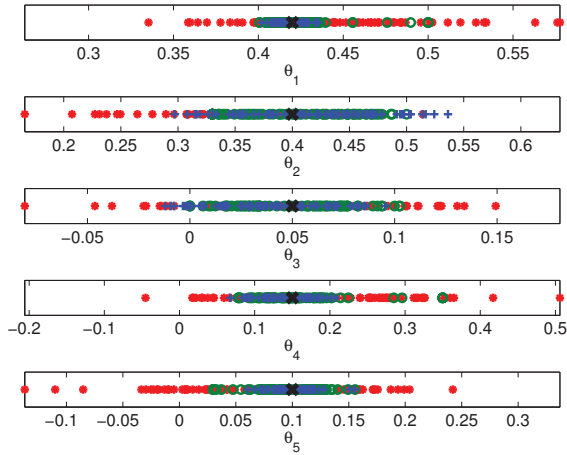
Fig. 2. Parameter estimates ($W_P = 1/3$).

does not work reliably due to inaccurate model predictions. In such situation, the model needs to be re-identified and the closed-loop identification experiment is performed only during a limited amount of time until sufficiently excited data are gathered and the model (and thus also the controller) performance is acceptable. Having accomplished that, the ordinary MPC can be used again.

To summarize the performance of the proposed algorithms, all variants provide more informative data for the price of non-critical deterioration of the controller performance. Here, slightly better informativeness results are obtained by the multi-sample approach. This can be attributed to the fact that when performing the informativeness optimization, this approach has more degrees of freedom at disposal since it optimizes M-sample subsequence of the input profile instead of optimizing just the first sample. However, the one-sample approach is more advantageous when looking for the better controller performance specified by the MPC cost criterion.

TABLE II
RESULTS COMPARISON.

	e_{ref}	ΔEC	ΔJ_{res}	$\det(S_{norm})$	$\lambda_{min,norm}$
AlgI.	4.1	2.3	3.0	5×10^{-4}	2.68
AlgII.	3.0	1.2	3.6	2×10^{-4}	3.54
AlgI.P	3.75	2.2	3.16	1.3×10^{-5}	2.46
AlgII.P	3.8	2.2	6.0	1×10^{-5}	3.56
MPC	1.3	0	0	1	1

V. CONCLUSION

In this paper, identifiability of a class of nonlinear systems with polynomial system dynamics controlled by a model predictive controller was studied. Bilinear systems were focused on and several formulations particularly advantageous for (but not restricted to) model predictive control tasks including bilinear system description were derived. PE condition was incorporated into the two-stage optimization procedure to ensure that the predictive controller provides sufficiently informative data and at the same time does not deteriorate the control performance compared to the nominal (non-exciting)

controller by more than a user-defined value. Two algorithms were developed and described in detail and their performance was verified on a set of numerical experiments. The resulting comparison shows that both developed algorithm successfully optimize the data informativeness which leads to significant improvement of the identifiability of the model parameters while respecting the maximal allowed controller performance deterioration.

REFERENCES

[1] Y. Zhu, *Multivariable system identification for process control*. Elsevier, 2001.
[2] L. Ljung, *System identification*. Wiley Online Library, 1999.
[3] ——, "Prediction error estimation methods," *Circuits, Systems and Signal Processing*, vol. 21, no. 1, pp. 11–21, 2002.
[4] I. Gustavsson, L. Ljung, and T. Söderström, "Identification of processes in closed loop—identifiability and accuracy aspects," *Automatica*, vol. 13, no. 1, pp. 59–75, 1977.
[5] C. A. Larsson, "Application-oriented experiment design for industrial model predictive control," 2014.
[6] J. Rathouský and V. Havlena, "Mpc-based approximate dual controller by information matrix maximization," *International Journal of Adaptive Control and Signal Processing*, vol. 27, no. 11, pp. 974–999, 2013.
[7] G. Marafioti, F. Stoican, R. Bitmead, and M. Hovd, "Persistently exciting model predictive control for siso systems," in *Nonlinear Model Predictive Control*, vol. 4, no. 1, 2012, pp. 448–453.
[8] E. Žáčeková, S. Prívara, and M. Pčolka, "Persistent excitation condition within the dual control framework," *Journal of Process Control*, vol. 23, no. 9, pp. 1270–1280, 2013.
[9] D. Williamson, "Observation of bilinear systems with application to biological control," *Automatica*, vol. 13, no. 3, pp. 243–254, 1977.
[10] A. Kelman and F. Borrelli, "Bilinear model predictive control of a hvac system using sequential quadratic programming," in *IFAC World Congress*, 2011.
[11] C. Olalla, I. Queinnec, R. Leyva, and A. El Aroudi, "Optimal state-feedback control of bilinear dc–dc converters with guaranteed regions of stability," *Industrial Electronics, IEEE Transactions on*, vol. 59, no. 10, pp. 3868–3880, 2012.
[12] P. Pardalos and V. A. Yatsenko, *Optimization and Control of Bilinear Systems: Theory, Algorithms, and Applications*. Springer Science & Business Media, 2010, vol. 11.
[13] E. Zacekova, M. Pcolka, S. Celikovsky, and M. Sebek, "Semi-receding horizon algorithm for "sufficiently exciting" mpc with adaptive search step," in *Decision and Control (CDC), 2014 IEEE 53rd Annual Conference on*. IEEE, 2014, pp. 4142–4147.
[14] S. Dasgupta, Y. Shrivastava, and G. Krenzer, "Persistent excitation in bilinear systems," *Automatic Control, IEEE Transactions on*, vol. 36, no. 3, pp. 305–313, 1991.
[15] G. C. Goodwin and K. S. Sin, *Adaptive filtering prediction and control*. Courier Corporation, 2014.
[16] Z.-Q. Luo, W.-K. Ma, A.-C. So, Y. Ye, and S. Zhang, "Semidefinite relaxation of quadratic optimization problems," *Signal Processing Magazine, IEEE*, vol. 27, no. 3, pp. 20–34, 2010.
[17] S. Boyd and L. Vandenberghe, *Convex optimization*. Cambridge university press, 2004.
[18] J. Currie and D. I. Wilson, "OPTI: Lowering the Barrier Between Open Source Optimizers and the Industrial MATLAB User," in *Foundations of Computer-Aided Process Operations*, N. Sahinidis and J. Pinto, Eds., Savannah, Georgia, USA, 8–11 January 2012.
[19] A. S. Bazanella, M. Gevers, D. Coutinho, R. Rui *et al.*, "Identifiability and excitation of a class of rational systems," in *53rd IEEE Conference on Decision and Control*, 2014.
[20] A. De Cock, M. Gevers, and J. Schoukens, "A preliminary study on optimal input design for nonlinear systems," in *Decision and Control (CDC), 2013 IEEE 52nd Annual Conference on*. IEEE, 2013, pp. 4931–4936.
[21] H. Hjalmarsson and J. Mårtensson, "Optimal input design for identification of non-linear systems: Learning from the linear case," in *American Control Conference, 2007. ACC'07*. IEEE, 2007, pp. 1572–1576.

Chapter 6

Conclusions

6.1 Summary

This thesis has summarized the author's research conducted on the development of algorithms handling the problem of identification for model predictive control under real-operation conditions. It has been divided into two part: in the first part, MRI techniques have been discussed while in the second one, contributions related to MPC with guaranteed persistence of excitation have been presented.

In the first part of this thesis, the algorithm for optimization of the multistep prediction has been developed. The identification procedure has been designed with respect to the issues occurring when tackling the task of identification from the real-life data. Unlike the methods available in the state-of-the-art literature, the method provided in this thesis has considered identification of multiple-input/multiple-output state-space structures and also constraints for the parameters of the identified structures have been handled.

The developed identification routines have been customized and exploited for identification of several models of the building of the Czech Technical University. Subsequently, the models have been deployed with the real-operation MPC, which also thanks to their use has spared more than 20 % of the energy consumed for heating as reported in [A.10] and [A.11].

The original procedure has been further extended and used for a medium-size office building in Hasselt, Belgium. Using a special two-stage procedure combining grey-box modeling and minimization of the multistep prediction error, a large model with 8 outputs and 11 inputs has been identified. Similarly to the previous story, the obtained model has

been employed as a predictor for the MPC controlling the temperature in the mentioned office building in real operation [A.3], [A.22]. In this case, the energy savings have reached about 20 % as well. The work published in *Applied Energy* [A.3] has brought, inter alia, a detailed discussion of the process of model validation and selection. For the analysis purposes, several identification datasets have been exploited differing from one another in number of available measurements, quality of the records and also in data richness. The analysis carried out in this publication has brought the following interesting revelations. While the predictions of the models identified by the MRI procedure have been sufficiently precise regardless of the identification dataset, the traditional grey-box method minimizing only one-step prediction error has been able to provide accurate long-term models mostly when fed with data of higher quality. Low-quality data, on the contrary, have yielded unreliable models with considerable prediction errors. This investigation has proven the theoretical analysis given in several pioneering works [Shook et al., 1991], [Shook et al., 1992] where the authors showed that the improvement in the predictions accuracy considering multistep prediction error minimization is proportional to size and complexity of the noise model and the unmodelled part of the system dynamic, respectively. This also makes the MRI identification a good candidate for the situations when data of questionable quality from the closed-loop operation are considered as the identification dataset.

Furthermore, this thesis has brought also a contribution in the area of nonlinear MRI identification. A novel method for identification of a broad class of nonlinear systems has been designed and successfully tested with results published in [A.4].

In the second part of the thesis, the topic of MPC guaranteeing perstistance of excitation has been studied. Two novel algorithms handling this problem have been designed. Both of them employ the following procedure: at first, the input sequence extremizing the original MPC cost function is computed and then, the excitation maximization task is solved with additional user-defined constraints on the deterioration of the performance with respect to the MPC cost function.

The first of them—the *one-sample algorithm*—takes advantage of the receding horizon principle and thanks to that, it solves a non-convex problem with the dimension reduced from M to 1. The second one—the *gradient algorithm*—utilizes local optimization. Both algorithms have been presented in several versions adapted to particular controller requirements and the structure of the identified system:

- the core version of the algorithms for linear systems governed by the standard MPC

minimizing a weighted combination of the control energy and reference tracking error [A.1], [A.13], [A.17].

- extension covering the zone MPCs (the control objective is to keep the output trajectory within the predefined zone) with linear system structure [A.15], [A.16].

- algorithm for a special class of systems with predictable disturbances controlled by a zone MPC; the manuscript [A.5] provides a detailed discussion about the choice of the tuning parameters. Moreover, it includes a rigorous debate on the conditions ensuring the problem feasibility and also a realistic case study representing optimization of the temperature control with use of a high-fidelity building model.

- adaptation of the algorithms for a class of nonlinear systems with polynomial nonlinearity governed by the standard version of the MPC [A.18].

All variants of the two designed algorithms for the persistently exciting MPC have been successfully tested. Thanks to the additional optimization of the data excitation, closed-loop data with considerably increased informativeness have been generated. Estimation errors of the model parameters obtained from these data have been several times lower and both the step and also frequency responses have been closer to the real ones than in case where common (non-excited) closed-loop data have been exploited. Despite substantial improvement in the parameters identifibility, only a modest degradation of the MPC performance has been observed. To be specific, the energy consumption increase has usually reached only several per cent and the reference tracking error or the zone violation, respectively, has been negligible.

Trying to compare the two algorithms, the following summary can be provided. When evaluating the performance (either from the control requirement degradation or the parameter identifibility point of view), the two alternatives are fairly equivalent. A more interesting is the comparison focusing on the computational complexity and adaptability. The *one-sample* algorithm is very fast and simple to implement especially for linear systems with the standard MPC since the "heart" of the algorithm consists in a line search. Increasing the complexity of either the model or the controller, the pre-processing phase preceding the one-dimensional optimization itself becomes more complicated. On the contrary, the complexity of the *gradient* algorithm is higher from the very beginning since the M-dimensional non-convex optimization has to be solved. However, it is also considerably versatile since with no special modifications, it can be used for a broad spectrum of the

controller/model structures. To sum up, both of them can be considered as good candidates for least costly closed-loop experiment design and the final choice strongly depends on the particular application and user preferences and requirements.

6.2 Future work

Speaking about the future research that could extend the work presented in this thesis, the following suggestions can be be made:

- **Combination of MRI and the persistently exciting MPC.** In the first part of this work, it has been shown that replacing the traditional identification methods with those minimizing multistep prediction error, significant improvement of the prediction properties of the identified models can be gained. It should be emphasized that especially the prediction properties are of key importance for the models that are intended to be used with MPC. However, the new algorithms proposed in the second part of the work consider only the common identification methods minimizing one-step prediction error. Therefore, the persistently exciting MPC algorithms should be tested in combination with the MRI method and they should be accordingly modified to enable the use of the MRI method in the role of the identification routine.

- **Combination of persistently exciting MPC and model mismatch detection methods.** To exploit the full potential of any model-based controller, it needs to be provided with an accurate model of the controlled system, which usually means that a continual maintenance is required. Although several algorithms capable of solving the problem of closed-loop identification experiment in an effective way with minimal expenses have been proposed in this thesis, *when* such experiment is actually necessary and *when* the use of the "pure" MPC suffices still remains to be answered. An extension of the current algorithm enabling detection of the model mismatch and therefore requesting excited data only when necessary (e.g. the model used by MPC becomes inaccurate and unusable) is one of the most peculiar future challenges. Such extension would lead to a fully automated re-identification and consequently to a maintenance-less MPC, which would be of huge interest for industrial control engineering practice.

- **Application in the fault detection area.** Since sufficient excitation is crucial not only for the needs of system identification but also for fault detection algorithms

that likewise need well-excited data for their proper functioning, the next area to be explored is the verification and potential adaptation of the algorithm in case that a failure in the controlled system occurs and needs to be detected and isolated.

Bibliography

[Aggelogiannaki and Sarimveis, 2006] Aggelogiannaki, E. and Sarimveis, H. (2006). Multiobjective constrained mpc with simultaneous closed-loop identification. *International Journal of Adaptive Control and Signal Processing*, 20(4):145–173.

[Alessio and Bemporad, 2009] Alessio, A. and Bemporad, A. (2009). A survey on explicit model predictive control. In *Nonlinear model predictive control*, pages 345–369. Springer.

[Anderson et al., 2018] Anderson, A., González, A., Ferramosca, A., D'Jorge, A., and Kofman, E. (2018). Robust mpc suitable for closed-loop re-identification, based on probabilistic invariant sets. *Systems & Control Letters*, 118:84–93.

[Bitmead, 1984] Bitmead, R. (1984). Persistence of excitation conditions and the convergence of adaptive schemes. *IEEE Transactions on Information Theory*, 30(2):183–191.

[Boyd and Vandenberghe, 2004] Boyd, S. and Vandenberghe, L. (2004). *Convex optimization*. Cambridge Univ Pr.

[Bustos et al., 2016] Bustos, G., Ferramosca, A., Godoy, J., and González, A. (2016). Application of model predictive control suitable for closed-loop re-identification to a polymerization reactor. *Journal of Process Control*, 44:1–13.

[Corriou, 2018] Corriou, J.-P. (2018). Model predictive control. In *Process Control*, pages 631–677. Springer.

[Darby and Nikolaou, 2012] Darby, M. L. and Nikolaou, M. (2012). Mpc: Current practice and challenges. *Control Engineering Practice*, 20(4):328–342.

[De Klerk and Craig, 2002] De Klerk, E. and Craig, I. (2002). Closed-loop system identification of a mimo plant controlled by a mpc controller. In *Africon Conference in Africa, 2002. IEEE AFRICON. 6th*, volume 1, pages 85–90. IEEE.

[Ebadat, 2017] Ebadat, A. (2017). *Experiment Design for Closed-loop System Identification with Applications in Model Predictive Control and Occupancy Estimation.* PhD thesis, KTH Royal Institute of Technology.

[Ebadat et al., 2017] Ebadat, A., Valenzuela, P. E., Rojas, C. R., and Wahlberg, B. (2017). Model predictive control oriented experiment design for system identification: a graph theoretical approach. *Journal of Process Control*, 52:75–84.

[Feng and Houska, 2018] Feng, X. and Houska, B. (2018). Real-time algorithm for self-reflective model predictive control. *Journal of Process Control*, 65:68–77.

[Forbes et al., 2015] Forbes, M. G., Patwardhan, R. S., Hamadah, H., and Gopaluni, R. B. (2015). Model predictive control in industry: Challenges and opportunities. *IFAC-PapersOnLine*, 48(8):531–538.

[Forssell and Ljung, 1998] Forssell, U. and Ljung, L. (1998). Closed-loop identification revisited Updated Version. *Report no. LiTH-ISY*.

[Forssell and Ljung, 2000] Forssell, U. and Ljung, L. (2000). A projection method for closed-loop identification. *Automatic Control, IEEE Transactions on*, 45(11):2101–2106.

[Genceli and Nikolaou, 1996] Genceli, H. and Nikolaou, M. (1996). New approach to constrained predictive control with simultaneous model identification. *AIChE journal*, 42(10):2857–2868.

[González et al., 2014] González, A. H., Ferramosca, A., Bustos, G. A., Marchetti, J. L., Fiacchini, M., and Odloak, D. (2014). Model predictive control suitable for closed-loop re-identification. *Systems & Control Letters*, 69:23–33.

[Gopaluni et al., 2004] Gopaluni, R., Patwardhan, R., and Shah, S. (2004). Mpc relevant identification—-tuning the noise model. *Journal of Process Control*, 14(6):699–714.

[Gopaluni et al., 2003] Gopaluni, R. B., Patwardhan, R., and Shah, S. (2003). The nature of data pre-filters in mpc relevant identification—open-and closed-loop issues. *Automatica*, 39(9):1617–1626.

[Gustavsson et al., 1977] Gustavsson, I., Ljung, L., and Soderstrom, T. (1977). Identification of processes in closed loop–identifiability and accuracy aspects. *Automatica*, 13(1):59–75.

[Heirung et al., 2013] Heirung, T. A. N., Ydstie, B. E., and Foss, B. (2013). An mpc approach to dual control. *IFAC Proceedings Volumes*, 46(32):69–74.

[Huang and Wang, 1999] Huang, B. and Wang, Z. (1999). The role of data prefiltering for integrated identification and model predictive control. *IFAC Proceedings Volumes*, 32(2):6751–6756.

[Klein, 1988] Klein, S. A. (1988). Trnsys-a transient system simulation program. *University of Wisconsin-Madison, Engineering Experiment Station Report*, pages 38–12.

[Larsson, 2014] Larsson, C. A. (2014). *Application-oriented experiment design for industrial model predictive control*. PhD thesis, KTH Royal Institute of Technology.

[Larsson et al., 2011] Larsson, C. A., Annergren, M., and Hjalmarsson, H. (2011). On optimal input design in system identification for model predictive control. In *Decision and Control and European Control Conference (CDC-ECC), 2011 50th IEEE Conference on*, pages 805–810. IEEE.

[Larsson et al., 2013] Larsson, C. A., Annergren, M., Hjalmarsson, H., Rojas, C. R., Bombois, X., Mesbah, A., and Modén, P. E. (2013). Model predictive control with integrated experiment design for output error systems. In *Control Conference (ECC), 2013 European*, pages 3790–3795. IEEE.

[Larsson et al., 2016] Larsson, C. A., Ebadat, A., Rojas, C. R., Bombois, X., and Hjalmarsson, H. (2016). An application-oriented approach to dual control with excitation for closed-loop identification. *European Journal of Control*, 29:1–16.

[Laurí et al., 2010] Laurí, D., Martínez, M., Salcedo, J., and Sanchis, J. (2010). Pls-based model predictive control relevant identification: Pls-ph algorithm. *Chemometrics and Intelligent Laboratory Systems*, 100(2):118–126.

[Laurı et al., 2010] Laurı, D., Salcedo, J., Garcıa-Nieto, S., and Martınez, M. (2010). Model predictive control relevant identification: multiple input multiple output against multiple input single output. *IET control theory & applications*, 4(9):1756–1766.

[Ljung, 1999] Ljung, L. (1999). *System identification*. Wiley Online Library.

[Ljung, 2001] Ljung, L. (2001). Prediction error estimation methods. In *Circuits, Systems, and Signal Processing*, pages 11–21. Birkhauser Boston.

[Lucia and Paulen, 2014] Lucia, S. and Paulen, R. (2014). Robust nonlinear model predictive control with reduction of uncertainty via robust optimal experiment design. *IFAC Proceedings Volumes*, 47(3):1904–1909.

[Ma et al., 2011] Ma, Y., Borrelli, F., Hencey, B., Coffey, B., Bengea, S., and Haves, P. (2011). Model predictive control for the operation of building cooling systems. *Control Systems Technology, IEEE Transactions on*, PP(99):1–8.

[Marafioti et al., 2010] Marafioti, G., Bitmead, R., and Hovd, M. (2010). Persistently exciting model predictive control using fir models. In *International Conference Cybernetics and Informatics*, volume 6.

[Mayne, 2014] Mayne, D. Q. (2014). Model predictive control: Recent developments and future promise. *Automatica*, 50(12):2967–2986.

[Oldewurtel et al., 2010] Oldewurtel, F., Parisio, A., Jones, C. N., Morari, M., Gyalistras, D., Gwerder, M., Stauch, V., Lehmann, B., and Wirth, K. (2010). Energy efficient building climate control using stochastic model predictive control and weather predictions. In *American control conference (ACC), 2010*, pages 5100–5105. IEEE.

[Potts et al., 2014] Potts, A. S., Romano, R. A., and Garcia, C. (2014). Improving performance and stability of mpc relevant identification methods. *Control Engineering Practice*, 22:20–33.

[Quachio and Garcia, 2014] Quachio, R. and Garcia, C. (2014). Application of the pls–ph method for identifying polynomial narx models. *Journal of Control, Automation and Electrical Systems*, 25(2):184–194.

[Quachio and Garcia, 2017] Quachio, R. and Garcia, C. (2017). Mpc relevant identification method for hammerstein models. *IFAC-PapersOnLine*, 50(2):47–52.

[Rathousky and Havlena, 2011] Rathousky, J. and Havlena, V. (2011). Multiple-step active control with dual properties. In *IFAC World Congress*, volume 18, pages 1522–1527.

[Rathousky and Havlena, 2013] Rathousky, J. and Havlena, V. (2013). Mpc-based approximate dual controller by information matrix maximization. *International Journal of Adaptive Control and Signal Processing*, 27(11):974–999.

[Razmara et al., 2015] Razmara, M., Maasoumy, M., Shahbakhti, M., and Robinett, R. (2015). Optimal exergy control of building hvac system. *Applied Energy*, 156:555–565.

[Rehor and Havlena, 2010] Rehor, J. and Havlena, V. (2010). Grey-box model identification–control relevant approach. *IFAC Proceedings Volumes*, 43(10):117–122.

[Rossiter and Kouvaritakis, 2001] Rossiter, J. and Kouvaritakis, B. (2001). Modelling and implicit modelling for predictive control. *International Journal of Control*, 74(11):1085–1095.

[Shook et al., 1991] Shook, D. S., Mohtadi, C., and Shah, S. L. (1991). Identification for long-range predictive control. In *IEE Proceedings D (Control Theory and Applications)*, volume 138, pages 75–84. IET.

[Shook et al., 1992] Shook, D. S., Mohtadi, C., and Shah, S. L. (1992). A control-relevant identification strategy for gpc. *IEEE Transactions on Automatic Control*, 37(7):975–980.

[Shouche, 1996] Shouche, M. (1996). *Closed-loop Identification and Predictive Control of Chemical Processes*. PhD thesis, Texas A&M University.

[Shouche et al., 2002] Shouche, M. S., Genceli, H., and Nikolaou, M. (2002). Effect of on-line optimization techniques on model predictive control and identification (mpci). *Computers & chemical engineering*, 26(9):1241–1252.

[Smarra et al., 2018] Smarra, F., Jain, A., de Rubeis, T., Ambrosini, D., D'Innocenzo, A., and Mangharam, R. (2018). Data-driven model predictive control using random forests for building energy optimization and climate control. *Applied Energy*.

[Tanaskovic et al., 2014] Tanaskovic, M., Fagiano, L., and Morari, M. (2014). On the optimal worst-case experiment design for constrained linear systems. *Automatica*, 50(12):3291–3298.

[Telen et al., 2016] Telen, D., Vallerio, M., Bhonsale, S., Logist, F., and Van Impe, J. (2016). Towards nonlinear model predictive control with integrated experiment design. In *American Control Conference (ACC), 2016*, pages 942–947. IEEE.

[Van den Hof, 1998] Van den Hof, P. (1998). Closed-loop issues in system identification. *Annual reviews in control*, 22:173–186.

[Van Den Hof and Schrama, 1993] Van Den Hof, P. and Schrama, R. (1993). An indirect method for transfer function estimation from closed loop data. *Automatica*, 29(6):1523–1527.

[Zhao et al., 2014] Zhao, J., Zhu, Y., and Patwardhan, R. (2014). Some notes on mpc relevant identification. In *American Control Conference (ACC), 2014*, pages 3680–3685. IEEE.

[Zhu, 2001] Zhu, Y. (2001). *Multivariable system identification for process control*. Elsevier Science.

Publications of the Author

Thesis related publications

Articles in journals with impact factor

[A.1] Zacekova, E., Privara, S., Pcolka, M. (2013, authorship: 80 %). *Persistent excitation condition within the dual control framework.* Journal of Process Control (2017 impact factor: 2,787). DOI: `10.1016/j.jprocont.2013.08.004`.

Citations (excluding auto-citations). *Web of Science*: 9. *Google Scholar*: 13.

[A.2] Privara, S., Cigler, J., Vana, Z., Oldewurtel, F., Zacekova, E. (2013, authorship: 25 %). *Use of partial least squares within the control relevant identification for buildings.* Control Engineering Practice (2017 impact factor: 2,616). DOI: `10.1016/j.conengprac.2012.09.017`.

Citations (excluding auto-citations). *Web of Science*: 13. *Google Scholar*: 19.

[A.3] Zacekova, E., Vana, Z., Cigler, J. (2014, authorship: 90 %). *Towards the real-life implementation of MPC for an office building: Identification issues.* Applied Energy (2017 impact factor: 7,900). DOI: `10.1016/j.apenergy.2014.08.004`.

Citations (excluding auto-citations). *Web of Science*: 19. *Google Scholar*: 32.

[A.4] Pcolka, M., Zacekova, E., Robinett, R., Celikovsky, S., Sebek, M. (2016, authorship: 29 %). *Bridging the gap between the linear and nonlinear predictive control: Adaptations for efficient building climate control.* Control Engineering Practice (2017 impact factor: 2,787). DOI: `10.1016/j.conengprac.2016.01.007`.

Citations (excluding auto-citations). *Web of Science*: 4. *Google Scholar*: 7.

Articles in journals with impact factor - under review

[A.5] Zacekova, E., Pcolka, M., Sebek, M. (2018; under review). *Zone MPC with Guaranteed Identifiability in Presence of Predictable Disturbances.* Journal of the Franklin Institute.

Conference proceedings - invited talks

[A.6] Pcolka, M., Zacekova, E., Robinett, R., Celikovsky, S., Sebek, M. (2014, authorship: 30 %). *From Linear to Nonlinear Model Predictive Control of a Building.* 19th World Congress of the International Federation of Automatic Control (IFAC 2014), Cape Town, South Africa. DOI: doi.org/10.3182/20140824-6-ZA-1003.02783.

Citations (excluding auto-citations). *Web of Science*: –. *Google Scholar*: 1.

[A.7] Pcolka, M., Zacekova, E., Robinett, R., Celikovsky, S., Sebek, M. (2014, authorship: 35 %). *Economical nonlinear model predictive control for building climate control.* American Control Conference (2014 ACC), Portland, U.S. (indexed in *Web of Science*). DOI: 10.1109/ACC.2014.6858928.

Citations (excluding auto-citations). *Web of Science*: 1. *Google Scholar*: 2.

[A.8] Zacekova, E., Pcolka, M., Tabacek, J., Tezky, J., Robinett, R., Celikovsky, S., Sebek, M. (2015, authorship: 40 %). *Identification and energy efficient control for a building: Getting inspired by MPC.* American Control Conference (2015 ACC), Chicago, U.S. (indexed in *Web of Science*). DOI: 10.1109/ACC.2015.7170973.

Citations (excluding auto-citations). *Web of Science*: 4. *Google Scholar*: 4.

Conference proceedings

[A.9] Zacekova, E., Vana, Z., Privara, S. (2011, authorship: 50 %). *Model predictive control relevant identification using partial least squares for building modeling.* Australian Control Conference (2011 AUCC), Melbourne, Australia.

Citations (excluding auto-citations). *Web of Science*: –. *Google Scholar*: 17.

[A.10] Zacekova, E., Privara, S. (2012, authorship: 60 %). *Control relevant identification and predictive control of a building.* 24th Chinese Control and Decision Conference

(2012 CCDC), Taiyuan, China (indexed in *Web of Science*). DOI: `10.1109/CCDC.2012.6244035`.

Citations (excluding auto-citations). *Web of Science*: 2. *Google Scholar*: 4.

[A.11] Zacekova, E., Ferkl, L. (2012, authorship: 80 %). *Building modeling and control using multi-step ahead error minimization.* 20th Mediterranean Conference on Control and Automation (MED 2012), Barcelona, Spain. DOI: `10.1109/MED.2012.6265674`.

Citations (excluding auto-citations). *Web of Science*: –. *Google Scholar*: 1.

[A.12] Zacekova, E., Vana, Z. (2012, authorship: 70 %). *Identification and model selection of building models.* 20th Mediterranean Conference on Control and Automation (MED 2012), Barcelona, Spain. DOI: `10.1109/MED.2012.6265853`.

Citations (excluding auto-citations). *Web of Science*: –. *Google Scholar*: 1.

[A.13] Zacekova, E., Privara, S., Komarek, J. (2012, authorship: 60 %). *On dual control for buildings using persistent excitation condition.* 51st Annual Conference on Decision and Control (2012 CDC), Maui, U.S. (indexed in *Web of Science*). DOI: `10.1109/CDC.2012.6426282`.

Citations (excluding auto-citations). *Web of Science*: 0. *Google Scholar*: 2.

[A.14] Zacekova, E., Vana, S., Cigler, J., Hoogmartens, J., Verhelst, C., Sourbron, M., Ferkl, L., Helsen, L. (2013, authorship: 40 %). *Identification for model based predictive control applied to an office building with a thermally activated building systems.* 11th REHVA world congress Clima, (2013 Clima), Prague, Czech Republic.

Citations (excluding auto-citations). *Web of Science*: –. *Google Scholar*: 0.

[A.15] Zacekova, E., Privara, S., Vana, S., Cigler, J., Ferkl, L. (2013, authorship: 50 %). *Dual control approach for zone model predictive control.* European Control Conference (ECC 2013), Zurich, Switzerland (indexed in *Web of Science*). DOI: `10.23919/ECC.2013.6669605`.

Citations (excluding auto-citations). *Web of Science*: 2. *Google Scholar*: 6.

[A.16] Zacekova, E., Pcolka, M., Sebek, M. (2014, authorship: 50 %). *On Satisfaction of the Persistent Excitation Condition for the Zone MPC: Numerical Approach.* 19th World Congress of the International Federation of Automatic Control (IFAC 2014), Cape Town, South Africa. DOI: `doi.org/10.3182/20140824-6-ZA-1003.02705`.

Citations (excluding auto-citations). *Web of Science*: –. *Google Scholar*: 0.

[A.17] Zacekova, E., Pcolka, M., Celikovsky, S., Sebek, M.(2014, authorship: 50 %). *Semireceding horizon algorithm for "sufficiently exciting" MPC with adaptive search step.* 53rd Annual Conference on Decision and Control (CDC 2014), Los Angeles, U.S. (indexed in *Web of Science*). DOI: `10.1109/CDC.2014.7040034`.

Citations (excluding auto-citations). *Web of Science*: 0. *Google Scholar*: 0.

[A.18] Zacekova, E., Pcolka, M., Sebek, M., Celikovsky, S. (2015, authorship: 50 %). *MPC for a class of nonlinear systems with guaranteed identifiability.* IEEE Conference on Control and Applications (CCA 2015), Sydney, Australia (indexed in *Web of Science*). DOI: `10.1109/CCA.2015.7320627`.

Citations (excluding auto-citations). *Web of Science*: 0. *Google Scholar*: 0.

Other publications

Articles in journals with impact factor

[A.19] Cigler, J., Privara, S., Vana, Z., Zacekova, E., Ferkl, L. (2012, authorship: 10 %). *Optimization of predicted mean vote index within model predictive control framework: Computationally tractable solution.* Energy and Buildings (2017 impact factor: 4,457). DOI: `10.1016/j.enbuild.2012.05.022`.

Citations (excluding auto-citations). *Web of Science*: 28. *Google Scholar*: 43.

[A.20] Privara, S., Vana, Z., Zacekova, E., Cigler, J. (2012, authorship: 10 %). *Building modeling: Selection of the most appropriate model for predictive control.* Energy and Buildings (2017 impact factor: 4,457). DOI: `10.1016/j.enbuild.2012.08.040`.

Citations (excluding auto-citations). *Web of Science*: 41. *Google Scholar*: 67.

[A.21] Privara, S., Cigler, J., Vana, Z., Oldewurtel, F., Sagerschnig, C., Zacekova, E. (2013, authorship: 10 %). *Building modeling as a crucial part for building predictive control.* Energy and Buildings (2017 impact factor: 4,457). DOI: `10.1016/j.enbuild.2012. 10.024`.

Citations (excluding auto-citations). *Web of Science*: 97. *Google Scholar*: 170.

[A.22] Vana, Z., Cigler, J., Siroky, J., Zacekova, E., Ferkl, L. (2014, authorship: 5 %). *Model-based Energy Efficient Control Applied to an Office Building.* Journal of Process Control (2017 impact factor: 2,787). DOI: `10.1016/j.jprocont.2014.01.016`.

Citations (excluding auto-citations). *Web of Science*: 8. *Google Scholar*: 23.

[A.23] Pcolka, M., Zacekova, E., Celikovsky, S., Sebek, M. (2017,authorship: 25 %). *Toward a Smart Car: Hybrid Nonlinear Predictive Controller With Adaptive Horizon.* IEEE Transactions on Control Systems Technology (2017 impact factor: 4,883). DOI: `10.1109/TCST.2017.2747504`.

Citations (excluding auto-citations). *Web of Science*: 0. *Google Scholar*: 0.

Conference proceedings

[A.24] Cigler, J., Privara, S., Vana, Z., Zacekova, E., Ferkl, L. (2012, authorship: 10 %). *On predicted mean vote optimization in building climate control.* 20th Mediterranean Conference on Control and Automation (MED 2012), Barcelona, Spain. DOI: `10.1109/MED.2012.6265854`.

Citations (excluding auto-citations). *Web of Science*: –. *Google Scholar*: 5.

[A.25] Vana, Z., Privara, S., Zacekova, E., Cigler, J. (2013, authorship: 20 %). *Building semi-physical modeling: On selection of the model complexity.* European Control Conference (ECC 2013), Zurich, Switzerland. DOI: `10.23919/ECC.2013.6669245`.

Citations (excluding auto-citations). *Web of Science*: 2. *Google Scholar*: 3.

[A.26] Vey, D., Lunze, J., Zacekova, E., Pcolka, M., Sebek, M.(2014, authorship: 25 %). *Control reconfiguration of full-state linearizable systems by a virtual actuator.* 9th IFAC Symposium on Fault Detection, Supervision and Safety of Technical Processes (Safeprocess 2015), Paris, France. DOI: `10.1016/j.ifacol.2015.09.550`.

Citations (excluding auto-citations). *Web of Science*: –. *Google Scholar*: 0.

[A.27] Pcolka, M., Zacekova, E., Robinett, R., Celikovsky, S., Sebek, M. (2015, authorship: 29 %). *Quantized nonlinear model predictive control for a building.* IEEE Conference on Control and Applications (CCA 2015), Sydney, Australia, (indexed in *Web of Science*). DOI: `10.1109/CCA.2015.7320653`.

Citations (excluding auto-citations). *Web of Science*: –. *Google Scholar*: 0.